The Role of Lymphotoxin Ligand-Receptor Interactions in Regulating Epithelial Cell Fate

Balid Albarbar

A thesis submitted to the University of Huddersfield in partial fulfilment of the requirements for the degree of Doctor of Philosophy

The University of Huddersfield
School of Applied Science

August 2016

Abstract

LTβR and HVEM are non-death domain-containing TNFRs that can induce cell death via possible recruitment of TNFR-associated factors (TRAF), thus may share similarities to other TNFR members (e.g. CD40). This thesis aimed to investigate the effects of soluble LT agonists on a panel of carcinoma cells of colorectal (CRC) and bladder (UCC) origins and to compare the ability of these agonists to induce cell death against membrane-bound LIGHT (mLIGHT), and to unravel for the first time the cell signalling pathways responsible for mLIGHT-mediated cell death.

Due to the complexity of some of the approaches used, a significant part of the experimental work involved optimisations involving not only soluble LT agonists, cytokines, specific pharmacological inhibitors but mainly optimisation for the first time of a co-culture system for the delivery of the mLIGHT signal to epithelial cells (involved co-culture of target cells with growth-arrested third-party L cells expressing surface mLIGHT). Several assays were also optimised for detection of cell viability, cell death (based on protease release, caspase activation and DNA fragmentation) and for detection of pro-inflammatory cytokine secretion. Moreover, immunoblotting techniques were optimised and utilised for detection of proteins associated with intracellular LTβR and HVEM-signalling. Transfection experiments using specific small interfering RNAs (siRNAs) were also employed to knockdown the expression of LTβR and HVEM proteins in CRC and UCC cells.

This project revealed for the first time that normal human urothelial cells (NHU), CRC and UCC cells express LTβR and HVEM, and that the activation of LTβR and HVEM by mLIGHT, in the absence of IFN-γ, is pro-apoptotic in carcinoma cells, whereas mLIGHT appeared to be cyto-protective in NHU cells. By contrast, soluble LT agonists were weakly pro-apoptotic and required IFN-γ to kill HT29 cells, yet this combination did not kill other, well-characterised carcinoma cell lines, in particular HCT116 and EJ cells. Moreover, mLIGHT caused some DNA fragmentation in HCT116, yet little DNA fragmentation was detected in HT29 and EJ cells. It was also found that mLIGHT caused IL-8 and GM-CSF secretion. mLIGHT triggered TRAF1 and TRAF3 induction and caused little detectable differences in phospho-ERK, -JNK and -p38 expression in CRC and UCC cells. Functional inhibition experiments showed that blockade of MEK/ERK abrogated death in all cell lines tested, and JNK inhibition attenuated death in HCT116 and EJ (but not HT29 cells) and p38 inhibition significantly attenuated, but not fully, mLIGHT-mediated cell death in CRC and UCC cells. Moreover, an NF-κB inhibitor partially reduced mLIGHT-mediated death in CRC cells and potentiated it in UCC cells, whereas, inhibition of AP-1 partially blocked mLIGHT-mediated death in HCT116 and EJ cells. By contrast, AP-1 blockade did not cause any statistically significant effect in mLIGHT-mediated death in HT29 cells. Moreover, mLIGHT-mediated death is ROS dependent in CRC and UCC cells as the antioxidant NAC attenuated death. The current work has also provided evidence for the first time that a role for NOX enzyme in cell death of HCT116 and EJ cells as it was found that mLIGHT induced the phosphorylation of p40phox (a subunit of NOX). Importantly, despite observing that ASK1 was activated in HCT116 cells, but not other cells, mLIGHT caused downregulation of Thioredoxin-1 expression in CRC and UCC. siRNA experiments for LTβR and HVEM knockdown showed some preliminary evidence that LTβR and HVEM might signal cooperatively in the context of LIGHT-mediated cell death.

Collectively, this thesis has demonstrated for the first time that triggering cell death in CRC and UCC is clearly dependent on signal quality, cell-type specificity and death is tumour cell-specific. The current study has also provided some mechanistic insight into how cell death induced by mLIGHT-LTβR/HVEM interactions occurs, which may involve a novel pathway of receptor-TRAF3-MAPK-NOX interactions, which utilise ROS for the activation of cell death pathways in CRC and UCC cells. These findings have not only improved our understanding of how TNFRs induce carcinoma cells death, but may also help in the design of better therapeutic strategies in the future.

ACKNOWLEDGMENTS

I would like to give big thank you to my supervisor Dr Nikolaos Georgopoulos for his help, support, and guidance throughout for four years of this PhD. A huge thank you to all the members of Nikolaos Georgopoulos group (NTG group) for making my time here enjoyable.

Special thanks must go to my country Libya for providing me a financial support. My thanks also go to the University of Huddersfield, in particular, the staff and the technician for their help and advices.

I would not be here today if it was not for the support of my parents and my wife, my children and extended my family, especially my brother Professor Al-hussein Albarbar.

I would like also to acknowledge everyone in the lab who helped with experience, ideas and discussions during my studies.

Thank you everyone!!

Table of contents

List of Figures

List of Tables

List of Abbreviations

ACD	Accidental cell death
AIF	Apoptosis inducing factor
AML	Amyloid leukaemia
ALL	Acute lymphoblastic leukaemia
AP-1	Activator protein-1
Apaf-1	Apoptosis protease-activating factor-1
ASK1	Apoptosis signalling kinase 1
APRIL	A proliferation-inducing ligand
ATP	Adenosine Triphosphate
APCs	Antigen presenting cells
Bad	Bcl-2 antagonist of cell death Bcl-2 binding protein
BAFF	B cell activating factor belonging to the TNF family
Bak	Bcl-2 antagonist killer
Bax	Bcl-2 associated X protein
BAX	Bcl-2-associated X protein
BCL-2	B-cell lymphoma 2
Bcl-w	Bcl-2 like 2 proteins (Apoptosis regulator Bcl-w)
Bcl-X_L	Bcl-2 extra large
Bcl-Xs	Bcl-2 related protein (short isoform)
B-CLL	B-chronic lymphocytic leukaemia
BCMA	B cell maturation antigen
Bid	BH3 interacting domain death agonist p22 BID
BID	BH3 interacting domain death agonist
BIK	Bcl-2 Interacting Killer
BIM	Bcl-2 interacting mediator of cell death
BAFF	B-cell activating factor belonging to the TNF family
BrdU	5-bromo-2-dedoxyuridine
BSA	Bovine Serum Albumin
CAD	Caspase activated DNase
CLL	Chronic lymphocytic leukaemia
CARD	Caspase activation and recruitment domain
Caspase	Cysteine aspartic acid-protease

c-FLIP	FLICE-inhibitory protein
Cyto-c	Cytochrome C
CDK	Cyclin dependant kinase
cDNA	Complementary DNA
CD	Cluster of Differentiation
CD40	CD40 receptor
CRD	Cysteine-rich domain
CXCL9	Chemokine 9
CXCL10	Chemokine 10
CRT	Calreticulin
DIABLO	Direct IAP binding protein with low PI
dATP	2'-deoxyadenosine triphosphate
DFF40	DNA Fragmentation Factor 40/CAD
DFF45	DNA Fragmentation Factor 45/ICAD
DISC	Death inducing signalling complex
DNA	Deoxyribonucleic acid
DNase	Deoxyribonuclease
DD	Death domain
DR	Death receptor
DcR	decoy receptor
DR4	Death receptor 4
DR5	Death receptor 5
DED	Death effector domain
DIF	Differentiation-inducing factor
DCs	Dendritic cells
DMEM	Dulbecco's modified Eagle's medium
DMSO	Dimethyl Sulphoxide
DPI	Diphenylene iodonium
Endo G	Endonuclease G
ERK1/2	Extracellular signal regulated Kinase1, 2
EDTA	Ethylenediaminetetraacetic acid
FAD	Flavine adinine dinucleotide
FADD	Fas-associated death domain

Fas	Fibroblast-associated cell-surface
FBS	Foetal Bovine Serum
GM-CSF	Granulocyte Macrophage – Colony Stimulating Factor
H_2DCFDA	6-carboxy-2,7 dichloro dihydrofluorescin diacetate
H_2SO_4	Sulphuric acid
HVEM	Herpes-virus entry mediator
IAP	Inhibitor of Apoptosis Proteins
ICAM-1	Intercellular adhesion molecule-1
ICD	Intracellular domain
IFN	Interferon
IFN-γ	Interferon-gamma
IU	International unit
IL	Interleukin
IP-10	Interferon gamma-induce protein 10
IκB	Inhibitor of NF-κB
IKK	IκB Kinase
IKKα	IκB Kinase alpha
IKKβ	IκB Kinase Beta
IKKγ	IκB Kinase gamma
JNK	C-jun N-terminal kinase
kDa	Kilo Dalton
LT	Lymphotoxin
LIGHT	Lymphotoxin-like exhibits Inducible expression and competes with herpes simplex virus Glycoprotein D for HVEM, HVEM being a receptor expressed on T lymphocytes
LTβR	Lymphotoxin beta receptor
LPC	Lysophosphatidylcholine
LPS	Lipopolysaccharide
Mac-1	Macrophage-1 antigen
MAPK	Mitogen activated Protein kinase
MEKK-1	MAP Kinase kinase-1
MHC-1	Major Histocompatibility Complex-1
MHC-2	Major Histocompatibility Complex-2

MMP	Metalloproteinase Matrix
MOMP	Mitochondrial outer membrane permeabilisation
mRNA	Messenger Ribonucleic acid
MAdCAM-1	Mucosal vascular addressin cell adhesion molecule
MIG	Monokine induced by gamma interferon
MMC	Mitomycine c
mg	Milligram
mM	Millimolar
NHU	Normal human urothelial cells
NF-κB	Nuclear factor kappa B
NAC	N-acetyl cysteine
NIK	NF-κB-inducing kinase
NK	Natural killer cells
NO	Nitric Oxide
NOX	NADPH oxidase
NGF	Nerve growth factor
OMM	Outer mitochondrial membrane
PBS	Phosphate buffer saline
PS	Phosphatidylserine
PVDF	Polyvinylidine difluoride membrane
RANTES	Regulated on Activation Normal T cell Expressed and Secreted
Redox	Reduction-oxidation
RFU	Relative Fluorescent unit
RLU	Relative Luminescence unit
RIP	Receptor-interacting protein
RNA	Ribonucleic acid
RNase	Ribonuclease
ROS	Reactive oxygen Species
RT	Room Temperature
RANK	Receptor activator of nuclear factor-kB
SAPK	Stress Activated Protein Kinase
sCD40L	Soluble CD40 ligand

sLIGHT	Soluble LIGHT
shRNA	Short hairpin RNA
siRNA	Small interfering RNA
Smac	Second mitochondrial activator of caspases
TACI	Transmembrane activator and CAML interactor
TIM	TRAF interacting motif
TNF	Tumour necrosis factor
TNFSF	TNF superfamily
TNFL	TNF ligand
TNFR	TNF receptor
TNFRSF	Tumour necrosis factor receptor superfamily
TNFR-I	Tumour necrosis factor receptor I
TNFR-II	Tumour necrosis factor receptor II
TRAIL	TNF-related apoptosis-inducing ligand
TRAIL-R	TRAIL receptor
TNF-α	Tumour necrosis factor-alpha
TRADD	Tumour necrosis factor receptor associated death domain
TRAF	Tumour necrosis factor receptor associated factor
TRAP	Tumour Necrosis Factor-related Activation Protein
TL1A	TNF-like molecule 1A
TF	Transcription factor
UV	Ultra violet
µl	Microlitre
µM	Micromolar
µg	Micro gram
VDAC	Voltage Dependent Anion Channel
XAF-1	XIAP- associated factor-1
XEDAR	X-linked ectodermal dysplasia receptor
xIAP	X-linked inhibitor of apoptosis protein

Chapter 1

Introduction

1.1 Programmed Cell Death–Overview

Organism homeostasis is maintained through a balance between cell growth or proliferation and cell death. Cell death or programmed cell death (PCD) is a physiological process that normally occurs during the life span of multicellular organisms, whose cells must die at some point, which is known as the “point of no return” during development or aging (Kroemer et al., 2009; Tower, 2015). PCD was first described in the mid-1960s (Kerr, 1965; Lockshin and Williams, 1964; Lockshin and Williams, 1965) and traditionally classified in 1973 by Schweichel and Merker (Schweichel and Merker, 1973) into three subtypes, apoptosis, autophagy, and necrosis.

Apoptosis (PCD type-I) is a form of regulated cell death that is characterized by cell rounding up, cell shrinkage, reduction in cell volume (pyknosis), plasma membrane blebbing, and chromatin and nuclear condensation (Kroemer et al., 2005) – this type of PCD will be largely discussed in section 1.2. Autophagic cell death (PCD type-II) is a regulated form of cell death characterized by double-membraned autophagic vacuoles; however, it lacks chromatin condensation (Galluzzi et al., 2007; Kroemer et al., 2005; Kroemer et al., 2009). Necrosis (PCD type-III) is different from apoptosis and autophagy in morphological features. It is traditionally known as an unregulated and passive form of cell death (unorganized events) where cells are killed accidently. Necrosis is characterized by swelling of the cell, disruption of the cell membrane, and release of cellular contents into the extracellular milieu, which in turn may damage the cells, resulting in local inflammation, and possibly promotion of tumour growth (Kroemer et al., 2009; Vakkila and Lotze, 2004). In addition, another type of PCD was identified as an alternative means of regulated cell death known as necroptosis (Degterev et al., 2005), which is characterized by the same morphological features as unregulated necrotic cell death. Necroptosis is not well understood and still under investigation (Degterev et al., 2014; Degterev et al., 2008; Zhou and Yuan, 2014).

PCD forms have been reviewed recently (Tower, 2015) and summarised in Table 1.1 and Figure 1.1. PCD usually refers to apoptosis; however, it is important to note that apoptosis and PCD are not synonymous because cell death and/or PCD occur during physiological development and PCD may also be characterized by nonapoptotic features (Baehrecke, 2002; Roach and Clarke, 2000).

The mechanisms and morphological features of apoptosis, autophagy, and necrosis are distinguishable and diverse. However, there are some overlapping features among them. PCD generally exhibits apoptotic morphology but could be also characterized by more necrotic features with the depletion of total intracellular adenosine triphosphate (ATP), inhibition of caspases (e.g., using pharmacological inhibitors), or elimination of caspase activators such as Apoptotic protease-activating factor 1 (Apaf-1) (Golstein and Kroemer, 2005; Kroemer and Martin, 2005; Nicotera et al., 1998). Because necrosis and apoptosis are characterized by the expression of shared biochemical molecules, this is often known as the “apoptosis–necrosis continuum” (Zeiss, 2003). This finding is supported by studies which demonstrated that receptor-interacting protein kinase (RIP) can inhibit ATP and adenosine diphosphate functions on mitochondrial membrane and causes TNF-induced necrosis (Temkin et al., 2006). Moreover, PCD can exhibit an autophagic phenotype, which can be converted to a necrotic morphology once the early steps of autophagy process are inhibited (Degenhardt et al., 2006; Golstein and Kroemer, 2007; Shimizu et al., 2004). The appearance of specific forms of PCD (whether apoptosis, autophagy, necrosis or necroptosis) depends on several factors such as the nature of death stimulus and cell or tissue type, thus it is highly context-specific (Fiers et al., 1999; Zeiss, 2003).

	Apoptosis	Autophagy	Necrosis	Necroptosis
Death mode	Programmed	Programmed	Accidental	Programmed
Triggers	Stress, UV, genotoxic substances, TNF-α, FasL, TRAIL, CD40L or LT ligands	Hypoxia, nutrient deprivation, histone deacetylase	Trauma, toxins	TNF-α, FasL, or TRAIL
Main signalling pathways	Intrinsic and extrinsic pathway caspase dependent	Caspase-independent, autophagosome and lysosome proteases	-	TNFR signalling, JNK activation, caspase independent RIP1/3 necrosome
Inflammation	No	No	Yes	Yes
Morphological features	non-lytic, shrinkage, DNA fragmentation, apoptotic bodies	non-lytic	Lytic, plasma membrane rupture	non-lytic, swollen, plasma membrane loss
Expression marker	PS Ecto-CRT	LPC PS	PS	LPC PS

Table 1.1. Summary of PCD forms and their features

The table shows the comparisons between PCD forms; apoptosis, autophagy, necrosis and necroptosis. Abbreviations: PS: phosphatidylserine. Ecto-CRT, calreticulin. LPC: lysophosphatidylcholine. JNK: c-Jun N-terminal kinase. Different markers are expressed by PCD forms, including ecto-CRT and LPC, on the cell membrane.

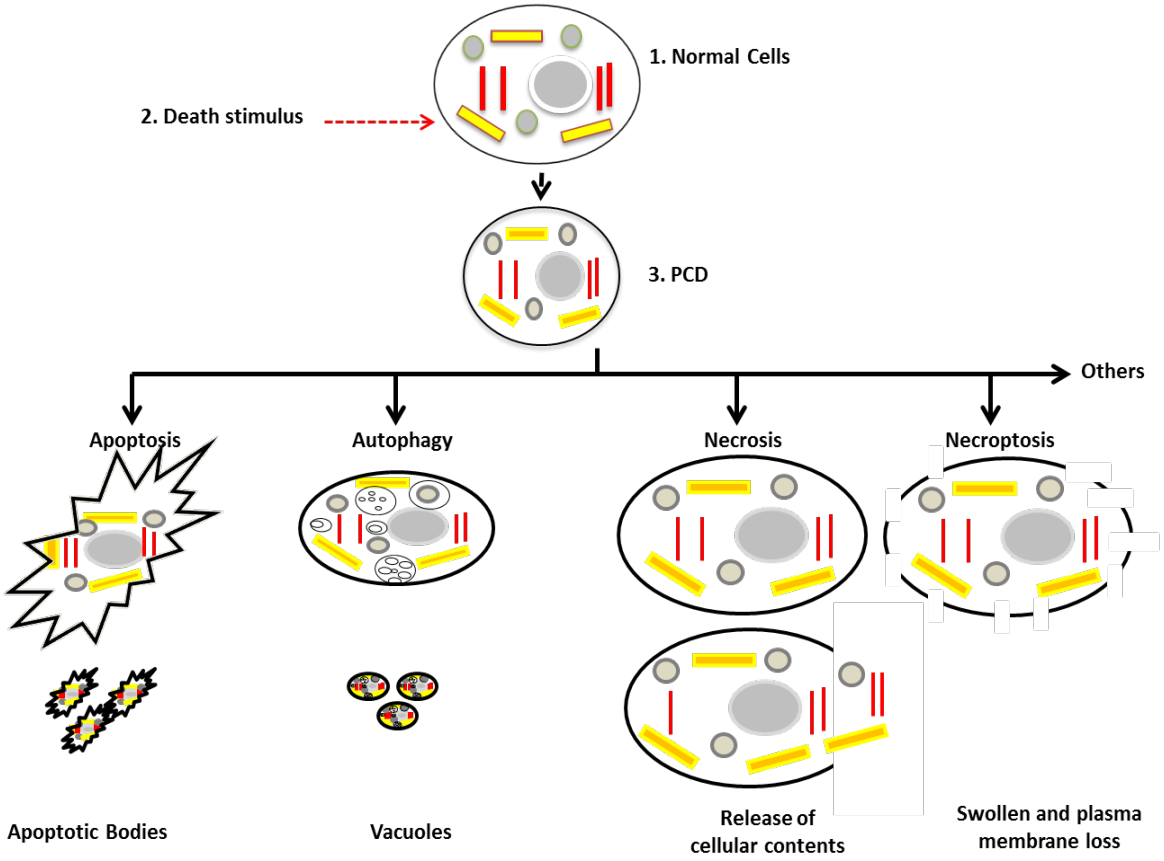

Figure 1.1. Schematic representation of the different forms of PCD

The figure shows the types of cell death, when normal cells are exposed to a stimulus. Apoptosis is triggered by the activation of various initiator caspases that play critical role in activating effector caspases in order to be cleaved and become active. Apoptotic cells are characterised by the condensation of their cytoplasmic and nuclear membrane, DNA damage, formation of apoptotic bodies, and maintenance of an intact plasma membrane. The apoptotic bodies are phagocytosed, and in the case of phagocytosis absence, apoptotic bodies may transform to apoptotic necrosis. Autophagy is characterised by degradation of cellular components within the intact dying cell in autophagic vacuoles; vacuolization is one of the morphological features of autophagy. Phagocytosis can take up the autophagic cells and degrade them. Necrosis exhibits cellular organelle swelling, membrane breakdown features and causing inflammatory cellular contents release. Necroptosis is one of the cell death types and has not been well characterised yet. Figure modified from (Labbe and Saleh, 2008).

1.2 Apoptosis – Background

The term ‘apoptosis’ derives from the Greek word ‘falling off’ as leaves fall from a tree. Apoptosis was described by Kerr and colleagues in 1972, after they observed similar specific features of toxin-treated liver cells to those embryonic cells during ontogenesis and development – this phenomenon was then named as apoptosis (Kerr et al., 1972). Apoptosis exhibits various features most of which are explained below.

1.2.1 Physiological and pathological roles of apoptosis

It is evident that apoptosis normally occurs during development and homeostasis, which maintains cell populations in tissues. Apoptosis appears to also be a key player in immune defence as it eliminates damaged cells (e.g. following immune reaction) or removes mutated cells (e.g. exposing cells to noxious agents), in order to keep the balance between cells under control and to comply with the rule “better death than wrong” (Kroemer et al., 2007; Norbury and Hickson, 2001). The process of apoptosis is essential and important for maintaining cell death and cell growth, and has to be neatly balanced, otherwise imbalance in apoptosis and cell growth can lead to autoimmune disease, oncogenesis and tumour progression (Koff et al., 2015), whereas excessive apoptosis contributes to degenerative diseases (e.g. stroke) and infectious diseases (e.g. intoxications and septic shock) (Reed, 2002; Thompson, 1995). Apoptotic bodies demonstrate typical features, such as chromatin condensation and DNA fragmentation, which subsequently can be taken up by phagocytic cells, and degraded within phagosomes (which fused with lysosome resulting in digestion of the foreign antigens) in macrophages (Savill and Fadok, 2000). This causes death of macrophages and leads to the engulfment of dying macrophages by dendritic cells in order to present theses antigens to T cells, and trigger innate and adaptive immune responses (Albert, 2004).

1.2.2 Biochemical components of apoptosis

1.2.2.1 Phosphatidylserine (PS)

During apoptosis PS (a phospholipid component of the cell's lipid bilayer) translocates from the intracellular to the extracellular surface of the plasma membrane. PS found on the surface of apoptotic cells is utilised as an 'eat-me' signal, as it is recognised by phagocytes. Studies have shown that Annexin I (cellular proteins found mostly in eukaryotic organisms) and calreticulin proteins are expressed on the cell surface during apoptosis. Also, Annexin V (a recombinant PS binding protein) can detect apoptosis, as it interacts strongly and specifically with PS residues (Arur et al., 2003; Bratton et al., 1997).

1.2.2.2 Caspases

Caspases exist in an inactive form as proenzymes, and when they activated they tend to cleave themselves, as well as other pro-caspases, allowing initiation of a protease cascade process (Cohen, 1997). Caspases are able to activate and cleave proteins at aspartic acid residues. This proteolytic cascade amplifies the apoptotic signalling pathway and thus leads to rapid cell death. To date, several caspases have been classified into three groups: initiator caspases (caspases-2, 8, 9, 10), inflammatory caspases (caspases-1, 4, 5) and executioner or effector caspases (caspases-3, 6 and 7) (Salvesen, 2002). Each of these caspases has different roles and specificities in the apoptosis cascade (Cohen, 1997; Hu et al., 1998; Rai et al., 2005).

1.2.2.3 Protein cross-linking and DNA fragmentation

Another characteristic of the apoptotic cell is extensive protein cross-linking and this is produced through the expression and activation of tissue transglutaminases (Nemes et al., 1996). During apoptosis, DNA is broken down by Ca^{2+} and Mg^{2+} dependent endonuclease in DNA fragments of 180 to 200 base pairs. These DNA fragments or "DNA ladder" can be observed by agarose gel electrophoresis with an ethidium bromide stain and ultraviolet illumination (Hengartner, 2000; Martinvalet et al., 2005).

1.3 Pathways of apoptosis

The decision for a cell to undergo apoptosis can be triggered by three pathways: a) the extrinsic (TNFR-mediated), b) the intrinsic (mitochondrial), and c) the perforin/granzyme pathways (that relates to cytotoxic T lymphocytes and NK cells) (Elmore, 2007; Martinvalet et al., 2005). These pathways converge at the execution caspase pathway (the execution pathway is initiated by caspase-3 and caspase-7, leading to the degradation of nuclear proteins, cell cytoskeleton, DNA fragmentation and the end form of apoptotic bodies) (Li and Yuan, 2008). The intrinsic and the alternative pathway of T-cell mediated cytotoxicity have been previously reviewed (Trapani and Smyth, 2002).

1.3.1 The perforin/granzyme pathway

This pathway involves immune cells and specifically cytotoxic T lymphocyte CD8 T cells (CTLs) and natural killer (NK) cells. These cells can kill their target cells (e.g. infected or transformed cells) by two mechanisms; the first mechanism (the extrinsic pathway – to be discussed below) is by the interaction of Fas and FasL, and a significant function of this pathway is to eliminate self-reactive lymphoid cells (van Parijs and Abbas, 1996). The second mechanism is to cause pores in the target cell membrane by delivering their protease toxins known as pore-forming protein ('perforin') and by inserting granzyme (granzyme A and B) leading to cell death of the target cells (Smyth and Trapani, 1995; Trapani and Smyth, 2002). Cell death via this pathway can be both caspase-dependent and caspase-independent (Sarin et al., 1997; Trapani et al., 1998).

Granzyme A is able to kill target cells via the cleavage of nuclear proteins, which ultimately leads to DNA degradation (Beresford et al., 1999), whereas, granzyme B acts differently and can cleave proteins at aspartate residues and is believed to be the most potent protease for caspase-mediated, as well as caspase-independent, cell death (Motyka et al., 2000).

The exact mechanism of perforin action is still unknown, but perforin polymerises once it is exposed to calcium and forms polyperforin. Polyperforin is able to induce pores in cell membranes and cause the release of proteins, thus causing necrosis of target cells. However, perforin alone is not sufficient to cause apoptosis for nucleated cells *in vitro* and both perforin and granzyme are important and required for the cleavage of specific substrates of death (Shresta et al., 1999).

It is reported that granzyme B can directly and cleaved pro-apoptotic BH3 only proteins, such as BH3-interacting domain death agonist (BID) (Alimonti et al., 2001). BID is able to trigger the release of pro-apoptotic mediators from mitochondria, such as cytochrome c, into cytosol (Alimonti et al., 2001). The alternative pathway of T-cell mediated cytotoxicity has been reviewed elsewhere (Trapani and Smyth, 2002).

1.3.2 The intrinsic pathway

The intrinsic pathway is also known as the mitochondrial pathway. Although mitochondrion is the main source of metabolic energy in the form of ATP to maintain cell survival, mitochondria are often in the ‘’centre’’ of apoptosis induction. Dysfunction in mitochondria, such as when triggered by stress (e.g. ultra violet, irradiation and drugs) causes mitochondrial outer membrane permeabilisation (MOMP) (Chipuk et al., 2006; Galluzzi et al., 2012). There are two suggested mechanisms for the initiation of MOMP and these are described briefly in the following sections.

1.3.2.1 Voltage dependent anion channel (VDAC)

The first mechanism or the alternative mechanism that mitochondria can be permeabilized by its proteins is voltage dependent anion channel 1 and 2 (VDAC1 and 2) - dependent mechanism and the adenosine nucleotide transporter (ANT), and under normal conditions both these proteins maintain mitochondrial homeostasis. However, during dysfunction, the presence of high concentration of Ca^{2+} results in pores in mitochondria known as mitochondrial permeability transition (MPT) (De Marchi et al., 2004), or hexokinase I and II (HKI and HKII)/ the voltage dependent anion channel 1 and 2 (VDAC1 and 2) -dependent mechanism (Rizzuto and Pozzan, 2006). VDAC is the most abundant protein present in the mitochondrial outer membrane (MOM) (Colombini, 2004), it has several physiological functions, and plays a critical role with HK-I and –II in triggering MPT and apoptosis induction (Pastorino et al., 2002; Pastorino et al., 2005; Robey and Hay, 2005; Shimizu et al., 1999; Tsujimoto and Shimizu, 2000; Zaid et al., 2005).

1.3.2.2 Bcl-2 members

The second mechanism for triggering MOMP is orchestrated by a family of proteins known as B cell lymphoma-2 (Bcl-2) family. Bcl-2 is a family of proteins that contains at least one Bcl-2 homology domain (BH) (Chipuk and Green, 2008), and this family is classified into three groups based on their functional activity and the presence of BH domain that is discussed below.

1.3.2.3 Anti-apoptotic Bcl-2 members

The first group of Bcl-2 proteins contains four BH domains (BH1, 2, 3, 4) and a C-terminal hydrophobic tail and referred to as anti-apoptotic proteins (possess anti-apoptotic activity). Archetypical members of this group are B-cell lymphoma 2 (Bcl-2) and B-cell lymphoma-extra-large (Bcl-X_L). This also includes other proteins, such as B-cell lymphoma w (Bcl-w), B-cell lymphoma-related protein; A1, myeloid cell leukaemia sequence 1 protein (Mcl-1), and Bcl-2 associated athanogenes (BAG) (Figure 1.2). The anti-apoptotic proteins are mainly present within the outer surface of mitochondria for the purpose of neutralising the pro-apoptotic proteins of the Bcl-2 family that induce MOMP and apoptosis (Green and Kroemer, 2004; Kroemer and Reed, 2000; Kroemer et al., 2007).

1.3.2.4 Pro-apoptotic (group I) Bcl-2 members

The second group contains three BH domains (BH1, 2, 3) and has a similar structure to the first group, apart from the fact that they mostly contain an N-terminal hydrophobic tail. Such of these members are Bcl-2 associated x protein (Bax), Bcl-2 homologous antagonist killer (Bak), Bcl-2-related ovarian killer (Bok), and p53 upregulated modulator of apoptosis (Puma) (Figure 1.2), which all share three domains and are all characterised by hydrophobic surface grooves (Fesik, 2000; Hengartner, 2000).

1.3.2.5 Pro-apoptotic (group II) Bcl-2 members

This third group is also referred to as pro-apoptotic proteins, but they differ in structure from the proteins Bcl-2 members in that they contain only one BH (BH3). Typical members of this group are BH3-interacting domain death agonist (Bid), Bcl-2-associated death promoter (Bad) and Bcl-2-like protein 11 known as Bim (Letai et al., 2002) (Figure 1.2). Taken together, both pro-apoptotic groups (I and II) are essential for apoptosis induction and damage-sensing, BH3-only proteins clearly depend on the activation of Bax/Bak, because they cannot kill cells lacking both Bax (cytosolic protein) and Bak (associated with the MOM) and it has been suggested that both Bax/Bak are important for apoptosis induction (Cheng et al., 2001; Wei et al., 2001; Zong et al., 2001).

On the other hand, it has been shown that p53 (the tumour suppressor protein) is transactivated by DNA damage and therefore it mediates apoptosis through the transcriptional regulation of several pro-apoptotic proteins of the Bcl-2 family, such as, Bax (Schuler and Green, 2001).

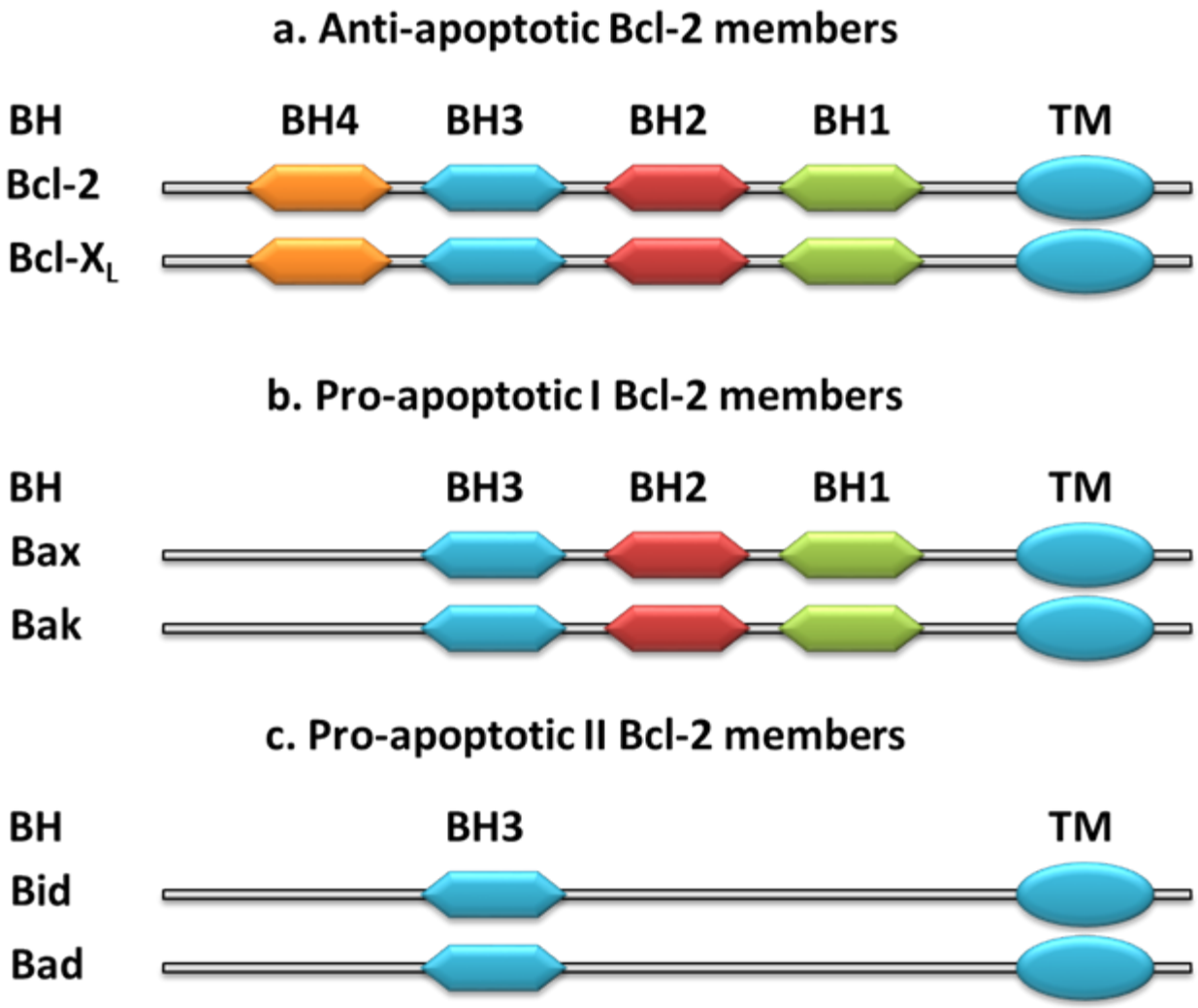

Figure 1.2. Classical examples of Bcl-2 members

Bcl-2 members consists of Bcl-2 homology domains (BH) and classified into three groups; (a) anti-apoptotic Bcl-2 members comprise of BH1, 2, 3, and 4 and a C-terminal transmembrane (C-TM) domain such as Bcl-2 and Bcl-X_L, (b) shows pro-apoptotic I Bcl-2 members which consist of BH1,2 and 3 and a TM, (c) pro-apoptotic II Bcl-2 members consist of BH3-only and a TM. Figure modified from (Giménez-Cassina and Danial, 2015).

1.3.3 Mitochondrial outer membrane permeabilisation (MOMP)

As part of the induction of the intrinsic apoptosis pathway, MOMP is initiated when the cytosolic pro-apoptotic protein Bax translocates to the MOM (Nechushtan et al., 2001; Wolter et al., 1997), that is thought to form supramolecular openings or pores for the MOM alone or with the help of other pro-apoptotic proteins, such as Bak or the active form of Bid, truncated Bid (tBid) (Kuwana et al., 2002; Li et al., 1998; Luo et al., 1998). The relocalisation of Bax from cytosol to MOM is essential for triggering apoptosis, otherwise if retained in cytosol, MOMP and apoptosis are inhibited. As a result of MOMP, apoptogenic factors are released from mitochondria, including either a) caspase-activating (leading to apoptosis via caspase-dependent pathway – discussed in section 1.3.3.1) molecules, such as cytochrome c (a component of the electron transport chain in mitochondria), second mitochondria derived activator of caspase/direct inhibitor of apoptosis protein (Smac/Diablo) and serine protease Omi/HtrA2, or b) apoptosis-inducing factor (AIF), endonuclease G (Endo G) and DNA proteolytic enzyme caspase-activated DNase (CAD) causing ultimately apoptosis via a caspase-independent pathway (Du et al., 2000; Fulda et al., 2002; Kroemer and Reed, 2000; van Loo et al., 2002).

1.3.3.1 Caspase-dependent apoptosis

Following its release into the cytosol, cytochrome c forms a complex with apoptosis protease-activator factor 1 (Apaf-1) and dATP and cytosolic procaspase-9, known as the high molecular weight caspase-activating complex “apoptosome” (Cain et al., 1999; Cain et al., 2000; Chinnaiyan, 1999; Hill et al., 2004; Li et al., 1997; Zou et al., 1997). Once the complex is formed, it leads to the activation of initiator caspase (procaspase-9) that triggers the activation of executioner caspases and then activates the other procaspases-2,-6,-8 and -10, which in turn lead to a feedback amplification of the apoptotic signal (Slee et al., 1999; Van De Craen et al., 1999).

The release of other molecules from mitochondria, such as Smac/Diablo and Omi/HtrA2, promotes caspase activation and prevent the effects of inhibitors, such as inhibitor of apoptosis proteins (IAPs) (Ferri and Kroemer, 2000). IAP proteins regulate both extrinsic and intrinsic pathways of apoptosis. However, IAP can inhibit the function of receptors containing death domain, such as TNFRI and Fas (Liston et al., 2003). Eight IAP human inhibitor proteins are well characterised, such as X-linked mammalian inhibitor of apoptosis protein (XIAP) and Survivin that inhibit IAP activity (Deveraux and Reed, 1999).

1.3.3.2 Caspase-independent apoptosis

Caspase-independent apoptosis can be triggered after MOMP releases molecules, which include apoptosis-inducing factor (AIF), endonuclease G and CAD. AIF interacts with endonuclease G and causes DNA fragmentation and CAD. DNA fragmentation and nuclear chromatin condensation are caused by AIF translocation into the nucleus, a process which is referred to as ‘stage I condensation’ (Joza et al., 2001). In addition, endonuclease G translocates to the nucleus and causes nuclear chromatin cleavage, which forms oligonucleosomal DNA fragments (Li et al., 2001). Both AIF and endonuclease G activation are mediated in a caspase-independent manner. CAD also causes oligonucleosomal DNA fragmentation, and chromatin condensation after the cleavage by caspase-3, a process which is referred to as ‘stage II condensation’ (Enari et al., 1998; Susin et al., 2000).

Also, some studies reported that there is a role for other members of the Bcl-2 family, such as Bad; Bad under normal conditions is sequestered in the cytosol and bound to 14-3-3 (a member of a family of multifunctional phosphoserine binding molecules). In case of dephosphorylation, non-phosphorylated Bad heterodimerizes with Bcl-X_L at membrane sites and contributes to cell death (Zha et al., 1996b).

1.3.4 The extrinsic pathway

The extrinsic pathway (also known as the death receptor pathway) is triggered by the ligand–induced activation of death or non-death receptors of tumour necrosis factor superfamily (TNFSF) members on the cell surface. In this regard, the best characterised extrinsic pathway of apoptosis is the one triggered by classical death receptors, such as Fas, TNFR-I and TNF-related apoptosis inducing ligands (TRAIL -R1 and -R2), which all known as death receptors (Scaffidi et al., 1998).

The TNFSF comprises a group of cytokines that have critical functional importance in immunity, inflammation, cytodifferentiation and apoptosis (Dempsey et al., 2003). The archetypal members of the TNFSF are discussed in greater detail in the following sections.

1.4 The TNFSF

The TNFSF consists of a large and complex network of ligands (TNFLs) and receptors (TNFRs) and each subgroup of the family may function in distinct ways, based on their signalling capacity and their ability to regulate specific gene expression and subsequently cell fate. By means of signalling triggered via interactions of these receptors with their cognate ligand(s), TNFRs play a critical role in cellular homeostasis (Li et al., 2004; Mauri et al., 1998; Remouchamps et al., 2011; Ruland and Mak, 2003).

TNFLs and TNFRs have multifunctional roles ranging from promotion of cell growth or induction of differentiation, to cytotoxicity by activation of cell death (mainly apoptosis) (Albarbar et al., 2015). The members of TNFLs and TNFRs are summarised in Table 1.2, with additional information on their cellular origins and recruited intracellular proteins (Gravestein and Borst, 1998; Screaton and Xu, 2000; Smith et al., 1994). Whilst, to date, 18 ligands and 29 receptors have been identified (Wiens and Glenney, 2011; Zhang, 2004), this thesis will focus on receptors and ligands of the Lymphotoxin (LT) system, and compare them with other closely related TNFSF systems that share structural and, particularly, functional similarities (Table 1.2).

1.4.1 TNFLs

TNFLs are type II transmembrane proteins that contain an intracellular N-terminus and extracellular C-terminus with the C-terminus region characterised by a conserved TNF homology domain (THD) (Bodmer et al., 2002; Idriss and Naismith, 2000). TNFLs are encoded by 18 genes clustered within the human leukocyte antigen (HLA) and major histocompatibility complex class three (MHC-III) regions, located on the short arm of chromosome 6 (Bodmer et al., 2002; Collette et al., 2003; Granger and Ware, 2001).

TNF-α is expressed in full-length on the cell surface as a 26kDa membrane ligand (mTNF-α) and as a 17kDa soluble cytokine (sTNF-α) after shedding (Aggarwal, 2000). By contrast, LT-α is always shed as a soluble cytokine, yet LTβ is expressed only in a membrane-bound form, as the latter does not contain a cleavage site. LTα and LTβ can assemble together and form two membrane bound complexes of LTαβ. The LTα1β2 complex consists of a single ββ and two unique αβ sites and exhibits high affinity to LTβR; LTα2β1 on the other hand binds to TNFR –I and TNFR –II, but with less affinity to LTβR (Ware, 2005). LIGHT also known as TNFSF14 or TL4, is encoded by a gene located on chromosome 19 and exists also in either a membrane bound form (29kDa) or a soluble form following cleavage by a yet undefined furin-like proteinase (Collette et al., 2003; Granger and Ware, 2001) and can bind both LTβR and the HVEM receptor, but not TNFR –I and TNFR –II (Ware, 2005).

1.4.2 TNFRs

The majority of the TNFRs are type I transmembrane glycosylated proteins with an extracellular N-terminus and an intracellular C-terminus, but some TNFRs are type III transmembrane proteins such as B cell maturation antigen/TNFRSF17 (BCMA), transmembrane activator and CAML interactor/TNFRSF13B (TACI), and X-linked ectodermal dysplasia receptor (XEDAR) (Bodmer et al., 2002). Structurally, TNFRs comprise three domains; an extracellular domain (ECD), a transmembrane domain (TMD) and an intracellular domain (ICD) (Albarbar et al., 2015). All TNFRs share a four cysteine-rich domain (CRD) in the ECD region, which is responsible for the specificity and affinity of these receptors for their cognate ligands (Banner et al., 1993). The genes encoding TNFRI, CD27 and LTβR are located on chromosome 12 in humans and chromosome 6 in the mouse, and the other receptors, with the exception of Fas, are located on chromosome 1p36 (Collette et al., 2003; Granger and Ware, 2001) (Table 1.2).

TNFR	Cellular origin	Signal	TNFL	Reference
TNFRI, TNFRSF1A, p55-60, and CD120a, TNFR60 and TNFRSF1A	Nucleated cells and all tissues	DD plus TRAF2,5	TNFα, cachectin, DIF, LTα3	(Armitage, 1994; Kitson et al., 1996; Loetscher et al., 1990; Terry Powers et al., 2010; Vince et al., 2009)
TNFRII, CD120b, p75-80 and TNFRSF1B	Inducible on immune cells and hematopoietic	TRAF1,2,3	LTα3, TNFα, LTα2β1	(Armitage, 1994; Cabal-Hierro and Lazo, 2012; Cabal-Hierro et al., 2014; Smith et al., 1990)
LTβR, TNFRSF3, CD18, TNFCR, TNFRIII	Fibroblast, epithelial, myeloid cells and most tumour cells	TRAF2,3,5	LTβ, LTα2β1, LTα1β2, LIGHT	(Bista et al., 2010; Crowe et al., 1994; Force et al., 1997; Kuai et al., 2003; Nakano et al., 1996; Sanjo et al., 2010; VanArsdale et al., 1997)
CD95, APO-1, Fas, TNFRSF6 APT1 and DR2	T and B cells and epithelial cells	DD plus TRAF2	FasL, APT1LG1 CD278, and TNFSF6	(Chinnaiyan et al., 1996; Leithäuser et al., 1993; Muntané, 2011; Pitti, 1998)
DR3, WSL-LR, TRAMP, TR3, LARD, APO-3, DDR3, TNFRSF12	Activated T cells and tissues of thymus, spleen and fetal kidney	DD plus TRAF2	APO-3L, TWEAK, DR3LG, TL1A, TNFSF12	(Bodmer et al., 1997; Chinnaiyan et al., 1996; Marsters et al., 1996; Screaton et al., 1997; Tan et al., 1997)
DR4, Apo2, TRAILR1 and TNFRSF10A	Most cells and cell lines	DD	TRAIL, Apo2L, TL2, TNFSF10	(Chaudhary et al., 1997; Kischkel et al., 2000; Pan et al., 1997; Schneider et al., 1997; van Geelen et al., 2011)
DR5, TRAILR2, KILLER, TRICK2 and TNFRSF10B	Most cells and cell lines	DD	TRAIL, Apo2L, TL2, TNFSF10	(Chaudhary et al., 1997; Kischkel et al., 2000; MacFarlane et al., 1997; Schneider et al., 1997; van Geelen et al., 2011)
DR6, TR-7, TNFRSF21	Lymphoid organs, tissues lymphoid cells and tumours	DD plus TRAF2	N.D	(Kitson et al., 1996; Pan et al., 1998a; Pan et al., 1998b).
DcR1, TRAILR3, TRID, Apo2, LIT and TNFSF10C	Various human tissues	Absent	TRAIL, TL2, TNFSF10	(Degli-Esposti et al., 1997c; MacFarlane et al., 1997; Marsters et al., 1997a; Pan et al., 1997; Sheridan et al., 1997)
DcR2, TRAILR4, TRUNDD	Various human tissues	Absent	TRAIL, TL2, TNFSF10	(Degli-Esposti et al., 1997a; Marsters et al., 1997a; Pan et al., 1998a)
DcR3, TR6, M68, TNFRSF6B	Monocytes, dendritic cells, lung tissues, adenocarcinomas	Absent	FasL, LIGHT, TL1A	(Pitti, 1998; Yu et al., 1999)
CD27, TNFRSF7, S152 and Tp55	T, B cell and some tumours	TRAF2,3,5	CD27L, TNFSF7 and CD70	(Akiba et al., 1998; Armitage, 1994; Camerini et al., 1991) (Nakano et al., 1999; Yamamoto et al., 1998)
CD30, TNFSF8	Lymphoid cells and some tumours	TRAF1,2,3,5	CD30L	(Armitage, 1994; Inoue et al., 2000; Smith et al., 1994; Wajant et al., 2001a)
CD40, GP39, HIGM1, IMD3, TNFRSF5, TRAP	T, B cells and some tumours	TRAF2,3,5,6	CD40L, CD154, CD140, HIGM1, TNFSF5	(Armitage, 1994; Bishop et al., 2007; Ishida et al., 1996a; Van den Oord et al., 1996)

OX40, gp34, TNFRSF4, TXGP1L,CD134, ACT35	T cells and some tumours	TRAF1,2,3,5,6	OX40L, TNFSF4, TXGP1	(Croft et al., 2009; Dürkop et al., 1995; Imura et al., 1997; Kawamata et al., 1998; Mallett et al., 1990; Wajant et al., 2001a)
NGFR, P75, P75NGFR, P75NTR, CD271, TNFRSF16	Nervous system, kidney, lung, hair follicles and some tumours	DD plus TRAF1,2,3,4,5,6	NGF, TNFSF16	(Geetha et al., 2012; Powell et al., 2009; Radeke et al., 1990; Roux and Barker, 2002; Wheeler et al., 1998)
AITR, GITR and TNFRSF18	T cells and some tumours	TRAF1,2,3,4,5	AITRL, TL6, hGITRL and TNFSF18	(Basak et al., 2007; Esparza and Arch, 2004; Esparza et al., 2006; Kim et al., 2007; Nocentini et al., 1997; Suvas et al., 2005)
HVEM, HveA, TL1, CD270, TNFRSF14, ATAR, TR2	T cells, lymphoid and non-lymphoid cells, and some tumours	TRAF1,2,3,5	LIGHT, LTα3, CD258, HVEM-L TL4, TNFSF14	(Hsu et al., 1997; Marsters et al., 1997b)
4-1BB, TNFRSF9, CD137 and ILA	T cells and thymocytes	TRAF1,2,3	4-1BBL and TNFSF9	(Inoue et al., 2000; Pollok et al., 1993; Vinay and Kwon, 1999; Wajant et al., 2001a)
RANK, TRANCE-R, TNFRSF11A	Activated T cells, dendritic cells, lymph nodes	TRAF1,2,3,5,6	RANKL, OPGL, ODF TRANCE, TNFRSF11A, TNFRSF11B	(Inoue et al., 2000; Kanazawa et al., 2003; Simonet et al., 1997; Wong et al., 1998)

Table 1.2. TNFLs and TNFRs members

The table summarises all known TNFRs and their cognate ligands, the cell types in which TNFRs are expressed and the adaptor proteins involved in signalling triggered by the receptor in each case. N.D, not determined.

1.4.3 Regulation of TNFLs and TNFRs function by shedding

Decoy receptors (DcRs) are not the only factors negatively modulating TNFR activation, because regulation of receptor signalling involves shedding of both ligands and receptors into soluble forms by the action of a family of metalloprotease known as sheddases. Shedding is often associated with attenuation of ligand-mediated receptor activation. Such enzymes include disintegrin and metalloproteinase such as a disintegrin and metalloprotease domain (ADAM-17). The latter is also referred to as TNF-alpha-converting enzyme (TACE) and was originally identified for its ability to shed membrane (mTNF-α) to soluble ligand (sTNF-α) (Figure 1.3). Importantly, there is evidence to suggest that cleavage of both mTNFRs and mTNFLs into soluble forms limits the bioavailability and thus concentrations of TNFLs and their respective TNFRs and this has a direct impact on receptor functionality (Black et al., 2002; Black et al., 1997; Moss et al., 1997; Vardouli et al., 2009).

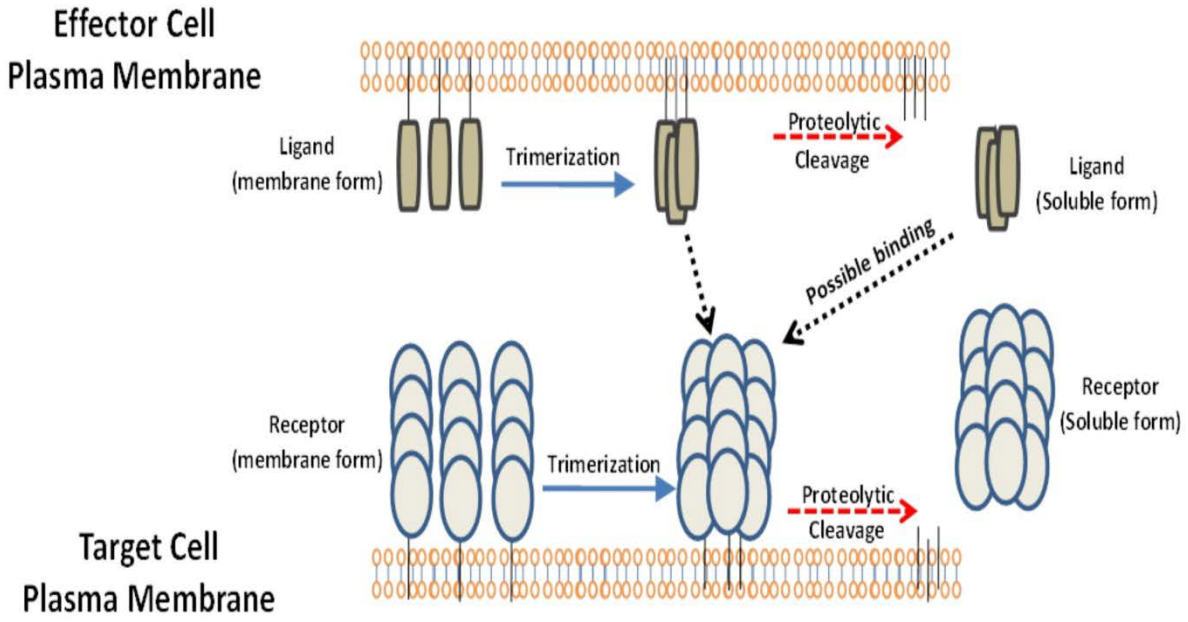

Figure 1.3. Mechanism of TNFLs and TNFRs shedding

TNFLs (top) and TNFRs (bottom) are expressed in two forms; membrane-bound (via a transmembrane domain anchoring the protein within the cell membrane) or a soluble trimeric form. Signalling via membrane-bound forms of TNFLs requires cell-cell contact to achieve activation of membrane-bound forms of TNFRs to induce receptor trimerisation and trigger intracellular signalling. Soluble TNFLs or TNFRs are membrane-bound forms that had been cleaved into soluble forms through metalloproteinase action.

1.5 TNFR signalling

In order to initiate TNFR-mediated cell signalling, TNFLs (either in soluble form or in membrane-bound form on the surface of an effector cell) induce TNFR clustering, aggregation and oligomerisation (cross-linking) on target cells. Downstream signalling is generally accepted to require trimeric ligands to drive/enable receptor trimerisation or possibly multimerization. However, TNFRs may not exist as monomers that trimerise only upon ligand binding. There is in fact evidence for the existence of a pre-ligand assembly domain (PLAD) residing within the CRD of the receptors, which appears to be critical for the function of the receptor (Chan, 2000; Chan, 2007). Studies reported that PLAD is formed for a number of receptors such as, Fas, TNFRI, and CD40. PLAD is located opposite to the receptor ligand binding site (Chan et al., 2000). Typically, once the receptor is activated, signal transduction is triggered via recruitment of adaptor proteins in order to ultimately activate transcription factors such as NF-κB or c-Jun N-terminal kinase/activator protein-1 (JNK/AP-1) for induction of either proliferation, differentiation or, more typically for a large proportion of the TNFSF, cell death (Albarbar et al., 2015). The precise nature, timing and extent of adaptor protein recruitment and overall TNFR activation are dependent on several factors, such as cell type, cellular context/state, and ‘quality’ of the signal i.e. the strength of ligand-receptor interaction (discussed further in subsequent sections) (Wajant, 2015). These factors are critical for adaptor protein recruitment and intracellular signalling and thus functional outcome (Georgopoulos et al., 2006).

1.6 TNFR sub-groups

TNFRs can be divided into three sub-groups based on the specific structural features that they contain within their ICD (Chung et al., 2002; Dempsey et al., 2003). An important characteristic defining the first and more classical TNFR group is that the ICD contains a death domain (DD) and includes members such as TNFR-I, Fas and TRAIL-Rs. The DD permits signalling initiation via adaptor protein recruitment; these adaptor proteins are modular, as they contain a DD (that allows interaction with the receptor) as well as a death effector domain (DED). Examples of such proteins include the TNFR-associated DD (TRADD) for TNFR-I and Fas-associated DD (FADD) for Fas and TRAIL-Rs. The existence of the DED permits induction of apoptotic signalling via recruitment of DED-comprising, initiator pro-caspases, in particular caspase-8 and in some cases caspase-10 (Dempsey et al., 2003; Engels et al., 2005; Micheau and Tschopp, 2003) (Figure 1.4).

The second TNFR group is characterised by the presence of another type of domain known as the TRAF-interacting motif (TIM). Receptor activation leads to recruitment of TNFR-associated factors (TRAFs), which are zinc RING finger proteins with a C-terminal region responsible for receptor binding, and these adaptors mediate recruitment and/or activation of downstream signalling pathways, mainly Mitogen Activated Protein Kinases (MAPKs) such as p38 and JNK (Arch et al., 1998; Inoue et al., 2000; Kuchroo et al., 2008) resulting in activation of transcription factors (TFs) such as NF-κB and AP-1 (Georgopoulos et al., 2006). To date, seven TRAF proteins have been identified and different TNFRs rely on distinct signalling pathways mediated by different TRAFs following receptor activation (Wajant and Scheurich, 2001; Wajant et al., 2001a; Zapata et al., 2001).

The third group of TNFRs is characterised by the lack of intracellular signalling function, due to the lack of an ICD in their cytoplasmic region. Yet, by maintaining the capacity to bind to TNFLs, these receptors act as decoy receptors and attenuate TNFR signalling (Zhan et al., 2011). The best characterised receptors of the third group are the TRAIL decoy receptors TRAIL-R3 (DcR1) and -R4 (DcR2) (Ashkenazi, 2002; Hehlgans and Pfeffer, 2005).

1.7 Death receptors

Death receptors (DRs) refer to unique sensor expressed within the cell surface. They are defined as CRD, and additionally contains homologous intracellular cytoplasmic sequence known as classical death domain (DD). DD is a potential receptor function to transmit the death signals from extracellular to intracellular causing cell apoptosis following the activation and recruitment of various proteins such as the TNFR-associated DD (TRADD) for TNFR-I and Fas-associated DD (FADD) for Fas and TRAIL-Rs TNFR-associated DD (TRADD) (Ashkenazi and Dixit, 1998). DD permits signalling initiation via adaptor protein recruitment following receptor activation. The existence of the DED permits induction of apoptotic signalling via recruitment of DED-comprising, initiator pro-caspases, in particular caspase-8 and in some cases involve the activation of caspase-10 (Dempsey et al., 2003; Engels et al., 2005; Micheau and Tschopp, 2003). The recruitment of these proteins form a complex called a death-inducing signalling complex (DISC) (Boldin et al., 1996; Debatin and Krammer, 2004; Muzio et al., 1996; Wang et al., 2001a). Once the caspase-8 is activated, the execution pathway of apoptosis is triggered by the activation of caspase 3 and 7 which results ultimately in apoptosis (Figure 1.4). However, in some conditions, apoptosis can be inhibited by cellular FLICE-inhibitory protein (c-FLIP) binding to FADD and caspase-8, preventing their function. It has been also shown that a potential protein known as Toso is able to block Fas-induced apoptosis in T lymphocytes via the inhibition of caspase-8 processing (Hitoshi et al., 1998; Kischkel et al., 1995; Scaffidi et al., 1999).

1.7.1 TNFRI and TNF-α ligand

TNF-α, the main ligand for the TNFR –I and –II receptors (where it can activate multiple signalling transduction pathways (Vilcek and Lee, 1991), is the archetypal pro-inflammatory cytokine and is a highly pleiotropic factor that plays critical roles in a variety of physiological mechanisms (Aggarwal, 2000; Beutler and Cerami, 1989). TNF-α is either secreted or maintained as a membrane-bound ligand by various immune and non-immune cell types including natural killer cells (NK), neutrophils, macrophages, monocytes, T cells, mast cells and granulocytes, as well as neurons, keratinocytes, smooth muscle cells, fibroblasts, endothelial cells and some malignant non-lymphoid cell lines (Aggarwal, 2000) (Table 1.2). An intriguing feature of the TNF-α/TNFR-I/II system is that differential receptor expression and/or receptor activation by TNF-α can regulate the balance between cell survival and apoptosis (Cabal-Hierro and Lazo, 2012).

Previous studies demonstrated that membrane-bound TNF-α induces stronger signalling via TNFR –I and –II than via its soluble counterpart, which can fundamentally alter the functional outcome of receptor activation (Ardestani et al., 2013b; Grell et al., 1995). Therefore, TNF-α exhibits both cell type- and context-specificity and TNF-α-mediated signalling can have highly pleiotropic effects. TNFRs –I and –II are mainly activated by TNF-α although receptor ligation can be induced by soluble LTα3 (due to its highly homologous structure to TNF-α) and by LTα2β1 (Williams-Abbott et al., 1997). TNFR-I is constitutively expressed on most nucleated cell types but is predominantly found on cells of epithelial and fibroblast origins (Armitage, 1994). Overall, TNFR-I has a greater abundance than TNFR-II, with TNFR-II mainly expressed on monocytic, lymphocytic, myeloid, hematopoietic, endothelial and neuronal cells (Grell et al., 1998; Hohmann et al., 1989; Tartaglia et al., 1993; Tartaglia et al., 1991). During inflammation, both TNFR-I and TNFR-II receptors can be quickly shed into soluble receptors believed to be important in down-regulating the inflammatory effects of TNF-α and these sTNFRs have been detected in human urine and blood serum of cancer patients (Engelmann et al., 1990; Idriss and Naismith, 2000; MacEwan, 2002).

Activation of TNFR –I and –II induces distinct signalling pathways; for instance, it has been demonstrated that the stimulation of individual TNFR –I or –II on mouse thymocytes and cytotoxic T cell line CT-6 by murine TNF (but not human TNF) induced differential effects in these cells (Tartaglia et al., 1991). Agonistic antibodies specific for TNFR-I caused cytotoxicity whereas antibodies for TNFR-II failed to reciprocate this. Moreover, TNFR-II stimulation triggered cell proliferation (Tartaglia et al., 1991).

Through its DD and TRADD, TNFR-I activation can activate the caspase-mediated pathway of apoptosis in numerous tumour cell lines (Andera, 2009; Ashkenazi and Dixit, 1998; Chinnaiyan et al., 1995; Gommerman and Summers deLuca, 2011; Hagemann et al., 2007; Nagata, 1997) (Figure 1.4). Activation of TNFR-I by TNF-α also induces the activation of NF-κB (Legler et al., 2003; Micheau and Tschopp, 2003) and this is a negative regulator for apoptosis mediated by TNFRs signalling (Karin and Lin, 2002; Ware, 2005). It has been shown that cell death could be augmented by the inhibition of NF-κB after TNF-α treatment (Karin and Lin, 2002; Varfolomeev and Ashkenazi, 2004) or the specific activation of TNFR-II (Wajant et al., 2003).

Pham and colleagues further demonstrated soluble TNF-α-induced apoptosis in NF-κB-deficient cells (Pham et al., 2004) which was due to JNK activation (Davis, 1998; Karin, 1998). TNFR-I also contains a TIM domain which interacts with TRADD, TRAF1 and TRAF2 and this triggers the activation of receptor interacting protein kinase (RIP). RIP and TRAF2 form a complex with TRADD in order to induce either MAPKs which lead to NF-κB, or c-Jun N-terminal kinase (JNK/AP-1) activation (Hehlgans and Pfeffer, 2005). RIP is a critical player that participates in various biological processes for intracellular and extracellular stresses and is found to stimulate TNF-induced apoptosis and necrosis (Hsu et al., 1996b; Kelliher et al., 1998; Lin et al., 2004; Zhang et al., 2010).

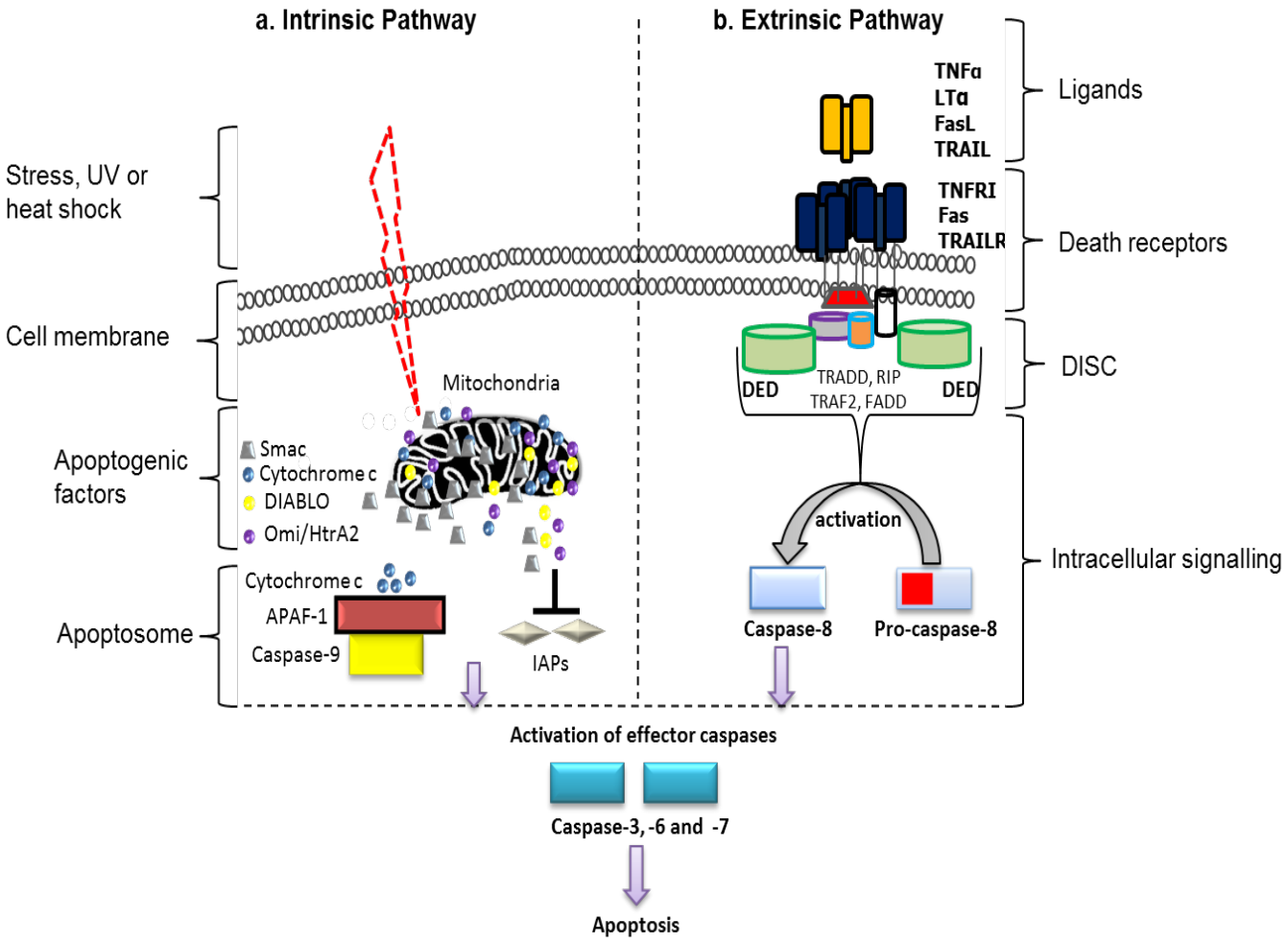

Figure 1.4. Schematic representation of the intrinsic and extrinsic pathways

This figure shows the two main mechanisms of apoptosis; intrinsic and extrinsic pathways. Each pathway is mediated by specific caspases, such as initiator caspases (8, 9, and 10) which lead to the activation of the executioner caspases. a, intrinsic pathway is initiated by cellular stress such as ultraviolet (UV) irradiation, chemotherapeutic or growth factor withdrawal. The cellular stress causes MOMP and promotes the release of cytochrome c, which subsequently interacts with Apaf-1 and triggers procaspase-9 activation. This results in the activation of procaspase-3, which leads to the activation of executioner pathway as well as apoptosis. b, extrinsic pathway is mediated by the activation of caspase-8, following activation of death receptors such as TNFRI, Fas or TRAIL-R. Consequently, death-inducing signalling complex (DISC) is formed and procaspase-8 is activated, which leads to the activation of other caspases such as, caspases-3, -6 and -7. Once activated, the extrinsic and intrinsic pathways converge at the executioner pathway which ultimately leads to cell changes including, cell shrinkage, chromatin condensation, and also membrane cytoplasmic bleb formation as well as apoptotic bodies. Figure modified from (de Vries et al., 2006).

1.8 Non-DD-containing TNFRs receptors

These receptors include TNFRII, CD40 and LT receptors that are discussed in depth in this chapter. Non-DD receptors have a lack of death domains and mediate their intracellular pathways via a domain known as the TRAF-interacting motif (TIM), which directly binds or interacts with specific TRAF proteins (Dempsey et al., 2003; Xie, 2013).

1.8.1 TRAF proteins

TRAFs are typically adaptor proteins that are characterised structurally by two domains the carboxyl-terminal half of the TRAF domain (highly conserved) known as TRAF-C (which functions to interact with TNFRs, forming homo- or heterodimers, or interaction with other signalling proteins) and a less conserved coiled-coil domain known as N-terminal portion (mostly consists of a RING finger and several zinc finger motifs that function to downstream signalling events) (Xie, 2013; Yang and Sun, 2015). To date, seven members of TRAFs have been identified and six are well described (TRAF1 to 6). A novel protein TRAF7 (it does not contain a TRAF homology domain) (Xu et al., 2004) (Figure 1.5). TRAF2, 3, 5 and 6, but not TRAF1, possess E3 ubiquitin ligase activities (Deshaies and Joazeiro, 2009; Ha et al., 2009; Häcker et al., 2011; Xie, 2013). They can induce downstream signalling of several kinases (such as the activation of NF-κB, AP-1, p38, JNK and other MAPKs), which can ultimately control and regulate cellular processes ranging from cell survival to cell death (Albarbar et al., 2015).

1.8.1.1 TRAF1

TRAF1 is a unique protein. It shares the structural features with other TRAFs that consist of a C and N-terminal, however, TRAF1 lacks both areas of zinc fingers and zinc ring in C-rich associated with RING and TRAF (CART) domains (Bradley and Pober, 2001) (Figure 1.5). TRAF1 has a restricted tissue distribution and its expression is upregulated by TNFLs/TNFRs interactions (Georgopoulos et al., 2006; Schwenzer et al., 1999). TRAF1 or TRAF2 triggers the activation of RIP. RIP and TRAF2 form a complex with TRADD in order to induce either MAPKs which may lead to NF-κB or JNK/AP-1 activation (Georgopoulos et al., 2006; Hehlgans and Pfeffer, 2005).

1.8.1.2 TRAF2

TRAF2 and TRAF1 were discovered as TNRFII-interacting proteins (Rothe et al., 1994; Rothe et al., 1995). Unlike TRAF1, TRAF2 contains of C-terminal TRAF domain as well as a zinc finger domain with a variable number of zinc fingers like other TRAFs (Ha et al., 2009) (Figure 1.5).

In terms of the functional role of TRAF2, it is reported that TRAF2 can regulate two distinct pathways of kinase cascades that contribute ultimately to the activation of NF-κB and MAPK, such as JNK (Jobin et al., 1999; Rothe et al., 1995). One finding reports NF-κB to be not activated but JNK activation was massively inhibited in transgenic mice following using dominant negative TRAF2 (Lee et al., 1997), but other studies demonstrate that TRAF2 plays a critical role in activation of inhibitor of kappa B kinase (IKK) and stress-activated protein kinases (SAPKs), JNK and p38 (Arch et al., 1998; Park et al., 2000).

1.8.1.3 TRAF3

TRAF3 is also known as CD40bp, LAP-1 or CRAF1 and was first described by several groups as an adaptor protein that binds to the cytoplasmic tail of CD40 and Epstein-Barr virus (latent membrane protein-1 (LMP-1) (Cheng et al., 1995; Hu et al., 1994; Kuhné et al., 1997; Mosialos et al., 1995; Sato et al., 1995a) (Figure 1.5). Studies reported that the C-terminal cytoplasmic domain of TRAF3 contains binding sites that is able to interact with other TRAF proteins, such as TRAF1, 2 and 5, which mediates EBV induced B cell proliferation and the activation of NF-κB (Izumi et al., 1999). Many studies report that TRAF3 is important for the induction of cell death, and mainly by CD40 (Eliopoulos et al., 1996; Georgopoulos et al., 2006). It is also reported that TRAF3 is recruited following the activation of LTβR that in turn inhibits the activation of NF-κB and results in the induction of cell death (VanArsdale et al., 1997), which was confirmed by a subsequent study which demonstrated that a dominant negative mutant of TRAF3 inhibits cell death that is triggered by LTβR signalling (Force et al., 1997).

1.8.1.4 TRAF5

TRAF5, TRAF1, TRAF2 and TRAF3 share binding to the same receptors (Figure 1.5). TRAF5 was discovered as an adaptor protein that can bind to CD40 and LTβR (Ishida et al., 1996a; Nakano et al., 1996). TRAF5 has been further investigated with other members of TNFRs and found to be implicated in NF-κB activation by CD27 and CD30 signalling (Aizawa et al., 1997; Akiba et al., 1998). A study demonstrated that overexpression of full-length TRAF5 in HEK392 cells (a human embryonic kidney cells) led to the activation of transcription factor NF-κB (Nakano et al., 1996).

1.8.1.5 TRAF6

TRAF6 shares structural similarities with TRAF4 (Figure 1.5), but both TRAF6 and TRAF4 are divergent from TRAF1, 2, 3 and 5 (Inoue et al., 2000). Based on crystallographic studies, the binding site of TRAF6 is different to other TRAFs and may interact with distinct peptides (Wong et al., 1998).

TRAF6 was first identified in 1996 as a signal transducer for IL-1 (Cao et al., 1996). It is reported that overexpression of TRAF6 activates NF-κB, JNK and p38 (Song et al., 1997). TRAF6 interacts with CD40, receptor activator of nuclear factor-kB (RANK), TNFR-II and nerve growth factor (NGF) receptors (Darnay et al., 1999; Galibert et al., 1998; Ishida et al., 1996b; Khursigara et al., 1999; Tsukamoto et al., 1999; Wong et al., 1998).

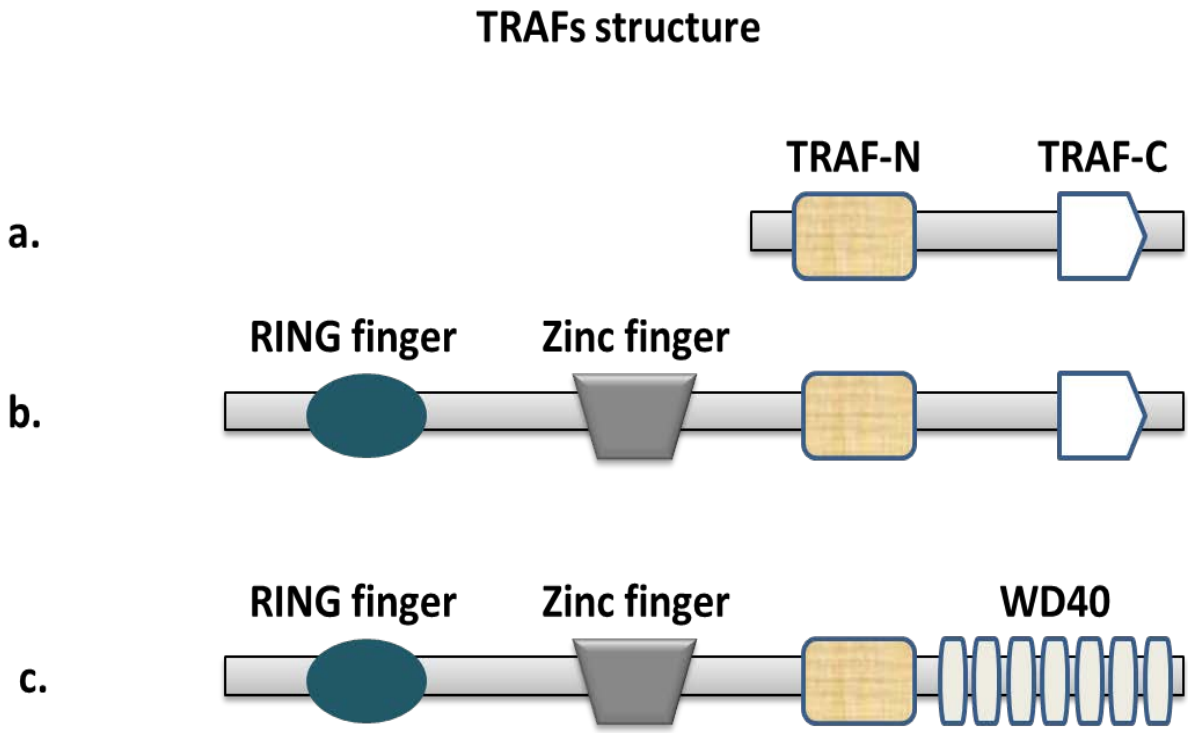

Figure 1.5. Structural organisation of TRAFs

TRAFs comprise the carboxyl-terminal of the TRAF domain (TRAF-C), a coiled-coil domain known as N-terminal portion (TRAF-N), zinc finger and RING finger motifs. a, TRAF1 domain organisation. b, TRAF2, 3, 4, 5 and 6 organisation. c, TRAF7 contains a RING finger domain, a zinc finger domain and also contains seven WD40 repeats instead of the archetypical C-terminus. Figure modified from (Zotti and Vito, 2012).

1.8.2 Mitogen-activated protein kinases (MAPKs)

Cells respond to extracellular stimuli (such as growth factors, cytokines and cell damaging agents) by triggering intracellular signalling cascades, and in response to these stimuli, TRAFs are recruited and relocated to membrane lipid rafts and subsequently MAPKs cascades are activated. MAPKs are components of intracellular pathways that regulate a number of cellular activities and are involved in regulation of gene expression, cell differentiation, cell survival and cell death (apoptosis) (Kim and Choi, 2010). Four subgroups of MAPKs have been identified in mammals: a) Extracellular signal-regulated kinases (ERK1 and ERK2); b) c-Jun amino-terminal kinases or stress-activated protein kinases (JNKs/SAPKs) (including JNK1, 2 and 3); c) p38 (isoforms α, β, γ and δ) and d) ERKs 3, 4 and 5 (Cargnello and Roux, 2011; Low and Zhang, 2016; Roux and Blenis, 2004).

1.8.2.1 ERK1/ERK2

ERK1 and 2 represent the classical mitogen kinase cascade signalling axis that consists of MAPK kinase kinases (MAPKKKs) such as A-Raf, B-Raf, Raf-1, MAPKKs (e.g. MEK1 and MEK2) which feeds into the MAPKs; ERK1 and ERK2 (Cargnello and Roux, 2011) (Figure 1.6). Briefly, following the extracellular stimulus, signals are transmitted by cell surface receptors, such as tyrosine kinases (RTK) and G protein-coupled receptors (GPCR), which transmit the activating signal through various isoforms of the small GTP-binding protein known as Ras to MAPKs Raf, MEK and ERK pathways (Campbell et al., 1998; Geyer and Wittinghofer, 1997; Wood et al., 1992) as reviewed elsewhere (Chong et al., 2003; Geyer and Wittinghofer, 1997). Once Raf is activated by Ras (proto-oncogene), it binds and phosphorylates MEK1 and 2, which in turn phosphorylates ERK1 and 2 through their conserved Thr-Glu-Tyr (TEY) motif (Hallberg et al., 1994). It is reported that MEK1 and 2 are specific for ERK activation (Figure 1.6) (Kyriakis and Avruch, 2012). Upon phosphorylation, a significant population of ERK1 and 2 translocates to the nucleus (Chen et al., 2001; Gonzalez et al., 1993; Lenormand et al., 1993; Pouysségur et al., 2002).

Activated ERK1 and 2 trigger the phosphorylation of a number of substrates in cellular compartments including membrane proteins (e.g. CD120a and calnexin), cytoskeleton proteins (e.g. paxillin and neurofilaments) and nuclear substrates (e.g. SRC-1 and c-Myc) (Chen et al., 2001).

1.8.2.2 JNK

The c-Jun NH_2-terminal kinase (JNKs) were first identified and isolated from rat livers treated with cycloheximide (Kyriakis and Avruch, 1990). JNK has three isoforms; JNK1 (SAPKγ), JNK2 (SAPKα) and JNK3 (SAPKβ). With the exception of JNK3, all JNKs are expressed ubiquitously, whereas JNK3 mainly presents in the brain and heart (Kyriakis and Avruch, 2001; Roux and Blenis, 2004). It has been demonstrated that JNKs are robustly activated by stimuli such as cytokines, UV, DNA-damaging chemicals, growth factors and G protein-coupled receptors (Roux and Blenis, 2004). It was found that JNK has a short from expressed at MW 46kDa and a long form expressed at MW 54kDa (Pulverer et al., 1991).

Like other kinases, ERK1, ERK2 and p38, JNK is activated by dual phosphorylation at tyrosine and threonine within the conserved Thr-Pro-Tyr (TPY) motif that is catalysed by MEK4 (also known as MKK4, SEK1, JNKK1 and SAPK-kinase 1) and MEK7 (also known as MKK7, JNKK2 and SKK4). MEK4 and 7 are phosphorylated by various MAPKKKs (e.g. MEKK1-4, MLK2 and 3, DLK, TAK1 and ASK1 and 2 (Kyriakis and Avruch, 2001) (Figure 1.6). It is reported that MEK4, but not MEK7, can also activate p38, whereas MEK7 phosphorylates all isoforms of JNKs (Kyriakis and Avruch, 2012). Once JNK is activated, JNK phosphorylation leads to the activation and phosphorylation of transcription factor AP-1 and related genes (c-Jun, JunD and ATF2) (Karin et al., 1997).

JNK cooperates with p38 and regulates several physiological processes, such as cell proliferation, cell survival and apoptosis (Dhanasekaran and Johnson, 2007). For example, activation of CD40 and Toll-like receptor 7 (TLR7) lead to the activation of JNK that enhances IL-6 secretion, which is crucial for B cell responses (Bush and Bishop, 2008). In mouse model studies, it has been shown that deficiency in JNK severely decreases susceptibility to diethylnitosamine-induced hepatocarcinogenesis (Sakurai et al., 2006). Other studies suggest that JNK can enhance tumour cell growth and can also act as anti-tumour target (Papachristou et al., 2003; Yang et al., 2003; Zenz and Wagner, 2006). Previous studies reported that JNK is activated in cell death triggered by chemotherapy drugs (Davis, 2000; Hayakawa et al., 2004; Potapova et al., 2001).

1.8.2.3 p38 MAPKs

p38 MAPKs were identified when first isolated as a protein with MW 38kDa that was quickly phosphorylated in response to lipopolysaccharide (LPS) (Han et al., 1993; Han et al., 1994). p38 MAPKs (also termed as CSBP, mHOG1, RK, SAPK2 and p40) are activated by cellular stress or extracellular stimuli (Han et al., 1994; Lee et al., 1994). p38 has four isoforms: p38α, p38β, p38γ and p38δ (Cuenda and Dorow, 1998; Jiang et al., 1996; Kumar et al., 1997; Lechner et al., 1996; Li et al., 1996) (Figure 1.6). p38 has multifunctional activities and participates in mediating T cell differentiation and apoptosis by controlling the production of IFN-γ (Ono and Han, 2000). It is also reported that p38 maintains specific cellular mRNAs that are involved and important for immune responses (Ono and Han, 2000).

p38 is activated by MEK3 and 6 (which is activated by MAPKKKs) (Figure 1.6). MEK3 and 6 are activated by physical or chemical stimuli, such as TNF-α or UV irradiation. MEK3 and 6 are specific for p38 activation (Cargnello and Roux, 2011). MEK6 phosphorylates all p38 isoforms, whereas MEK3 preferentially activates p38α and β (Chen et al., 2001). Activation of p38 is as a result of MEK3 and 6 phosphorylation at a conserved threonine and tyrosine (Thr-Gly-Tyr (TGY) motif residues (Enslen et al., 2000).

p38 is the best studied MAP kinase and was found to be expressed in most cell types and present in cytoplasm and nucleus. However, following stimulation, one study suggests that active p38 translocates from the cytoplasm to the nucleus (Raingeaud et al., 1995) and another study reported that active p38 is also present in the cytoplasm (Ben-Levy et al., 1998).

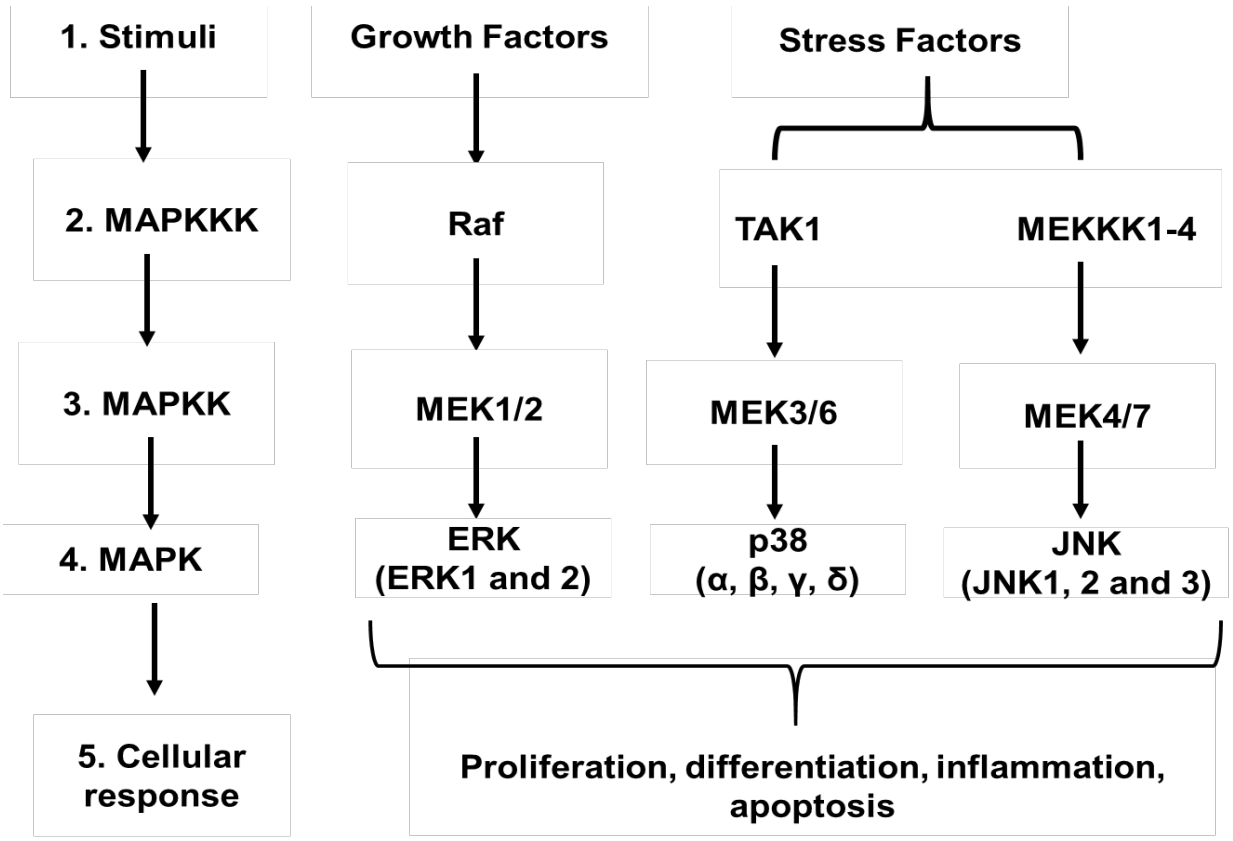

Figure 1.6. Simplified schematic representation of MAPK signalling pathway

(1) An extracellular stimulus (e.g. growth factors or stress factors) activates (2) MAPKKK such as Raf1, TAK1 and MEKKK1-4, MAPKKK phosphorylates and activates (3) MAPKK (MEK1/2, MEK3/6 and MEK4/7), which phosphorylates and activates (4) MAPK (ERK1/2, p38 and JNK), leading to (5) various cellular biological response. Modified from (Kim and Choi, 2010).

1.8.3 Transcription factors (TFs)

TFs are central components in a number of signalling pathways that control gene expression and their activation is triggered by several physiological and environmental stimuli (Baldwin Jr, 1996; Pahl, 1999). TFs can be involved in many physiological processes e.g. inflammation, development, differentiation, oncogenesis and cell death (Li and Verma, 2002; Shaulian and Karin, 2002).

The activation of TFs is often regulated by phosphorylation or dephosphorylation via the involvement of several intracellular signalling pathways. Such as two very well-characterised TFs are AP-1 and NF-κB (Collins et al., 2000; Devary et al., 1993; Yasumoto et al., 1992).

1.8.3.1 AP-1

AP-1 is a family of proteins of homotrimers and heterodimers, which are comprised of basic region-leucine zipper (bZIP) proteins that are main components for Jun (c-Jun, JunB and JunD) Fos (c-Fos, FosB, Fra-1 and Fra-2), Jun dimerization partners including JDP1 and JDP2 and other members, such as ATF2, LRF1, ATF3 and B-ATF (Johnson and Nakamura, 2007). Jun proteins can form a stable dimeric complex that is able to bind to AP-1 DNA recognition site known as TREs (Shaulian and Karin, 2002). Evidence suggests that proteins of the Fos sub-family are not able to form a complex directly, but they indirectly form heterodimers with Jun proteins resulting in DNA binding, (previously reviewed (Shaulian and Karin, 2002). It is reported that AP-1 regulates cell cycle controlling Cyclin D1 (Cyclin D1 is a protein involved in cell cycle regulation and it is important for the initiation and transition of G1 to G1/S phase, respectively) (Baldin et al., 1993), p53, p21, cell proliferation, cell survival and cell death (Shaulian and Karin, 2001). c-Jun of AP-1 is activated following JNK activation (Biswas et al., 2006).

Most cells contain the predominant form of AP-1 heterodimers Fos/Jun that bind to the AP-1 site with high affinity, whereas other forms of homodimers Jun/Jun bind to the AP-1 site with less affinity (Ransone and Verma, 1990; Shaulian and Karin, 2002). The induction of AP-1 is initiated by the activation of ERK subgroup of MAPKs that translocates to the nucleus (Cavigelli et al., 1995; Hipskind et al., 1994; Rao and Reddy, 1994; Shore and Sharrocks, 1994; Wang and Prywes, 2000). Members of transcriptional factor AP-1, such as Fos, FosB and others, are regulated in their promoters mainly by serum responsive elements (SREs) (Sassone-Corsi and Verma, 1987; Verma and Sassone-Corsi, 1987).

1.8.3.2 NF-κB

NF-κB was identified in 1986 as a factor in the nucleus that binds the promoter of the kappa chain of immunoglobulins in B cells (Aggarwal, 2004). NF-κB is a nuclear transcription factor that regulates expression of a number of genes and plays essential roles in inflammation, apoptosis, tumourigenesis and various autoimmune diseases (Davies et al., 2005a). NF-κB consists of a family of proteins including: NF-κB1 (p50/p105), NF-κB2 (p52/p100), RelA (p65), RelB, and c-Rel. NF-κB family proteins that share similarity in possessing highly conserved Rel (is a proto-oncogene and one of NF-κB subunits) homology domain (RHD; ~300 aa) with bi-functional roles, are responsible for DNA binding and for interacting with IκB (intracellular inhibitor of NF-κB). NF-κB is present in the cytosol of cells as an inactive protein bound to its inhibitor IκBs, but during stress or any stimulus NF-κB is activated and causes the phosphorylation for IκB and ultimately degradation, which results in NF-κB gene translocation to the nucleus (Baldwin Jr, 1996; Bonizzi and Karin, 2004). NF-κB is the best studied TF and is a critical transcriptional activator of many genes involved in innate and adaptive immunity, inflammatory responses, as well as development and maintenance of the immune system (Bonizzi and Karin, 2004; Ghosh and Karin, 2002; Karin and Greten, 2005).

The NF-κB participates in two pathways; the classical (canonical) and alternative (non-canonical). In the context of the TNFSF, the canonical pathway often mediates inflammatory responses, while the non-canonical pathway is involved in immune cell proliferation, maturation and is responsible for secondary lymphoid organogenesis and previously reviewed (Ghosh and Karin, 2002; Hayden and Ghosh, 2008; Sun, 2010; Vallabhapurapu and Karin, 2009).

1.9 The TNFR-II and TNF-α system

TNFR-II binds to mTNF-α with high affinity, thus it has been suggested that there must be cell-cell contact in order for TNF-α to activate TNFRII effectively (Goetz et al., 2004; Grell et al., 1995). TNFR-II also recruits TRAF1 and TRAF2, and the latter plays a critical role in activation of IKK and stress kinases JNK and p38 (Arch et al., 1998; Park et al., 2000) (Table 1.2). Activation of these is regulated by reactive oxygen species (ROS) release, which can occur either from nicotinamide adenine dinucleotide phosphate-oxidase (NADPH or NOX) or following mitochondrial disruption (Devin et al., 2003; Hsu et al., 1996a; Hsu et al., 1995; Hsu et al., 1996b; Stanger et al., 1995; Westwick et al., 1994).

More recently, mTNF-α was shown to be highly cytotoxic to carcinoma cells due its ability to cause ROS-mediated necrosis (Ardestani et al., 2013a). Interestingly, it was confirmed that apoptosis was driven by mTNF-α-mediated ligation of TNFR –II and not –I (Ardestani et al., 2013a; Ardestani et al., 2013b) (Figure 1.7).

1.10 The CD40 and CD40L system

CD40 was first functionally characterised in B cells (although originally identified as an antigen expressed in bladder carcinomas) and was found to share homology with NGFR (Stamenkovic et al., 1989). CD40 is a type I transmembrane protein with a MW 40-45kDa and is constitutively expressed on activated T cells, B cells, dendritic cells (DCs), antigen presenting cells (APCs), but also at low level on monocytes, platelets, as well as fibroblasts, epithelial, endothelial, neuronal cells and is also found to be expressed in a variety of carcinomas (Table 1.2) (Bourgeois et al., 2002; Kooten and Banchereau, 1997; Larsen and Pearson, 1997; Stamenkovic et al., 1989; Tan et al., 2002; Van den Oord et al., 1996).

The ligand of the CD40 receptor is CD40L (CD154), a type II transmembrane protein with MW between 31-39kDa (van Kooten and Banchereau, 2000) (Figure 1.7). CD40L is predominantly expressed on activated $CD4^+$ T cells and B cells, activated APCs (such as DCs) as well as platelets (Danese et al., 2003; Higuchi et al., 2002). The CD40/CD40L dyad is critical in cellular and humoral immune responses, and is essential for lymphocyte proliferation as well as differentiation and maturation (Korniluk et al., 2014). CD40/CD40L engagement mediates DC activation and the activated DCs promote the upregulation of other co-stimulatory molecules such as B7 family members which result potent production of pro-inflammatory cytokines in order to enhance productive immune responses (Table 1.2) (Yang and Wilson, 1996). The role of CD40L/CD40 interaction in humoral immunity for the production immunoglobulins such as IgA, IgE, IgG and IgM (Ma and Clark, 2009). The absence of CD40L/CD40 interaction results in severe defect in production of immunoglobulins IgA, IgE and IgG and causes patients with symptoms of hyper IgM syndrome (HIM) (Aruffo et al., 1993). The role of CD40/CD40L in immune system has been reviewed recently elsewhere (Elgueta et al., 2009; Korniluk et al., 2014).

One interesting characteristic of the CD40 system, is that receptor expression is not restricted only to normal cells but it is also expressed in both mouse and human in many cancers such as lymphocytic leukaemia, lymphoma, multiple myeloma, acute myeloid leukaemia (AML) as well as in both non-Hodgkin's lymphomas (NHLs) and Hodgkin's lymphomas (Aldinucci et al., 2002; Kato et al., 1998; Pellat-Deceunynck et al., 1996; Teoh et al., 2000). Moreover, CD40 is expressed on non-lymphoid cells where receptor engagement by CD40L contributes to cytokine and chemokine secretions and also can lead to fibroblast and endothelial cell proliferation (Dallman et al., 2003; Kawabe et al., 2011). Although CD40 expression is low on normal epithelial cells, it is often particularly highly expressed on solid tumours such as melanoma and lung cancers as well as in carcinomas of the nasopharynx, bladder, cervix and in ovarian cancer although it appears to be absent from prostate carcinomas (Agathanggelou et al., 1995; Altenburg et al., 1999; Cooke et al., 1999; Gallagher et al., 2006; Tan et al., 2002; Young et al., 1989) (Figure 1.7). The outcome of CD40/CD40L signalling ranges from proliferation and differentiation to growth inhibition and cell death in a cell type- and context-dependent manner (Korniluk et al., 2014). With regards to its function in tumour cells, CD40 ligation was found to have growth inhibitory effects in carcinoma cell lines of ovarian, breast, bladder (urothelial) and colorectal tumour cells *in vitro* when such cells were treated with a soluble form of CD40L or agonistic anti-CD40 antibodies (Bugajska et al., 2002; Georgopoulos et al., 2006; Jiang et al., 2008).

CD40 signalling starts with the recruitment of adaptor proteins, in particular, TRAF1, TRAF2, TRAF3, TRAF5 and TRAF6 (Gommerman and Summers deLuca, 2011). It has been shown that TRAF2, TRAF3 and TRAF6 bind directly to cytoplasmic tail of CD40 whereas TRAF1 and TRAF5 are recruited indirectly via interactions with TRAF2 and TRAF3, respectively (Bishop et al., 2007; Hauer et al., 2005; Pullen et al., 1999a; Pullen et al., 1998; Pullen et al., 1999b). Following TRAF recruitment, signalling cascades triggered include the p38 MAPK, AKT, JNK/AP-1, signal transducer and activator of transcription 5 (STAT5) pathways and the activation of canonical and noncanonical pathways of NF-κB. The activation of such cascades is dependent and attributed to the precise TRAF protein recruitment pattern (Albarbar et al., 2015). In B cells, for instance TRAF2 and MEKK1 recruitment activates the JNK, p38 mitogen activated protein kinase

(MAPK) and AKT pathways (Gallagher et al., 2006; Hostager et al., 2003; Lee et al., 1997), whereas TRAF5 and TRAF3, are found to be required for canonical and noncanonical pathways of NF-κB activation (Bishop et al., 2007; Hauer et al., 2005; Nakano et al., 1999).

Overall, a number of signalling and functional properties appear to be shared by CD40 with other members of TNFRs such as LTβR. It has been reported that these receptors are able to induce the maturation and immunogenic activity for DCs, and this is because they share similarities in activating adaptor proteins as part of their intracellular signalling, e.g. TRAF3 induction activates the noncanonical pathway (Moore and Bishop, 2005) (Figure 1.7). Previous studies also reported that LIGHT cooperates with CD40 in signalling that activates B cells (Duhen et al., 2004; Pasero et al., 2009a). Moreover, LIGHT cooperates with CD40L (CD154) resulting in DC maturation (Morel et al., 2001; Zou and Hu, 2005).

1.11 The Lymphotoxin system: receptors

1.11.1 LTβR

This receptor is mainly expressed on stromal fibroblasts, epithelial cells, monocytes, DCs and mast cells but is absent on lymphocytes (Browning et al., 1997; Stopfer et al., 2004) (Table 1.2).

1.11.1.1 Role of LTβR in the immune system

Expression of LTβR by stromal cells in the intestine is important for normal production of IgA after antigen recognition (Kang et al., 2002). Constitutive LTβR-mediated signalling leads to the development of autoimmune disease, including Sjogren's disease and experimental autoimmune encephalomyelitis (EAE). Moreover, $LT\alpha^{-/-}$ and $LT\beta R^{-/-}$ mice demonstrated a reduction in chemokine and adhesion molecule expression within lamina propria lymphocytes (Kang et al., 2002). Blocking of LT pathways in normal adult mice using soluble receptor-immunoglobulin fusion protein (LTβR-Ig) caused inhibition of splenic germinal centre formation and defective humoral responses (Mackay et al., 1997).

Thus, such studies using genetically modified mice indicate that LTβR is a key molecule involved in lymphoid organogenesis and in adaptive humoral immunity (Fütterer et al., 1998; Locksley et al., 2001; Mackay and Browning, 1998). LTβR is activated by three ligands; the two heterotrimeric LTαβ complexes and the homotrimeric LIGHT (Ware, 2005) (Figure 1.7). Two studies using a fusion protein to inhibit LTβR signalling through LTα1β2 and LIGHT attenuation, have also shown that LT receptors regulate the normal development lymph nodes of mice offspring (Fava et al., 2003; Rennert et al., 1996). More recent studies have indicated that little LTβR expression is found in normal human colon tissue and adenomas, but receptor expression is increased on colon adenocarcinomas (Hu et al., 2013), thus indicating that LT receptor expression may increase during carcinogenesis.

1.11.1.2 Role of LTβR in epithelial cells

Activation of the LTβR receptor *in vitro* by either LIGHT mutein (LIGHT-R228E – which is mutated form of LIGHT that preferentially interacts with LTβR over HVEM) or agonistic anti-LTβR antibody, induces chemokine (IL-8) secretion in HEK293 and 375 melanoma cells and inhibits the growth of 375 melanoma cells, and this appears to be due to differential modulation of the MAPKs signalling molecules ASK1, JNK1/2, AP1, and NF-κB (Chang et al., 2002; Chen et al., 2003; Degli-Esposti et al., 1997b; Hehlgans and Männel, 2001; Sabapathy et al., 2004; Tobiume et al., 2001). Unlike TNFRI which activates the canonical pathway of NF-κB, LTβR can activate both NF-κB pathways (Dempsey et al., 2003; Hehlgans and Pfeffer, 2005) (Table 1.2).

Lukashev et al. (2006) have previously demonstrated that agonistic multivalent pentameric anti-LTβR antibody CBE11 can reduce the growth of colon and cervical tumours *in vivo*. More recently, Hu et al. (2013) demonstrated that LTβR activation using LTβR agonistic antibody BS-1 was found to induce growth inhibition (as well as NF-κB activation) in colon carcinoma cell lines HT29 and CT26, mammary carcinoma 4T1 and soft-tissue sarcoma CMS4.

Moreover, BS-1 was able to trigger the activation of caspase -8 and -3 as well as the release of cytochrome c in tumour cells, all of which were mediated by LTβR activation (Hu et al., 2013). This provides evidence that cell growth inhibition of these tumour cells could be partially driven by caspase-dependent mechanism (Hu et al., 2013). The aforementioned study also reported that the activation of LTβR by using a different monoclonal anti-LTβR antibody (ACH6) suppressed the colon carcinoma metastasis *in vivo* (Hu et al., 2013). These findings are in support of previous work by Browning and colleagues demonstrating that anti-LTβR monoclonal antibody alone caused cell death *in vitro* (Browning et al., 1996). Therefore, signalling through LTβR either by its natural ligands or via agonistic anti-LTβR antibodies triggers cell death for a variety of tumour cell lines (Browning et al., 1996; Rooney et al., 2000).

In vivo studies involving the inhibition of tumour growth in mice deficient in LTα1β2 demonstrated the requirement for LTβR activation and signalling on the tumour cells by host cell-derived LTα1β2 (Hehlgans et al., 2002). The growth of colon and cervical carcinoma cell lines in xenograft models was shown to be inhibited by agonistic antibody LTβR (CBE11) and this potentiated tumour responses to chemotherapeutic treatment (Lukashev et al., 2006). *In vitro*, however, some contradictory findings have been reported, as the activation of LTβR with an agonistic LTβR antibody in melanoma cell lines (Hs294T, SKMel5, SKMel28, and WM115) leads to the activation of the NF-κB and enhances tumour cell proliferation (Dhawan et al., 2008). Mackay and colleagues reported that activation of LTβR with either soluble LTα1β2 or agonistic anti-LTβR antibody (CBE11) induced activation of NF-κB in HT29 and WiDr human adenocarcinoma lines and human lung fibroblasts WI-38 (Mackay et al., 1996), however, Browning et al. (1996) demonstrated that recombinant LTα1β2 together with IFN-γ were cytotoxic to an array of carcinoma cell lines, including HT29 and WiDr, breast adenocarcinoma cell line (MDA-MB-468) and cervical carcinoma (HT-3) cells

1.11.1.3 The LTβR signalling pathway

Signal transduction through LTβR involves recruitment of adaptor proteins such TRAF -2, -3, and -5 to the cytoplasmic tail of the receptor upon its ligation (Nakano et al., 1996; Rooney et al., 2000; VanArsdale et al., 1997) (Figure 1.7) and these interactions regulate TFs activation. TRAF2 and TRAF5 recruitment lead to NF-κB activation, but TRAF3 was found to be a negative regulator for NF-κB activation and associated with induction of cell death, as shown in the tumour cell line HT29 and in human embryonic kidney cells (HEK293T) (Force et al., 1997; Sanjo et al., 2010; VanArsdale et al., 1997). Their findings are in accordance with such an effect for TRAF3 in signalling triggered by other TNFSF members (Bechill and Muller, 2014; Hauer et al., 2005).

A study by Kim and colleagues also demonstrated using HeLa cells *in vitro* that TRAF2 and TRAF3 were recruited following the LIGHT/LTβR ligation and their recruitment led to the activation of NF-κB and JNK in HeLa cells (Kim, 2005). Bista and colleagues reported that TRAF3 functions as a pro-survival molecule during LTβR activation, through canonical and noncanonical NF-κB function. In fact, LTβR-induced signalling complexes enhanced TRAF3 recruitment, but decreased TRAF2 recruitment which attenuated the phosphorylation of Ikβα and RelA genes of NF-κB (Bista et al., 2010).

Triggering LTβR signalling in WI-38 cells was also found to activate NF-κB and induced cell proliferation, whereas, there was no observation of NF-κB activation in human umbilical vein endothelial cells (Chen et al., 2003; Dempsey et al., 2003). Another study has demonstrated that hepatocytes are LTβR responsive cells whilst the inhibition of LTβR in LTαβ transgenic mice with hepatitis suppresses the formation of hepatocellular carcinoma (Haybaeck et al., 2009).

Moreover, Chen and colleagues demonstrated using human hepatoma cells (Hep3BT2), HeLa and HEK293 cells that the activation of LTβR by using either LIGHT mutein (LIGHT-R228E) or agonistic monoclonal antibody anti-LTβR (clone 31G4D8) led to the recruitment of TRAF3 and TRAF5 and the production of ROS, which in turn activated ASK1 to induce caspase-dependent and caspase-independent LTβR-mediated death (Chen et al., 2003).

1.11.2 HVEM

This receptor is expressed by lymphoid and non-lymphoid cells, but primarily it is expressed transiently by NK cells and constitutively on naive $CD4^+$ and $CD8^+$ T cells (Table 1.2), and it binds to two ligands LIGHT and LTα (Fan et al., 2006; Kwon et al., 1997; Sedy et al., 2004; Ware, 2005) (Figure 1.7).

1.11.2.1 Role of HVEM in the immune system

HVEM has dual roles acting both as receptor and as a ligand and it was first described as a receptor for herpes simplex virus-1 (HSV-1) glycoprotein D (HSV-gD), the main component of the HSV envelope for entry into human and mouse cells (Montgomery et al., 1996; Spear et al., 2006). HVEM functions as ligand and binds the immunoglobulin (Ig) superfamily members, B and T lymphocyte attenuator (BTLA), and CD160 (glycosylphosphatidylinositol-anchored member of immunoglobulin (Ig) domain protein), and is expressed by many immune cells (Šedý et al., 2014). Two studies found that BTLA and CD160 bind to the first cysteine-rich domain at the N-terminus of HVEM, compared with LIGHT, which most likely binds to the second and third cysteine-rich domains on the opposite face (Cai et al., 2008; Compaan et al., 2005).

However, other studies reported that soluble LIGHT binds to HVEM without binding to BTLA, and also found that soluble LIGHT and LTα can enhance the binding of BTLA with HVEM forming a trimolecular complex (Cheung et al., 2005; Gonzalez et al., 2005). Cai and colleagues reported that HVEM is critical for T cell activation depending on the engagement of HVEM with CD160 and BTLA as well as T lymphocytic LIGHT.

CD160 also functions as a negative regulator of $CD4^+$ T cell activation via the interaction with HVEM receptor (Cai et al., 2008). The binding of LIGHT to HVEM-expressing T cells *in vitro* acts also as a co-stimulatory signal for their activation, proliferation and cytokine secretion via NF-κB activation. Other studies also found that blocking the interaction of LIGHT and HVEM by using HVEM-Ig inhibited proliferation of T cells (Harrop et al., 1998a; La et al., 2002; Wang et al., 2001b). Moreover, the differentiation of effector cells T helper cell 2 (Th2) and (Th1) into memory cells depends on the LIGHT and HVEM signaling (Soroosh et al., 2011).

1.11.2.2 Role of HVEM expression in carcinoma

It is reported that in most B cell malignancies including B-chronic lymphocytic leukaemia (B-CLL), mantle cell lymphoma, acute lymphoblastic leukaemia (ALL) and Burkitt's lymphoma express HVEM. HVEM is also expressed by all primary myeloma cells and in plasma cell leukaemia (Costello et al., 2003) (Table 1.2).

It has been demonstrated that engagement of soluble LIGHT with HVEM-expressing U937 cells induced a weak increase in NF-κB activity (Harrop et al., 1998b). Overexpression of HVEM in 293 cells enhances the recruitment of adaptor proteins, TRAF -1, -2, -3, and -5, which result in activation of NF-κB and AP-1 (Hsu et al., 1997; Marsters et al., 1997b). By contrast, other studies demonstrated that HVEM activation more likely recruits TRAF2 and TRAF5, which are key mediators for the activation of NF-κB as well as AP-1 (Kim, 2005; Kuai et al., 2003; Marsters et al., 1997b; Nakano et al., 1996).

Pasero and colleagues demonstrated that LIGHT-mediated HVEM signalling is able to induce cell death in freshly isolated B-CLL tumour cells, while LTβR was not expressed or expressed at low levels. The mechanisms responsible for cell death in the B-CLL tumour cells related to expression of FasL, p53, Bax, Bid, Bcl-Xs and mitochondrial cytochrome c release (Pasero et al., 2009b).

Interestingly, it was found that broad caspase inhibition via z-VAD-FMK did not prevent apoptosis, suggesting that both intrinsic and extrinsic pathways of apoptosis were active (Gross et al., 1999; Korsmeyer et al., 1994; Pasero et al., 2009b). This data suggests that despite the co-stimulatory and co-inhibitory role for HVEM during immune regulation, HVEM could in fact function as a tumour suppressor if utilised in the correct context. However, there is evidence to suggest that the way HVEM modulates cell fate might be indirect and more complex than the aforementioned studies suggested (Bechill and Muller, 2014).

1.11.3 DcR3

Decoy receptor 3 (DcR3) is a secreted protein which is closely related to osteoprotegerin (which is a member of TNFRSF) (Simonet et al., 1997) and is classified as a TNFRSF member which can bind to several TNFLs, such as LIGHT, FasL and TL1A (Migone et al., 2002; Pitti, 1998) (Table 1.2). Reports demonstrated that DcR3 is expressed in some normal tissues including colon, stomach, spleen, lymph node and lung (Hsu et al., 1996b; Pitti, 1998) and interestingly it is found in serum of rheumatoid arthritis patients. DcR3 is also overexpressed in tumours, such as those derived from primary lung, colon (SW480), gastrointestinal and hepatocellular, and its overexpression might help tumour growth by neutralization of the cytotoxicity and regulatory effects of LIGHT, Fas and TL1A (Migone et al., 2002; Pitti, 1998; Yu et al., 1999) (Figure 1.7).

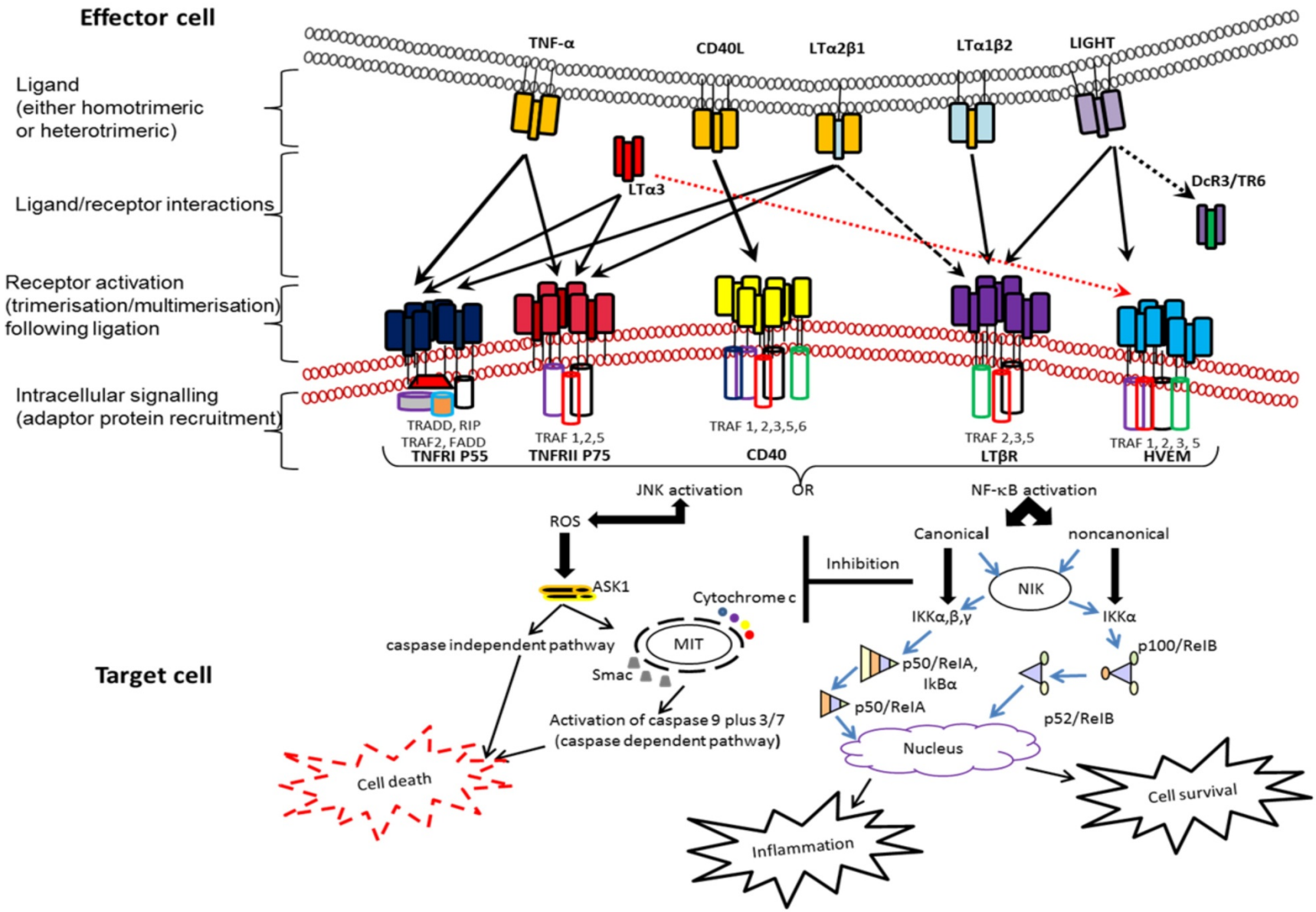
Effector cell
Ligand
(either homotrimeric
or heterotrimeric)
Ligand/receptor interactions
Receptor activation
(trimerisation/multimerisation)
following ligation
Intracellular signalling
(adaptor protein recruitment)
TNF-α
CD40L
LTα2β1
LTα1β2
LIGHT
LTα3
DcR3/TR6
TRADD, RIP
TRAF2, FADD
TNFRI P55
TRAF 1,2,5
TNFRII P75
TRAF 1, 2,3,5,6
CD40
TRAF 2,3,5
LTβR
TRAF 1, 2, 3, 5
HVEM
OR
JNK activation
ROS
ASK1
caspase independent pathway
Cytochrome c
MIT
Smac
Activation of caspase 9 plus 3/7
(caspase dependent pathway)
Cell death
NF-κB activation
Canonical
noncanonical
Inhibition
NIK
IKKα,β,γ
IKKα
p100/RelB
p50/RelA,
IkBα
p50/RelA
p52/RelB
Nucleus
Cell survival
Inflammation
Target cell

Figure 1.7. TNF and LT associated intracellular signalling pathways

Schematic representation of TNFL and TNFR interactions and associated signalling, with the upper portion showing TNFL expression by an effector cell and lower portion showing TNFR expression by target cell. TNFα can be both either membrane-bound or secreted and binds to and activates TNFRI and TNFRII, whereas LTα3 exists in soluble homotrimeric form. LTβ is not shed into soluble form and can bind with LTα to form LTαβ complexes. Heterotrimeric LTα1β2 binds LTβR and LTα2β1 binds with TNFRI, TNFRII as well as LTβR. LIGHT binds LTβR and HVEM as well as soluble receptor DcR3. Arrows indicate high affinity interactions, the dotted red arrow indicates possible binding and the dashed lines indicate binding with low affinity. TNFR-mediated signalling is triggered via intracellular proteins associating with either the death domain (as for TNFRI) or a TRAF binding motif (as for CD40, LTβR). Members of the TRAF family are indicated: TRAF1 (purple), TRAF2 (black), TRAF3 (green), TRAF5 (red), and TRAF6 (blue). The two main signalling axes are JNK and NF-κB (for precise explanations see text). Activation of ROS triggers ASK1 and subsequently cell death which can be either caspase-dependent or independent. Activation of NF-κB may involve canonical (classical) and noncanonical (alternative) pathways. The canonical pathway depends on NIK and activation of trimeric complex of IKKαβγ and phosphorylation of IKBα to p50/RelA; the noncanonical pathway of NF-κB is dependent on NIK and IKKα and followed by activation of p100/RelB to p52/RelB. The activity of p50/RelA and p52/RelB in the nucleus leads to activation of specific gene transcription.

1.12 The Lymphotoxin system: ligands

1.12.1 LTα

The discovery of LTα came shortly after the discovery of TNF-α. Both ligands are able to interact with both TNFR –I and –II receptors, albeit with different affinities (Table 1.2). Unlike other TNFRs such as Fas, TRAIL-R or CD40 which almost exclusively have a single cognate ligand, the LT system is far more complex with ligands LTα, LTβ, LTα1β2, LTα2β1, and LIGHT being able to interact with the two main transmembrane receptors LTβR and HVEM, the TNFRs –I and –II as well as the soluble receptor DcR3 (Ware, 2005) (Figure 1.7).

LTα is a ligand and often used as a term to describe the biologically active trimer LTα3 (Ware, 2005; Ware et al., 1996), but can exist in three different forms; soluble homotrimeric LTα3, or as two transmembrane heterotrimeric complexes termed LTα1β2 and LTα2β1 (Tracey et al., 2008). LTα1β2 and LTα2β1 complex formation occurs when soluble LTα binds to LTβ bound on the cell membrane. Thus signalling via LTαβ-LTβR interaction requires target-effector cell contact (Tracey et al., 2008; Ware, 2005). In addition to binding to TNFR, LTα3 may bind HVEM, although this binding has been reported to be with low affinity (Mauri et al., 1998). LTα is secreted by activated lymphocytes, resting B cells, non-hematopoietic and myeloid lineage cells. Like TNF-α, LTα secretion has been found in some immortalised T cell lines including Jurkat and Hut78 (Gommerman and Browning, 2003). It is also found to be secreted following stimulation of Raji B lymphocytes with phorbol ester (Ware et al., 1992). It has been shown that when LTα is mutated at either D50N or Y108F, it will only remain as a homotrimer which is not able to bind TNFRI or TNFRII and is not able to induce HT29 cell apoptosis. The modified LTα ligand, however, co-assembled with LTβ, formed a stable ligand heterotrimer complex (LTαβ), which was functionally active and able to trigger cell death in the adenocarcinoma cell line due to its capability to bind LTβR (Williams-Abbott et al., 1997).

In addition, Browning and colleagues reported that the LTα1β2 with mutated LTα was functionally active on HT29 and WiDr cells (Browning et al., 1996). Interestingly, over-secretion of LTα has been associated with an increased risk of bladder, endometrial, cervical, prostate, bone, breast and gastric cancer, as well as various lymphomas thus overall suggesting it may contribute to carcinogenesis (Niwa et al., 2005; Nonomura et al., 2006). Although how LTα increases carcinogenesis is unknown, evidence implies this is due to over activation of LTβR and not due to its concomitant ability to activate TNFRII (Browning et al., 1996; Degli-Esposti et al., 1997b; Wilson and Browning, 2002; Winter et al., 2007; Yang et al., 2007).

1.12.2 LTβ and LTαβ complexes

The non-cleavable membrane LTβ ligand is active when homotrimeric and it ligates with LTβR (Williams-Abbott et al., 1997) (Figure 1.7). LTβ is known to be expressed in splenic naive B cells in the adult spleen, $CD4^+$ T cells, and mature DCs (Edwards et al., 2003; Junt et al., 2006). Evidence suggests that the expression of LTβ on these lymphocytes enhances the immune response, and is also responsible for antiviral immunity on non-lymphocytes by facilitating antigen presentation by APCs (Junt et al., 2006). LTβ remains largely under-researched, not only perhaps due to its lack of malignant cell toxicity, but because it mainly assembles with LTα in order to form membrane stable complexes of LTαβ (Williams-Abbott et al., 1997) (Table 1.2).

As in the case of LTβ, the effects of LTαβ complexes (via LTβR activation) remain relatively under investigated, despite the ability of LTαβ ligands to induce cytotoxic effects *in vitro* and *in vivo* (Browning et al., 1996; Williams-Abbott et al., 1997). The expression of both LTα1β2 and LTα2β1 complexes is regulated by IL-2, which leads to their induction on human peripheral blood T cells (Ware et al., 1992). Interestingly, LTαβ ligands exhibit differential receptor binding specificities due to the differences in their stoichiometry (Ware, 2005).

In murine studies, LTαβ expression shows induction on splenic T cells in response to the cytokines IL-4 and IL-7 and the chemokines CCL19 and CCL21 (Browning et al., 1993; Luther et al., 2002), but it is still not yet reported how this relates to humans. The interaction of LTαβ with its receptor LTβR is also important for the maintenance of the gut-associated lymphoid tissues (GALT), including, lymph nodes and Peyer's patches and also for the formation of germinal centres (Gommerman and Browning, 2003; Ware, 2005). This suggests that the system is important in normal development and immune regulation following adulthood. There is a report that LTα1β2 can be secreted following its cleavage by ADAM17 metalloproteinase (MMP) and MMP-8 and the soluble form was detected in serum of patients with rheumatoid arthritis (Young et al., 2010). Some studies have looked at the importance of the LTαβ complexes in signal transduction (Androlewicz et al., 1992; Browning et al., 1991; Browning et al., 1995; Ware et al., 1995; Ware, 2005). Of the two types of LTαβ membrane complexes, recombinant LTα1β2 was able to induce cell death in a range of human carcinoma cell lines such as HT29 and HT-3 cells in the presence of IFN-γ (Browning et al., 1996).

1.12.3 LIGHT

Lymphotoxin-like exhibits inducible expression and competes with herpes simplex virus glycoprotein D for HVEM, HVEM being a receptor expressed on T lymphocytes (LIGHT) was identified and classified as a TNFL member when it showed sequence homology with TNFα (27%), LTα (27%), LTβ (34%), FasL (31%) and CD40L (26%) (Table 1.2) (Mauri et al., 1998). LIGHT is constitutively expressed on myeloid cells, primary immature DCs and its expression can be induced on the surface of activated T cells and macrophages (Harrop et al., 1998b; Mauri et al., 1998; Morel et al., 2000).

1.12.3.1 Role of LIGHT in the immune system

LIGHT can ligate both LTβR and HVEM receptors (and can bind to soluble receptor DcR3) (Figure 1.7) to regulate cell proliferation, differentiation and growth inhibition (Black et al., 2002; Granger et al., 2001; Mauri et al., 1998). The interaction of LIGHT with LTβR and HVEM plays an important role in the induction of positive co-stimulatory signals between immune cells as reviewed in detail elsewhere (Steinberg et al., 2011; Ware and Šedý, 2011). LIGHT also plays a crucial role in regulating gene expression in innate and adaptive immune system against pathogens but also conversely may be linked to disease (autoimmunity and cancer) (Gommerman and Browning, 2003).

Work in transgenic mice showed that LIGHT is important for T cell proliferation and in regulation of T cell homeostasis (Wang et al., 2001c). Two further studies *in vitro* showed that LIGHT induces T cell proliferation, IFN-γ secretion and NF-κB activation (Tamada et al., 2000a; Tamada et al., 2000b). Morel and colleagues demonstrated that LIGHT also cooperates with CD40 ligand (CD154) contributing to DC maturation (Duhen et al., 2004; Morel et al., 2001; Pasero et al., 2009a).

LIGHT induces the expression of chemotactic molecules (CCL21), adhesion molecules such as Mucosal vascular addressin cell adhesion molecule (MAdCAM-1), MIG/CXCL9 and IP-10/CXCL10 most likely via LTβR signalling (Farber, 1997; Ngo et al., 1999; Sharma et al., 2003; Yu et al., 2004). The release of MIG and IP-10 possibly reduces tumour angiogenesis and enhances the infiltration of activated tumour antigen-specific T cells, which may lead to tumour regression (Tamada et al., 2000a; Yu et al., 2004). A study by Petreaca and colleagues demonstrated in a cutaneous wound-healing model that LIGHT promotes apoptosis in local macrophages via LTβR in order to reduce inflammation (Petreaca et al., 2008).

Conversely, however, LIGHT may enhance severe inflammation in non-lymphoid tissues (Ware, 2005). *In vivo*, tumours expressing LIGHT have been reported to undergo autocrine LIGHT mediated apoptosis thus LIGHT overall has a tumour suppressive effect (Zhai et al., 1998). Other studies in mice have also shown that the expression of LIGHT caused activation of localised NK cells and the infiltration of cytotoxic CD8 T cell lymphocytes (CTL) which assisted tumour eradication (Fan et al., 2006; Yu et al., 2004). Mortarini and colleagues further reported that the expression of LIGHT in microvesicles attracted and enhanced lymphocytic infiltration (Mortarini et al., 2005). Transfected murine fibrosarcoma with stable membrane LIGHT resulted in tumour rejection and eradication *in vivo* and LIGHT expression enhanced the anti-tumour response mainly by priming T cells (Tamada et al., 2000b; Yu et al., 2004).

1.12.3.2 Role of LIGHT in epithelial cells

Soluble LIGHT can trigger apoptosis of human tumour cells *in vitro* but this appears to require the presence of IFN-γ (Zhai et al., 1998). The combination of LIGHT/IFN-γ in fact has the capacity to cause apoptosis of p53-normal and p53-deficient HT29 adenocarcinoma cells (Chang et al., 2004; Kim et al., 2004; Walczak and Krammer, 2000), MDA-MB-231 breast cancer cells (Wu et al., 2003), caspase-3 deficient MCF-7 breast cancer cells and human hepatoma cells (Chen et al., 2003; Tamada et al., 2000b). It was reported that LIGHT treatment triggers the activation of caspase-3 with concomitant downregulation of anti-apoptotic protein Bcl-2 in HCT116 colorectal carcinoma cells (Wang et al., 2013). This is in support of previous studies suggesting that the LIGHT/IFN-γ combination induces apoptosis via downregulation of anti-apoptotic Bcl-2 family members, where the contribution of the Bcl-2 families (pro-apoptotic and anti-apoptotic) appears to be cell type-dependent (Tamada et al., 2000b; Wu et al., 2003).

Interestingly, LIGHT can ligate with two transmembrane receptors of LT (LTβR and HVEM) and one soluble receptor DcR3 (Figure 1.7). A number of studies have suggested that the functional outcome of LTβR and HVEM receptor activation by LIGHT is dependent on the presence or relative expression levels of these receptors on the target cells. Some elegantly performed studies by Ware and colleagues using an HVEM-selective LIGHT mutant that cannot bind LTβR showed that IFN-γ assisted activation of LTβR alone is sufficient and necessary for LIGHT-induced apoptosis in HT29 cells, and apoptosis was TRAF3-dependent (Rooney et al., 2000). Interestingly, however, LIGHT-induced growth inhibition occurs in carcinoma cells MDA-MB-231 and HT29 cells which express both receptors LTβR and HVEM, and also LIGHT was not cytotoxic to cells that expressed only one of these receptors (Zhai et al., 1998). In that study, LIGHT induced growth inhibition in the prostate cancer cell line PC-3 which only expresses LTβR but not HVEM. This evidence highlighted two important points: a) LIGHT may not cause cell death for target cells expressing one of the receptors LTβR or HVEM, b) LIGHT engagement with LTβR or HVEM may trigger different biological mechanism in target cells (Zhai et al., 1998).

However, such findings contrast previous studies by Pasero et al. (2009b) in cells from patients with chronic lymphocytic leukaemia, which suggested that when HVEM is the primary available receptor, soluble and mainly membrane-presented LIGHT promoted cell death. Interestingly this was found to occur via cross-talk of LIGHT-mediated signalling with other TNFSF members, in particular by induction of endogenous TNF-α, which enhanced HVEM mediated cell-death.

Therefore, the effect of LIGHT-induced signalling on cell fate appears complex and studies like those discussed above have not only suggested receptor level-related effects, but also, as soluble LIGHT does not bind to other TNFRs, e.g. Fas, DR4, or DR5 shown by *in vitro* binding assays (Chen et al., 2003), it is possible that indirect signalling (via cross-talk) may be important, too.

1.13 LT receptor cross-linking and functional outcome

One fundamental property of the TNFSF that despite its clear importance is very rarely highlighted relates to how “signal quality” (i.e. the degree of receptor activation or cross-linking) affects or determines the outcome of receptor ligation. There is a plethora of reports in the literature clearly indicating that highly cross-linked agonistic antibodies, cross-linked soluble recombinant ligands and particularly membrane-presented ligand (achieved by co-culture of target cells with growth-arrested, ligand-expressing third-party cells) induce a greater extent of carcinoma cell death in *vitro* in comparison to non-cross-linked agonists.

Studies in the CD40 system have demonstrated how ligand valency, and consequently the extent of receptor cross-linking, can dictate cell death against survival signals (Bugajska et al., 2002). Specifically in carcinoma cell lines, membrane-presented CD40 ligand (mCD40L), but not soluble agonists (e.g. sCD40L), induces high level of pro-inflammatory cytokine secretion and causes extensive cell apoptosis (Bugajska et al., 2002; Engels et al., 2005; Zapata et al., 2001), whilst remaining a tumour-cell specific death signal (Bugajska et al., 2002; Shaw et al., 2005). CD40 activation can induce downstream signalling pathways of both pro- and anti-apoptotic nature; this is entirely dependent on the type of tumour and the state of differentiation of the target cells (Elgueta et al., 2009; Korniluk et al., 2014; Tong and Stone, 2003). This is not a unique property of CD40, for instance it has been reported that mTNF-α generates higher cytotoxicity than soluble ligand in certain tumour cell lines leading even to necrotic cell death (Ardestani et al., 2013b).

In the context of LT signalling, the majority of previous studies have focused on the activation of LTβR, and to a lesser extent on HVEM, by soluble LT agonists. It is well established in carcinoma cell lines that cross-linking of LTβR in Hep3BT2, HeLa and HEK293 cells by soluble mutein LIGHT (LIGHT-R228E), which activates LTβR, and agonistic anti-LTβR monoclonal antibody (clone 31G4D8) were able to induce cell death in these cells (Chen et al., 2003; Rooney et al., 2000). Degli-Esposti and colleagues (1997b) reported that cross-linking of LTβR with immobilized agonistic anti-LTβR monoclonal antibody (M12) induced secretion of IL-8 and RANTES in A375 cells, but not cell death, and similar observations were made with membrane-bound LTβ and LTαβ (ligands for LTβR).

On the other hand, Browning and colleagues (1996) demonstrated that immobilised agonistic monoclonal antibody anti-LTβR (CBE11) induced cell death efficiently for HT29, WiDr, MDA-MB-468 and HT-3 better than when the agonist was added to cultures in non-cross-linked form. Importantly, the activation of LTβR was more enhanced when the same agonistic antibody was engineered and converted into an IgM-like oligomer and thus delivered in pentameric form (CBE11p). The pentameric agonistic antibody was shown to inhibit cell proliferation and induced cell death for HT29 in the presence or absence of IFN-γ to a greater extent than did the monomeric mAb form CBE11 (Lukashev et al., 2006).

Interestingly, soluble recombinant LTα1β2 (another ligand for LTβR) was toxic when combined with IFN-γ in adenocarcinoma cell lines (Browning et al., 1996) and these studies by Browning and colleagues using different cross-linked forms of LT ligands (e.g. LTα1β2) and antibodies for LTβR activation have provided some evidence for the importance of the degree of receptor cross-linking in functional outcome for a number of cell lines *in vitro*. Of note also, there is evidence that cross-linking of HVEM receptor in CLL-derived cells (showing weak or no expression of LTβR) with agonistic antibody could induce downstream signalling involving pro- and anti-apoptotic proteins, which was more enhanced when LIGHT was presented in a membrane-bound form (Pasero et al., 2009b). Moreover, recent studies by Bechill et al. (2014) have demonstrated that LTβR and HVEM in HeLa and HT29 cells activated by membrane-bound LIGHT (via target cell co-culture with CHO cells expressing LIGHT ligand) or mutant LIGHT (LIGHT-R228E) in the presence of IFN-γ induced high levels of secretion of the CXCL10 chemokine.

An interesting, yet related, aspect of the LT system is the clear requirement for synergy with IFN-γ for the induction of apoptosis. There is evidence that when LT receptor activation by LIGHT is combined with IFN-γ this enhanced LIGHT cytotoxicity (Zhai et al., 1998), in accordance with studies that cross-linking LTβR alone with soluble LIGHT in presence of IFN-γ is sufficient to induce cell death (Rooney et al., 2000). The studies by Bechill et al. (2014) showing that in HeLa and HT29 cells LIGHT/IFN-γ induced a higher level of cytokine secretion compared with LIGHT treated cell alone further support this notion.

Therefore, there is an emerging picture that although the activation of LT receptors (LTβR and/or HVEM) requires the synergistic action of IFN-γ to induce adequate cytotoxicity, membrane-presented agonist may engage the apoptotic pathway more effectively thus negating the need for IFN-γ synergy. These observations on the importance of the quality of the signal in determining functional outcome following LT system-triggered signalling demonstrate intriguingly clear parallels with the mode of operation of the CD40/CD40L dyad, where membrane-bound agonist provides a stronger pro-apoptotic signal that overrides anti-apoptotic mechanisms (Bugajska et al., 2002; Georgopoulos et al., 2006).

This complexity is evident at the signal transduction level as well as the level of receptor activation. For instance, there is clear difference between the ability of TNF agonists to trigger cell signalling when presented in a soluble versus membrane-bound form. Often soluble agonists lack cytotoxic potency when administrated as a single treatment (without synergism by co-treatment with cytokines) yet membrane-presented ligands are superior. And although such studies have been informative to a great extent, the use of a variety of ligand/agonist format (soluble or membrane) between different studies *per se* often makes it difficult to form a collective understanding into the function of the ligand.

Moreover, there is often a lack of consistency when it comes to the cell models used to study the functional role of receptor-ligand interactions. This perhaps may explain some of the inconsistencies evident in the literature. It is thus essential that well-characterised *in vitro* models (e.g. cell lines representative of tissues of origin) are employed to study the role of TNFRs mainly LT receptors. Equally, it is important that the effect of LT receptors signalling is also tested in the normal counterparts of such cells to examine tumour cell specificity.

1.14 Aims and objectives

The effect of LTβR and HVEM ligation by LT agonists and membrane-bound LIGHT (mLIGHT) in well-characterised *in vitro* models (e.g. cell lines representative of tissues of origin) has not yet been investigated. The main aim of this thesis was to investigate the effects of LT agonists on a panel of carcinoma cells of colorectal (CRC) and bladder (UCC) origins and compare the ability of these agonists to induce cell death to mLIGHT. Moreover the project investigated the molecular mechanisms of mLIGHT-mediated apoptosis.

More specifically:

- **Chapter Three:** The effects of LTβR and HVEM activation triggered by LT agonists (receptor-specific anti-LTβR – BS-1) and soluble ligand (LIGHT) on carcinoma cell lines were investigated using a number of assays for detection of cell death, such as cell viability assay (MTS), CytoTox-Glo and flow cytometry.

- **Chapter Four:** Establishment and optimisation for a co-culture system to activate LTβR and HVEM by mLIGHT (co-culture target cells with growth-arrested third party L cells expressing mLIGHT). Several assays were performed to detect cell death, caspase activity, DNA fragmentation and cytokine secretion.

- **Chapter Five:** Using the co-culture system for induction of mLIGHT-mediated cell death, immunoblotting techniques and functional inhibition experiments (using specific pharmacological inhibitors) were carried out to determine early events in LT-associated signalling.

- **Chapter Six:** Based on the co-culture system, immunoblotting techniques for pro-apoptotic mediator detection, pharmacological inhibitors, flow cytometry and CytoTox-Glo, reactive oxygen species (ROS) detection and inhibition, caspase inhibitors and RNA interference (RNAi) were utilised to determine the nature of the mLIGHT-associated apoptotic pathways.

Chapter 2

Materials and Methods

2.1 Cell culture

All tissue cultures were set using aseptic techniques under a HEPA filtration CellGarda microbiological safety class II cabinet manufactured by NUAIRE (Triple Red Technologies). To avoid any possible contamination, all cell culture working areas of the cabinet were cleaned before and after use with diluted ethanol 70% (w/v). For a monthly routine sterilisation, the hood was disinfected by using Mikrozid® (Gompel Healthcare). Contaminated and unwanted cells and solutions were treated with 10% (w/v) Virkon for at least 30mins before removal to a domestic waste drain. For centrifugation, a Hettich Zentrifugen Universal 320 bench top centrifuge was used for cell isolation and freezing, and the cell suspension was spun for 5mins at 1200rpm. Cells were then incubated at 37°C in 5% (v/v) CO_2 conditions in a humidified atmosphere in an incubator manufactured by NUAIRE (Triple Red Technologies).

2.2 Growth medium

All cells, with the exception of normal human urothelial (NHU) cells, were maintained in a 1:1 (v/v) mixture of Dulbecco's Modified Eagle Medium (DMEM) (Gibco-BRL) and Roswell Park Memorial Institute (RPMI-1640) medium (Sigma-Aldrich), supplemented with 5% (v/v) of foetal Bovine Serum (FBS) and 1% (v/v) (2mM) L-Glutamine (Sigma-Aldrich), and this medium was named DR 5%. Normal Human Urothelial (NHU) cultures were established in a keratinocyte serum free medium (KSFM), and supplemented with 50µg/mL bovine pituitary extract and epidermal growth factor (EGF). Growth medium and supplements are detailed in Table 2.1.

Culture medium	Cat. No	Application	Supplier
DMEM (high glucose) with sodium bicarbonate, without L-Glutamine	D6546-6X500ML	Growth medium	Sigma-Aldrich
RPMI-1640 with sodium bicarbonate, without L-Glutamine	R0883-6X500ML	Growth medium	Sigma-Aldrich
Foetal bovine serum (FBS) 500ml (qualified foetal bovine serum) – (FBS)	F7524-500ML	Supplements	Sigma-Aldrich
L-Glutamine 200mM solution	G7513-100ML	Supplements	Sigma-Aldrich
Keratinocyte-SFM Medium	VX17005075	Growth medium	Fisher scientific
Supplements for keratinocyte-SFM	13028-014	Supplements	Fisher scientific
DPBS (10x concentrated) liquid 500ml	14200-067	Cell washing	Invitrogen
Trypsin-EDTA solution 0.25%	T4174-20ML	Cell detachment	Sigma-Aldrich
HANKS' balanced salt solution	H9394-6X500ML	Cell detachment	Sigma-Aldrich

Table 2.1. Growth medium, supplements and other reagents

2.3 Cell lines

2.3.1 Normal Human Urothelial (NHU)

Normal human urothelial (NHU) cells were kindly provided by Professor Jenny Southgate (York University). NHU cells were isolated and maintained in complete KSFM and incubated at 37°C in 5% (v/v) CO_2, as previously described (Crallan et al., 2006; Southgate et al., 2002).

2.3.2 Carcinoma cell lines

Three urothelial cell carcinoma (UCC) derived cell lines were studied: RT4, RT112 and EJ. RT4 represents well-differentiated papillary non-invasive. RT112 cells are moderately differentiated malignant non-invasive cells, whereas EJ is a model of an undifferentiated highly invasive malignant UCC cell line (Crallan et al., 2006). Also, three colorectal cell carcinoma (CRC) derived tumour cell lines were used that were HT29, SW480 and HCT116. HT29 and SW480 cells represent colon adenocarcinomas, whereas HCT116 are colon carcinoma cells. CRC cell lines were purchased from Sigma-Aldrich (depositor from ATCC) as shown in Table 2.2. CRC cells were maintained in recommended medium and then were adapted gradually in DR 5%. Cultured cells were incubated at 37°C and 5% (v/v) CO_2 until these reached a confluency of approximately 80% and were then harvested (for more details see the cell detachment and sub-culturing section 2.7) for cell expansion. Stocks were frozen in liquid nitrogen for future work.

2.3.3 LTK murine fibroblast (L cells)

LTK murine fibroblasts (L cells) transfected with human cDNA encoding LIGHT (LIGHT-transfected L cells) were kindly provided by Professor Daniel Olive, Cancer Research Centre of Marseille (CRCM, France); these cells were named mLIGHT-L cells. Non-transfected L cells (NT-L-cells) were also used in this study as control cells (Table 2.2). To simplify the work, both cell lines were gradually adapted in a DR medium supplemented with 10% (v/v) FBS, 1% (v/v) L-Glutamine, with the addition of 1mg/mL Hygromycin (Invivogen cat # ant-hm-5; supplied by Source Bioscience) for mLIGHT-L cells (in order to maintain transgene expression).

Cell lines	Tissue type	Cancer type
HT29	Epithelial	CRC/Adenocarcinoma
SW480	Epithelial	CRC/Adenocarcinoma
HCT116	Epithelial	CRC/Carcinoma
RT112	Epithelial	UCC/Carcinoma
EJ	Epithelial	UCC/Carcinoma
NT-L	Fibroblast	N/A
mLIGHT-L	Fibroblast	N/A

Table 2.2. Epithelial and fibroblast cell lines

2.4 Soluble agonists

Agonistic antibody (tetravalent LTβR agonistic BS-1 antibody) specific for LTβR activation and soluble ligands (human recombinant LIGHT) were used to activate LTβR and HVEM. Recombinant cytokines IFN-γ and TNF-α were used for some experiments as presented in Table 2.3. All agonistic antibodies and soluble ligands were aliquoted and stored at -20°C according to the manufacturer's instructions.

Reagents	Cat	Target	Supplier	Stock conc.	Optimal conc.
MOPC-21	N/A	Non-specific	A kind gift from Biogen Idec – USA	3.3mg/mL	10µg/mL
BS-1	N/A	LTβR receptor	A kind gift from Biogen Idec – USA	5mg/mL	30µg/mL
LIGHT Human Recombinant	167310-09B-B	LTβR and HVEM	Tebu-bio	15µg	1µg/mL
IFN-γ Human Recombinant	167300-02-B	IFN-γ receptor	Tebu-bio	$20x10^6$ Unit	180U/mL
TNF-α Human Recombinant	167300-01A-B	TNFRI and TNFRII	Tebu-bio	$20x10^6$ Unit	1000U/mL

Table 2.3. Soluble agonists: agonistic antibodies and soluble ligands

2.5 Pharmacological inhibitors

Functional inhibitors used included cycloheximide (CHX) to inhibit general protein synthesis (Sigma-Aldrich). Inhibitors for caspase-3 (z-DEVD-FMK), caspase-8 (z-IETD-FMK), caspase-9 (z-LEHD-FMK), caspase-10 (Z-AEVD-FMK) and pan-caspase (z-VAD) were all purchased from R&D Systems. MAPK kinase inhibitors for JNK, p38, MEK and NF-κB were purchased from Santa Cruz. All inhibitors were dissolved in DMSO and solvent control (vehicle) controls were included in all experiments. The antioxidant inhibitors used were NAC and DPI and were purchased from Sigma-Aldrich. Optimal concentrations were obtained after the chemical inhibitors were pre-titrated. Dose-response experiments were performed using the CellTiter 96® AQ_{ueous} One Solution Cell Proliferation assay. Table 2.4 lists all inhibitors used in this study.

Inhibitors	Cat	Target	Supplier	Stock conc.	Optimal conc.
Cycloheximide (CHX)	C4859-1ML	Cell protein synthesis	Sigma-Aldrich	100mg/mL	0.05-0.1µg/mL
z-DEVD-FMK	FMK004	Caspase-3&7	R&D systems	20mM	50-100µM
z-IETD-FMK	FMK007	Caspase-8	R&D systems	20mM	50-100µM
z-LEHD-FMK	FMK008	Caspase-9	R&D systems	20mM	50-100µM
z-AEVD-FMK	FMK009	Caspase-10	R&D systems	20mM	50-100µM
z-VAD-FMK	FMK001	All caspases	R&D systems	20mM	50-100µM
SP600125	sc-200635	JNK	Santa Cruz	100mM	5-10µM
SB202190	sc-202334B	p38	Santa Cruz	200mM	25µM
U0126	sc-222395A	MEK/ERK	Santa Cruz	100mM	10-20µM
NF-κB Activation inhibitor III	sc-204818	NF-κB	Santa Cruz	100mM	5µM
NAC	A7250-5g	ROS	Sigma-Aldrich	20mM	1.25-2.5mM
DPI	D2926-10MG	NADPH oxidase	Sigma-Aldrich	30mM	0.01562-0.03125µM

Table 2.4. Common pharmacological inhibitors

2.6 Reagents and antibodies

Different antibodies were used to detect the protein of interest. For example, surface protein expression was detected by flow cytometry (Table 2.5a), or total protein expression or phosphorylated proteins was detected by western blotting (Table 2.5b). Secondary antibodies were applied when unconjugated primary antibodies were used (Table 2.5c).

a.

Ab/format	Cat#/Clone	Host	Reactivity	Application	Supplier
TNFRI(CD120a)-Purified	550514/mAb TNFRI-B1	Mouse	Human	FC	BD Bioscience
TNFRII (CD120b)-PE	552418/hTNFR-M1	Rat	Human	FC	BD Bioscience
IgG1-isotype control PE	556650/MOPC-21	/	N/A	FC	BD Bioscience
CD40-PE	555589/5C3	Mouse	Human	FC	BD Bioscience
CD54 / (ICAM-1) PE	555511/HA58	Mouse	Human	FC	BD Bioscience
LIGHT/CD258-PE	FAB664P/115520	Mouse	Human	FC	R&D System
HVEM/CD270-PE	MAB356/94801	Mouse	Human	FC, WB, ELISA	R&D System
HVEM/CD270-PE	318806/122	Human	Human	FC	Biolegend
LTα (TNF-β) PE	554556359-81-11	Mouse	Human	FC	BD Bioscience
LTβR-PE	551503/hTNFR-RP-M12	Mouse	Human	FC	BD Bioscience
Annexin V-FITC	556547	N/A	N/A	FC	BD Bioscience
Propidium Iodide	556547	N/A	N/A	FC	BD Bioscience

b.

Antibody	Cat/Clone	Host	Reactivity	Dilution	Application	MW	Supplier
HVEM	MAB356/94801	Mouse	Human	1:500 in 0.1% Tween20	WB	~50	R&D Systems
TRAF1	sc-7186/(H-186)	Rabbit	Human	1:500 in 0.1% Tween20	WB	52	Santa Cruz Biotechnology
TRAF2	sc-876/(C-20)	Rabbit	Human	1:500 in 0.1% Tween20	WB	50	Santa Cruz Biotechnology
TRAF3	sc-949/(C-20)	Rabbit	Human	1:500 in 0.1% Tween20	WB	65	Santa Cruz Biotechnology
TRAF5	sc-7220/(H-257)	Rabbit	Human	1:500 in 0.1% Tween20	WB	55	Santa Cruz Biotechnology
TRAF6	sc-8409/(D-10)	Rabbit	Human	1:500 in 0.1% Tween20	WB	60	Santa Cruz Biotechnology
Phospho-p44/42 MAPK (Erk1)/(Erk2)	5726S (D1H6G)	Mouse	Human	1:1000 in 5% w/v non fat dry milk, 0.1% Tween20	WB	42-44	Cell Signalling
Phospho-JNK/SAPK (Thr183/Tyr185)	9255S	Mouse	Human	1:1000 in 5% w/v non fat dry milk, 0.1% Tween20	WB	46-54	Cell Signalling
Phospho-p40phox (Thr154)	4311	Rabbit	Human	1:1000 in 5% w/v non fat dry milk, 0.1% Tween20	WB	40	Cell Signalling
Phospho-ASK-1 (Thr845)	3765S	Rabbit	Human	1:1000 in 5% w/v BSA, 0.1% Tween20	WB	155	Cell Signalling
Phospho-p38 MAPK (Thr180/Tyr182)	4511P	Rabbit	Human	1:1000 in 5% w/v BSA, 0.1% Tween20	WB	43	Cell Signalling
Thioredoxin 1	2285S	Rabbit	Human		WB	12	Cell Signalling
Bax	2282-MC-100/YTH-2D2	Mouse	Human	1:500 in 0.1% Tween20	WB	21	R&D Systems
Bak	AF816	Rabbit	Human	1:500 in 0.1% Tween20	WB	28	R&D Systems
Anti-β-actin	A5441/AC15	Mouse	Human	1:10.000 in 0.1% Tween20	WB	42	Sigma-Aldrich
Anti-Cytokeratin 8	[X] 18-0185Z/ C51	Mouse	Human	1:1000 in 0.1% Tween20	WB	52.5	Invitrogen
Anti-Cytokeratin 18	C 8541/CY-90	Mouse	Human	1:1000 in 0.1% Tween20	WB	~50	Sigma-Aldrich

c.

Antibody	Cat#/Clone	Host	Reactivity	Dilution	Application	Supplier
Goat anti-mouse IgG, Alexa Fluor 680 conjugate	A-21084	Goat	Mouse	1:10.000 in 0.1% Tween20	WB	Invitrogen
Goat anti-rabbit IgG conjugated (IRDye 800)	039611-132-122	Goat	Rabbit	1:10.000 in 0.1% Tween20	WB	Tebu-bio

Table 2.5. Flow cytometry and immunoblotting antibodies

2.7 Cell detachment and sub-culturing

In order to establish cell cultures, all solutions were warmed at room temperature. Cultures that reached confluency of approximately 80% were harvested by the removal of cultured medium through an aspirator. Subsequently, cultured cells were incubated with 0.1% (w/v) in ethylenediaminetetraacetic acid (EDTA) in PBS for 3-5mins at 37°C (to remove residual FBS and break calcium mediated contacts between neighbouring cells) and this is only applied for NHU and epithelial carcinoma cells. Recipe for EDTA preparation can be found in Appendix I. Fibroblast cells were washed with 1x PBS (to remove any remaining FBS-containing medium). The PBS/EDTA or 1x PBS solution was aspirated and cells were incubated with Hank's buffered salt solution containing 0.25% (w/v) trypsin and 0.02% (w/v) EDTA [250 and 750µL for T25cm^2 tissue culture flasks and T75cm^2 tissue flasks, respectively] (Table 2.6) for 3mins at 37°C in 5% (v/v) CO_2 (or until cells detached from the culture flask). Trypsin was neutralised by the addition of KSFM containing 1% (v/v) FCS for NHU or addition of standard growth medium for carcinoma and fibroblast cells to achieve cell suspension, and then transferred to a universal tube to perform centrifugation and to pellet the cells. Cell centrifugation was performed at 1200rpm for 5mins to remove any traces of trypsin. Supernatants were discarded by aspiration and fresh medium was added to the pelleted cells, cell suspension was well-mixed and appropriate splitting ratio was performed.

Cells were imaged by using an EVOS™ XL Core inverted microscope (PeqLab) on a daily basis. Images were taken by using a 100x immersion objective lens with an embedded operating system with image software for image capture. There was a routine passage system during this study, NHU cells sub-culturing passages involved 3 passages and 6-8 passages were performed for epithelial carcinoma and fibroblast cells. Following that fresh cultures were used.

2.8 Cell counting

Briefly, after cell centrifugation, cells were resuspended in growth medium and then diluted at an appropriate ratio (usually 1:5) with growth medium. When cell suspension was not being manipulated, this was incubated at 37°C and 5% (v/v) CO_2 at a humidified atmosphere. Cells were counted manually by using a haemocytometer (Neubauer-Improved Chamber) (Table 2.6) and, only bright, healthy cells were counted. The following formula was used to calculate the cell number per mL:

$$\text{Cells No/mL} = \text{Average counted cells in 4 squares} \times \text{dilution factor} \times 10^4$$

2.9 Cell cryopreservation

For cell cryopreservation, cultured cells were harvested (as described above) and collected by centrifugation at a 1200rpm for 5mins. The cell pellet was resuspended in the appropriate volume of freezing medium, (ice-cold growth medium consisting of 10% (v/v) FBS and 10% (v/v) dimethylsulphoxide (DMSO)) at a cell density not less than $1x10^6$ cells/mL (for epithelial cells). The freezing medium of NT-L cells and mLIGHT-L cells was different to the freezing medium was used for epithelial cells; it consisted of 90% (v/v) FBS and 10% (v/v) DMSO, as these cells would not recover when frozen in freezing medium of epithelial cells. Cells were aliquoted in a total of 1mL to polypropylene cryovials and then transferred to an ice-cold Nalgene “Mr Frosty” (Fisher, UK) containing 250mL of isopropanol (Fisher) to control the cooling rate to 1°C/minute (Table 2.6). Cells were cryopreserved and stored gradually at first in -20ºC and then -80°C (for at least 4hrs and usually overnight), and on the second day were placed and stored in liquid nitrogen (Statebourne Storage Dewar, at -196°C) for long term storage.

For thawing cryopreserved cells, frozen vials were thawed partially until only a portion of the contained solution was still in ice form. Then the liquid/ice mix (drop by drop with growth medium) was transferred rapidly in a 10mL volume of growth medium and spun at 1200rpm for 5mins at room temperature (this was to remove any DMSO from the medium). The supernatant was discarded and fresh medium was added and mixed with the cell pellet, and then cultured in either T25 or T75 tissue culture flasks for cell growth as usual (Table 2.6). On the following day, the cultured medium was replaced with fresh medium to enhance cell recovery.

Item	Cat	Application	Supplier
Haemocytometer	MNK-420-010N	Cell counting	Fisher
Haemocytometer spare chambers	MNK-504-030M	Cell counting	Fisher
T25cm^2 Tissue culture flask	83.1810.002	Cell growth	Sarstedt
T75cm^2 Tissue culture flasks	83.1813.002	Cell growth	Sarstedt
Nalgene Mr frosty	CRY-120-010T	Cell cryopreservation	Fisher
Polypropylene cryovials	72.38	Cell cryopreservation	Sarstedt

Table 2.6. Tissue culture materials

2.10 Cell transfection with siRNAs

Gene silencing or short interfering (siRNA) is a technique used for down-regulating the specific expression of genes in living or mammalian cells by introducing a complementary RNA (a double-stranded RNA) that degrades the mRNA of interest. It has been reported that the optimal siRNA molecule contains 21 base pairs (bp), which can be used to transfect mammalian cells (Elbashir et al., 2001a; Elbashir et al., 2001b)**.**

To knockdown the expression of LTβR or HVEM, Accell SMARTpool siRNAs (Dharmacon, supplied by Fisher) were used that can target three sequences simultaneously of each of protein expression as described below (Table 2.7).

a.

Reagents	Cat	Target	Supplier	Stock conc.	Optimal conc.
RNA free water	B-003000-WB-100	Diluent	Fisher	N/A	N/A
5x siRNA buffer	B-002000-UB-100	Diluent	Fisher	N/A	N/A
DharmaFECT 2 Transfection Reagent	T-2002-01	Cell membrane	Fisher	N/A	N/A
Accell Human LTβR siRNA, SMARTpool	E-008023-00-0005	LTβR	Dharmacon	5nmol	100nM
Accell Human HVEM siRNA, SMARTpool	E-008096-00-0005	HVEM	Dharmacon	5nmol	100nM

b.

Target mRNA	Accell Human SMARTpool siRNA	Target Sequence
LTβR	A-008023-14	GCAUGAAGAUGAAAUUAUA
	A-008023-15	CAAGUGUAUUUAUAUUGUA
	A-008023-16	CCCAUUUCUGGAGAUGUUU
	A-008023-17	GCCCAAGGAACCAAUUUAU
TNFRSF14 (HVEM)	A-008096-13	UCGUCAUCGUCAUUGUUUG
	A-008096-14	GUGUGGUGUUUAGUGGAUA
	A-008096-15	CUCCUGUUUUCUAUUUGUC
	A-008096-16	GGAGGAUGUAAAUAUCUUG

Table 2.7. siRNA molecules and their target sequences for LTβR and HVEM expression knockdown

2.10.1 siRNA delivery

Cell knockdown for the surface expression of LTβR and HVEM is difficult to achieve efficiently. The successful delivery of the siRNA depends on the cell type, because different cell types have varying sensitivities to the introduction of nucleic acids or siRNA. In addition, successful transfection requires careful optimisation of conditions, so a series of optimisations were performed to determine the conditions that would provide effective knockdown and maintain levels of cell death for co-cultured cells. Therefore, both improved protein knockdown and cell death were considered during optimisation experiments, and described in the following sections.

2.10.2 siRNA preparations

Dharmacon transfection reagents were used to deliver siRNA into cultured mammalian cells in 96-well plates. Tubes containing siRNA were briefly centrifuged to ensure the siRNA pellet was collected at the bottom of the tube. siRNA was resuspended in RNase-free 1x siRNA buffer (prepared as a mix of four volumes of sterile RNase-free water with one volume of 5x siRNA buffer) to achieve the desired final concentration at 20µM. The solution was pipetted gently up and down 3-5 times and placed on an orbital shaker for 30mins at room temperature to ensure solution homogeneity. Then the solution was aliquoted in RNase and DNase free eppendorf tubes and stored in -80C.

For siRNA preparations (LTβR siRNA and HVEM siRNA), the working solution was prepared, and the siRNA solution (stock 20µM) was mixed with an appropriate volume of serum-free medium KSFM (to make a concentration of 100nM) and pipetted gently up and down 4-5 times before incubation for 5mins at room temperature. In a separate tube, each 2µL of DharmaFECT transfection reagent was diluted with 1mL of KSFM (as transfection in serum-free medium was necessary), gently pipetted and incubated for 5mins. After the incubation time, the contents of both tubes were mixed and pipetted carefully up and down 4-5 times and further incubated for 20mins at room temperature. This achieved the final concentration 50nM of siRNA and 1µL/1mL of transfection reagent.

2.10.3 Transfection optimisation

After reagent preparations, the cell transfection step was performed, where the culture medium was removed from the 96-well plate and 100µL of appropriate transfection working medium was added to each well. Plates were incubated at 37°C in 5% (v/v) CO_2 for 24hrs. Three methods of transfection were attempted for co-cultured cells, and discussed in the following sections.

2.10.4 siRNA transfection using manufacturer's protocol

Target cells were seeded in a 96-well plate and incubated overnight at 37°C in 5% (v/v) CO_2 On the second day, the culture medium was aspirated and replaced with the prepared transfection reagent (as mentioned above) and incubated for 24hrs at 37°C for the purpose of successful transfection. On the following day, the transfection reagent was removed and MMC-treated effector cells were added to the growth medium, and post-ligation was conducted. Cells were incubated at 37°C in 5% (v/v) CO_2 for 72hrs. After the incubation time, cell death of non-transfected and transfected cells was detected by the CytoTox-Glo assay.

2.10.5 Modified protocol for siRNA delivery

Two methods of transfection optimisation were performed, where cells were transfected either twice with siRNA (conc. 50nM) or transfected once with a double concentration of siRNA (100nM). Transfection with 100nM of siRNA enhanced silencing in protein expression, LTβR or HVEM, as detected by flow cytometry. The first method involved a number of cells being split or cultured before transfection, and cells were about 40-60% confluent on the day of transfection. Transfection reagents were prepared, and the culture medium was removed and replaced with the transfection reagent. Cells were incubated for 24hrs at 37°C in 5% (v/v) CO_2. After the incubation time, the transfection reagent (siRNA conc. 50nM) was replaced with growth medium, and cells were placed in the incubator overnight to grow. On the following day, cells were split 1:2 and grown for 24hrs. A second transfection (siRNA conc. 50nM) was carried out for 24hrs, and after incubation time the cells were harvested and co-cultured with effector cells for 72hrs.

To achieve effective siRNA delivery into cultured mammalian cells, an appropriate number of target cells was seeded in a T25 flask for overnight at 37°C in 5% (v/v) CO_2. On the second day, the culture medium was aspirated and replaced with prepared transfection reagent (conc. 100nM) and incubated for 24hrs at 37°C. In the meantime, MMC-treated effector cells were seeded in 96-well plate and incubated overnight at 37°C in 5% (v/v) CO_2. On the following day, the transfection reagent was removed from flasks, and target cells were harvested, counted and co-cultured with MMC-treated effector cells. Cells were incubated at 37°C in 5% (v/v) CO_2 for 72hrs. After the incubation time, the cell death of non-transfected and transfected cells was determined by the CytoTox-Glo assay.

2.11 Flow cytometry

Flow cytometry is a technique primarily used to identify specific extracellular or intracellular proteins on live or dead labelled cells using a fluorochrome conjugated antibody which can be detected by passing the cell suspension through the flow cytometer. The fluorescent signal is proportional to the level of expression. For successful assessment for expression of surface proteins, in all experiments matched isotype control fluorochrome either fluorescein isothiocyanate (FITC) or Phycoerythrin (PE) was used to determine cell background. Also, cells were labelled with a fluorescent marker of the protein of interest. The fluorescence intensity emitted by cells corresponds to the quantity of binding sites for the fluorescent antibody on the cells. So the more levels of protein expression there are, the more fluorescence is emitted, and therefore the higher on the fluorescence intensity scale the data appears in comparisons to fluorescence intensity scale of background data (isotype control). In some experiments, median fluorescence intensity (MFI) was calculated for cell background (matched isotype control) and the protein of interest that has been examined.

Experiments were performed to detect the expression of lymphotoxin receptors on the cell surface of NHU and tumour cells. Cells were labelled with conjugated or non-conjugated monoclonal antibodies (mAbs). Appropriate isotype control (isotype controls such as, PE or FITC) was included. mAbs against any specific protein were added per test tube. Test tubes were vortexed very well and incubated for 25-30mins at 4°C in the dark conditions. Samples were protected from light during incubation to

avoid bleaching the fluorochrome of the conjugated antibodies. After incubation, labelled cells were washed with FACS buffer (PBS/1% (v/v) FBS) and centrifuged at 1500rpm for 5mins. After centrifugation, the supernatant was discarded and cells were resuspended in 300 or 400µL of FACS buffer. Samples were analysed on a Millipore Guava EasyCyte flow cytometer and 5,000 to 10,000 events were routinely acquired. Using gating on live and healthy cells, the results were analysed using InCyte2.6 Guava software (Millipore).

2.12 LT receptor cross-linking

For LT receptor activation, three approaches were used (to activate LTβR alone or activate both LTβR and HVEM on target cells) as described below:

1. Incubation of target cells with soluble agonists;
    a. Agonistic antibody BS-1.
    b. Soluble recombinant trimeric ligand LIGHT.
2. Co-culture of target cells with fibroblast cells that were transfected to constitutively express membrane-presented ligand LIGHT (mLIGHT).

Cells were incubated at 37°C in 5% (v/v) CO_2 for the indicated times, and the effects of soluble agonists and mLIGHT were determined by using several assays as discussed in the following section.

2.13 Determination of cell death

Cell death of treated cells was measured by utilising various assays as explained below, but before explaining these assays, it is essential to address the steps of cell treatments and the co-culture system.

1- For cell treatment with soluble agonists, cells were seeded in 96-well plates and treated with either soluble a) agonistic antibody (BS-1 – to activate only one receptor LTβR) or b) soluble ligand (LIGHT – to activate both receptors LTβR and HVEM) in the absence or presence of IFN-γ. In some experiments, CHX was also used in combination with soluble agonists to inhibit cell protein synthesis.

2- For the co-culture system, NT-L-cells (control cells) and a membrane LIGHT- (mLIGHT) bearing fibroblast cell line were used. Both NT-L-cells and mLIGHT-L cells were pre-treated with Mitomycin C (MMC) at conc. 15µg/mL and incubated for 2hrs (this is to cause effector cell growth-arrest). Cells were subsequently washed with sterile 1x PBS three times to remove any excess MMC. Subsequently, cells were harvested from flasks by trypsinisation and were resuspended in DR 5% medium and counted. Cells were seeded at cell density $2x10^4$ cells/well in 96-well plates and incubated overnight at 37˚C and 5% (v/v) CO_2 in order to allow cell attachment. On the second day, target cells were harvested, counted and seeded onto fibroblasts at a ratio of 1:0.8, and incubated for 72hrs at 37˚C and 5% (v/v) CO_2. An optimal ratio of cell number (effector:target) and incubation time was determined after a series of optimisations (see Chapter 4 Results).

The functional outcome of receptor(s) ligation and cell death was determined using CytoTox-Glo assay.

2.13.1 Cell biomass measurement (MTS assay)

The CellTiter 96® Aqueous One Solution Cell Proliferation kit was used to measure cell biomass. The kit contains a tetrazolium compound 3-(4,5-dimethylthiazol-2-yl)-5-(3-carboxymethoxyphenyl)-2-(4-sulfophenyl)-2H-tetrazolium, inner salt (MTS); this is coupled with an electron reagent known as phenazine methosulfate (PES). PES acts to form a stable solution with MTS (Table 2.8). MTS is a colorimetric method for the measurement of viable cells. The principle of MTS is that mitochondria in viable cells will reduce MTS to a water-soluble coloured formazan product in multi-well plates. Formazan levels correspond to cell biomass, which can be quantified by a FLUOstar OPTIMA (BMG Labtech) plate reader at a wavelength of 492nm.

The MTS assay was used only for cell treatment experiments, but not for co-culture experiments. Cells were seeded in a 96-well flat bottom cell culture plate and treated immediately with either agonistic antibody (BS-1) or treated with soluble ligand (LIGHT). In some experiments, IFN-γ and CHX were used in combination with BS-1 or LIGHT to enhance the cytotoxicity of BS-1 and LIGHT. Treated cells (in a final volume of 100µL) were then incubated for 72hrs or 96hrs at 37°C and 5% (v/v) CO_2.

Following incubation time, 20µL of CellTiter reagent was added to plates and incubated for 4hrs at 37°C and 5% (v/v) CO_2, in order to allow complete reaction. Absorbance was measured on a FLUOstar OPTIMA (BMG Labtech) plate reader at a wavelength of 492nm. Cell biomass percentage (%) was calculated using the formula (Abs T/Abs C) x 100, where Abs T refers to absorbance of treated cells and Abs C corresponds to absorbance of control cultures.

2.13.2 Cell Death assay (CytoTox-Glo)

Cell death was measured by performing a cell death assay known as CytoTox-Glo (Promega). The assay uses a luminogenic peptide substrate (alanyl-alanyl-phenylalanyl-aminoluciferin; AAF-Glo™ Substrate) to measure “dead-cell protease activity”, which is released from dead cells that have lost their membrane integrity (Table 2.8). The AAF-Glo is cleaved as a result of the release of protease and cleavage of AAF-Glo generates a luminescence signal (Figure 2.1), which was detected by luminescence measurements on a FLUOstar OPTIMA (BMG Labtech) plate reader.

All CytoTox-Glo™ reagents were thawed at room temperature and all components were mixed well to ensure homogeneity of the solution. The CytoTox-Glo™ reagents were prepared by transferring the contents of one bottle of assay buffer to the AAF-Glo™ substrate and steps were followed according to the manufacturer’s protocol. 50µL of working solution was added to each well of either treated cells or co-cultured cells (as mentioned in the section 2.13) to measure dead cell numbers and the Gain function on the MARS software was applied (to ensure the measurements were taken within the dynamic range of the instrument) and subsequently, the relative luminescence unit (RLU) was measured by the plate reader to determine cell death. For cell death calculation for co-cultured cells, where target cells were co-cultured with control (NT-L) and mLIGHT-L cells, control (NT-L) and mLIGHT-L cells cultures alone were included, control (NT-L) and mLIGHT-L cells background luminescence values were subtracted pair wise as appropriately, i.e. “control/target cells – control” and “mLIGHT/target cells – mLIGHT” readings. Fold increase relative to control was generated from background corrected data by comparing mLIGHT/target cell *versus* control/ target cell co-cultures. In all experiments, blank controls were included as appropriate.

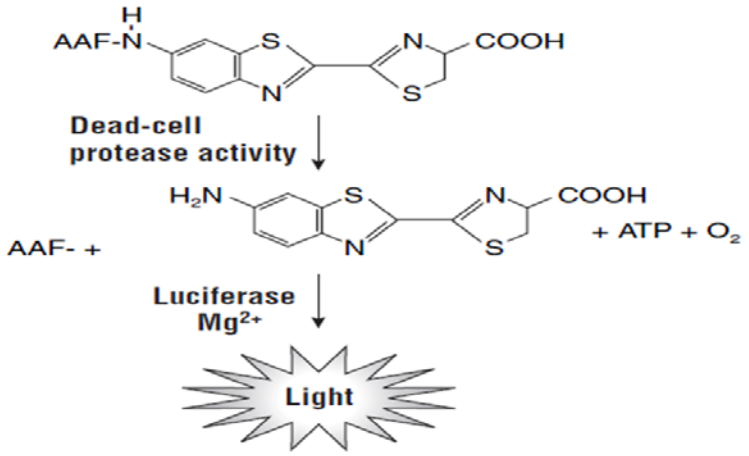

Figure 2.1. Cytotoxicity assay (CytoTox-Glo™) principle

Cleavage of luminogenic AAF-Glo™ substrate occurs by dead-cells, which release protease. A substrate for luciferase (aminoluciferin) is released resulting in the luciferase-mediated production of light, which can be detected by the plate reader. Figure was adapted from Promega's manual protocol for the CytoTox-Glo assay.

2.13.3 Annexin V/PI assay

One of the hallmarks of programmed cell death (apoptosis) is loss of plasma membrane integrity. This leads to the membrane phospholipid phosphatidylserine (PS) being translocated from the intracellular to the extracellular side of the plasma membrane, and exposes PS to the cell surface. To detect this, recombinant Annexin V conjugated to fluorochrome FITC was used, which is a phospholipid-binding protein that has a high affinity for PS and mainly binds to cells with exposed PS in order to determine apoptotic cells by flow cytometric analysis (Table 2.8). Also, propidium iodide (PI) was used in conjunction with Annexin V in order to detect late stage of cell death (dead cells), as the membranes of dead and damaged cells are permeable to PI. This study considered and calculated the percentage of total dead cells that were collected.

Cells were seeded in a 24-well plate (a conversion factor was used to determine cell number) and treated with soluble agonists. Cells were incubated for 72hrs at 37˚C and 5% CO_2. Steps of the Annexin V and PI procedure were performed according to the manufacturer's protocol. Cells were trypsinised, collected and centrifuged at 1500rpm for 5mins, and then washed once with cold PBS and resuspended in 50µL of 1x of binding buffer (BD Biosciences). Cells were then stained with Annexin V-FITC and PI and incubated for 10-20min at room temperature in dark. After the incubation time, 200 - 300µL of 1x binding buffer was added to each tube and cells were then analysed by flow cytometry within 1hr. Data analysis was performed on GuavaSoft 2.6 software and cell death was calculated.

2.13.4 Caspase activity assay (caspase-3/7 activity detection)

This assay detects and measures the activity of executioner caspase-3/7 as in Table 2.8. The principle of this kit is that it contains AFC caspase-3/7, which directly measures caspase-3/7 activity in cell culture. The assay (SensoLyte® Homogeneous AMC Caspase-3/7 Assay Kit) utilises the Ac-DEVD-AMC substrate as the fluorogenic indicator for assaying caspase-3/7 activities via the cleavage of caspase-3/7, and the substrate Ac-DEVD-AMC generates the AMC fluorophore as shown in Figure 2.2, and this was detected using a FLUOstar OPTIMA (BMG Labtech) plate reader at Excitation 380nm/Emission 500nm, respectively.

All kit components were thawed at room temperature and a working solution was prepared according to the manufacturer's protocol. Before adding the substrate, 50µL of DR 5% medium was added to cultures to ensure each well contained a total volume of 150µL, according to manufacturer's protocol. Subsequently, 50µL of substrate was added to cells and incubated for few minutes, and the Gain function on the MARS software was applied (to ensure the measurements were taken within the dynamic range of the instrument) and then the fluorescence signal was measured every 10min. For calculation of caspase levels in co-culture cells, where target cells were co-cultured with control (NT-L) and mLIGHT-L cells, control (NT-L) and mLIGHT-L cells cultures alone were included, control (NT-L) and mLIGHT-L cells background fluorescence values were subtracted pair wise as appropriately, i.e. "control/target cells – control" and "mLIGHT/target cells – mLIGHT" readings. Fold increase relative to control was generated from background corrected data by

comparing mLIGHT/target cell *versus* control/ target cell co-cultures. In all experiments, blank controls were included as appropriate.

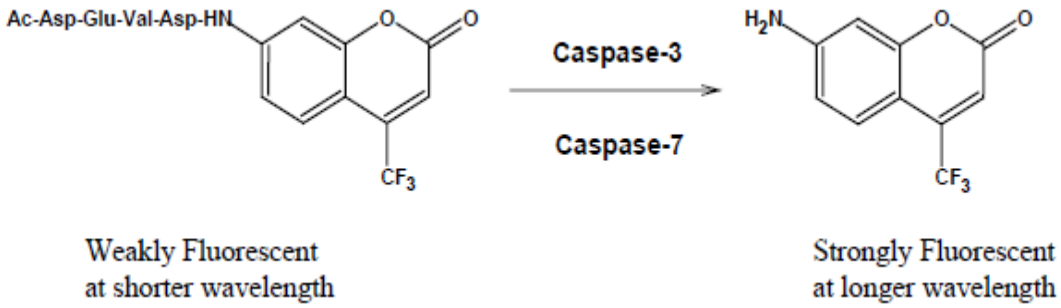

Figure 2.2. The principle of caspase-3/7 activity

The SensoLyte® Homogeneous AMC Caspase-3/7 Assay Kit uses Ac-DEVD-AMC as the fluorogenic indicator for assaying caspase-3/7 activities. Upon activation of caspase-3/7, the cleavages of substrate Ac-DEVD-AMC generates the AMC fluorophore that has bright blue fluorescence, which can be detected at Excitation 380nm/Emission 500nm respectively, and the reading was measured as a relative fluorescence unit (RFU). Figure was adapted from manual protocol for SensoLyte® Homogeneous AMC Caspase-3/7 Assay.

2.13.5 DNA fragmentation assay

Cell death was also investigated by performing DNA fragmentation assay, as DNA fragmentation is a hallmark of apoptosis. This assay detects the fragmentation of DNA in supernatants of treated cells.

Prior to LT receptor ligation, target cells were pre-treated and labelled with 5-bromo-2-deoxyuridine (BrdU) at a concentration of 10µM and incubated for 2hrs at 37°C and 5% (v/v) CO_2 (Table 2.8). This allows the DNA of target cells to be labelled with BrdU before ligation, in accordance with the manufacturer's instructions. After the incubation time, cells were harvested and co-cultured with NT-L or mLIGHT-L cells and incubated for 72hrs. Unlike the CytoTox-Glo and caspase assay, no cells alone background were needed in this assay as epithelial cells pulsed with BrdU were included instead. Treated cells with 5µM of staurosporine were served as positive control.

ELISA plate was coated with an anti-DNA antibody (overnight before the end of incubation time for co-cultured cells) and on the following day, the ELISA plate was blocked to remove any non-specific binding sites, followed by several washes to remove any blocking buffer. Supernatants from cell cultures were collected and added at 100µL (which may contain DNA fragments that were pulsed with BrdU, if cells underwent apoptosis). Then, a secondary enzyme-linked antibody was added in order to recognise BrdU. Ultimately, an enzyme substrate was added, which was converted into a blue colour by the secondary enzyme-linked antibody. After sufficient colour change (a deep yellow colour representative of and proportional to cell apoptosis, the reaction was stopped by adding diluted sulphuric acid (H_2SO_4) and absorbance was measured at 455nm on a FLUOstar OPTIMA (BMG Labtech) plate reader. Data were collected using MARS software and percentage (%) apoptotic cells were calculated as follows:-

$$\% \text{ Apoptotic cells} = \frac{\text{mLIGHT-L/target cells}}{\text{Cells treated with staurosporine}} \times 100$$

Reagents	Cat	Application	Supplier
CellTiter 96(R) AQueous One Solution Assay, 5,000 assays	G3581	Spectrophotometry	Promega
CytoTox-Glo cytotoxicity assay (5x10ml)	G9291	Spectrophotometry	Promega
SensoLyte homogenous AFC caspase -3/7 assay kit	ANA-71114	Spectrophotometry	Cambridge bioscience
Cellular DNA Fragmentation ELISA	11585045001	Spectrophotometry	Roche
Annexin V-FITC/Propidium Iodide	556547	Flow cytometry	BD Bioscience

Table 2.8. Reagents of cell death assays

2.14 Detection of ROS

2.14.1 H_2DCFDA

Chloromethyl derivative of 6-carboxy-2', 7'-dichlorodihydrofluorescein diacetate (CM-H_2DCFDA) (Fisher Cat 11530166) is a cell-permeant indicator for ROS in cells. CM-H_2DCFDA passively diffuses into cells, and is non-fluorescent itself, but gives green fluorescence when acetate groups are removed by intracellular esterases and oxidation in the cells. CM-H_2DCFDA was dissolved in DMSO in a nitrogen (oxygen free) environment and aliquoted and stored at -80°C, as recommended by the manufacturer. When co-cultures were carried out, effector cells were not MMC-treated and seeded overnight. On the second day, target cells were co-cultured and incubated for 2, 3, 4 and 6hrs post-ligation. Cells were first washed with PBS to remove any culture medium and were then treated with 1, 2 and 4µM of H_2DCFDA in pre-warmed (37°C) PBS for 30mins at 37°C in 5% (v/v) CO_2. Following H_2DCFDA treatment, cells were washed once and 100µL of PBS was added to each well. Fluorescence was then measured by a FLUOstar OPTIMA (BMG Labtech) plate reader at Excitation 485nm/Emission 520nm. Data were analysed by using MARS software.

2.14.2 ROS-Glo

ROS is superoxide anion radical that is generated in cells and acts as a signalling molecule, which can lead to cell damage or death. Most ROS are converted to H_2O_2 and has the longest half-life of all ROS in cultured cells. A change in H_2O_2 level can correspond to ROS level. Therefore, the ROS-Glo kit (Promega G8820) was used to measure H_2O_2 levels. The kit contains a substrate that reacts with H_2O_2 to generate a luciferin precursor. The addition of ROS-Glo™ detection reagent containing recombinant luciferase and d-Cysteine generates a luminescent signal (which is proportional to H_2O_2 level) that was detected by luminescences measurements as shown in Figure 2.3.

To perform ROS-Glo assay, effector cells were seeded overnight (without pretreatment with MMC) in a 96-well plate. On the second day, target cells were harvested and pretreated with H_2O_2 substrate at conc. 25µM for 30mins in suspension and incubated in incubator at 37°C and 5% (v/v) CO_2. Then target cells were co-cultured with effector cells and incubated for 3 and 4hrs post receptor ligation. Before just adding the second reagent (ROS-Glo), H_2O_2 was added at final conc. 2mM which served as positive control. ROS-Glo reagent was prepared and added at volume 100µL/well and luminescence was then measured on a FLUOstar OPTIMA (BMG Labtech) plate reader. Data were analysed by using MARS software.

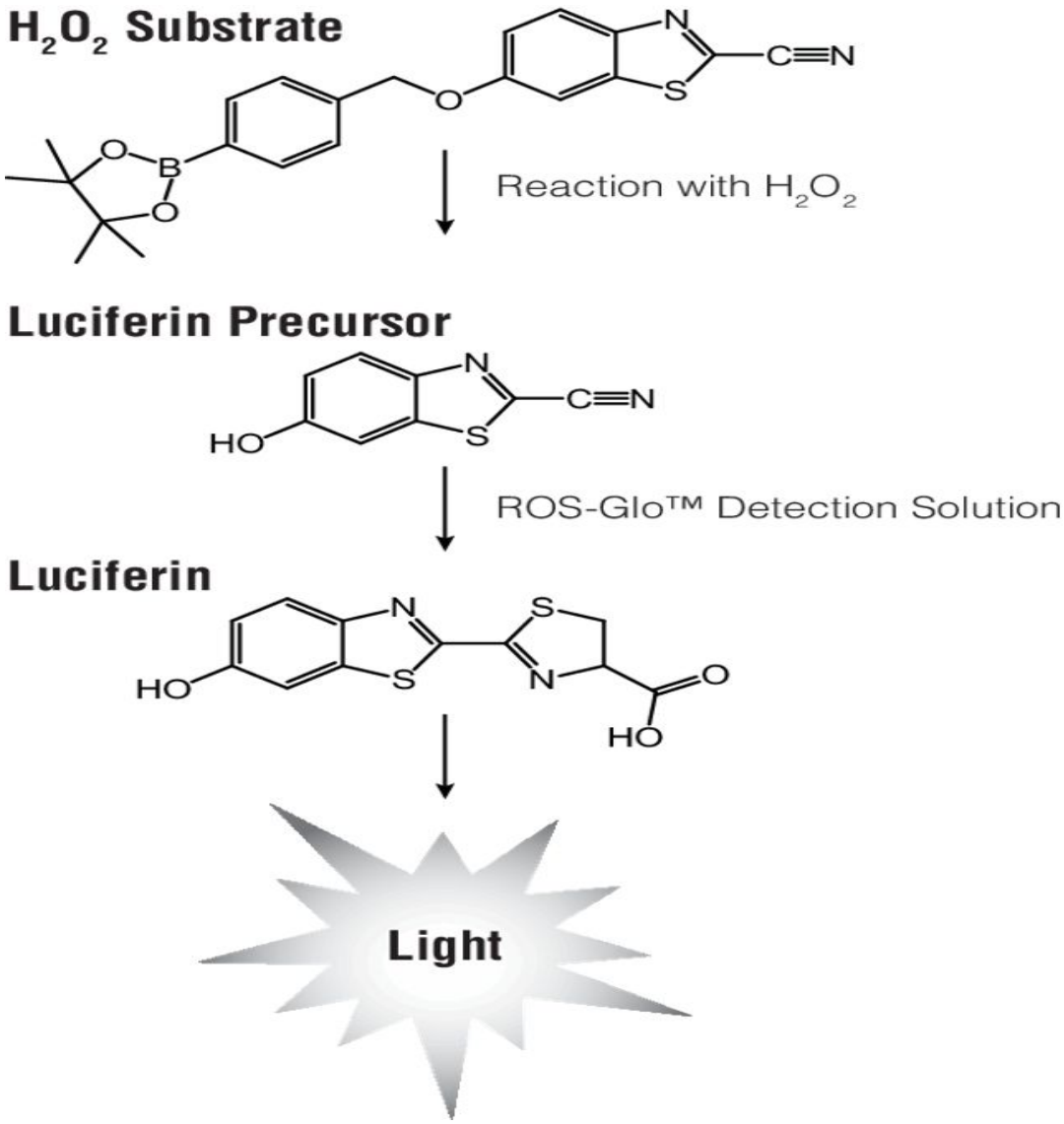

Figure 2.3. ROS-Glo assay principle

The addition of H_2O_2 substrate produces luciferin precursor as a result of the presence of H_2O_2. Then the addition of ROS-Glo™ detection reagent reacts with luciferin precursor generates a luminescent signal (Light) that can be detected by the plate reader. The luminescent signal is proportional to H_2O_2 level which corresponds to ROS level. Figure was adapted from Promega's manual protocol for the ROS-Glo assay.

2.15 Measurement of cytokine secretion

Cell culture supernatants were collected at specific times of post receptor ligation: 6, 12, 24, 36 and 48hrs, centrifuged, aliquoted and stored in -80°C. Secretion of IL-6, IL-8 and granulocyte-macrophage colony stimulating factor (GM-CSF) following LTβR and HVEM ligation was measured by using human specific monoclonal antibodies IL-6 (DY206-05), IL-8 (DY208-05) and GM-CSF kit (DGM00). Steps were followed as recommended by the manufacturer (R&D Systems).

2.15.1 Reagent preparation

All antibodies and standards were brought to room temperature and then were reconstituted and working dilutions were prepared and used immediately as recommended by the manufacturer's protocol.

2.15.2 Plate preparation

For IL-6 and IL-8 investigations, plates were coated with 100µL/well of prepared capture antibody in PBS (without carrier protein). For GM-CSF investigation, GM-CSF plate was pre-coated by the company and ready for blocking step. After plate coating, plates were sealed and incubated overnight at room temperature. Next day, each well was aspirated and washed with 400µL of wash buffer for three times and liquid was completely removed by inverting the plate and blotting it against clean paper towels to ensure good performance. Plates were then blocked by adding 300µL of blocking buffer to each well and incubated 1hr at room temperature; after incubation plates were washed three times as in previous step.

2.15.3 Assay procedure

After plate coating and blocking step, 100µL of sample supernatants or diluted standards in reagent diluent was added to each well. Plates were then covered with adhesive strip and incubated for 2hrs at room temperature. After incubation time, a washing step was repeated as previously. 100µL of the detection antibody (diluted in reagent diluent) was added to each well and plates were covered with adhesive strip and incubated for 2hrs at room temperature. Washing step was repeated and 100µL of working dilution of secondary antibody (Streptavidin-HRP) was added to each well and incubated for 20mins at room temperature in the dark. Washing step was repeated again as in previous step. Then 100µL of substrate solution was added to each well and incubated for 20mins at room temperature. After incubation for 20mins, 50µL of stop solution was added to each well and plates were gently tapped to ensure thorough mixing. Absorbance was measured at wavelength 455nm, data were analysed and presented as concentration in pg/mL.

2.16 Western blotting

Western blot is a powerful technique that is used to separate and identify proteins (from a mixture of proteins extracted from cells) according to their molecular weight. There are four main aspects for performing western blot: 1) quantify the protein concentration of cell lysate (by using Bradford Assay); 2) separate proteins by size using Sodium Dodecyl Sulphate-Polyacrylamide Gel Electrophoresis (SDS-PAGE); 3) protein transfer to solid to polyvinylidinedifluoride membrane (PVDF); and 4) immunolabelling of target protein using an appropriate primary and secondary antibody to visualise antibody binding.

2.16.1 Protein extraction

Cell lysates were prepared from treated cells with soluble agonists or from co-cultures. Culture medium was aspirated and then cells were washed two times with PBS to remove any medium cell debris and/or dead cells. Subsequently, sodium dodecyl sulphate (SDS) sample buffer was prepared and aliquoted as 1mL (see Appendix I). A working solution or complete lysate buffer was made by addition of Dithiothreitol (DTT) (DTT is a reducing agent). Also, protease inhibitor cocktail (PI) was added as dilution (1:500) with SDS. Complete lysate buffer was mixed very well and an appropriate volume was used; for example, 150µL was added per T75 flask, and 50µL per T25 flask or 6 well plates. Cell scraper was inserted into flasks to remove and collect the lysates from the flask surface or plates. Cell lysates were collected in eppendorf tubes and then were stored at -20°C for future use, or placed on ice to be immediately processed.

The following step was cell lysate sonication, as cell lysates were sonicated (at 75% amplitude for 10 seconds) and then were placed immediately back on ice for 30mins. Lysate suspension was centrifuged at a high speed of 13000-14000rpm at 4°C for 30mins. Supernatants were collected carefully without disturbing the pellets and aliquoted into small clean eppendorf tubes and stored at -20°C, or kept at -80°C for long-term storage.

2.16.2 Protein Quantification

Protein concentration of cell lysates was determined for each individual sample by using the Bradford Assay (Coomassie protein reagent assay kit, Pierce). Cell lysates were diluted as (1:12.5) with dH_2O in small eppendorf tubes. Protein standards curve of 0-1000µg/mL BSA (Pierce) were added separately as 10µL, dH_2O was served as a blank (zero concentration), and protein standards were 25, 125, 250, 500, 750 and 1000 µg/mL. Samples and standards were added in duplicate in 96-well flat bottom plates. Subsequently, 200µL of ambient temperature Coomassie reagent was added to each well and mixed gently (bubbles were avoided). The addition of Coomassie reagent generates a blue colour, which corresponds to protein sample concentration. The absorbance was then measured at 595nm using a FLUOstar OPTIMA (BMG Labtech) plate reader (Thermo Fisher) against a dH_2O control data and to plot a standard curve for the BSA from MARS analysis software 2.0 (BMG Labtech) (Figure 2.4).

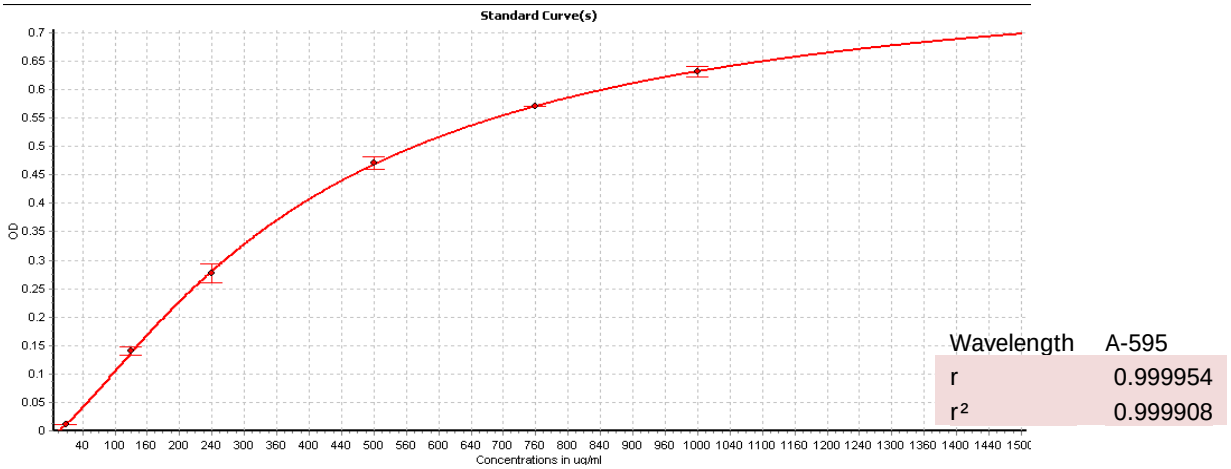

Figure 2.4. An example of protein Standard Curve

Standard curve of used standards solutions 25, 125, 250, 500, 750 and 1000µg/mL. Absorbance was measured at 595nm. Error bars were applied as shown.

2.16.3 Sodium dodecyl sulphate Polyacrylamide gel Electrophoresis (SDS-PAGE)

A total of 20 or 40µg of protein lysate was calculated (see Table 2.9) and was then diluted with dH_2O to make a total volume of 13µL. Following this, lithium dodecyl sulphate (LDS) sample buffer (which allows for maximum activity of the reducing agent) and reducing agent (to reduce disulphide bonds in protein samples for optimal separation by PAGE) were diluted (4x) and (10x), respectively. Samples were centrifuged and then were denatured by warming up to 70°C for 10mins in a water bath. After incubation time, 10-well Novex™ electrophoresis pre-cast gels were placed into an XcellSurelock™ mini-cell upright electrophoresis tank. MES running buffer was prepared (1:20) with dH_2O mix well and was then poured into the inner and outer chambers within the tank. NuPAGE™ antioxidant was added (to prevent re-oxidation of sensitive amino acids) to the inner chamber prior to loading of the samples (cathode). All-Blue Precision PlusProtein™ standard was loaded alongside as a marker of protein size and sample lysates were loaded into the other wells (Table 2.9).

Where available a positive control lysate known to express the protein of interest was included and used for some experiments. The gel was then run at 200V for 35mins. This process allowed proteins to be separated according to their molecular weight (MW).

	UCC cell lines			CRC cell lines			CRC Transfected	Fibroblast cell lines	
	RT4	**RT112**	**EJ**	**SW480**	**HT29**	**HCT116**	**SW480CD40**	**3T3-Neo**	**3T3-CD40L**
µg/mL	5159.5	6392.7	4188.6	2127.4	5869.2	1499.7	9652.8	3044.1	3234.2
µg/µL	5.1	6.3	4.1	2.1	5.8	1.4	9.6	3	3.2
sample µL	**3.9**	**3.1**	**4.8**	**9.4**	**3.4**	**13.34**	**2.1**	**6.6**	**6.2**
dH_2O µL	**9.1**	**9.9**	**8.2**	**3.6**	**9.6**	**0**	**11**	**6.4**	**6.8**
Final µL	13	13	13	13	13	13.34	13	13	13
RA (µL)	2	2	2	2	2	2.05	2	2	2
LDS µL	5	5	5	5	5	5.13	5	5	5
Total µL	**20**	**20**	**20**	**20**	**20**	**20.52**	**20**	**20**	**20**

Table 2.9. Calculations for protein concentration from cell lysates

Samples of cell lysates were diluted with dH_2O in small eppendorf tube (dilution factor 12.5) and mix well (for the purpose of protein concentration dilution and to ensure the protein concentration readout by plate reader). 10µL of diluted lysates and protein standards were placed in Microplate (96 well) in duplications. 200µL of Commassie blue reagent was added and incubated between 5-10mins at room temperature. The absorbance of protein concentration was then measured by using a FLUOstar OPTIMA (BMG Labtech) plate reader at 595nm against dH_2O control. MARS analysis software 2.0 (BMG Labtech) was used to plot a standard curve for the BSA and to estimate the protein concentration for each sample dH_2O = de-ionised water. RA = Reducing agent. LDS = lithium dodecyl sulfate.

2.16.4 Electrophoretic membrane transfer

Before the end of SDS-PAGE, blotting pads and filter paper were soaked in transfer buffer and pre-cut (size of blot pad normally) transfer membrane Immobilon-FL polyvinylidinedifluoride membrane (PVDF) was dipped in 10mL of methanol in a square dish for a few seconds, and then immediately rinsed with dH_2O and then kept in transfer buffer (see Table 2.10).

Once SDS-PAGE complete, the gel was taken from tank and the gel knife was used to open the cassette and unwanted and extra gel was cut and then placed on an equal cut of soaked filter paper on top. The gel was loosened using the gel knife and slit at the bottom, and with the aid of gravity the gel was gently prised off onto a blot pad, so the filter paper was at the bottom. Forceps were used to place a transfer membrane on top of the gel that was protected with more filter paper, and then air bubbles were removed very carefully. The gel membrane sandwich was assembled cathode to anode as follows: 3x blot pads, filter paper, gel, PVDF membrane, filter paper, 3x blot pads and blot module was secured into the ‘x cell sure lock system’ and then filled with transfer buffer. The outer chamber was filled with ice-cold dH_2O and the transfers were performed on ice at 25V for 2hrs.

2.16.5 Immunolabelling and detection of antibody binding

Membranes were blocked in 50:50 (v/v) Odyssey blocking buffer with 10mM TBS pH 7.4 on a plate rocker for 1hr at room temperature to block for non-specific antibody binding. Once the primary antibody was pre-diluted (as required and as recommended by the manufacturer's protocol) in TBS+0.1% (v/v) Tween-20 to total volume 8mL and then was poured on membranes and incubated on a rocker overnight at 4°C. On the second day, membranes were washed quickly with TBS only, and then followed with three washes in TBS/Tween-20 (0.1%) (v/v) for 5mins for each wash. Subsequently, secondary antibody was pre-diluted with TBS/Tween-20 (0.1%) (v/v) (secondary antibody dilution can vary) and incubated with membranes for 1hr and then placed on a rocker (at speed between 10-20rpm) at room temperature. After incubation, three washes were repeated and then TBS buffer was added to membranes, before visualisation using an Odyssey™ Infra-red Imaging system (Li-Cor). To detect this correctly, membranes were placed face down on the Li-cor scanner protein. Equal loading protein loading was confirmed by using several loading control antibodies such as β-actin or Cytokeratin (CK) -8 or -18.

Item	Cat	Application	Supplier
DTT	D9779-5g	Cell lysate	Sigma
Protease inhibitor cocktail set	535140-1	Cell lysate	VWR
Cell scraper individually wrapped sterile 250mm handle x 18mm blade	11597692	Cell lysate	Fisher
Coomassie blue protein assay kit	PN23236	Protein assay	Fisher
BSA pre-diluted protein assay	PN23208	Protein assay	Fisher
NuPAGE Sample Reducing Agent (10x)	NP0009	WB	Invitrogen
NuPAGE LDS sample Buffer (4x)	NP0007	WB	Invitrogen
NuPAGE antioxidant	NP0005	WB	Invitrogen
NUPAGE 4-12% BT GEL 1.0MM10W	NP0321BOX	WB	Invitrogen
NuPAGE MES SDS Running buffer (x20)	NP0002	WB	Invitrogen
Improved Millipore membrane (PVDF)	fdr-523-020q	WB	Fisher
Whatman Filter paper	11435248	WB	Fisher
Odyssey® Blocking Buffer (PBS), 500mL	927-40000	WB	Li-Cor
Precision plus all blue protein standards	161-0373	WB	Biorad

Table 2.10. Reagents and materials for immunoblotting

2.17 Statistical Analysis

Results were collected and analysed by using Microsoft Excel. All data were presented as mean values and standard deviation ±S.D. Statistical analysis was performed by using statistical software (Minitab 17). P-value was generated by using two tailed paired student t-test.

Chapter 3

The effects of LTβR and HVEM signalling triggered by soluble receptor agonists in carcinoma cells

3.1 Introduction

LT receptors LTβR and HVEM (and their cognate ligand LIGHT) belong to the TNF family. Both LT receptors are widely expressed in a number of immune and non-immune cells (Fan et al., 2006; Kwon et al., 1997; Sedy et al., 2004; Ware, 2005). The ligand LIGHT is expressed on myeloid cells, primary immature DCs and on activated T cells and macrophages (Harrop et al., 1998b; Mauri et al., 1998; Morel et al., 2000). LTβR and HVEM signalling plays roles in regulating cell fate both in the immune system and in non-lymphoid tissues (Albarbar et al., 2015; Ware, 2005). For example, the binding of LIGHT to HVEM on T cells functions as a co-stimulatory signal for T cell activation (Harrop et al., 1998a; La et al., 2002; Wang et al., 2001b), whereas LTβR and HVEM signalling in tumour cells through receptor engagement by LIGHT may lead to cell death (Zhai et al., 1998). The majority of previous studies on LT-related effects on epithelial cells have focused on the role of activation of LTβR and HVEM using almost exclusively the colorectal cell line HT29. Such studies have shown that soluble agonists can induce cytotoxicity only in the presence of IFN-γ. LTβR activation by agonistic multivalent antibody BS-1 induces growth inhibition and soluble LIGHT (which activates both LTβR and HVEM) combined with IFN-γ triggers cell death in HT29 cells (Hu et al., 2013; Zhai et al., 1998).

As LT receptor expression and signalling have been demonstrated only in limited carcinoma cells, we aimed in this chapter:

- To perform flow cytometry to investigate the protein expression levels of LT receptors LTβR and HVEM in a panel of CRC and UCC carcinoma cell lines.
- To examine the regulation of LT receptors on carcinoma cells by pro-inflammatory cytokine (IFN-γ and TNF-α) treatment.
- To perform activation of LTβR and HVEM by LT agonists on the panel of carcinoma cells and compare them to the widely used HT29 cells.

3.2 Detection of LT receptors and their regulation by pro-inflammatory cytokines on carcinoma cells

The surface expression of LT receptors (LTβR and HVEM) in parallel with other TNFRs (TNFRI, TNFRII and CD40) and its regulation by pro-inflammatory cytokine were investigated on a panel of carcinoma cells of CRC and UCC origins, alongside expression of intercellular adhesion molecule-1 (ICAM-1). Studies demonstrated that TNFRs can be regulated by pro-inflammatory cytokines (IFN-γ or TNF-α); in particular, CD40 expression was shown to be upregulated in epithelial cells following IFN-γ or TNF-α treatment (Bugajska et al., 2002; Schwabe et al., 2001; Wingett et al., 1998). Moreover, Rissoan and colleagues demonstrated that IFN-γ is more effective than TNF-α in upregulation CD40 expression in positive cells (Rissoan et al., 1996). Like CD40, ICAM-1 has been shown to be expressed on tumour cells and upregulated following IFN-γ treatment (Duff et al., 1997; Look et al., 1994).

To examine the expression of LT receptors, CD40 and ICAM-1 and their regulation by IFN-γ or TNF-α in the panel of CRC and UCC lines, epithelial cells were seeded and either left untreated or were treated with 1000U/mL of IFN-γ or TNF-α in 6-well plates and incubated for 48hrs. For flow cytometry analysis, cells were harvested and labelled with mAb for detection of LTβR, HVEM, TNFRI, TNFRII, CD40 and ICAM-1 for the panel of CRC and UCC cells. Gating strategies for flow cytometry results are shown in Figure 3.1 and representative results are shown in Figure 3.2. Moreover, microscopy images were taken to observe any morphological changes (as an indication of cytotoxicity) in response to IFN-γ or TNF-α treatment compared with untreated cells (Figure 3.3)

LTβR and HVEM expression were detected in CRC lines HT29, SW480 and HCT116 (Figure 3.2a), and in UCC lines RT4, RT112 and EJ (Figure 3.2b). By contrast, CD40 expression was only detected in HCT116 and EJ cells but not in HT29, SW480, RT4 and RT112 cells, in agreement with previous reports (Georgopoulos et al., 2006; Georgopoulos et al., 2007). TNFR-I, TNFR-II and ICAM-1 expression was detected in some CRC and UCC cell lines (Figure 3.2).

Following cell treatment with pro-inflammatory cytokines (IFN-γ and TNF-α), the flow cytometry results showed that IFN-γ treatment upregulated LTβR expression in RT112, whereas TNF-α treatment upregulated LTβR expression in RT4 and HCT116 cells compared with untreated cells (Figure 3.2). There was upregulation of HVEM expression in HT29, SW480, HCT116, RT4, RT112 and EJ cells in response to IFN-γ treatment compared with untreated cells. By contrast, TNF-α treatment increased HVEM expression in HT29, HCT116, EJ and RT4 cells (Figure 3.2). As expected and in agreement with previous reports (Georgopoulos et al., 2006; Georgopoulos et al., 2007), EJ and HCT116 cells showed an increase in CD40 expression following IFN-γ treatment (Figure 3.2), whilst treatment with neither IFN-γ nor TNF-α could induce CD40 expression in CD40-negative cells. A massive upregulation of ICAM-1 expression was observed in all treated CRC and UCC cell lines with IFN-γ, with the exception of RT4 cells, which showed downregulation of ICAM-1 but ICAM-1 expression was indeed enhanced by TNF-α treatment in RT4 cells (Figure 3.2).

Following cell treatment with IFN-γ and TNF-α, phase-contrast microscopy showed that IFN-γ and TNF-α exhibited cell growth inhibitory effects on bladder lines RT112 and RT4 (Figure 3.3). IFN-γ and TNF-α treatment appeared to promote cell growth or had no effects on the cell growth of HT29, SW480, HCT116 and EJ cells (Figure 3.3). Our observations are in agreement with a study which demonstrated that there are some carcinoma cells types (of the bladder) where TNF-α can be growth-promoting (Bugajska et al., 2002).

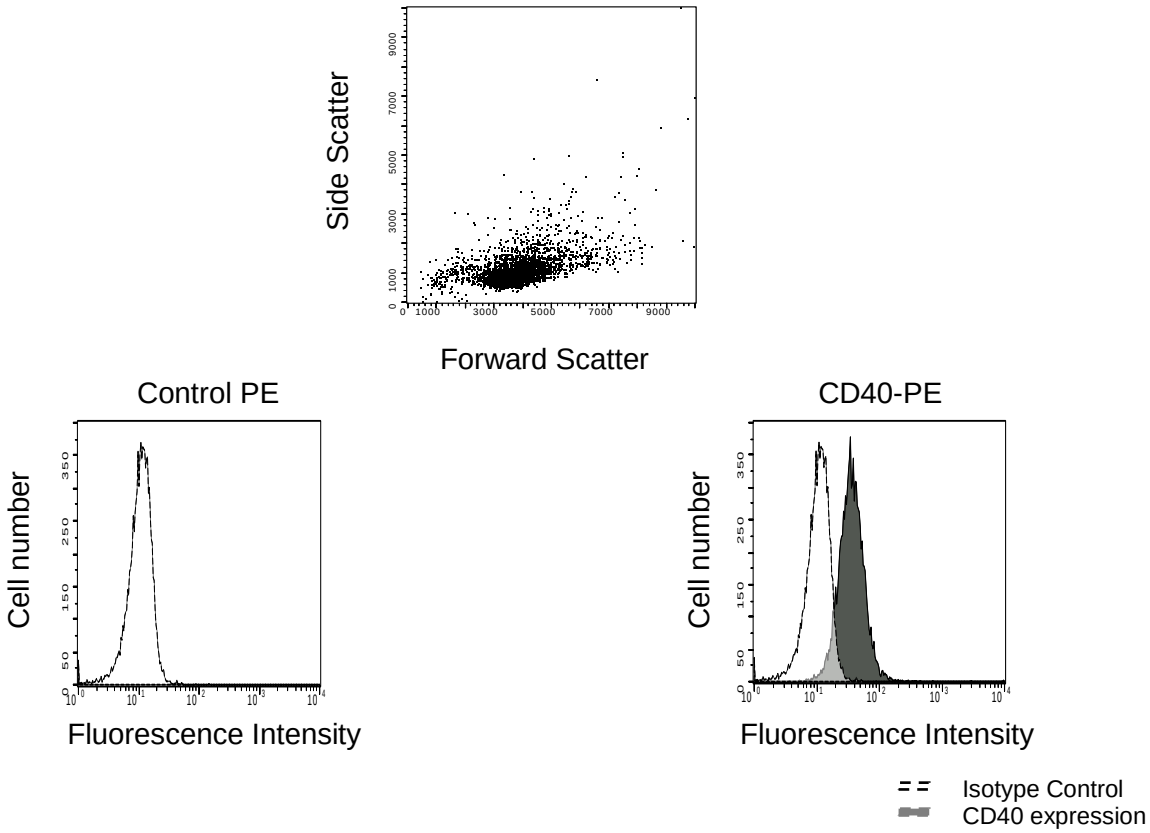

Figure 3.1. Gating strategies during flow cytometry to detect protein expression on carcinoma cells

Following acquisition, fluorescence intensity was determined following gating on viable populations based on forward scatter and side scatter properties, as indicated in R1 in the top histogram. Data shown were derived from the HCT116 cell line. Control isotype antibody PE was used (dashed white left histogram). CD40 expression was determined by using PE-conjugated anti-CD40 antibody (filled grey histograms) and this was compared with control PE.

a.

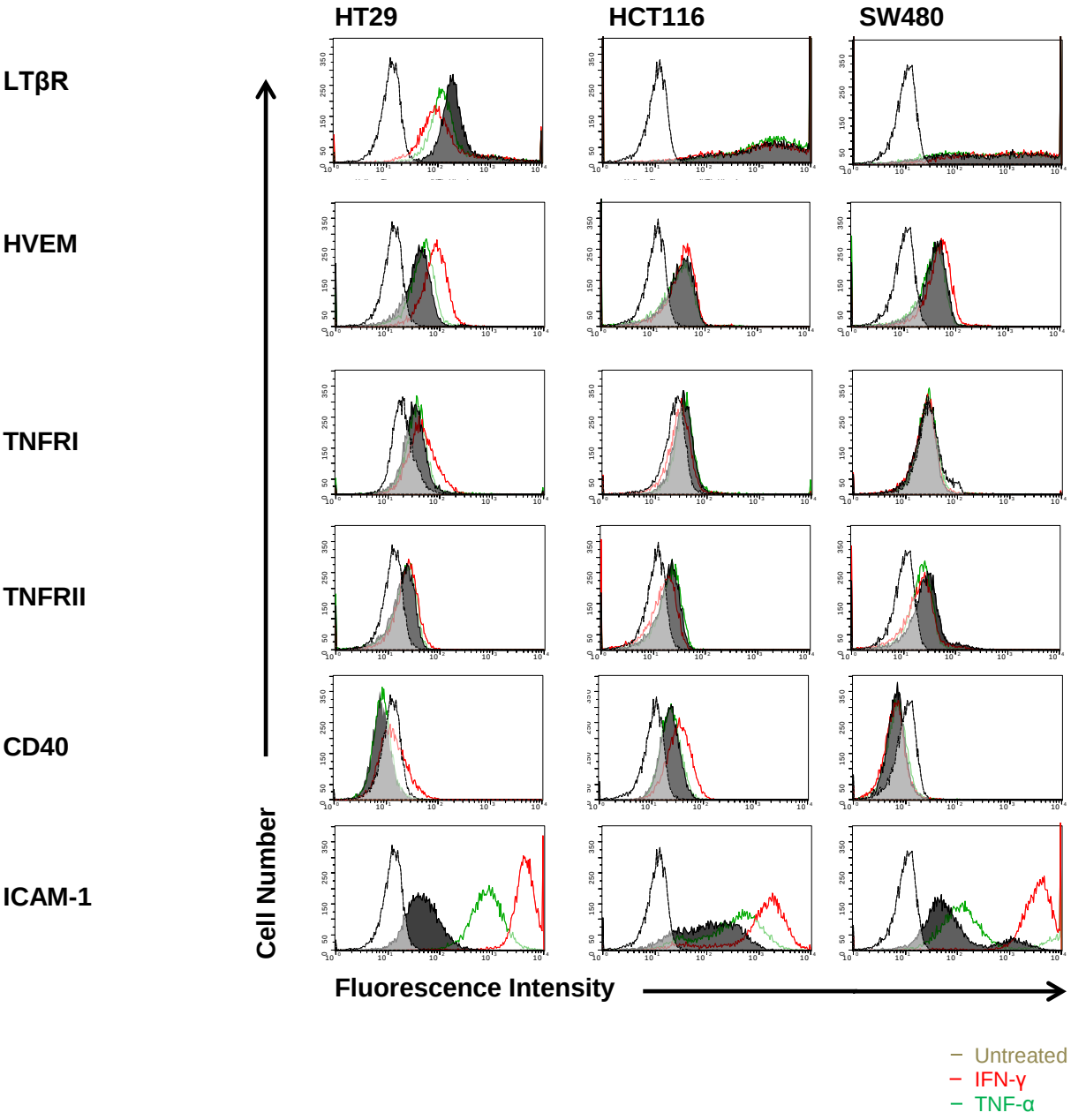
HT29
HCT116
SW480
LTβR
HVEM
TNFRI
TNFRII
CD40
ICAM-1
Cell Number
Fluorescence Intensity
Untreated
IFN-γ
TNF-α

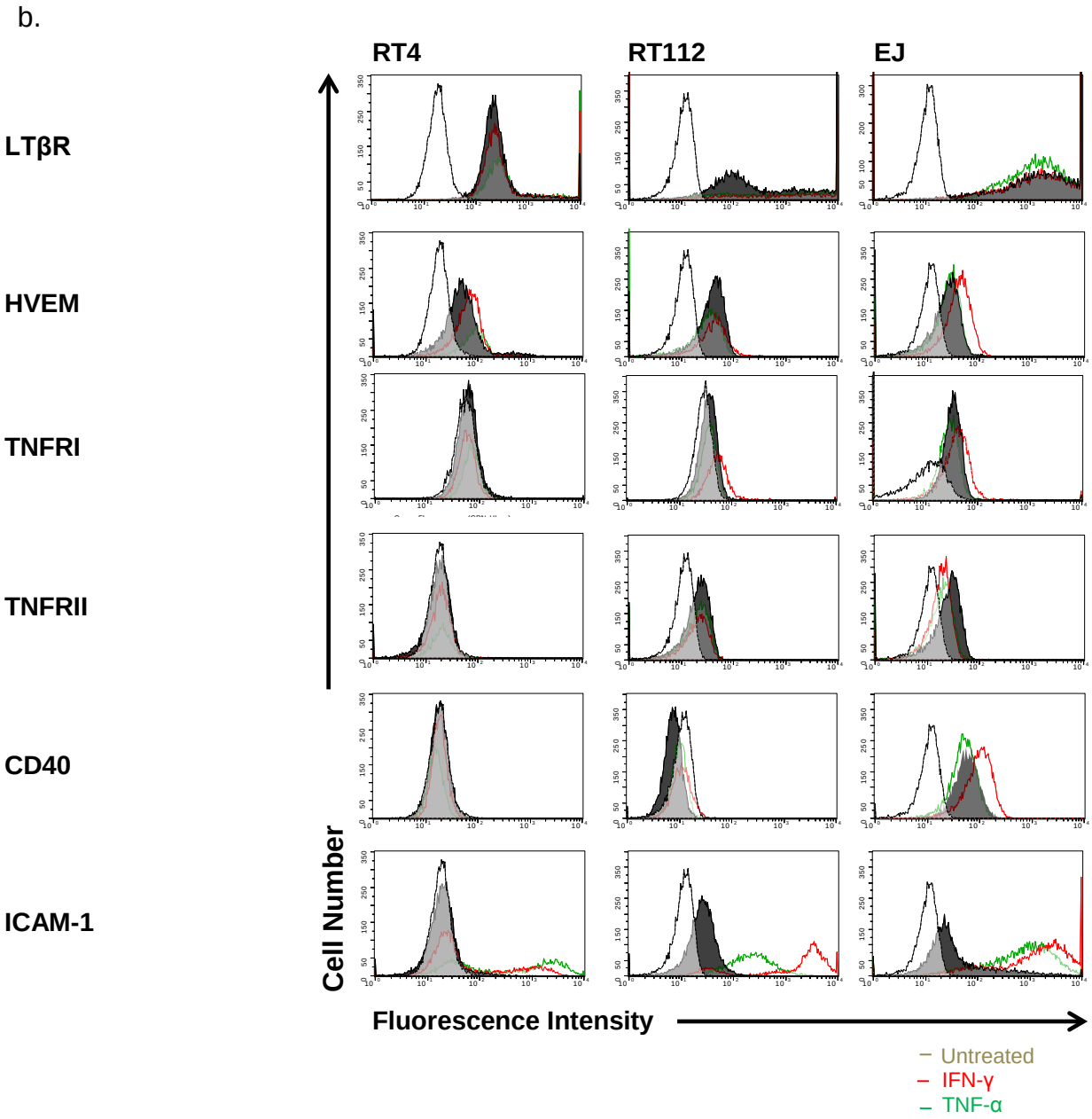

Figure 3.2. The regulation of expression of LT receptors and other TNFRs by IFN-γ and TNF-α

Cells were seeded and left untreated or were treated with IFN-γ or TNF-α for 48hrs in 6-well plates. Cells were harvested and labelled with anti-LTβR, TNFRII, HVEM, CD40 and ICAM-1 directly and PE-conjugated antibody except for TNFRI, which involved labelling with primary TNFRI and followed with Alexa fluor 488-conjugated secondary antibody. Matched isotype was also used as control (open dashed white histogram), whilst omission of primary antibody was performed for TNFRI labelling. Untreated cells (filled grey histograms) were treated with 1000U/mL of IFN-γ (red histograms) or TNF-α (green histograms) and then analysed by flow cytometry after 48hrs and at least 10,000 cells were collected: a. CRC cell lines b. UCC cell lines.

a.

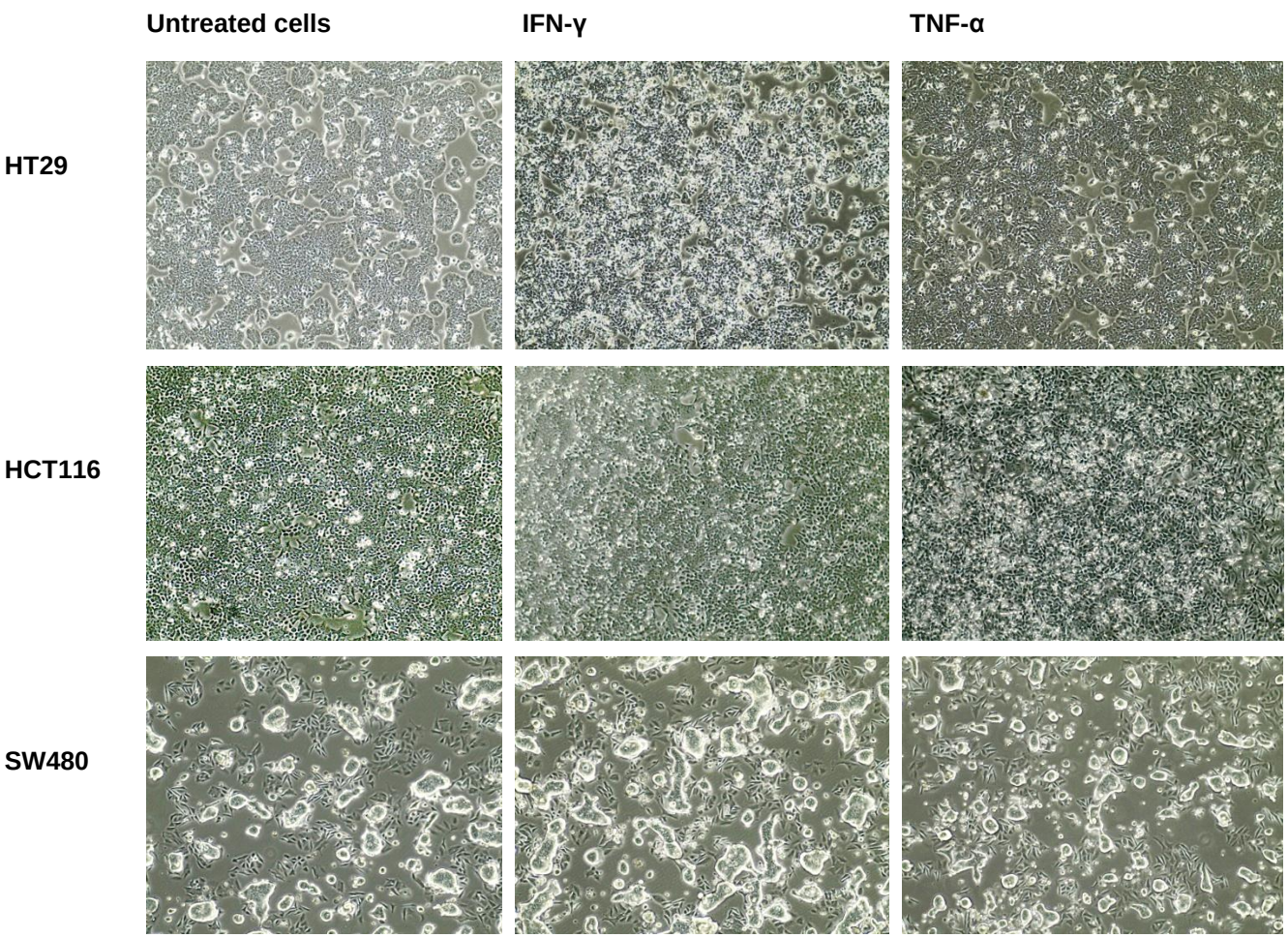

b.

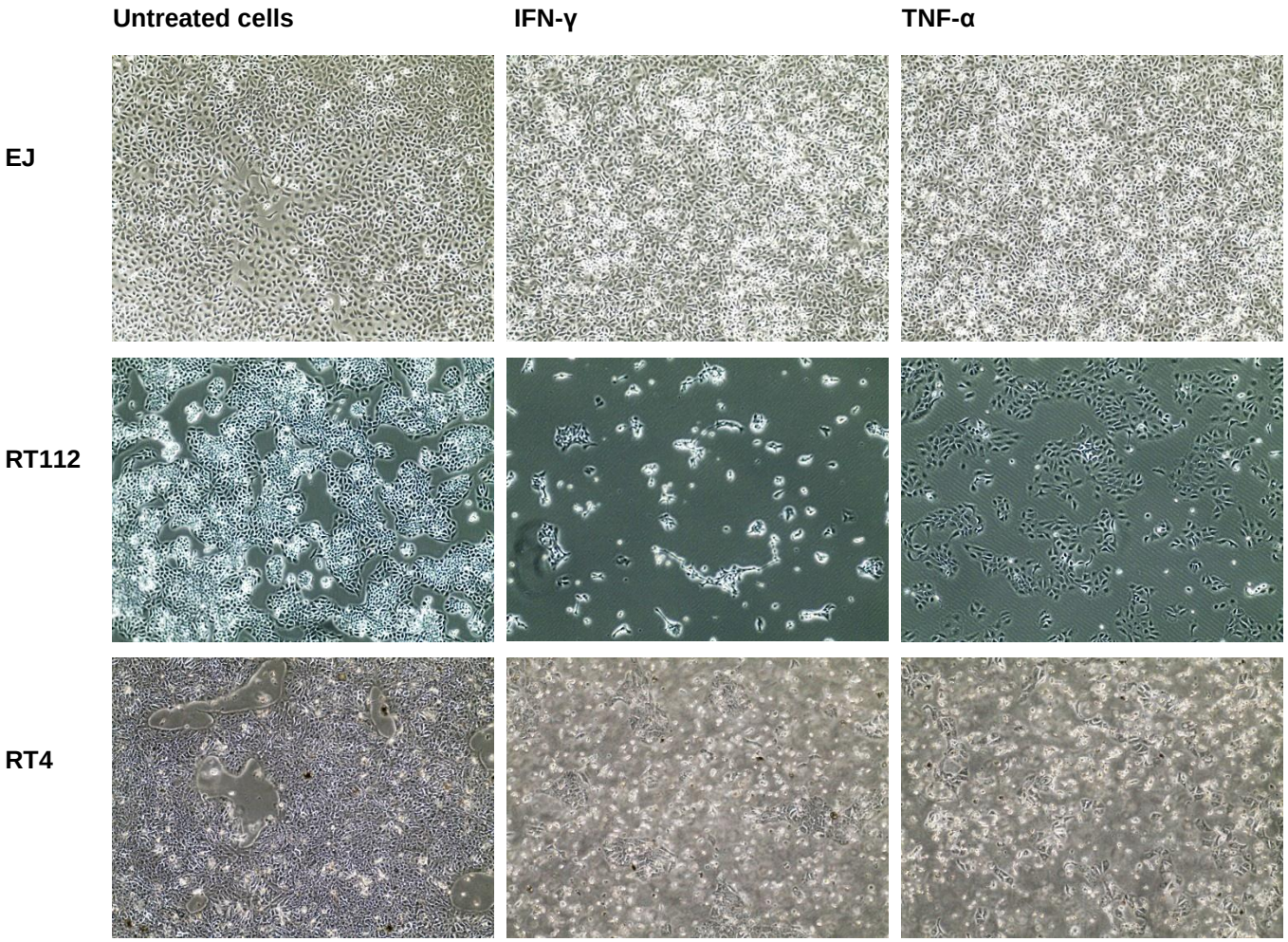

Figure 3.3. Microscopy images of untreated and treated cells with IFN-γ and TNF-α

Cells were seeded in 6-well plates overnight. On the following day, cells were treated with 1000U/mL of either IFN-γ or TNF-α and incubated for 48hrs at 37°C. Figures show untreated cells, treated cells with IFN-γ (1000U/mL) and treated cells with TNF-α (1000U/mL): a. shows CRC cell lines (HT29, HCT116 and SW480) while b. shows UCC cell lines (EJ, RT112 and RT4), as indicated. Photos were taken at magnification a 100x using an EVOSXL inverted microscope (PeqLab).

3.3 Activation of LT receptors by soluble agonists

Based on the finding that all cell lines are positive for LTβR and HVEM expression, the effects of soluble LT agonists were tested on the carcinoma cells above as we have previously extensively characterised them for their responses to other TNFR members and particularly CD40 (Bugajska et al., 2002; Georgopoulos et al., 2007; Hill et al., 2008) and compared them to the widely used HT29 cells. To induce activation of LTβR alone or activation both of the LT receptors LTβR and HVEM on target cells, the following reagents were used:

a. Agonistic antibody [tetravalent (BS-1)] (Browning et al., 1996) to activate LTβR.
b. Soluble ligand (commercially available recombinant human trimeric LIGHT) for activating both LTβR and HVEM on the target cells.

In some experiments, to enhance the effects of the agonists, cells were treated with agonist (BS-1 or soluble LIGHT) plus IFN-γ or cycloheximide (CHX). Following cell treatment, the effects of LT agonists were determined by utilising various assays including: MTS (Promega Cell Titer assay), CytoTox-Glo (Promega CytoTox-Glo Cytotoxicity assay) and flow cytometry using Annexin-V and Propidium iodide (PI); however, due to space limitations, Annexin-V/PI data is not presented in this thesis.

3.4 Assessment of cytotoxicity by detection of changes in cell viability

3.4.1 LTβR activation using BS-1 antibody

Using the panel of CRC and UCC lines, we first activated LTβR on target cells by using agonistic antibody (BS-1) and determined whether the outcome of this activation is cell growth or cell death. Cells were treated with control antibody (MOPC-21) and agonistic antibody (BS-1) in the absence or presence of IFN-γ (Chapter 2 section 2.13). IFN-γ is a cytokine that enhances inflammation by the upregulation of the co-stimulatory molecules and it has also been shown to synergise and enhance the cytotoxicity of soluble agonists (IFN-γ titration can be found in Appendix II). Cell viability was determined and analysed as shown in Figure 3.4.

Treatment of cells with agonistic antibody BS-1 alone did not have significant effects on cell growth, unless combination of BS-1 and IFN-γ was employed. Our results showed that most cells are resistant to the BS-1; in some cells, growth was enhanced by BS-1 antibody, thus at certain concentrations the agonist showed a 'bi-phasic' effect (Figure 3.4).

a.

b.

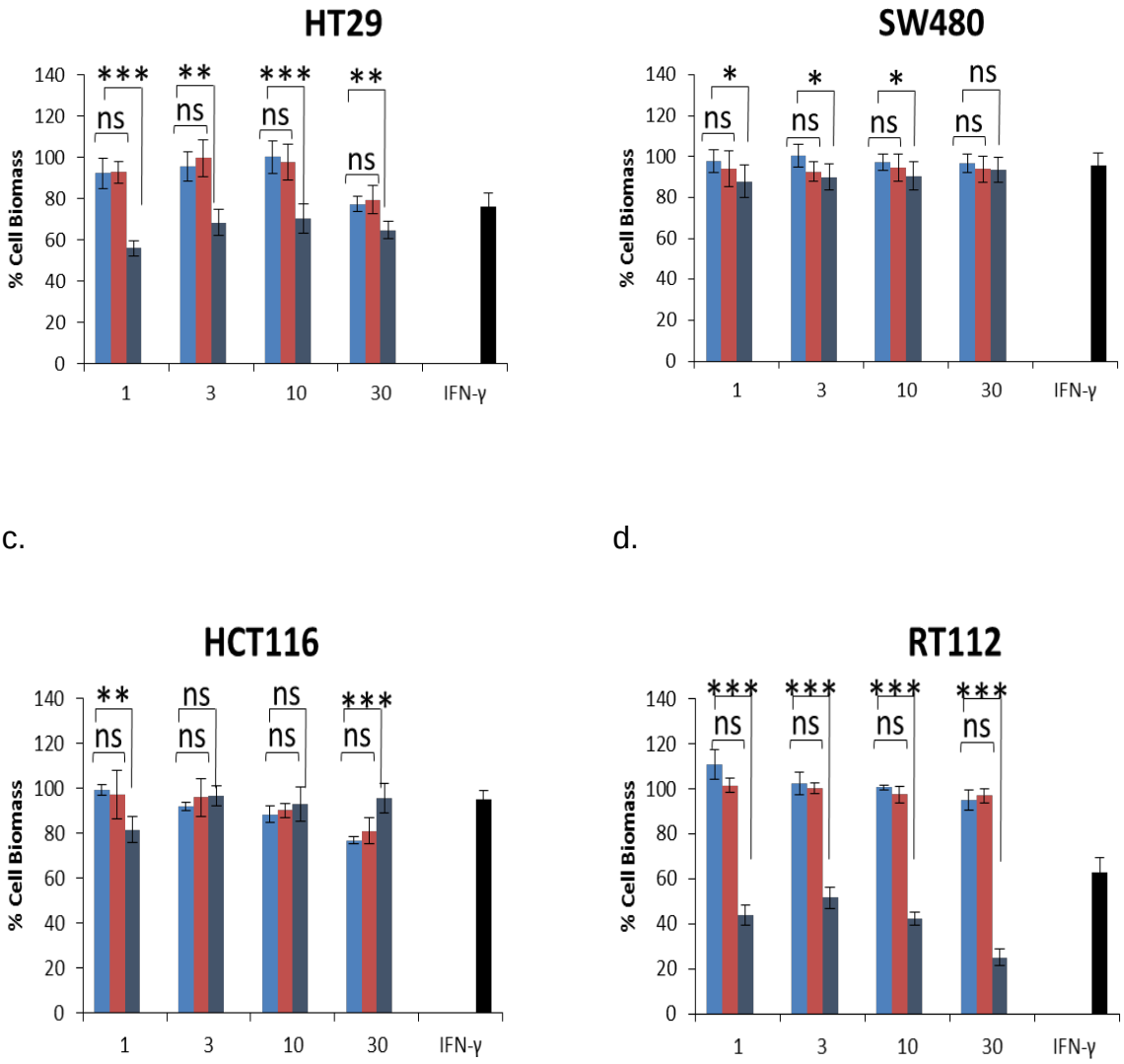
HT29
SW480
HCT116
RT112
% Cell Biomass
0
20
40
60
80
100
120
140
1
3
10
30
IFN-γ
ns
*
**
***
Antibody Conc. µg/ml
MOPC-21
BS-1
BS-1/IFN-γ
IFN-γ (200U/ml)

c.

d.

e.

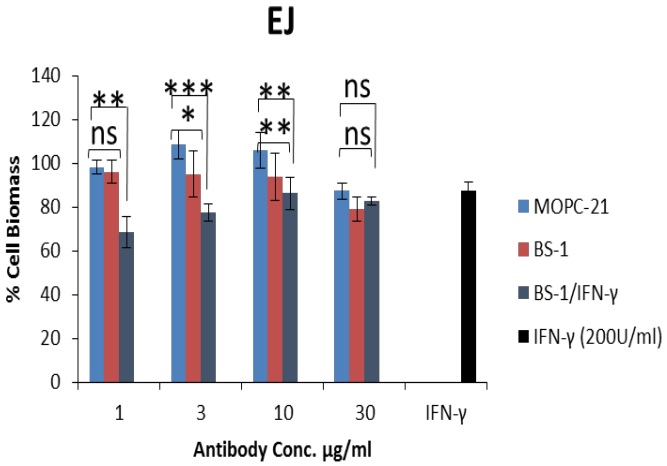

Figure 3.4. Effects of BS-1 and BS-1/IFN-γ treatment on carcinoma cell viability

HT29, SW480, HCT116, RT112 and EJ were seeded in 96-well plates alone or treated with control antibody (MOPC-21), BS-1, BS-1/IFN-γ or IFN-γ alone, as indicated, and incubated for 96hrs. 20µL of MTS solution was added to each well and incubated for approximately 4hrs. Cell viability was determined by a FLUOstar OPTIMA (BMG Labtech) plate reader at a wavelength of 492nm. a, b, c, d and e show HT29, SW480, HCT116, RT112 and EJ cells, respectively. Figures represent % cell biomass = (sample/control)*100. Data are represented as mean values of 4-5 replicates ±S.D. Stats: ns. non-significant; *, $p < 0.05$; **, $p < 0.01$; ***, $p < 0.001$, paired student t-test for MOPC-21 treated cells vs BS-1 or BS-1/IFN-γ treated cells, as indicated.

Cells were treated with BS-1 antibody combined with CHX aiming to potentially enhance the cytotoxic activity of BS-1 on target cells. CHX was used as it acts as an inhibitor for protein synthesis and is used in combination with pro-apoptotic agonists in many studies *in vitro*. Previous studies reported that CD40 ligation caused apoptosis when soluble CD40 agonist was combined with CHX (Bugajska et al., 2002).

Following initial pre-titration experiments, it was found that the addition of CHX to cultures was cytotoxic at concentrations 0.125µg/mL and above, compared with controls. Treatment of cells with 0.025µg/mL of CHX appeared to have little effect on cell viability (see Appendix II). Therefore, the concentration of 0.1µg/mL was selected and used in combination with soluble agonists as presented in Figure 3.5.

Our data showed that treatment with BS-1 in presence of CHX has significant effects on cell viability of HCT116 and EJ but no other cells. Our results suggest that activating one receptor may not sufficient to induce cell death for most cells even if IFN-γ and CHX were used. Therefore, both receptors LTβR and HVEM were activated using recombinant LIGHT.

a.

b.

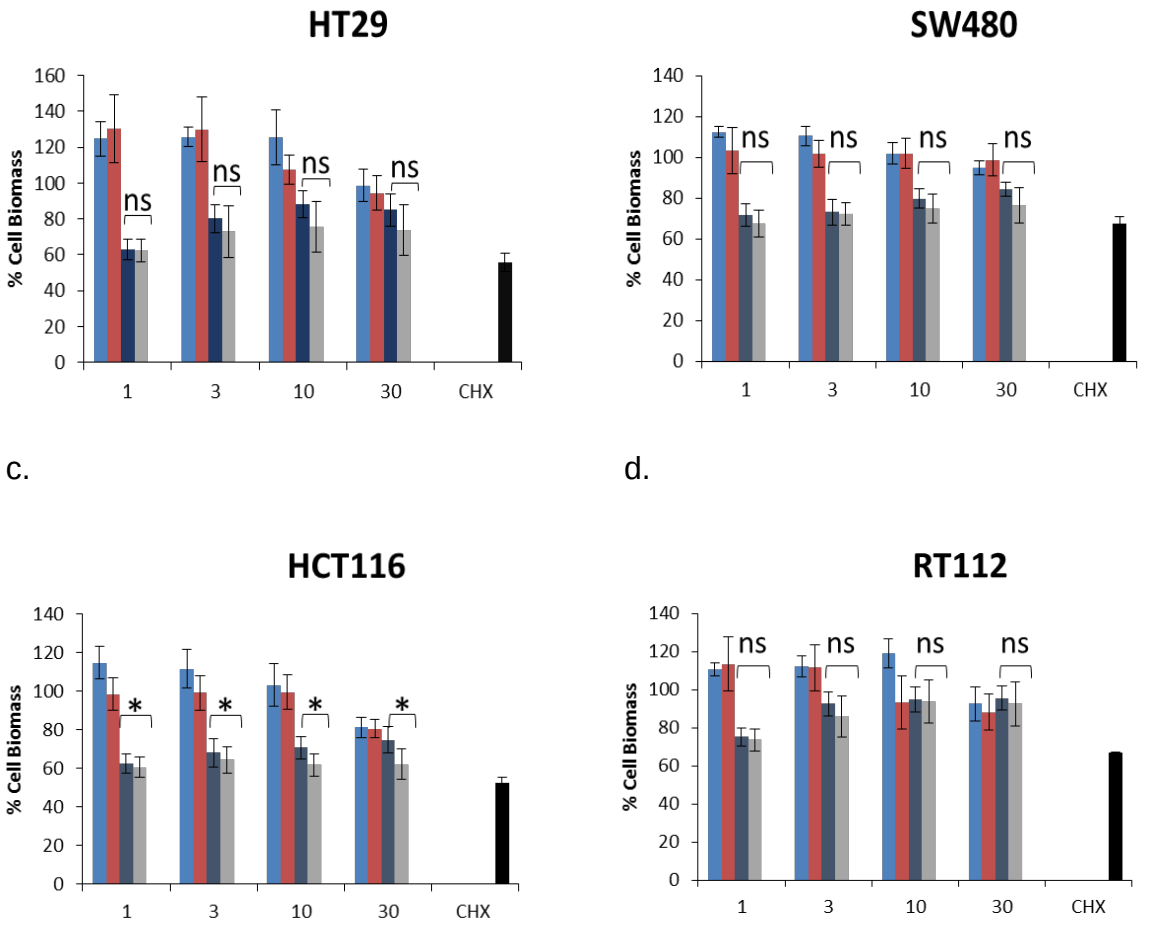
HT29
SW480
HCT116
RT112
% Cell Biomass
ns
*
1
3
10
30
CHX
Antibody Conc. µg/ml
MOPC-21
BS-1
MOPC-21/CHX
BS-1/CHX
CHX (0.1µg/ml)

c.

d.

e.

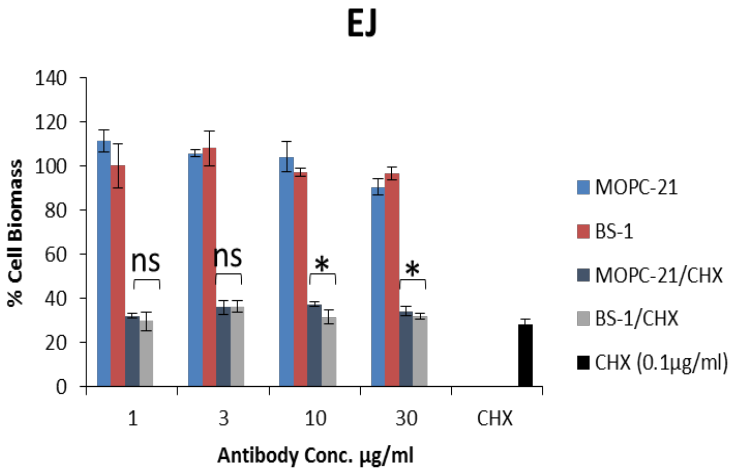

Figure 3.5. Effects of BS-1 and BS-1/CHX treatment on carcinoma cell viability

HT29, SW480, HCT116, RT112 and EJ were seeded in 96-well plates. Cells were treated with MOPC-21 and BS-1 alone or in combination with CHX, as indicated, and incubated for 96hrs. 20µL of MTS solution was added to each well and incubated for 4hrs. Cell viability was determined by a FLUOstar OPTIMA (BMG Labtech) plate reader at a wavelength of 492nm. a, b, c, d and e show HT29, SW480, HCT116, RT112 and EJ cells. Figures represent % cell biomass = (sample/control)*100. Data are represented as mean values of 3-4 replicates ±S.D. Stats: ns. non-significant; *, $p < 0.05$; **, $p < 0.01$; ***, paired student t-test for MOPC-21/CHX treated cells vs treated cells with BS-1/CHX.

3.4.2 LTβR and HVEM activation using recombinant LIGHT

In the previous section we demonstrated that BS-1, which activates only LTβR, induced weak cytotoxicity in some cells. Our findings suggest that activating LTβR alone without activating HVEM may not be sufficient to trigger cell signalling. Therefore, we treated cells with soluble recombinant LIGHT ligand, which interacts with and activates both receptors (LTβR and HVEM). A study by Zhai and colleagues reported that LIGHT is cytotoxic to tumour cells that express both LTβR and HVEM. Zhang and colleagues reported that human breast cancer cell lines (MDA-MB-231 and MCF-7), colon cancer cell line (HT29) and cervical cancer cell line (HT3) are the most susceptible cells to LIGHT-induced cell growth arrest, whereas embryonic kidney (293T), human breast cancer cell line (MCF-10A), prostate cancer (PC-3) and Jurkat cells were found to be resistant to LIGHT (Wu et al., 2003). It was also shown that cells which express both receptors were sensitive to LIGHT-induced cell growth inhibition, whereas cells that expressed only one of the receptors was found to be resistant to LIGHT-induced cell growth inhibition (Zhai et al., 1998).

CRC and UCC cells were treated with LIGHT and LIGHT-mediated cytotoxicity was examined in these cells and compared with HT29 cells. Treatment of cells with LIGHT in the absence or presence of IFN-γ was performed as in the case of the BS-1 agonistic antibody and data are shown in Figure 3.6.

a.

b.

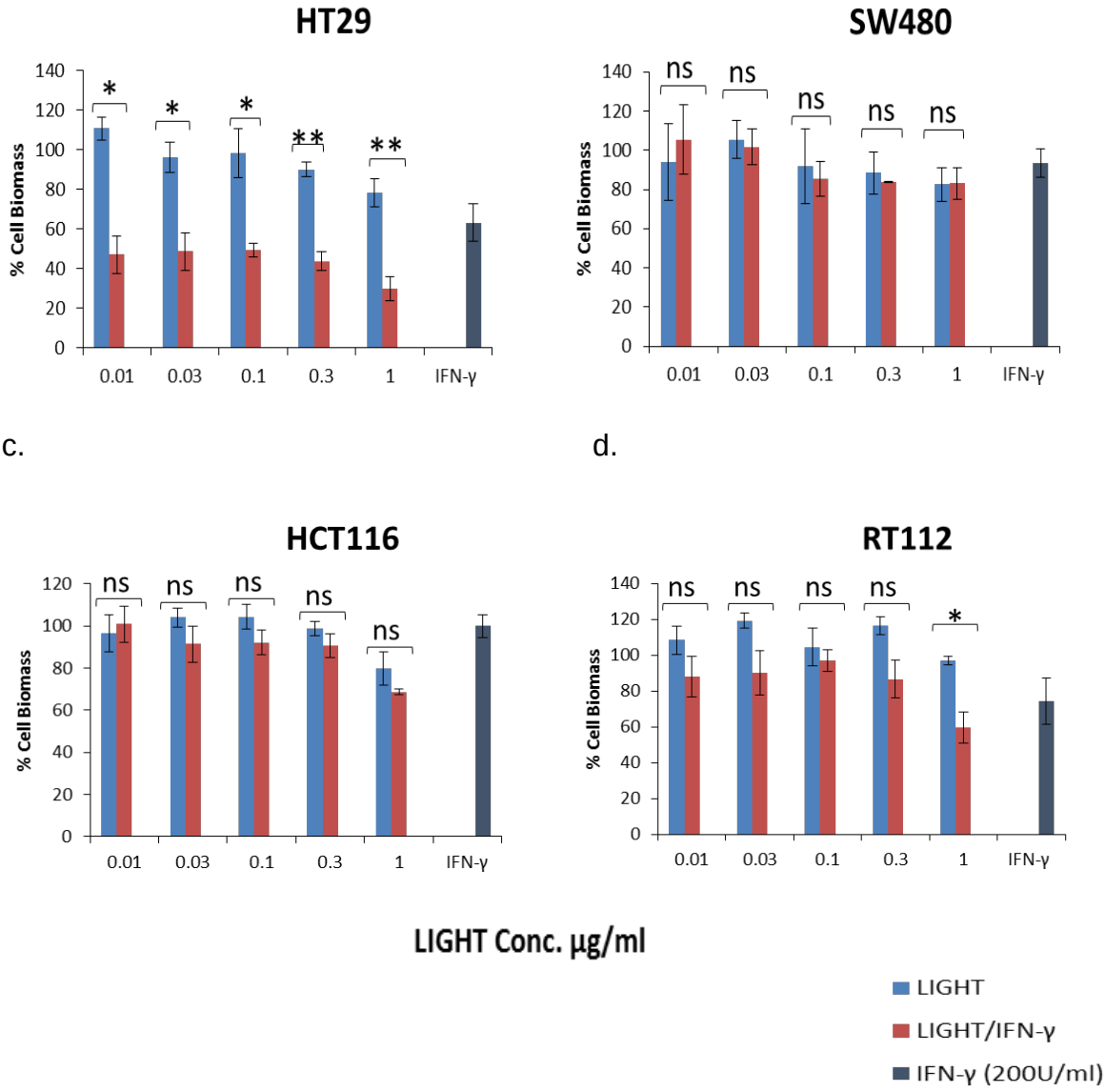
HT29
SW480
HCT116
RT112
% Cell Biomass
0
20
40
60
80
100
120
140
*
**
ns
0.01
0.03
0.1
0.3
1
IFN-γ
LIGHT Conc. µg/ml
LIGHT
LIGHT/IFN-γ
IFN-γ (200U/ml)

c.

d.

e.

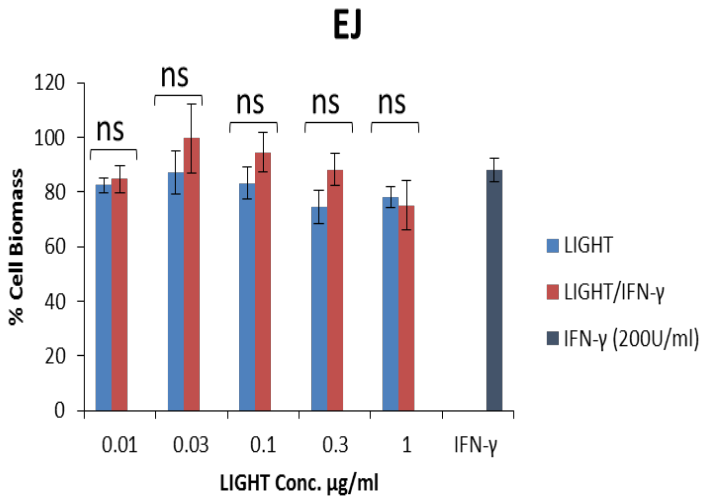

Figure 3.6. Effects of LIGHT and LIGHT/IFN-γ treatment on carcinoma cell viability

HT29, SW480, HCT116, RT112 and EJ were seeded in 96-well plates. Cells were treated with LIGHT in the absence or presence of IFN-γ, at different concentrations as indicated and incubated for 96hrs. 20µL of MTS solution was added to each well and incubated for 4hrs. Cell viability was determined by a FLUOstar OPTIMA (BMG Labtech) plate reader at a wavelength of 492nm. a, b, c, d and e show HT29, SW480, HCT116, RT112 and EJ cells. Figures represent % cell biomass = (sample/control)*100. Data are represented as mean values of 3-4 replicates ±S.D. Stats: ns. non-significant; *, $p < 0.05$; **, $p < 0.01$; ***, $p < 0.001$, paired student t-test for LIGHT treated cells vs treated cells with LIGHT and IFN-γ.

Our results showed that HT29 and RT112 are susceptible to LIGHT and combined LIGHT/IFN-γ treatment (Figure 3.6). Statistically, LIGHT/IFN-γ treatment significantly inhibited cell growth of HT29 and RT112 cells. SW480 cells appeared to be resistant to LIGHT and LIGHT/IFN-γ treatment (Figure 3.6). Treatment with LIGHT alone shows little effects on reduction of cell viability of EJ and HCT116 cells. Notably, in some cells growth was enhanced by low concentrations of LIGHT alone and thus showing 'bi-phasic' effects.

As there is a possibility that the cytotoxicity of LIGHT/IFN-γ may be dose-dependent on IFN-γ concentration and based on the differential effect results of IFN-γ on our cells, we next treated our cells with LIGHT with various concentrations of IFN-γ (at 60, 120 and 180U/mL). This allowed us to determine the maximum cytotoxicity effects of LIGHT in presence of IFN-γ (Figure 3.7).

a.

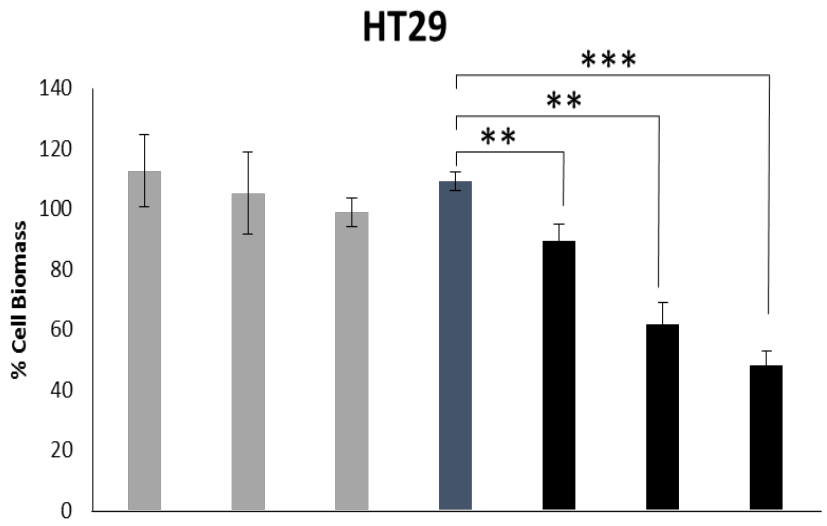
HT29
% Cell Biomass
140
120
100
80
60
40
20
0
***
**
**

b.

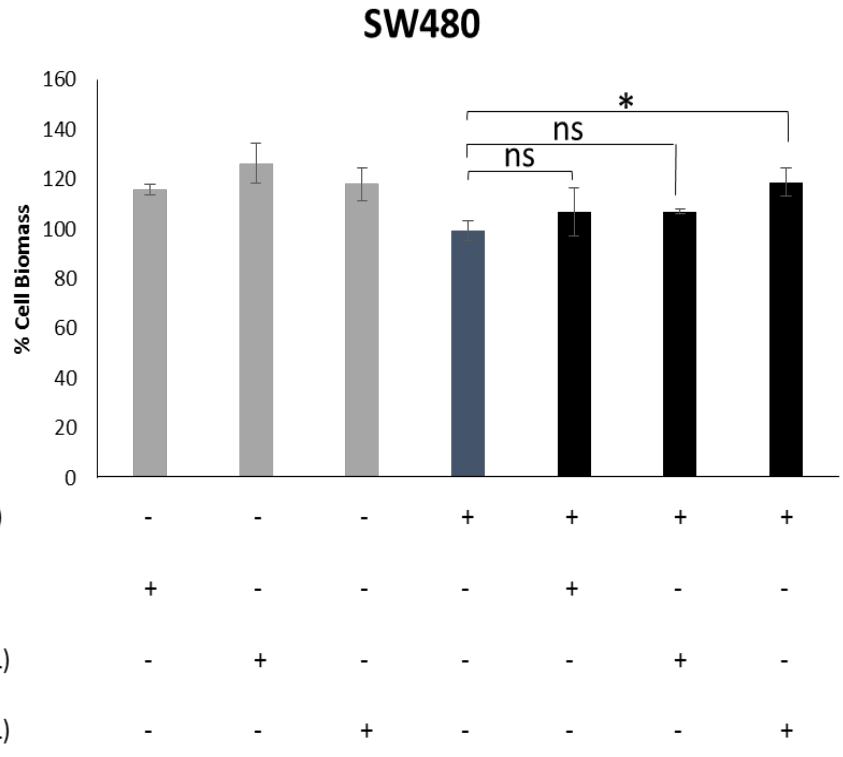
SW480
% Cell Biomass
160
140
120
100
80
60
40
20
0
*
ns
ns
LIGHT (1µg/mL) - - - + + + +
IFN-γ (60U/mL) + - - - + - -
IFN-γ (120U/mL) - + - - - + -
IFN-γ (180U/mL) - - + - - - +

c.

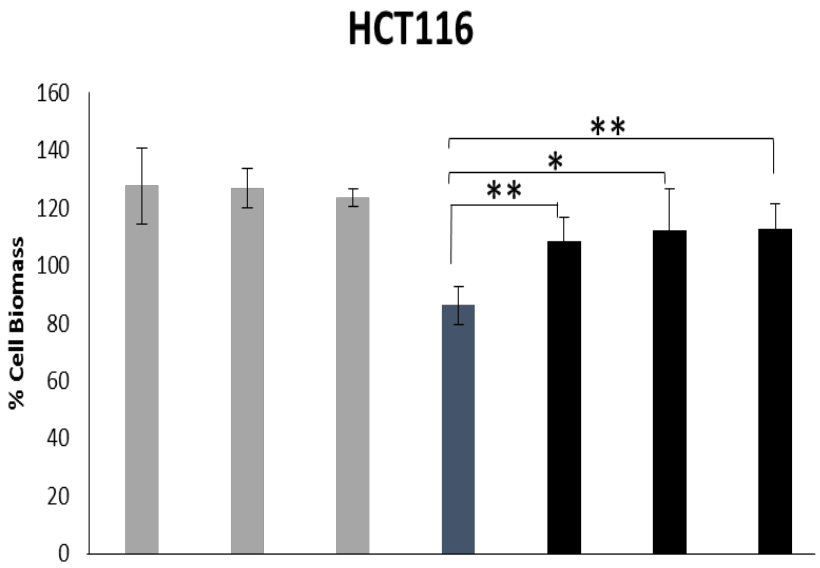

d.

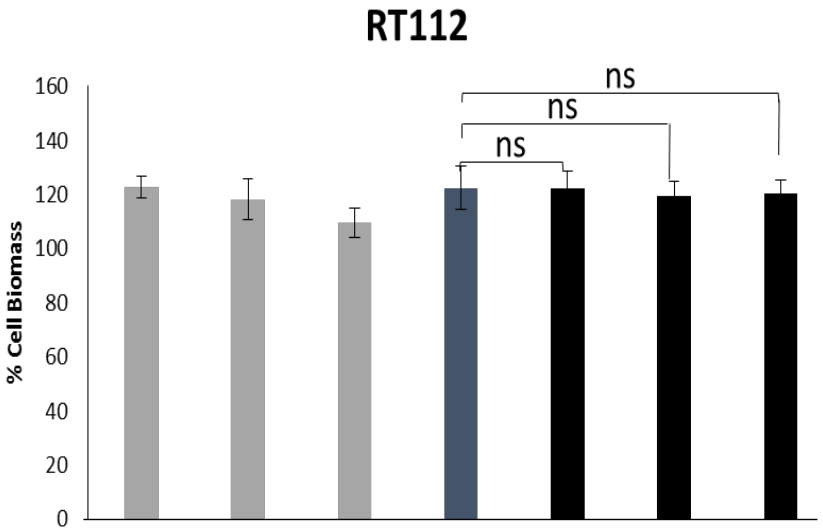

LIGHT (1µg/mL)	-	-	-	+	+	+	+
IFN-γ (60U/mL)	+	-	-	-	+	-	-
IFN-γ (120U/mL)	-	+	-	-	-	+	-
IFN-γ (180U/mL)	-	-	+	-	-	-	+

e.

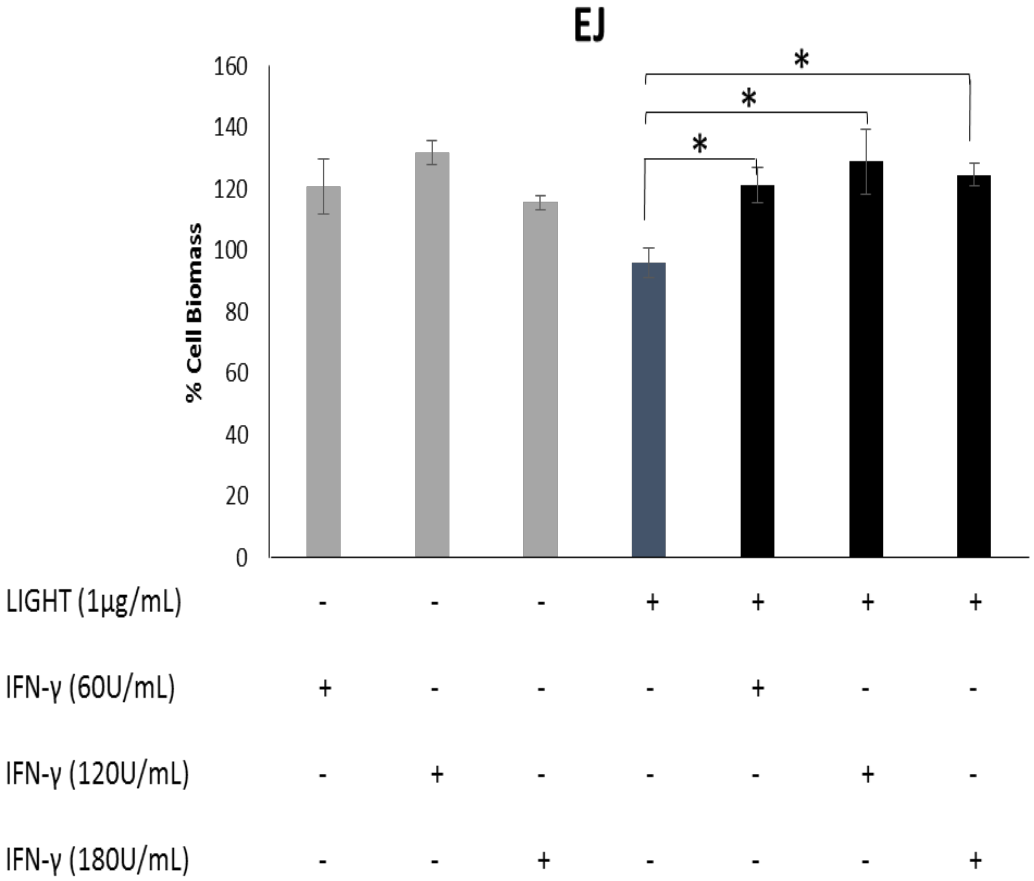

Figure 3.7. Effects of LIGHT treatment combined with varying concentrations of IFN-γ on carcinoma cell viability

HT29, SW480, HCT116, RT112 and EJ were seeded in 96-well plates. Cells were treated with LIGHT in the presence or the absence of IFN-γ (60, 120 and 180U/mL), as indicated, and incubated for 96hrs. 20µL of MTS solution was added to each well and incubated for 4hrs. Cell viability was determined by a FLUOstar OPTIMA (BMG Labtech) plate reader at a wavelength of 492nm. a, b, c, d and e show HT29, SW480, HCT116, RT112 and EJ cells. Figures represent % cell biomass = (sample/control)*100. Data represented as mean values of 3 replicates ±S.D. Stats: ns. non-significant; *, $p < 0.05$; **, $p < 0.01$; ***, $p < 0.001$, paired student t-test for LIGHT treated cells vs treated cells with LIGHT and IFN-γ.

Our data showed that the cytotoxic effects of LIGHT combined with IFN-γ is dose-dependent only in HT29 cells, and that combined LIGHT with IFN-γ (at concentration 120 or 180U/mL) induced significant reduction cell viability (about 50%) of HT29 compared with controls (Figure 3.7). By contrast, the same dose of IFN-γ combined with LIGHT treatment enhanced cell viability (cytoprotected) in SW480, HCT116 and EJ cells.

Cells were treated with LIGHT in the absence or presence of inhibitor of protein synthesis (CHX) to demonstrate LIGHT cytotoxicity on growth of CRC and UCC cells. Two optimal concentrations of CHX (0.05 and 0.1µg/mL) were selected to ensure there is no cytotoxicity by CHX alone and data were presented as shown in Figure 3.8. Treatments of cells with LIGHT/CHX caused a significant reduction in cell biomass of SW480, HCT116 and EJ cells. LIGHT/CHX has little effects on HT29 cells viability and the results in RT112 cells seem the same compared with control (Figure 3.8).

a.

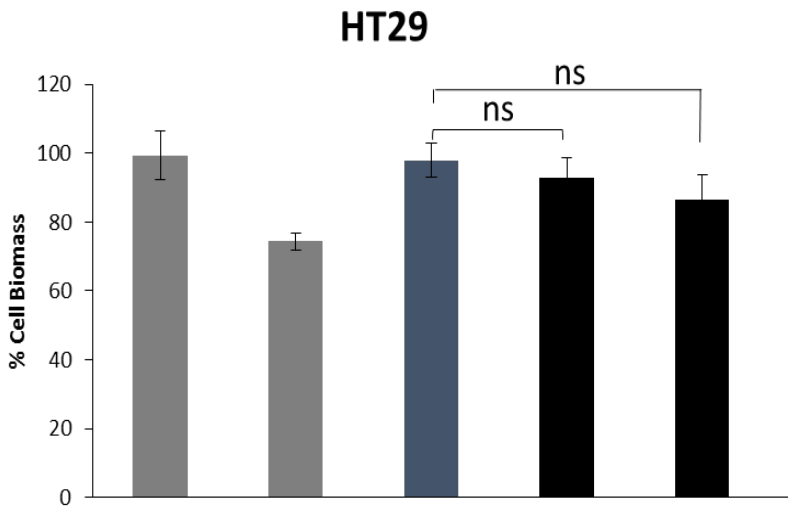

b.

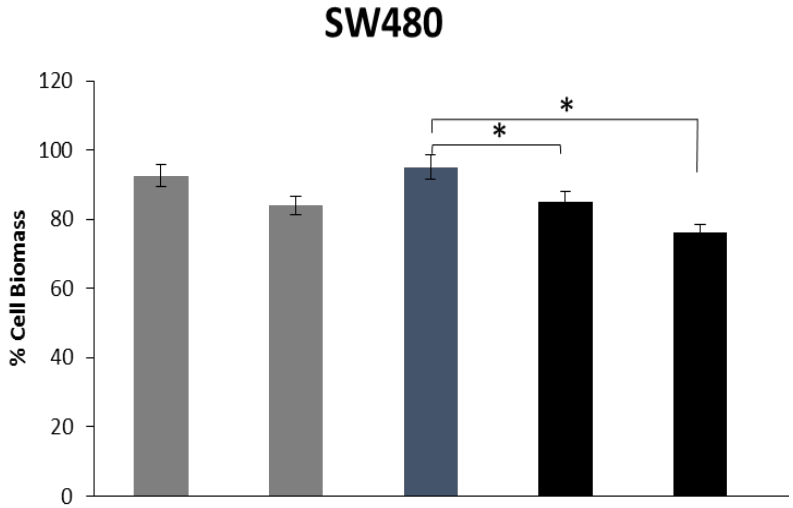

LIGHT (1µg/mL)	-	-	+	+	+
CHX (0.05µg/mL)	+	-	-	+	-
CHX (0.1µg/mL)	-	+	-	-	+

c.

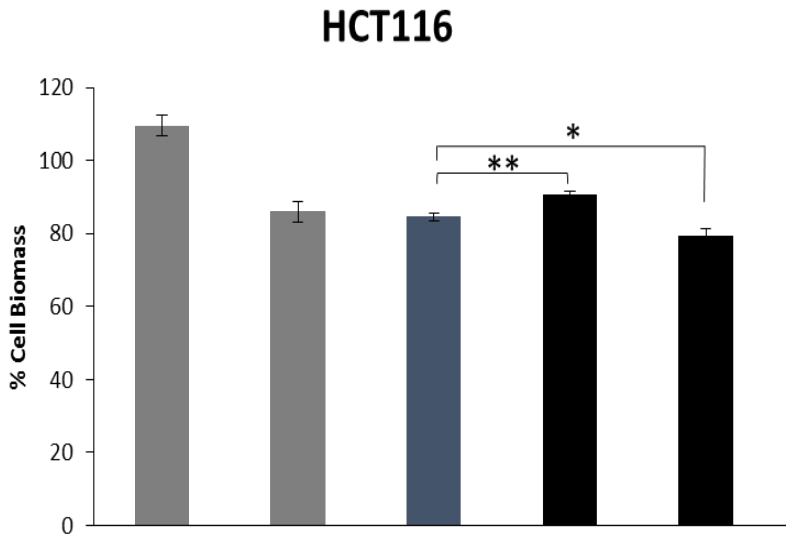

d.

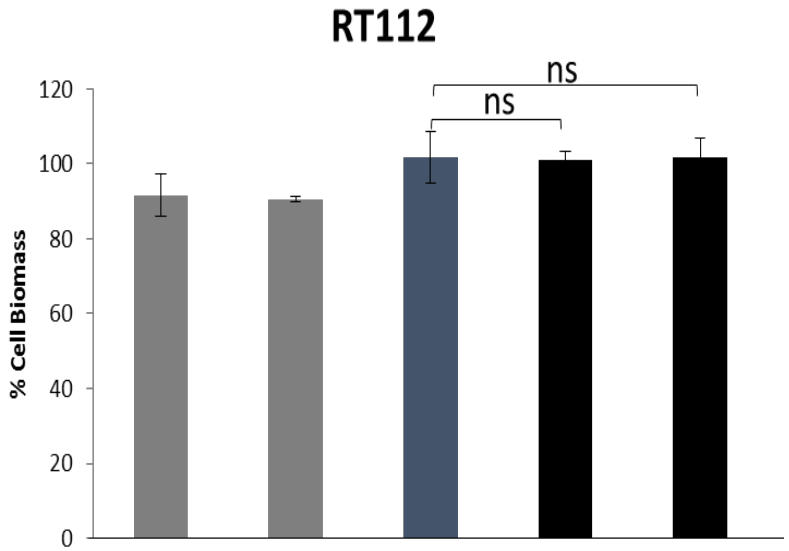

LIGHT (1µg/mL)	-	-	+	+	+
CHX (0.05µg/mL)	+	-	-	+	-
CHX (0.1µg/mL)	-	+	-	-	+

e.

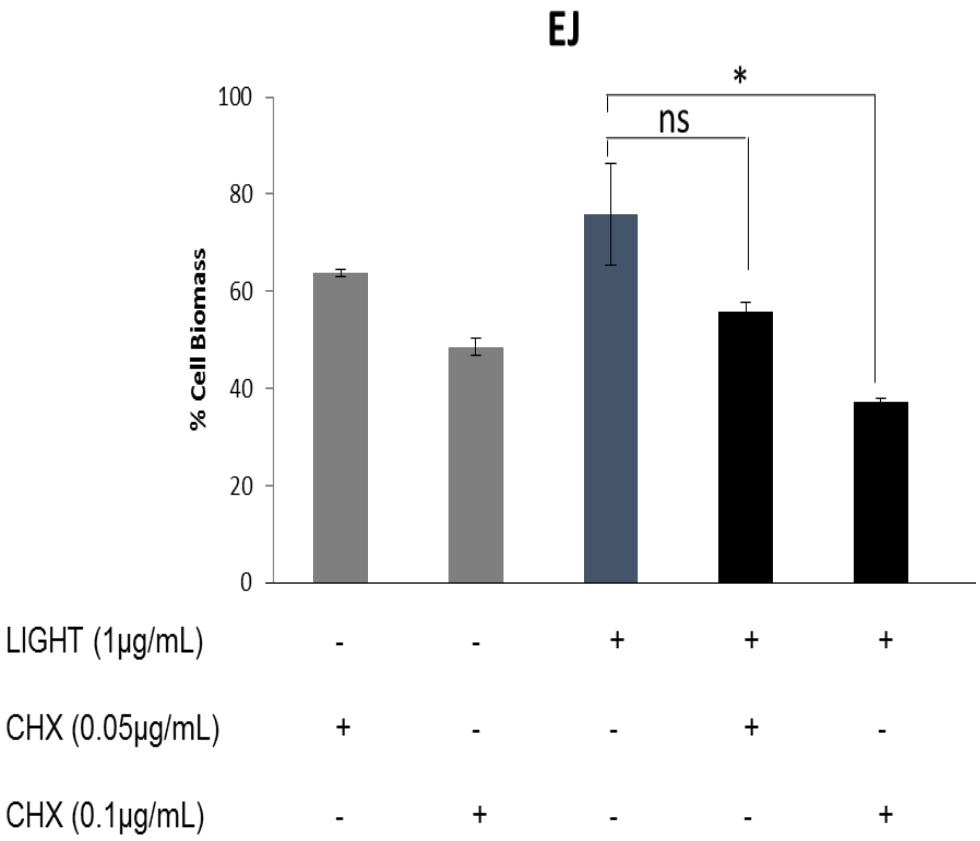

Figure 3.8. Effects of LIGHT and LIGHT/CHX treatment on carcinoma cell viability

HT29, SW480, HCT116, RT112 and EJ were seeded in 96-well plates. Cells were treated with LIGHT, CHX, or LIGHT/CHX at various concentrations as indicated and incubated for 96hrs. 20µL of MTS solution was added to each well and incubated for 4hrs. The control bar represents cell alone without treatment. Cell viability was determined by a FLUOstar OPTIMA (BMG Labtech) plate reader at a wavelength of 492nm. a, b, c, d and e show HT29, SW480, HCT116, RT112 and EJ cells, respectively. Figures represent % cell biomass = (sample/control)*100. Data are represented as mean values of 3 replicates ±S.D. Stats: ns. non-significant; *, $p < 0.05$; **, $p < 0.01$; ***, $p < 0.001$, paired student t-test for LIGHT treated cells vs treated cells with LIGHT and CHX, as indicated.

3.5 Assessment of cell death using the CytoTox-Glo assay

3.5.1 LTβR activation using BS-1 antibody

Because the MTS assay detects effects of cell viability but strictly does not measure cell death, and based on previous recommendations that more than one assay should be utilised to investigate cell death *in vitro* (Kroemer et al., 2009), in addition to the MTS assay, the CytoTox-Glo assay was employed to detect cell death.

The basis of the CytoTox-Glo (Promega) is that it uses a luminogenic peptide substrate (alanyl-alanyl-phenylalanyl-aminoluciferin; AAF-Glo™ Substrate) to measure "dead-cell protease activity" that is released from dead cells (cells have lost their membrane integrity). The AAF-Glo is cleaved as a result of the release of protease and cleavage of AAF-Glo generates a luminescence signal, which was detected by luminescence measurements on a FLUOstar OPTIMA (BMG Labtech) plate reader (section 2.13.2).

In this part of the study, cells were treated with control antibody (MOPC-21), BS-1 in the absence or presence of effective dose concentration of IFN-γ (see Chapter 2 section 2.13 and 2.13.2). Cells were treated with soluble agonists and incubated for two time points; 72 and 96hrs (results of cell treatment with BS-1 for 96hrs can be found in Appendix III), and this is because it was observed there was a difference in cell biomass at 96hrs so it is likely by 72hrs cell death would be observed or initiated. Data was presented as raw data and fold increase of luminescence of treated cells *versus* untreated cells as shown in Figure 3.9.

Our results demonstrated that HCT116 cells showed some detectable death in response to BS-1 treatment whereas, treatment with BS-1/IFN-γ caused significant cell death ($p < 0.001$) in HT29, HCT116 and RT112 cells (Figure 3.9). SW480 cells showed no detectable death in response to BS-1 and BS-1/IFN-γ and it appeared to be resistant to the treatments and this is in agreement with the MTS data (Figure 3.9).

a.

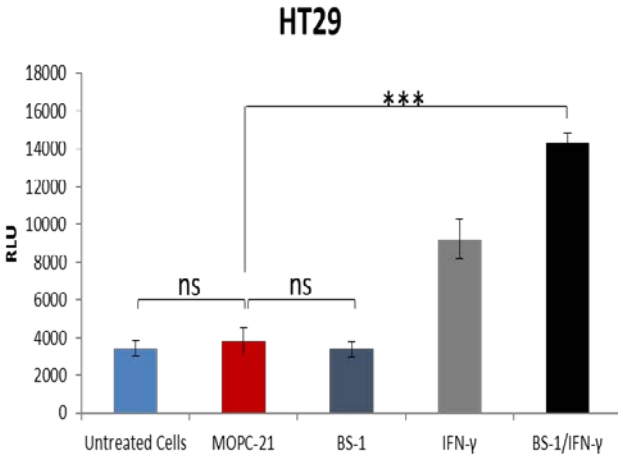
HT29
RLU
18000
16000
14000
12000
10000
8000
6000
4000
2000
0
***
ns
ns
Untreated Cells
MOPC-21
BS-1
IFN-γ
BS-1/IFN-γ

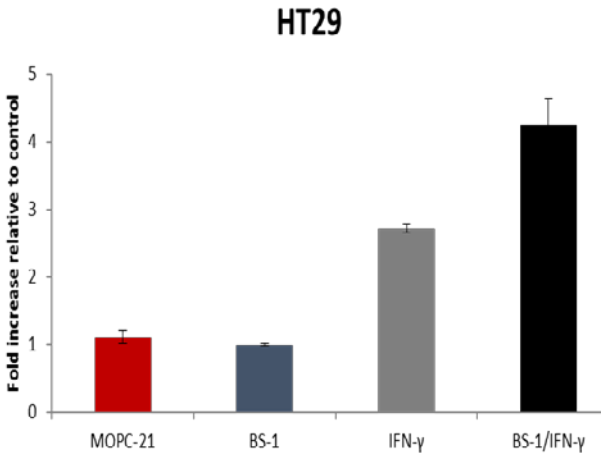
HT29
Fold increase relative to control
5
4
3
2
1
0
MOPC-21
BS-1
IFN-γ
BS-1/IFN-γ

b.

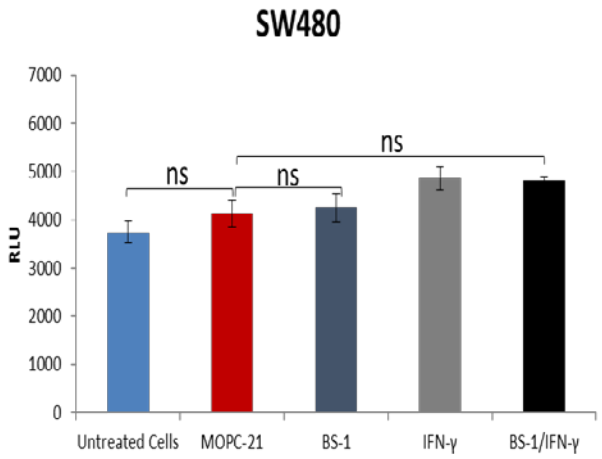
SW480
RLU
7000
6000
5000
4000
3000
2000
1000
0
ns
ns
ns
Untreated Cells
MOPC-21
BS-1
IFN-γ
BS-1/IFN-γ

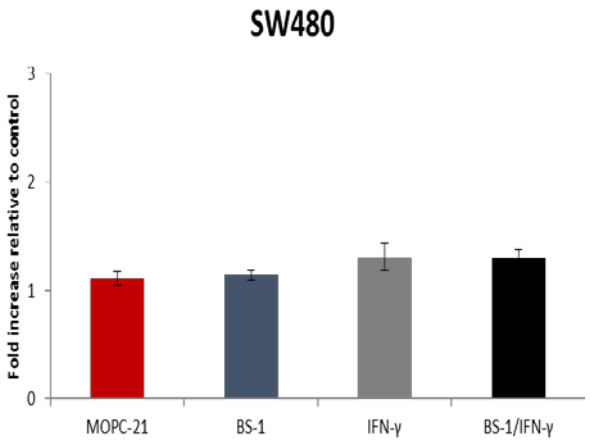
SW480
Fold increase relative to control
3
2
1
0
MOPC-21
BS-1
IFN-γ
BS-1/IFN-γ

c.

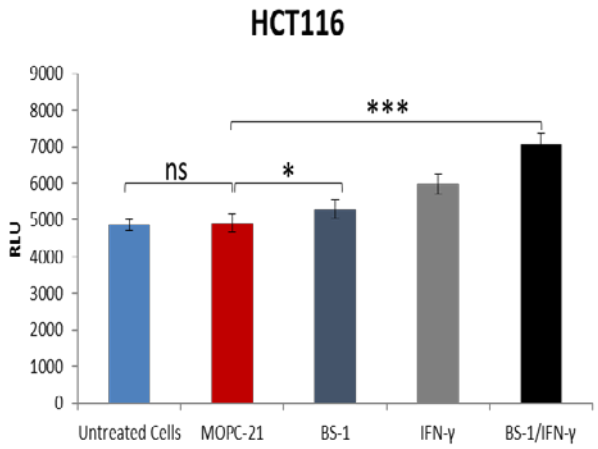
HCT116
RLU
9000
8000
7000
6000
5000
4000
3000
2000
1000
0
***
ns
*
Untreated Cells
MOPC-21
BS-1
IFN-γ
BS-1/IFN-γ

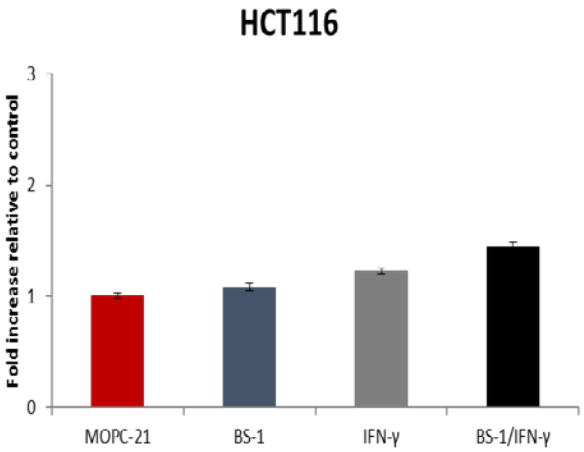
HCT116
Fold increase relative to control
3
2
1
0
MOPC-21
BS-1
IFN-γ
BS-1/IFN-γ

d.

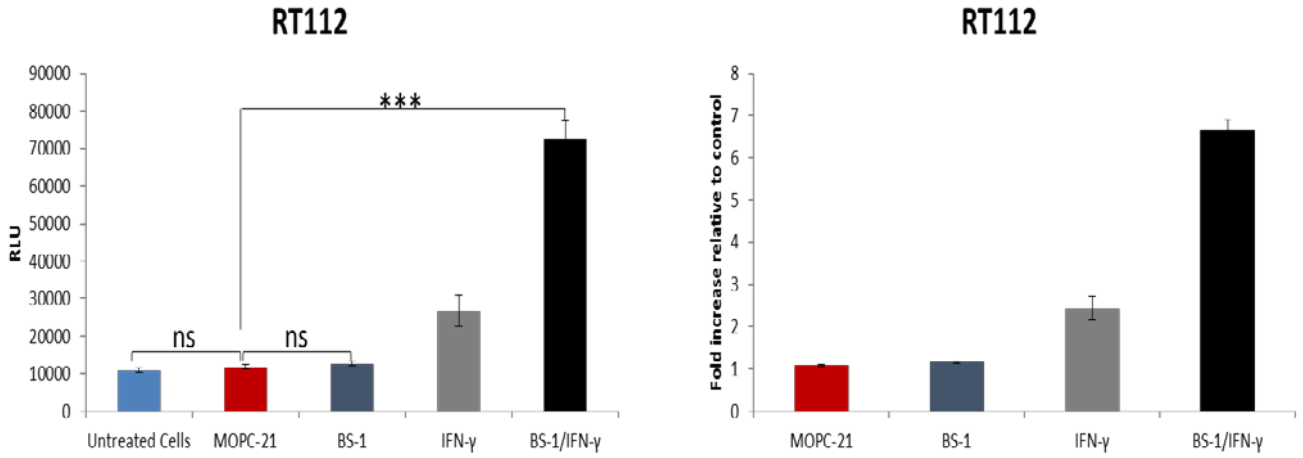

e.

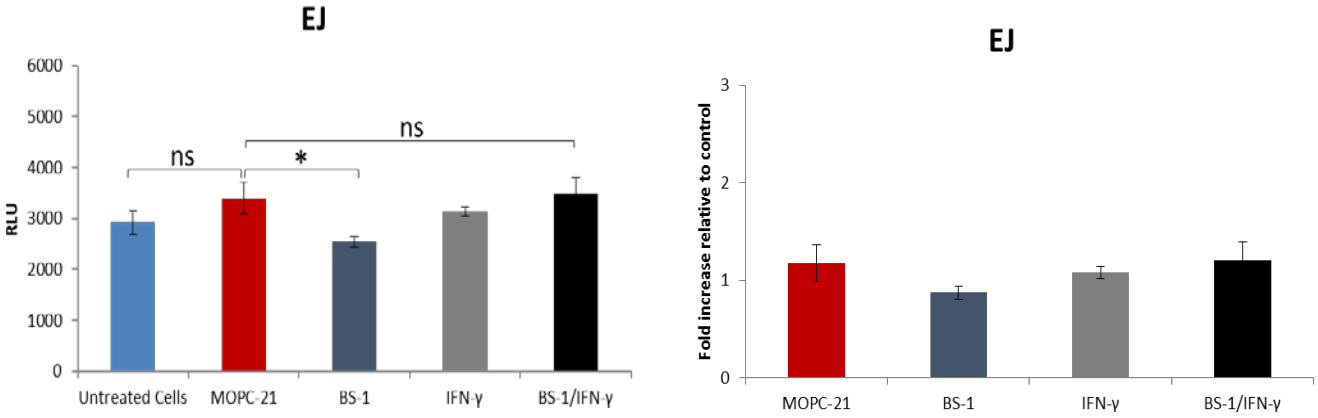

Figure 3.9. Detection of cell death following carcinoma cell treatment with BS-1 and BS-1/IFN-γ

HT29, SW480, HCT116, RT112 and EJ were seeded in 96-well plates. Cells were treated with BS-1 (30µg/mL), MOPC-21 (10µg/mL), in the absence or presence of IFN-γ (180U/mL) and incubated for 72hrs. CytoTox-Glo reagents were prepared and added to each well and then relative luminescence unit (RLU) was measured by a FLUOstar OPTIMA (BMG Labtech) plate reader. The intensity of the RLU signal corresponds to the degree of dead cells in a population (as described in section 2.13.2). Raw data are presented in left panels and fold increase relative to control was generated from raw RLU data (left panels) by comparing treated cells *versus* untreated cells as shown in right panels. a, b, c, d and e show HT29, SW480, HCT116, RT112 and EJ cells, respectively. Data are represented as mean values of 4-5 replicates ±S.D. Stats: ns. non-significant; *, $p < 0.05$; **, $p < 0.01$; ***, $p < 0.001$, paired student t-test for control cells vs treated cells, as indicated.

3.5.2 LTβR and HVEM activation using recombinant LIGHT

Based on previous section data, activating LTβR alone by BS-1 is insufficient to kill (hence no death) and required IFN-γ help to kill some cells by using the CytoTox-Glo assay. As BS-1 is not efficient to kill, therefore, cells were treated with LIGHT to activate both receptors LTβR and HVEM for 72 and 96hrs and death were assessed by the CytoTox-Glo assay. The reason for using incubation 72hrs is because we thought that if there is a difference in cell biomass by 96hrs, then it is likely by 72hrs cell death would have been initiated. We found that activation of LTβR and HVEM by LIGHT for 72hrs showed better cell death than 96hrs (results of cell treatment with LIGHT for 96hrs can be found in Appendix III). For this reason, data of 72hrs incubation time were only presented here as raw data and fold increase of luminescence of treated cells *versus* untreated cells as shown in Figure 3.10.

Treatment HCT116 cells with LIGHT induced significant cell death and LIGHT co-treatment with IFN-γ was significantly cytotoxic on HT29, HCT116, and RT112 cells. Our results also showed that SW480 cells show no response to LIGHT/IFN-γ treatments (Figure 3.10).

a.

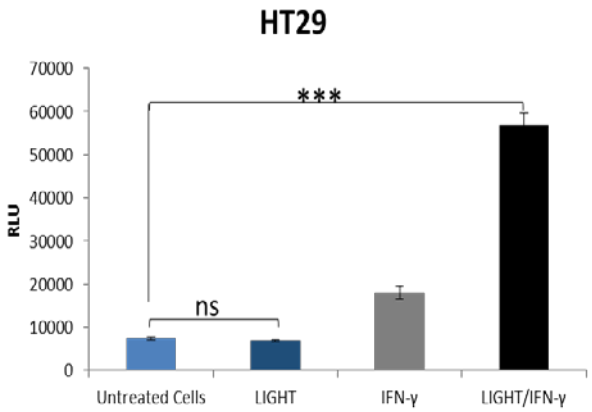
HT29
RLU
70000
60000
50000
40000
30000
20000
10000
0
***
ns
Untreated Cells
LIGHT
IFN-γ
LIGHT/IFN-γ

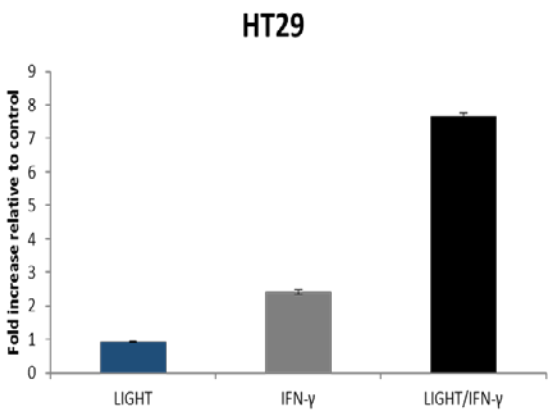
HT29
Fold increase relative to control
9
8
7
6
5
4
3
2
1
0
LIGHT
IFN-γ
LIGHT/IFN-γ

b.

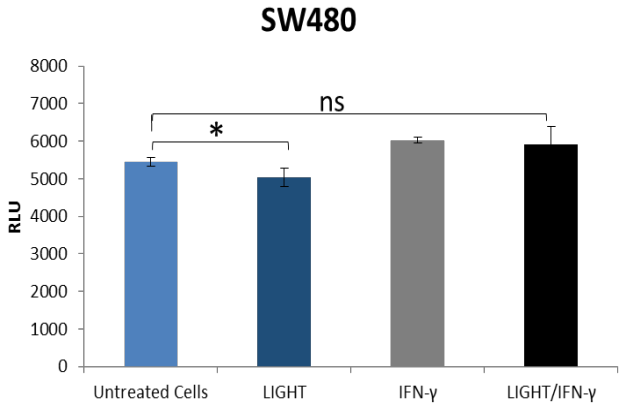
SW480
RLU
8000
7000
6000
5000
4000
3000
2000
1000
0
ns
*
Untreated Cells
LIGHT
IFN-γ
LIGHT/IFN-γ

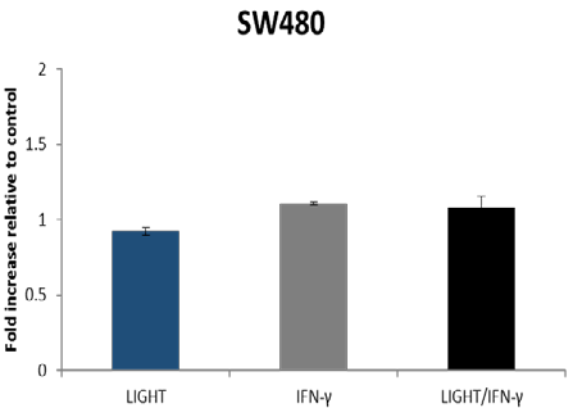
SW480
Fold increase relative to control
2
1.5
1
0.5
0
LIGHT
IFN-γ
LIGHT/IFN-γ

c.

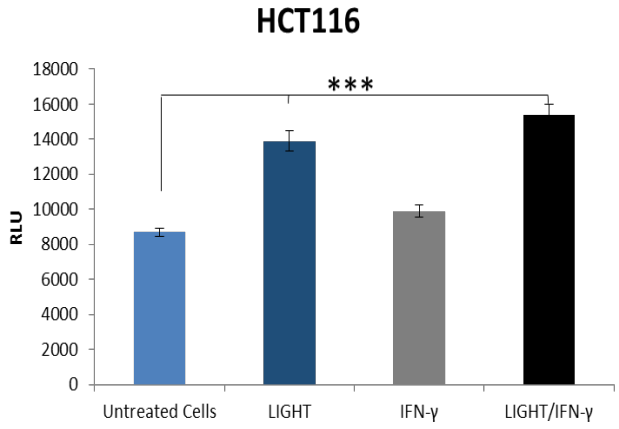
HCT116
RLU
18000
16000
14000
12000
10000
8000
6000
4000
2000
0
***
Untreated Cells
LIGHT
IFN-γ
LIGHT/IFN-γ

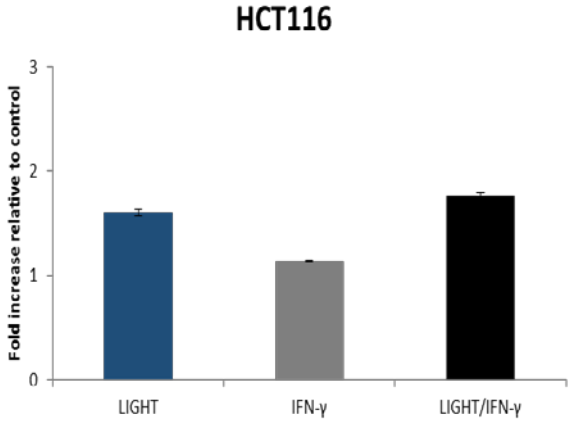
HCT116
Fold increase relative to control
3
2
1
0
LIGHT
IFN-γ
LIGHT/IFN-γ

d.

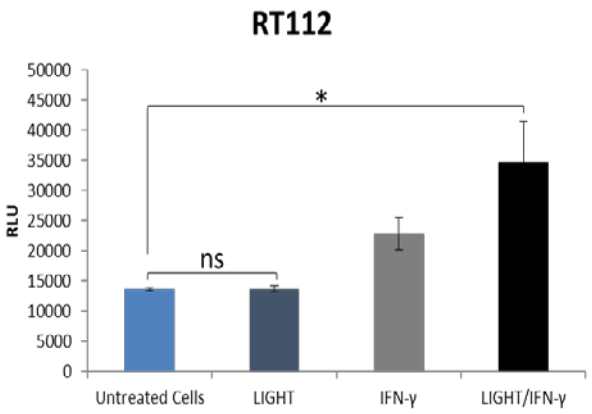

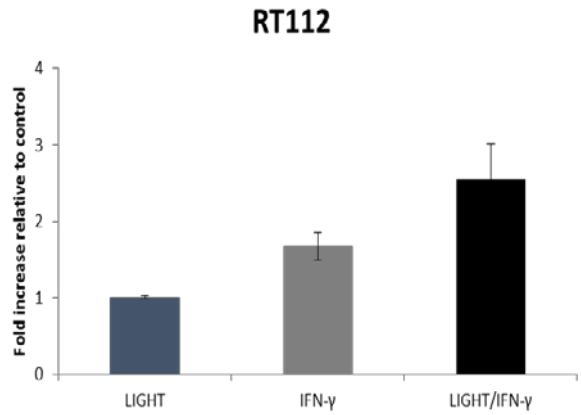

e.

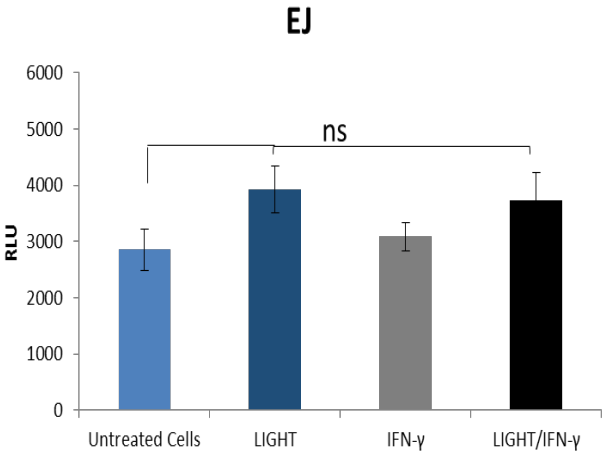

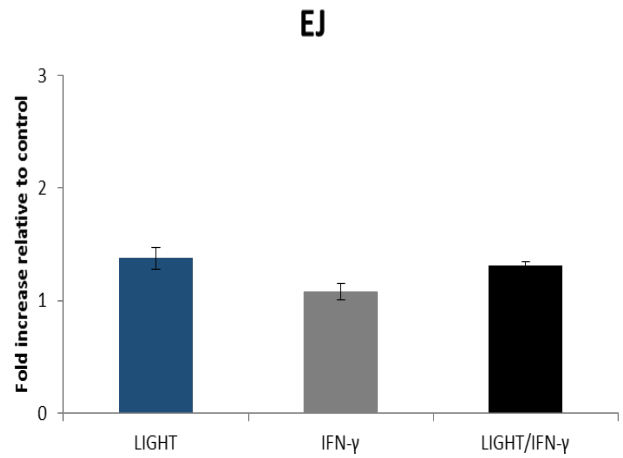

Figure 3.10. Detection of cell death following carcinoma cell treatment with LIGHT and LIGHT/IFN-γ

HT29, SW480, HCT116, RT112 and EJ were plated in 96-well plates. Cells were treated with LIGHT (1µg/mL), in the absence or presence of IFN-γ (180U/mL) and incubated for 72hrs. CytoTox-Glo was prepared and added to each well and then relative luminescence unit (RLU) was measured by a FLUOstar OPTIMA (BMG Labtech) plate reader. The intensity of the RLU signal corresponds to the degree of dead cells in a population (as described in section 2.13.2). Raw data are presented (left panels) and fold increase relative to control was generated from raw RLU data used in left panels by comparing treated cells *versus* untreated cells as shown in right panels. a, b, c, d and e show HT29, SW480, HCT116, RT112 and EJ cells, respectively. Data are represented as mean values of 4 replicates ±S.D. Stats: ns. non-significant; *, $p < 0.05$; **, $p < 0.01$; ***, $p < 0.001$, paired student t-test for untreated cells vs treated cells, as indicated.

Summary

- CRC and UCC cells expressed LTβR, HVEM, TNFRI, TNFRII and ICAM-1. Moreover, HCT116 and EJ were detectable for CD40 expression, whereas HT29, SW480, RT4 and RT112 were negative for CD40 expression in agreement with previous studies (Georgopoulos et al., 2006; Georgopoulos et al., 2007).

- Pro-inflammatory cytokines IFN-γ / TNF-α (and in particular IFN-γ) upregulated LTβR in RT112, and also HVEM expression in HT29, SW480, HCT116, RT4, RT112 and EJ cells compared with untreated cells.

- Treatment of cells with soluble receptor agonists (BS-1 or recombinant soluble LIGHT) alone has no effect on carcinoma cell viability, but co-treatment with IFN-γ caused a significant growth inhibition for HT29 and RT112 cells but not SW480, HCT116 and EJ cells.

- The cytotoxic effects of LIGHT/IFN-γ was IFN-γ dose dependent (at concentration 120 or 180U/mL) and showing reduction in cell viability only in HT29 cells, whereas the same treatment showed cytoprotected effects in SW480, HCT116 and EJ cells.

- Cells treatment with BS-1 or LIGHT in the presence of protein synthesis inhibitor CHX caused a significant reduction in cell viability mainly in HCT116 and EJ cells but not on other cells.

- Using the cell death assay (CytoTox-Glo), the combinatorial treatment with BS-1/IFN-γ or LIGHT/IFN-γ resulted in extensive cell death in HT29 cells, some CRC and UCC lines; HCT116 and RT112 cells, respectively, also exhibited significant cell death whereas other (e.g. the highly malignant EJ cells) showed little if any cell death. SW480 cells showed no response to the cytotoxic effects of BS-1 or LIGHT combined with IFN-γ.

Chapter 4

Optimisation of a co-culture system to investigate membrane LIGHT (mLIGHT)-mediated death in carcinoma cells

4.1 Introduction

The findings presented in Chapter 3 demonstrated that activating either a) single LT receptor, i.e. LTβR using soluble agonist (BS-1 mAb) (section 3.5.1), or b) both LT receptors (LTβR and HVEM) using soluble recombinant agonist (LIGHT) induced weak or failed to induce cell death in most cells, while there was more substantial cytotoxicity in some cells (but not all) when both receptors (LTβR and HVEM) were activated by treatment with soluble recombinant LIGHT in combination with IFN-γ (LIGHT/IFN-γ) (section 3.5.2). Collectively, these suggest that activating LTβR alone may not be sufficient to induce cell death, whilst little cell death was observed when both receptors LTβR and HVEM were activated by soluble LIGHT. Significant cytotoxicity was observed only upon co-treatment with IFN-γ and that was only for a proportion of the cell lines tested.

These findings have provided evidence that the quality of LT signal may be important in determining the functional outcome of receptor ligation. Therefore, treatment with soluble agonists was weakly pro-apoptotic and significant cytotoxicity was not observed unless synergism with IFN-γ was employed. This apparent lack of cytotoxicity by soluble agonists and potential importance of signal quality is consistent with studies in the CD40 system which have demonstrated that ligand valency, and consequently the extent of receptor cross-linking, can dictate cell death against survival signals (Bugajska et al., 2002; Georgopoulos et al., 2006). Specifically in carcinoma cell lines, membrane-presented CD40 ligand (mCD40L), but not soluble agonists (e.g. sCD40L), induces high level of pro-inflammatory cytokine secretion and causes extensive cell apoptosis (Bugajska et al., 2002; Engels et al., 2005; Zapata et al., 2001), whilst remaining a tumour-cell specific death signal (Bugajska et al., 2002; Hill et al., 2008; Shaw et al., 2005).

Therefore, this study aimed to examine for the first time the hypothesis that membrane-presented LIGHT (mLIGHT) may represent a more potent pro-apoptotic signal in comparison to soluble agonists. For this purpose, the study employed a co-culture system that was based on the use of growth-arrested, third-party cells (fibroblasts) that were L-cells engineered to express mLIGHT and control cells (non-transfected L cells/NT-L cells) (Pasero et al., 2009b). These effector cells were co-

cultured with target epithelial cells to deliver the LT signal. The steps involved in these co-culture experiments are described in detail in the Methods (section 2.13).

The aims of the work presented in this chapter were to:

- adapt the effector mLIGHT expressing cells (mLIGHT-L) in appropriate cell culture medium and confirm expression of mLIGHT in comparison to control (NT-L) cells.

- optimise several parameters of the co-culture system (including to determine the optimal Mitomycin C concentration for the purposes of growth arresting the effector cells, ensure LIGHT expression on effector cells following treatment, and optimisation of the effector:target cell ratios) for the delivery of mLIGHT.

- detect mLIGHT-mediated cell death using cytotoxicity assays, caspase activation and DNA fragmentation as well as determine cytokine secretion in carcinoma cells following receptor ligation.

- study the effects of mLIGHT on carcinoma cells of CRC and UCC origins (HT29, HCT116, SW480, RT112 and EJ cells) and for the first time on normal epithelial cells (normal human urothelial, NHU, cells).

4.2 Confirmation of LIGHT expression on effector cells

The mLIGHT-L cells (Pasero et al., 2009b) were originally cultured in RPMI medium containing the necessary supplements and appropriate concentration of antibiotic for the maintenance of transgene (LIGHT cDNA) expression (see section 2.3.3 in the Methods). In order to simplify the experimental work and conform with routine laboratory procedures for the culture of other effector cells, such as 3T3-CD40L cells for the delivery of mCD40L (Bugajska et al., 2002; Georgopoulos et al., 2006), mLIGHT-L and control (NT-L) cells were adapted into DR medium (section 2.3.3) supplemented with 10% (v/v) FBS, and 1% (v/v) L-Glutamine. Following gradual adaptation, and due to possible risk of genetic drifting during culture, it was important to ensure that the process of adaptation did not affect LIGHT expression in the mLIGHT-L cells.

Therefore, following adaptation, flow cytometry was performed to examine the expression of mLIGHT in the adapted cells compared to the original cells (that were maintained in RPMI medium). As shown in Figure 4.1, adapted mLIGHT-L cells showed similar levels of mLIGHT expression in comparison to the original mLIGHT-L cells (Figure 4.1). Control experiments were also carried out using the same LIGHT-specific antibody to confirm lack of LIGHT expression on control NT-L cells, which confirmed antibody specificity for LIGHT (shown in Appendix IV).

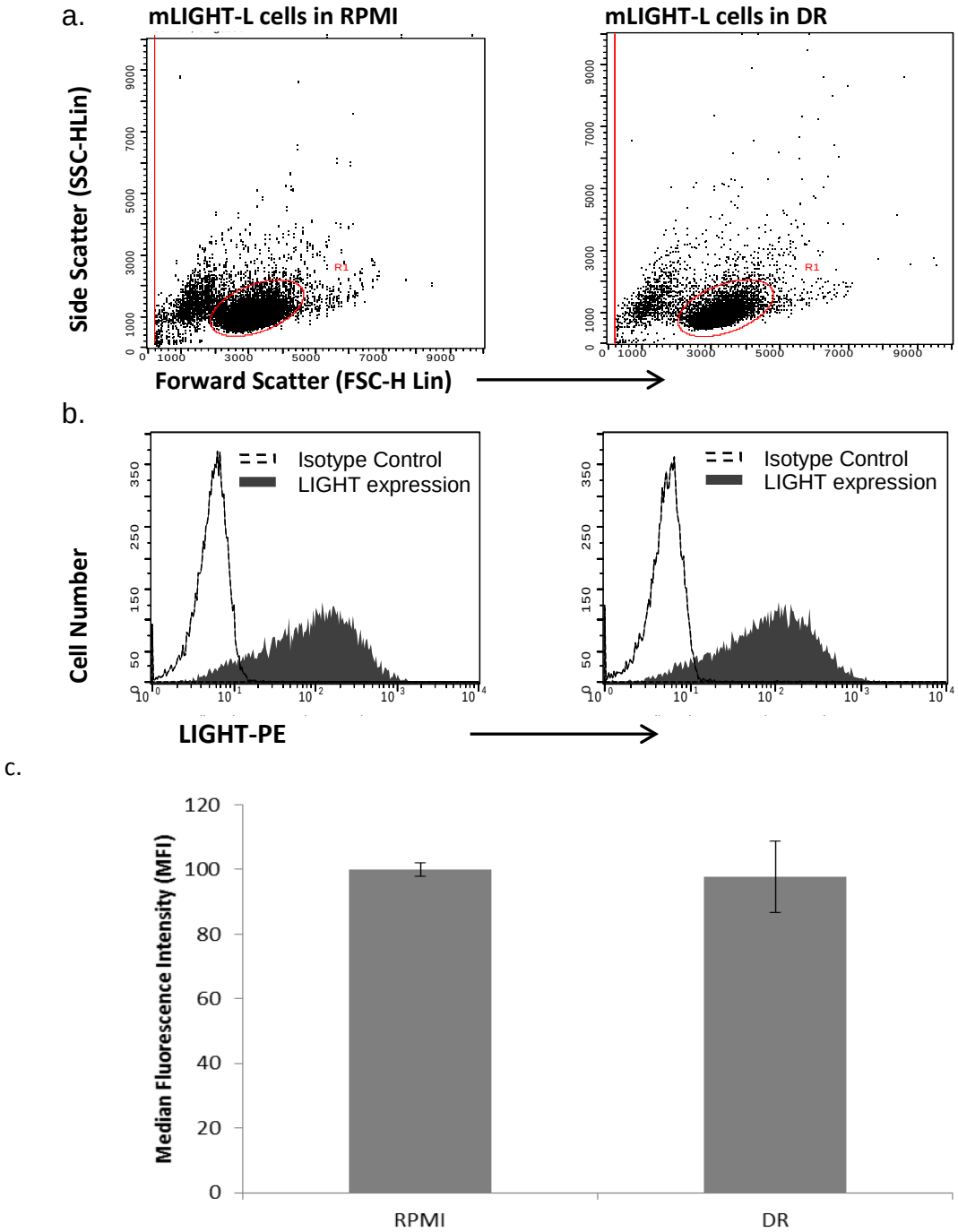

Figure 4.1. LIGHT expression on original and adapted mLIGHT-L cells

mLIGHT-L cells were adapted into DR/10% FBS/10% (v/v) L-glutamine medium. Original (mLIGHT-L cells maintained in RPMI/10% FBS/1% (v/v) L-glutamine) and adapted cells were harvested and labelled with anti-LIGHT or isotype control antibody PE-conjugated for 20-30mins. Cells were then washed and re-suspended in FACS buffer. Samples were acquired on an EasyCyte Guava flow cytometer and data analysed using InCyte2.6 Guava software (Millipore). a, Forward and side scatter plots for acquired cells; b, mLIGHT-L cells maintained in original medium RPMI on the left, adapted cells in DR on the right; c, Mean values of MFI readings for LIGHT expression for 2 replicates. Isotype control PE antibody was used to determine background (MFI = 6±1).

4.3 Confirmation of LIGHT expression after MMC treatment

The purpose of MMC treatment is to inhibit cell growth and therefore avoid the artefacts of cell overgrowth. In order to induce growth-arrest in the effector (mLIGHT-L and NT-L cells) for use in co-culture with target carcinoma cells, it was essential to determine the optimal concentration of Mitomycin C (MMC). Cells were therefore treated with a range of MMC (10, 15 and 20µg/mL) and incubated for 48 and 72hrs and cell viability of untreated and MMC-treated cells was determined.

Using routine microscopy MMC-treated cells appeared to be growth-arrested using MMC treatment at 15µg/mL; by contrast, treatment with a concentration of 10µg/mL appeared ineffective, whereas the 20µg/mL dose seemed toxic on cells (Appendix IV). In agreement with microscopy observations, cell viability experiments demonstrated that MMC treatment used at the concentration 15µg/mL effectively caused growth-arrest in mLIGHT-L and control cells without significant cytotoxicity (Figure 4.2).

a.

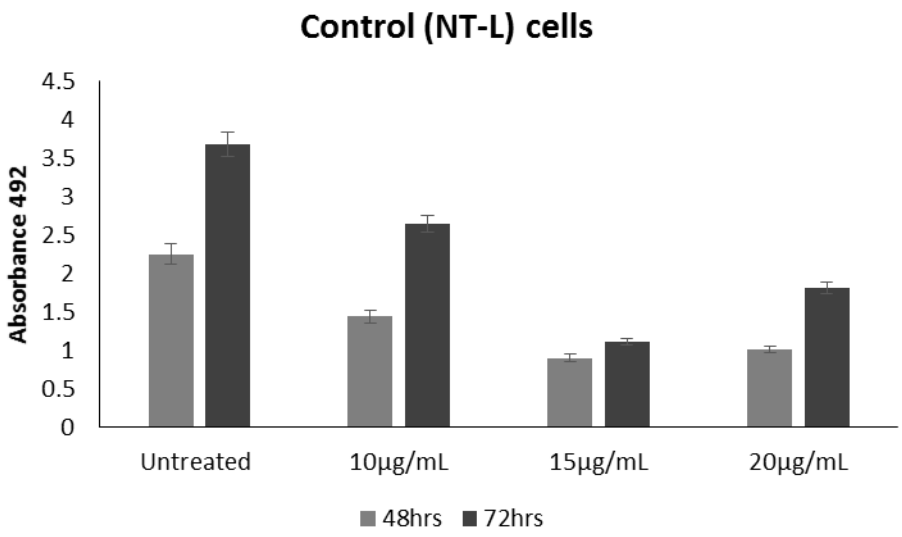

b.

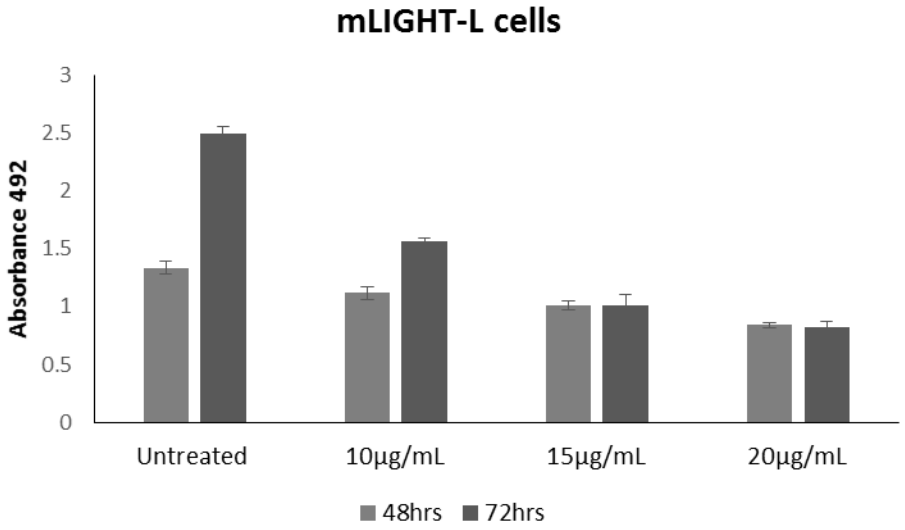

Figure 4.2. Effects of MMC treatments on control (NT-L) and mLIGHT-L cells

Control (NT-L) and mLIGHT-L cells were cultured in T25 flasks until they reached approximately 75% confluency. Cells were treated with the indicated concentrations of MMC and incubated for 2hrs at 37°C and 5% CO_2. After 2hrs, cells were washed with PBS and seeded in 96-well plates. After incubation for 48 and 72hrs, 20µL of MTS solution was added to each well and incubation for 4hrs followed. Cell viability was determined by a FLUOstar OPTIMA (BMG Labtech) plate reader at a wavelength of 492nm. Data are represented as mean values of 4-5 replicates ±S.D. a. MMC-treated NT-L control cells, b. MMC-treated mLIGHT-L cells.

To exclude the possibility that MMC treatment may have an effect on LIGHT expression in mLIGHT-L cells, LIGHT expression following MMC treatment was tested by flow cytometry. As shown in Figure 4.3, LIGHT expression remained stable after the treatment with MMC.

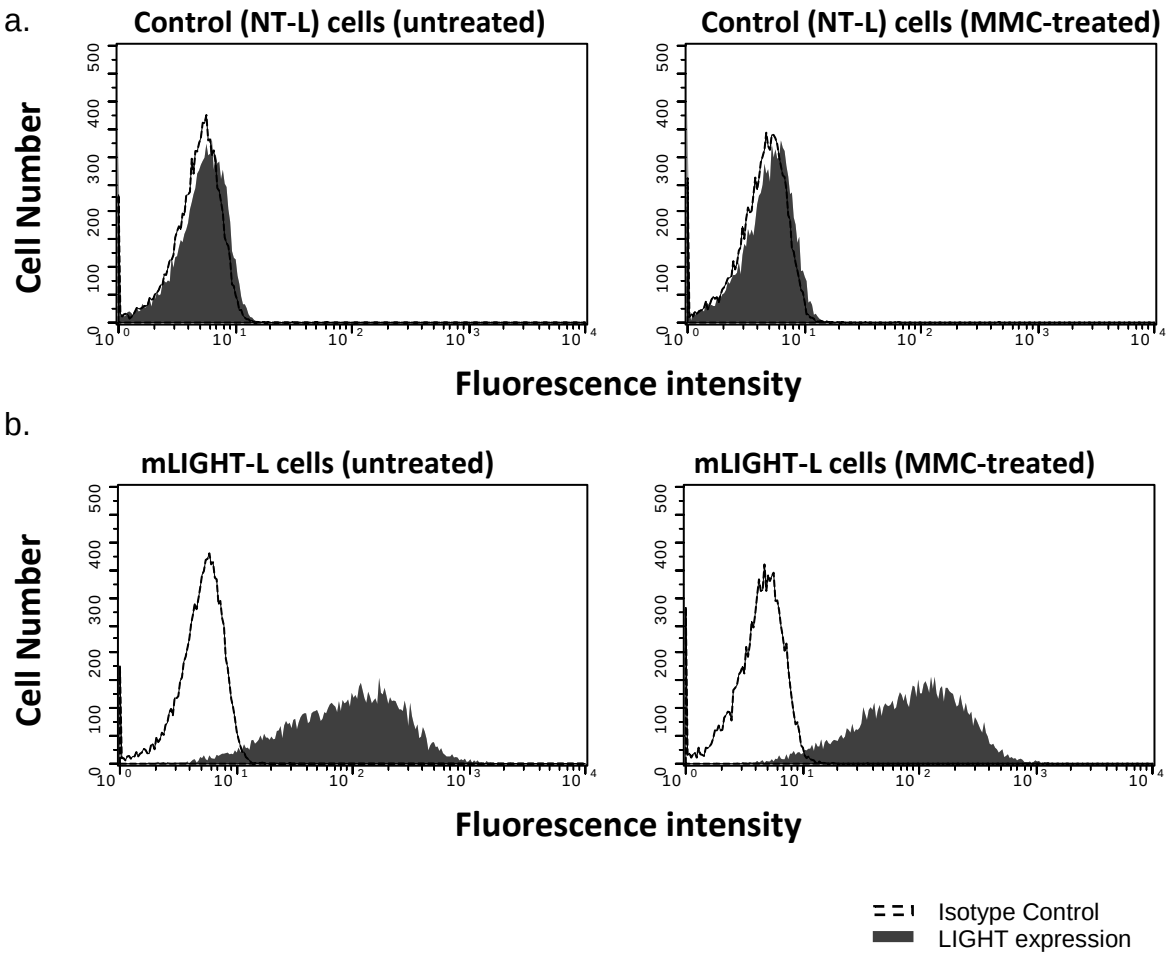

c.

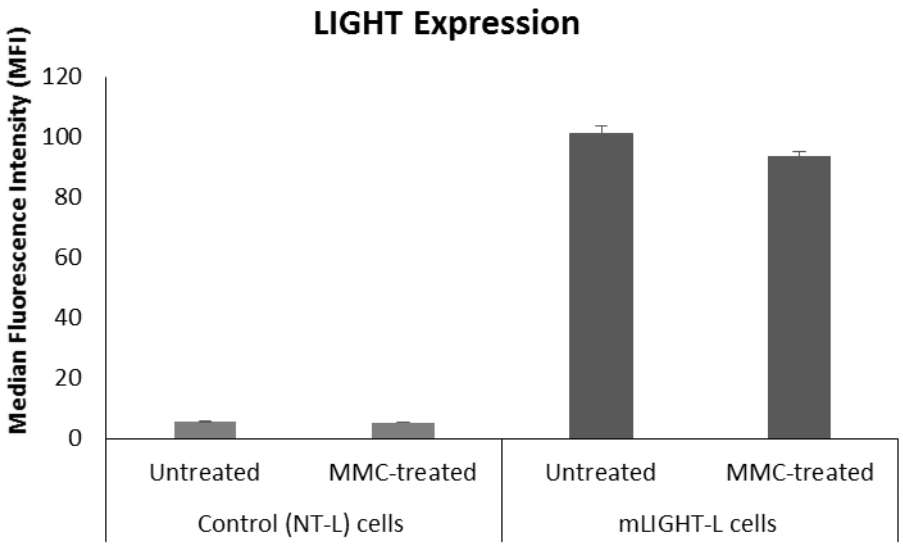

Figure 4.3. Detection of LIGHT expression on effector cells following MMC treatment

Untreated and MMC-treated control (NT-L) and mLIGHT-L cells were labelled with LIGHT-PE or control PE-conjugated isotype antibody and incubated for 20-30mins. Cells were then washed and re-suspended in FACS buffer. Samples were analysed on an EasyCyte Guava flow cytometer and data analysed using InCyte2.6 Guava software (Millipore): a, overlay histograms of untreated (left) and MMC-treated control (NT-L) cells (right), b. untreated (left) and MMC-treated mLIGHT-L cells (right). In these plots, isotype control PE antibody was used and shown as an open black histogram, and PE-conjugated anti-LIGHT is shown as filled grey histogram, c. Mean values of MFI readings for LIGHT expression for 2 replicates.

4.4 Determination of optimal effector:target cell densities for detection of mLIGHT-mediated death using CytoTox-Glo

As part of the optimisation of the co-culture system, it was important to determine optimal cell densities of effector and target cells. NT-L, mLIGHT-L and target cells were seeded at ratios 1:0.6, 1:0.8 and 1:1 (with $1x10^4$ effector cells/well) or co-cultured using the same ratio but the number of effector cells was doubled (i.e. $2x10^4$ cells/well of effector cells used). The use of two densities was due to the fact that the size of the mLIGHT-L cells are relatively small, so there was adequate surface area in the wells to double the overall cell number, which may enhance ligation and cell death; in fact, it was observed that doubling the densities resulted in higher levels of cell death as presented in this chapter (see below).

Using the optimal MMC concentration (15µg/mL, as determined above), effector cells were growth-arrested and co-culture experiments were performed (as detailed in section 2.13.2) using a panel of UCC and CRC lines. CytoTox-Glo was used to detect cell death and results are shown in Figure 4.4 and are presented as raw data (following background correction) as well as fold increase in target cell death for mLIGHT-L versus NT-L co-cultures (Figure 4.4). Raw RLU data and fold increase relative to controls were calculated using the parameters and equations described in section 2.13.2.

The results showed that co-culture of target cells with mLIGHT-L cells resulted in high levels of cell death in CRC and UCC cells with the exception of SW480 cells which appeared relatively resistant to mLIGHT, whilst RT112 cells were moderately susceptible. Therefore, unlike soluble agonists that alone do not cause significant levels of cell death and even in combination with IFN-γ only some cell lines undergo significant levels of death, mLIGHT causes high levels of cell death in nearly all cell lines tested and in the absence of IFN-γ treatment (Figure 4.4).

a.

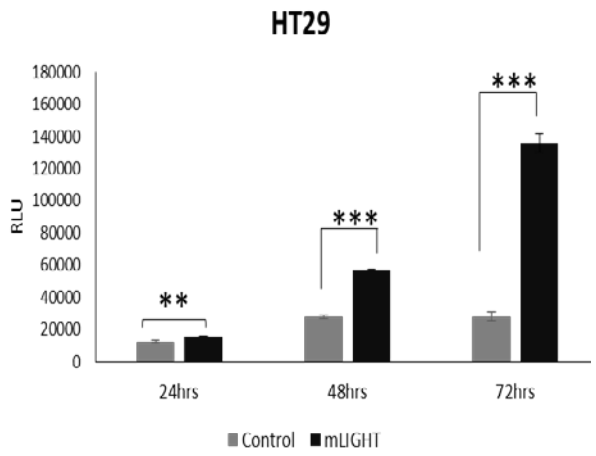
HT29
RLU
180000
160000
140000
120000
100000
80000
60000
40000
20000
0
**
***
***
24hrs
48hrs
72hrs
Control
mLIGHT

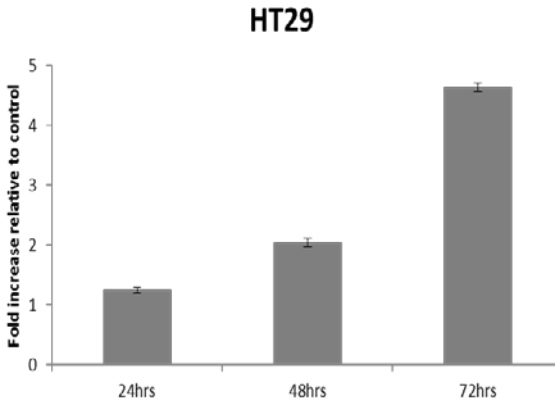
HT29
Fold increase relative to control
5
4
3
2
1
0
24hrs
48hrs
72hrs

b.

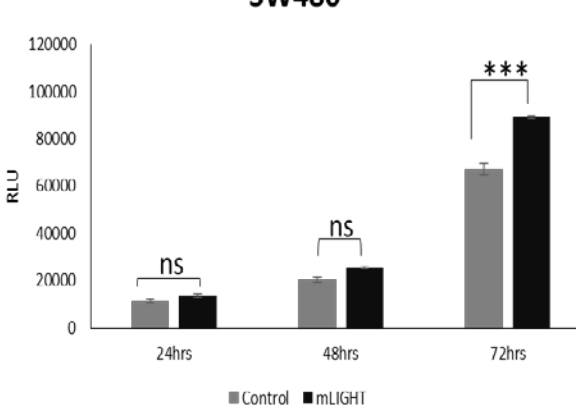
SW480
RLU
120000
100000
80000
60000
40000
20000
0
ns
ns
***
24hrs
48hrs
72hrs
Control
mLIGHT

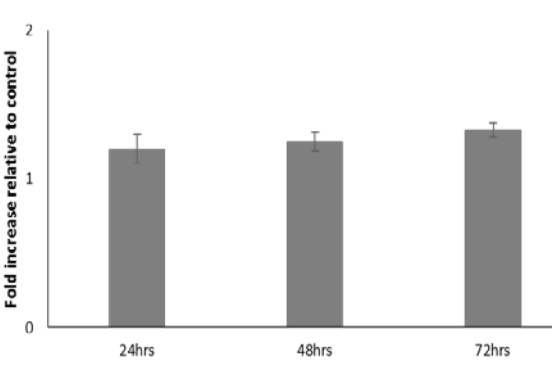
SW480
Fold increase relative to control
2
1
0
24hrs
48hrs
72hrs

c.

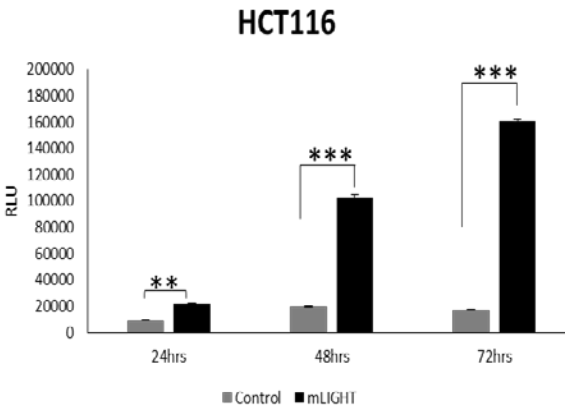
HCT116
RLU
200000
180000
160000
140000
120000
100000
80000
60000
40000
20000
0
**
***
***
24hrs
48hrs
72hrs
Control
mLIGHT

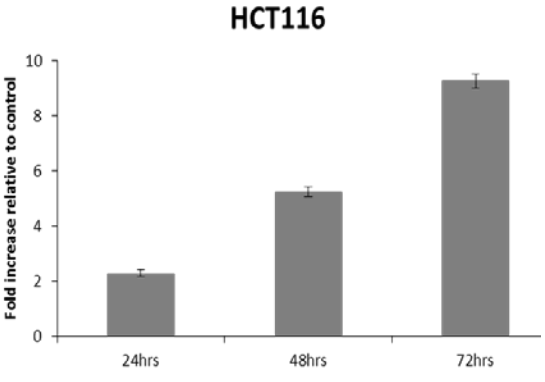
HCT116
Fold increase relative to control
10
8
6
4
2
0
24hrs
48hrs
72hrs

d.

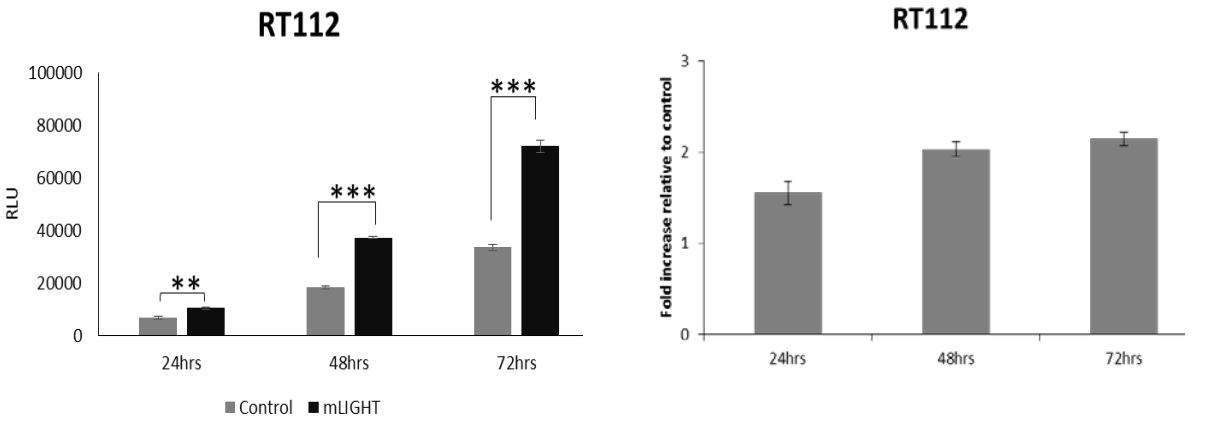

e.

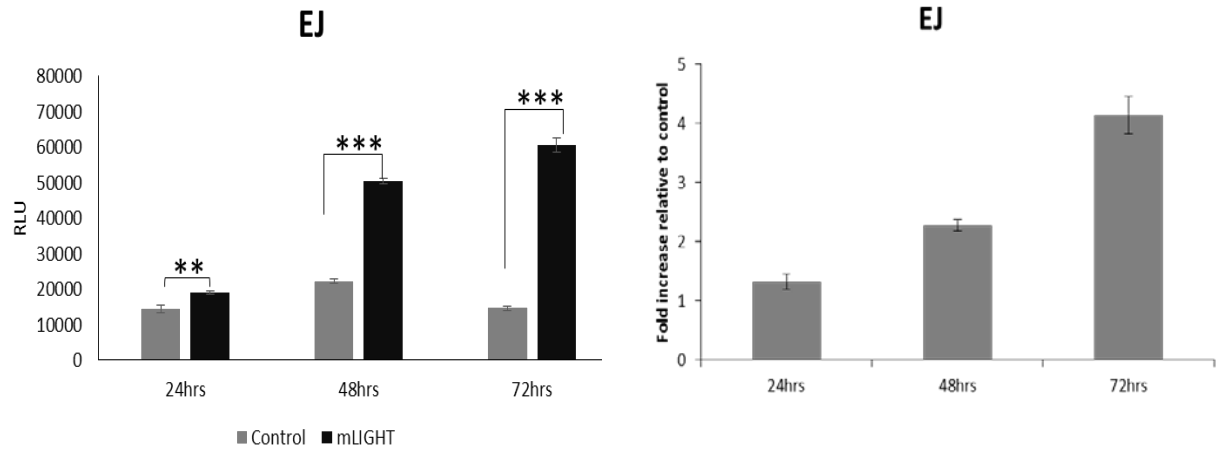

Figure 4.4. Detection of mLIGHT-mediated cell death in carcinoma cells

MMC-treated control (NT-L) and mLIGHT-L cells were seeded at $2x10^4$ cells/well in 96-well white plates overnight and on the following day $1.6x10^4$ of HT29, SW480, HCT116, RT112 or EJ cells were co-cultured with the control or mLIGHT-L cells. Cells were incubated for 24, 48 and 72hrs at 37°C and 5% of CO_2. After that, 50µL of CytoTox-Glo substrate were added to each well and luminescence was measured on a FLUOstar OPTIMA plate reader. Control and mLIGHT alone cultures were included for background correction. Background corrected relative luminescence units (RLU) raw data was generated using the equation: ''control/target cell RLU – control RLU'' and ''mLIGHT/target cell RLU – mLIGHT RLU'' as shown in the left panels. Fold increase relative to control was generated from background corrected data by comparing mLIGHT/target cell *versus* control/ target cell co-cultures (as detailed in section 2.13.2) as shown in right panels. a, b, c, d, and e show HT29, SW480, HCT116, RT112 and EJ cells, respectively. Bars correspond to mean values of 4 replicates ±S.D. Stats: ns. non-significant; *, $p < 0.05$; **, $p < 0.01$; ***, $p < 0.001$, paired student t-test, target cells/control vs target cells/mLIGHT, as indicated.

4.5 Detection of caspase activation by mLIGHT using the SensoLyte caspase-3/7 assay

Caspases-3 and -7 are structurally related enzymes and are classified as effector caspases. The activation of caspase-3/7 is involved in cell death (apoptosis) and contributes to mitochondrial events (Lakhani et al., 2006). Caspase-3 plays a critical role in controlling DNA fragmentation as well as morphological features of apoptosis, whereas caspase-7 is less involved in these processes but it plays a role in the loss of cell viability (Lakhani et al., 2006).

As the CytoTox-Glo assay detects both apoptotic and necrotic cells and also based on published recommendations that cell death should be detected using more than one assay (Galluzzi et al., 2007), the activation of caspase-3 and -7 following treatment of carcinoma cells with mLIGHT using the co-culture system above was detected after 72hrs using the Sensolyte Homogenous caspase-3/7 assay (as detailed in section 2.13.4). Results are shown in Figure 4.5 and are presented as raw data (following background correction) as well as fold increase in target cell death for mLIGHT versus NT-L co-cultures. Raw RFU data and fold increase relative to controls were calculated using the parameters and equations provided in section 2.13.4.

The results demonstrate that mLIGHT induced the activation of caspase-3/7 in HT29, HCT116, RT112 and EJ cells after 72hrs, whereas SW480 showed no caspase activation (Figure 4.5) which is in agreement with the lack of cell death in SW480 when assessed by CytoTox-Glo (Figure 4.4). As RT112 cells were moderately susceptible to mLIGHT and SW480 cells were completely refractory to mLIGHT-mediated apoptosis, this study focused on HT29, HCT116 and EJ cells to further characterise the nature, biological consequences and the underlying mechanisms of mLIGHT-mediated death, whereas the cell lines RT112 and SW480 were not investigated further in detail.

a.

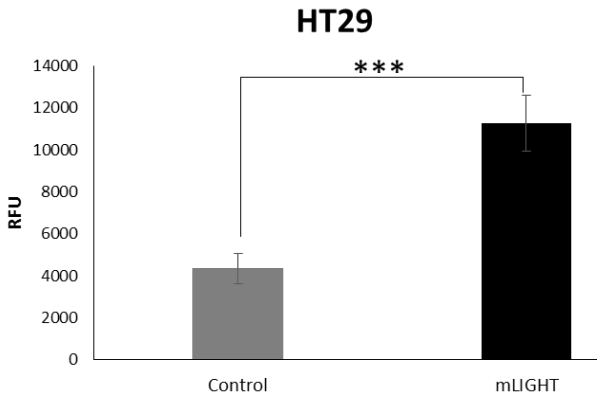
HT29
***
RFU
14000
12000
10000
8000
6000
4000
2000
0
Control
mLIGHT

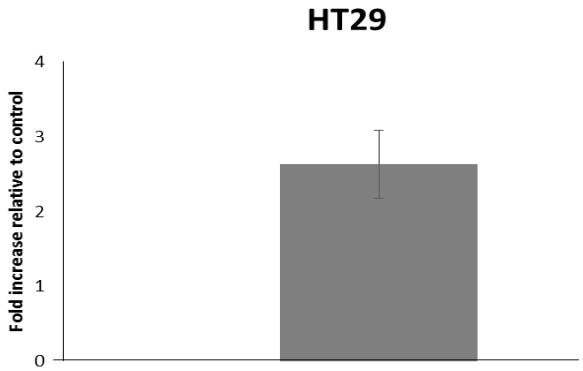
HT29
Fold increase relative to control
4
3
2
1
0

b.

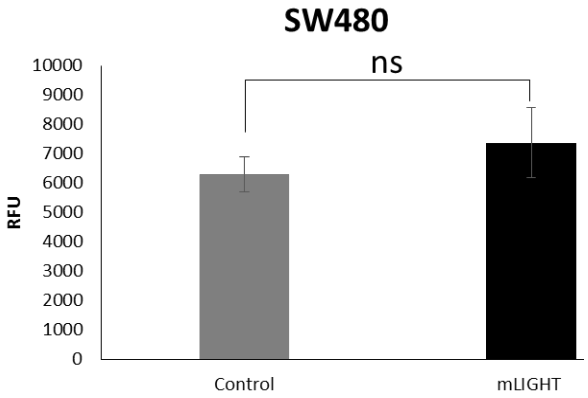
SW480
ns
RFU
10000
9000
8000
7000
6000
5000
4000
3000
2000
1000
0
Control
mLIGHT

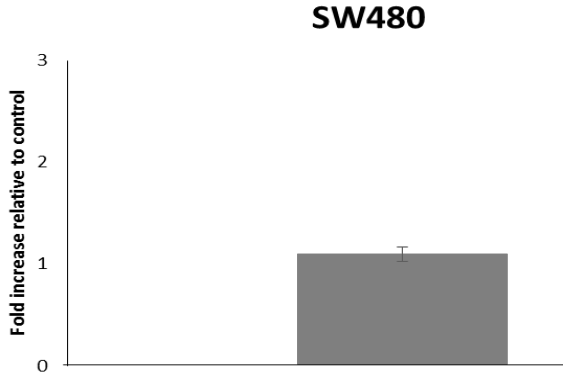
SW480
Fold increase relative to control
3
2
1
0

c.

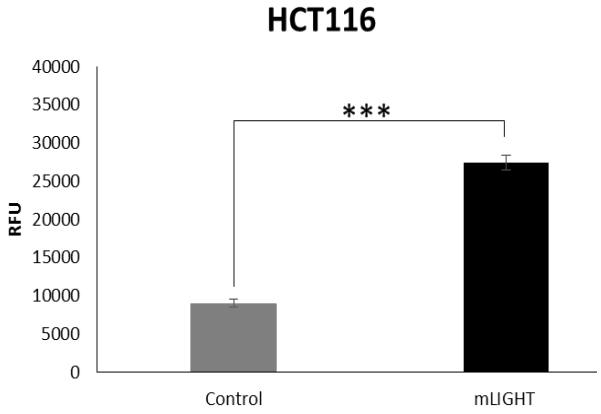
HCT116
***
RFU
40000
35000
30000
25000
20000
15000
10000
5000
0
Control
mLIGHT

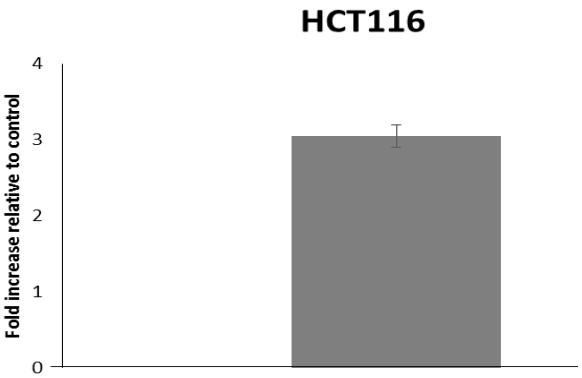
HCT116
Fold increase relative to control
4
3
2
1
0

d.

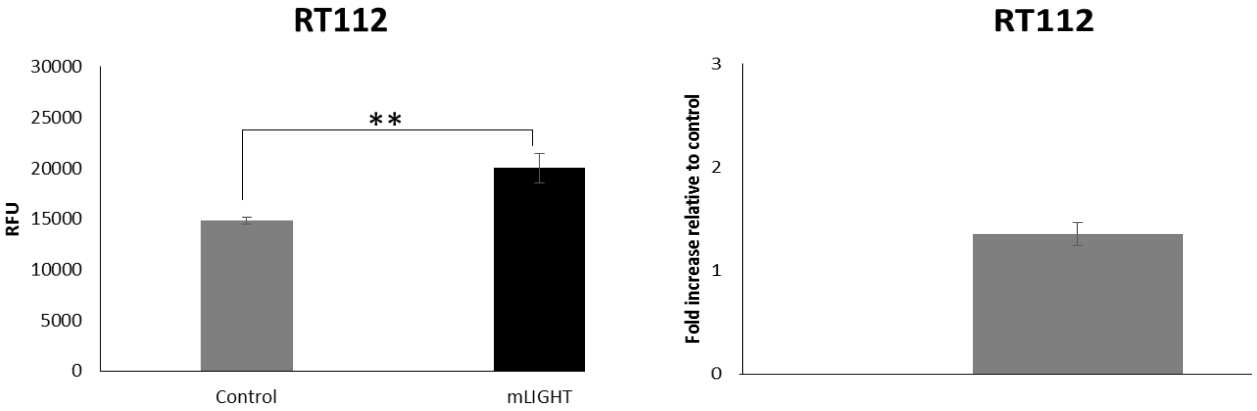

e.

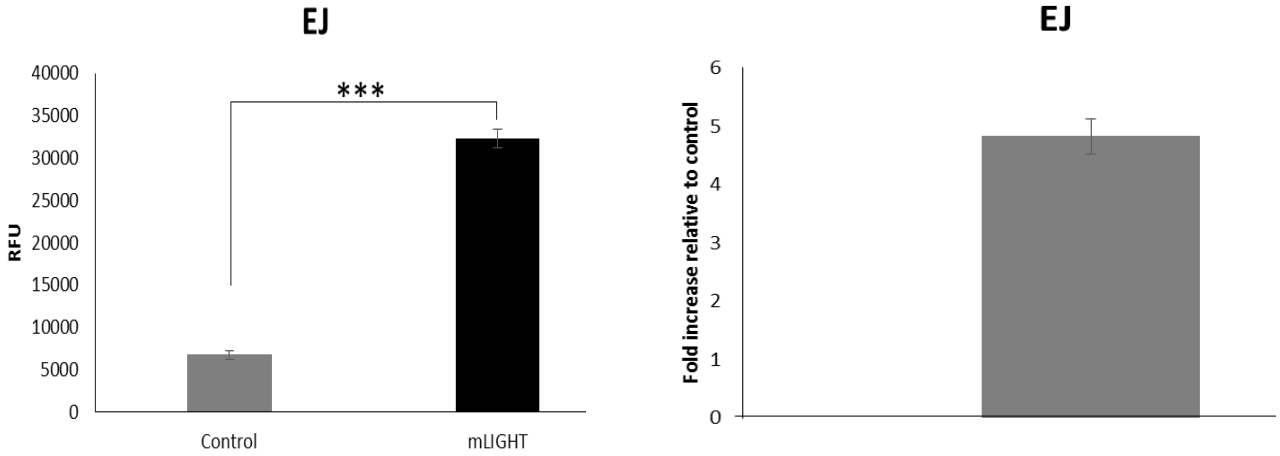

Figure 4.5. Induction of caspase-3/7 activation by mLIGHT ligation

MMC-treated control (NT-L) and mLIGHT-L cells were seeded at $2x10^4$ cells/well in 96-well white plates overnight and on the following day $1.6x10^4$ of target cells HT29, SW480, HCT116, RT112 or EJ cells were co-cultured with control or mLIGHT-L cells and incubated for 72hrs at 37ºC and 5% CO_2. 50µL of medium was added and then 50µL of substrate of the Anaspec reagent was added to each well. Fluorescence was measured by a FLUOstar OPTIMA (BMG Labtech) plate reader. Relative Fluorescence Units (RFU) is relative to total levels of caspase-3/7 activation. RFU values were subtracted pair wise as appropriately, i.e. "control/target cells – control" and "mLIGHT/target cells – mLIGHT" readings (left panels). Fold increase relative to control was generated from background corrected RFU data by comparing mLIGHT/target cell *versus* control/ target cell co-cultures (right panels) and as detailed in section 2.13.4. a, b, c, d and e show HT29, SW480, HCT116, RT112 and EJ cells, respectively. Bars correspond to mean values of 4 replicates ±S.D. Stats: ns. non-significant; *, $p < 0.05$; **, $p < 0.01$; ***, $p < 0.001$, paired student t-test, target cells/control vs target cells/mLIGHT, as indicated.

4.6 Detection of DNA fragmentation following mLIGHT ligation

In addition to cell death detection using the CytoTox-Glo assay (which measures the release of an active protease from dead cells with a structurally compromised cell membrane) and the SensoLyte assay (which measures cellular caspase-3/7 activity and thus apoptosis), cell death also was measured using a DNA fragmentation ELISA assay (see section 2.13.5). DNA fragmentation is a powerful and robust technique to detect apoptosis (as DNA fragmentation is a hallmark of apoptotic cell death) and has been shown to be a reliable tool to detect apoptosis in our laboratory (Bugajska et al., 2002; Georgopoulos et al., 2006; Georgopoulos et al., 2007) and others (Abreu-Martin et al., 1995; Browning et al., 1996; Dealtry et al., 1987). It should, however, be noted that members of the TNFSF do not always induce DNA fragmentation, particularly when the type of death induced displays both apoptotic and non-apoptotic features, as has been reported for TNFRs, such as members of the LT family (Wilson and Browning, 2002) and TRAIL-R (Steele et al., 2006). Finally, an additional advantage of the technique is that, as part of the methodology, only target cells are labelled (with BrdU) for detection (see section 2.13.5 for details) which negates the need to include “effector cell-alone” controls for background subtraction (as in the case of the CytoTox-Glo assay), thus excluding any possibility of interference of the effector cells in the experimental readings obtained.

We therefore examined the level of DNA fragmentation following treatment of carcinoma cells with mLIGHT and experiments were performed as detailed in section 2.13.5. Data were collected and presented as the percentage (%) of apoptotic/dead epithelial cells which was calculated with respect to staurosporine readings (as detailed in section 2.13.5) and representative results are shown in Figure 4.6. mLIGHT caused relatively low levels of DNA fragmentation in HT29 cells (15% in comparison to with 11% for control) and EJ cells (18% compared with 13% for control), whereas in HCT116 cells, mLIGHT resulted in more significant levels of DNA fragmentation (50% compared with 15% for control) (Figure 4.6).

a.

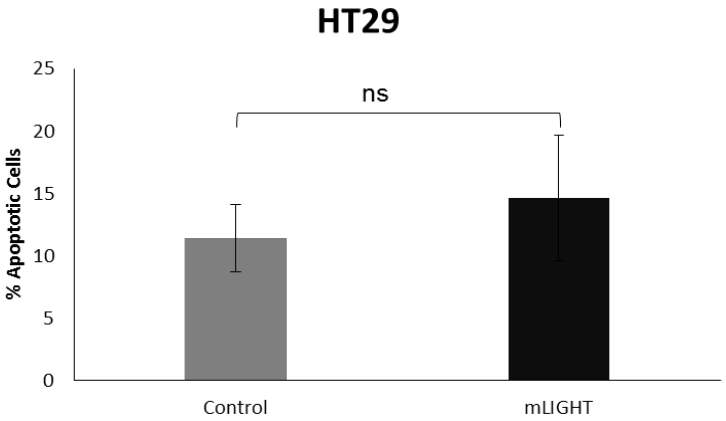

b.

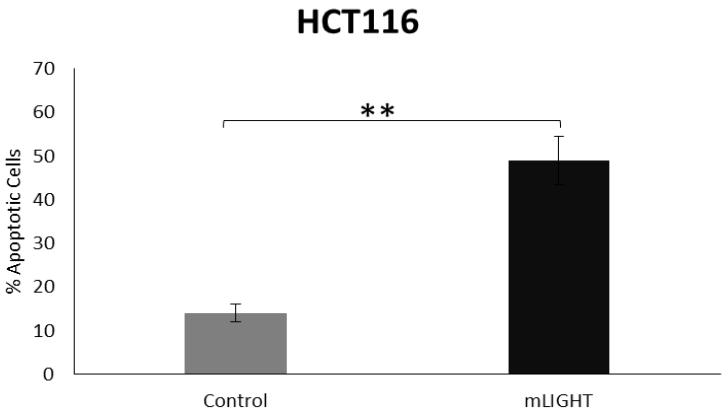

c.

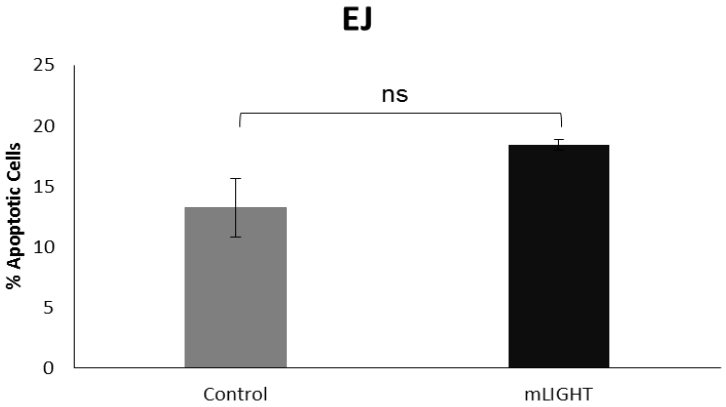

Figure 4.6. Detection of DNA fragmentation mediated by mLIGHT

$1.6x10^4$ of BrdU labelled HT29, HCT116 and EJ cells were co-cultured with $2x10^4$ cells/well of control (NT-L) or mLIGHT-L cells and incubated for 72hrs. ELISA assay was performed and absorbance was measured by a FLUOstar OPTIMA plate reader and the percentage of apoptotic cells was calculated (as described in 2.13.5). a, b, and c show HT29, HCT116 and EJ cells, respectively. Bars correspond to mean values of 3 replicates ±S.D. Stats: ns. non-significant; *, $p < 0.05$; **, $p < 0.01$, paired student t-test for co-cultured HT29, HCT116 or EJ/control (NT-L) cells vs mLIGHT-L/HT29, HCT116 or EJ cells, as indicated.

4.7 Effects of LT receptors ligation by mLIGHT in normal human urothelial (NHU) cells

This study has shown that mLIGHT can efficiently kill CRC and UCC cell lines, however no other studies have previously assessed the effects of LT receptors ligation in normal cells of epithelial origin. Thus, to determine whether mLIGHT-mediated death is tumour cell-specific or not, the effects of mLIGHT in urothelial cell carcinoma (UCC)-derived cell lines were compared to their normal counterparts, normal human urothelial (NHU cells). NHU cells were isolated and used in this study (see section 2.3.1) as described elsewhere (Crallan et al., 2006; Southgate et al., 2002). Before employing the co-culture system to deliver mLIGHT, it was important to examine the LTβR and HVEM expression on NHU cells. NHU cells were immunolabelled as above (Chapter 3) for detection of LTβR and HVEM by flow cytometry and results are shown in Figure 4.7. The flow cytometry results showed that NHU cells demonstrated high levels of expression for both the LTβR and HVEM receptors (Figure 4.7).

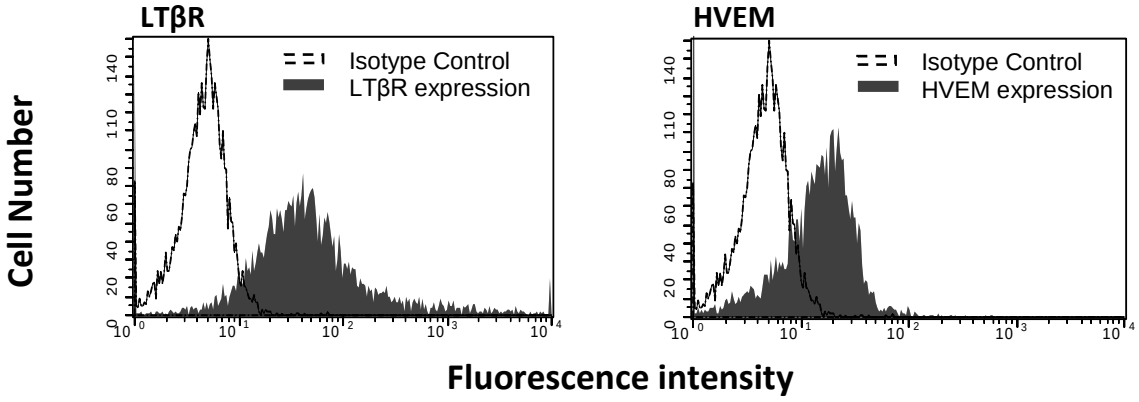

Figure 4.7. Detection of LTβR and HVEM expression on NHU cells

NHU cells were labelled with control PE-conjugated isotype antibody, anti-LTβR or anti-HVEM and incubated for 20-30mins. Cells were then washed and re-suspended in FACS buffer. Samples were analysed on an EasyCyte Guava flow cytometer and data analysed using InCyte2.6 Guava software (Millipore): overlay histograms of LTβR expression (left) and HVEM expression on NHU (right). Isotype control PE antibody labelling of cells is shown as an open black histogram; PE-conjugated anti-LTβR or anti-HVEM labelled cells are shown as filled grey histogram.

In order to activate LTβR and HVEM by mLIGHT and determine the effects of mLIGHT-mediated receptor ligation in normal cells, NHU cells were co-cultured with control (NT-L) or mLIGHT-L cells in KSFM culture medium for 48 and 72hrs. It is of note that both effector and NHU cells were co-cultured in serum-free (KSFM) culture medium to ensure that NHU cells maintained their undifferentiated state (Crallan et al., 2006) whilst it was also essential to ensure that MMC-treated NT-L (control) or mLIGHT-L effector cells do not undergo cell death (due to lack of serum) and thus delivered the mLIGHT signal to NHU cells. Phase contrast microscopy images for control (NT-L) or mLIGHT-L cells alone and co-cultured cells were taken to observe any morphological changes as shown in Figure 4.8.

It appeared that KSFM culture medium had no or little effect on growth arrested control (NT-L) or mLIGHT-L cells as shown in Figure 4.8. In agreement with microscopy observations, when co-culture experiments were performed and determined by the CytoTox-Glo assay, it was found that the background values of control (NT-L) or mLIGHT-L cells in KSFM medium were relatively similar to background values of that cells cultured in DR (data not shown) confirming lack of changes in effector cell viability. CytoTox-Glo cell death detection assay was performed as with the carcinoma cells (see above section 4.4). Results are presented in Figure 4.9 as raw data (following background correction) as well as fold increase relative to control in NHU for mLIGHT versus NT-L co-cultures. Raw RLU data and fold increase relative to controls were calculated using the parameters and equations provided in section 2.13.2.

Strikingly, as can be seen in Figure 4.9, unlike carcinoma cells that responded to mLIGHT by cell death, mLIGHT showed a cyto-protective effect on normal (NHU) cells.

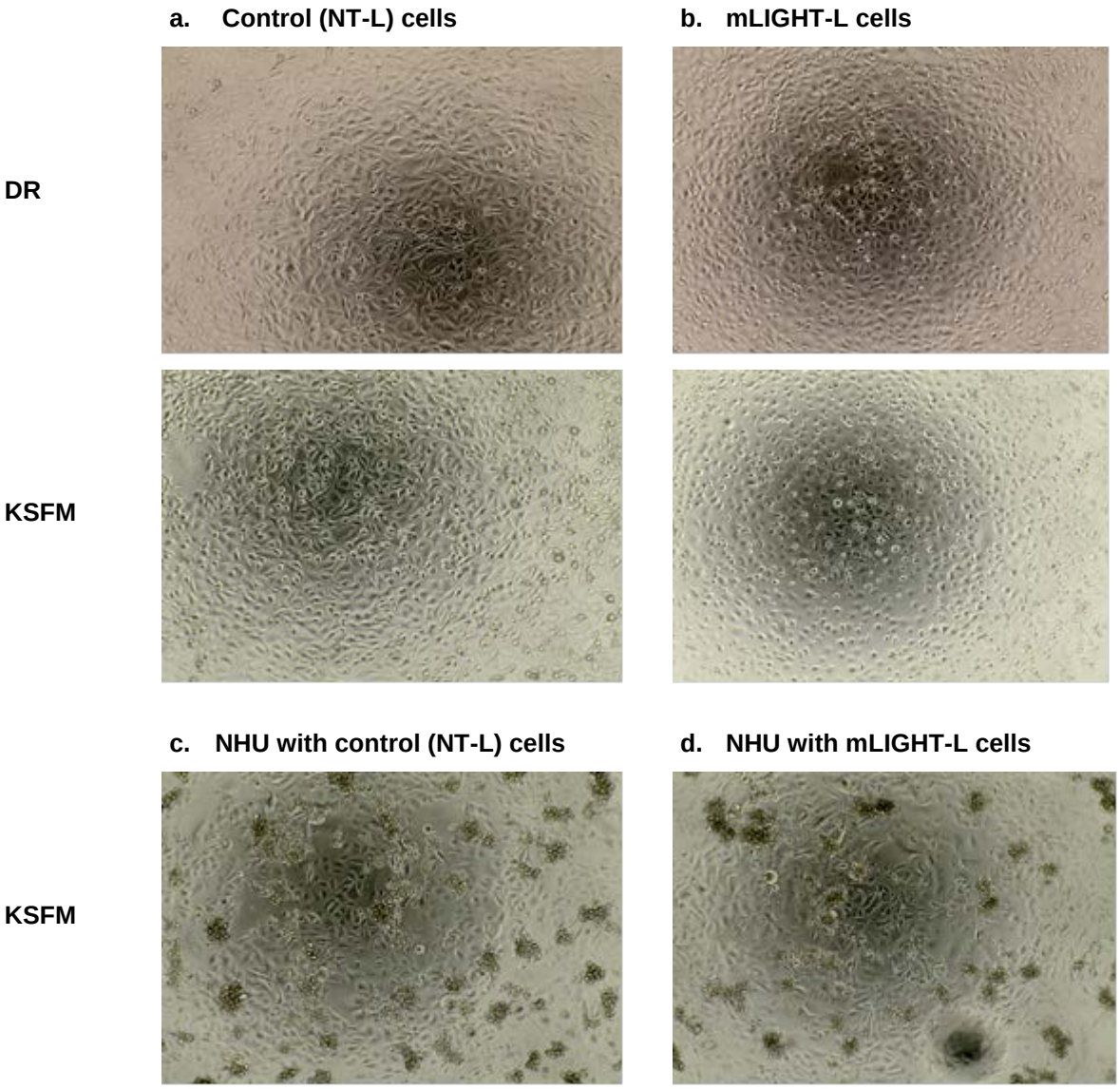

Figure 4.8. Microscopy images of control (NT-L), mLIGHT-L cells and co-cultured with NHU cells

MMC-treated cells control (NT-L) and mLIGHT-L cells were seeded at $2x10^4$ cells/well in 96-well plates in DR 10% (v/v) or complete KSFM and incubated at 37°C for 72hrs. a, shows control (NT-L) cell cultured in DR 10% (upper images) and in KSFM (lower images). b, shows mLIGHT-L cells cultured in cultured in DR 10% (upper images) and in complete KSFM (lower images). c and d show co-culture of NHU cells with MMC-control (NT-L) (left) and mLIGHT-L cells (right), respectively, for 72hrs. Photos were taken at a 100x magnification using an EVOSXL inverted microscope (PeqLab).

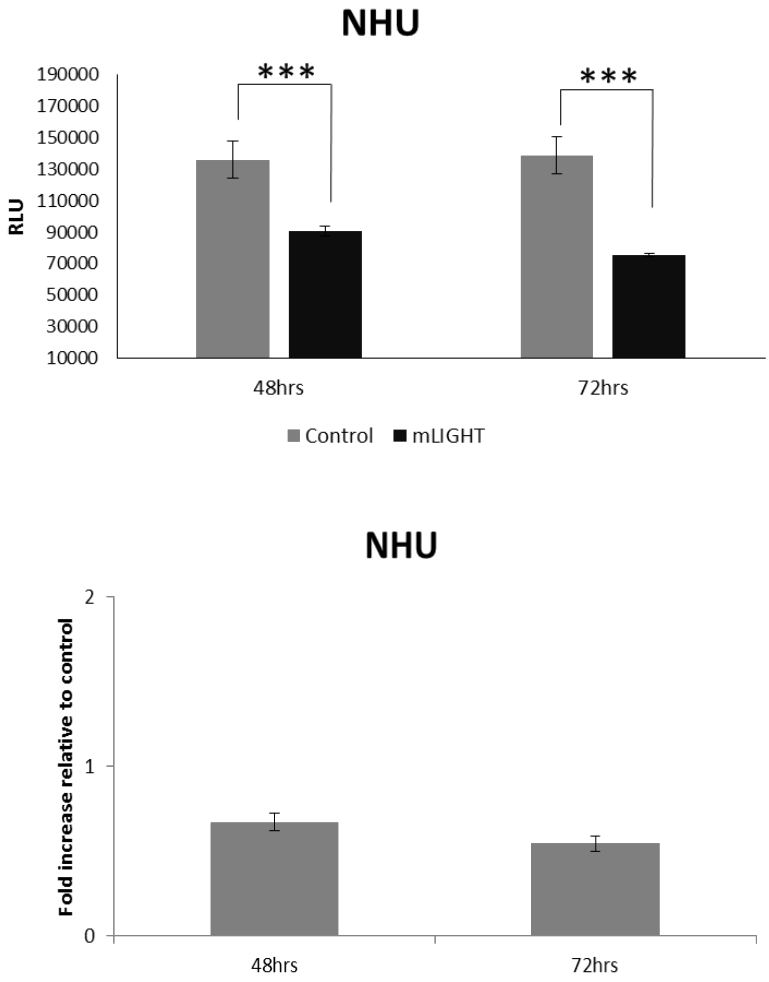

Figure 4.9. Effect of mLIGHT in normal human urothelial (NHU) cells

MMC-treated control (NT-L) and mLIGHT-L cells were seeded at $2x10^4$ cells/well in 96-well white plates overnight and on the following day NHU cells were seeded at $1.6x10^4$. Cells were incubated for 48 and 72hrs at 37°C and 5% (v/v) of CO_2. After that, 50µL of CytoTox-Glo substrate were added to each well and luminescence was measured on a FLUOstar OPTIMA plate reader. Results are presented as relative luminescence units (RLU) following background correction (top figure). Fold increase relative to control was generated from background corrected data as detailed in section 2.13.2 and as described in Figure 4.4 (bottom figure). Bars correspond to mean values of 4-5 replicates ±S.D. Stats: ns. non-significant; *, $p < 0.05$; **, $p < 0.01$; ***, $p < 0.001$, paired student t-test, NHU cells/control vs NHU cells/mLIGHT, as indicated.

4.8 Induction of pro-inflammatory cytokine secretion following LTβR and HVEM ligation by mLIGHT

There is evidence that ligation of TNFR members can induce cytokine secretion in epithelial cells. A study reported that HT29 cells exhibited IL-8 secretion in response to TNF-α and Fas treatment (Abreu-Martin et al., 1995). Moreover, previous studies on the highly related TNFR member CD40 have shown that ligation by membrane presented CD40L (mCD40L) induced secretion of cytokines IL-6, IL-8 and GM-CSF in some carcinoma cell lines of CRC and UCC origins (Georgopoulos et al., 2007). Interestingly, although soluble CD40 agonist could induce IL-8 (and to a lesser extent IL-6 secretion), only mCD40L could induce GM-CSF secretion (Georgopoulos et al., 2007). The secretion of IL-6 and IL-8 was reported to be dependent on NF-κB activation in normal and malignant epithelial cells and also in human colonic fibroblasts (Cagnoni et al., 2004; Gallagher et al., 2002; Gelbmann et al., 2003; Schwabe et al., 2001). Others have demonstrated that LTβR activation with immobilised agonistic anti-LTβR monoclonal antibody (M12) induced secretion of IL-8 and RANTES in A375 cells, but not cell death, and similar results were observed when LT receptor was cross-linked with membrane-bound LTβ and LTαβ (both ligands for LTβR) (Degli-Esposti et al., 1997b).

As the secretion of pro-inflammatory cytokines in carcinoma cells by mLIGHT is not yet investigated, this study examined whether mLIGHT can induce the secretion of cytokines IL-6, IL-8 and GM-CSF at various time points of 6, 12, 36 and 48hrs post receptor ligation. Detection of cytokines secretion was quantified by ELISA assays and data were analysed (see section 2.15).

Results showed that mLIGHT caused a decrease in IL-6 levels in HT29 cells (Figure 4.10a); by contrast it induced the increase of IL-6 secretion in EJ cells (Figure 4.10b), whilst there was no IL-6 secretion by HCT116 cells (data not shown). mLIGHT triggered significant IL-8 secretion in all cells tested compared with controls in a time-dependent fashion (Figure 4.10c, d and e). Moreover, mLIGHT caused secretion of GM-CSF in HT29 and HCT116 (Figure 4.10f and g) and more dramatic secretion of GM-CSF was observed in EJ cells, compared with controls (Figure 4.10h).

a.

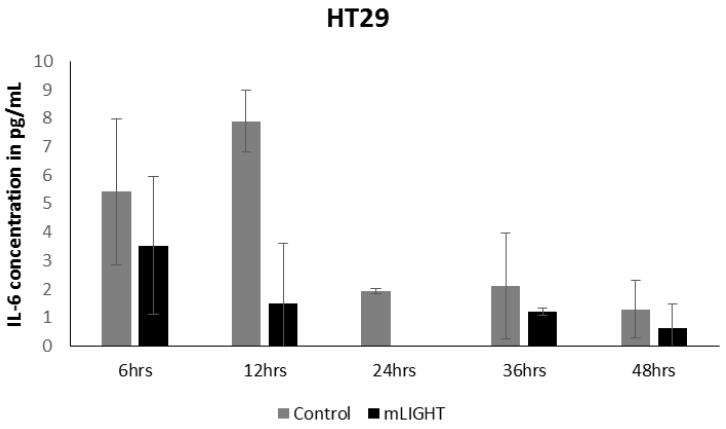
HT29
IL-6 concentration in pg/mL
10
9
8
7
6
5
4
3
2
1
0
6hrs
12hrs
24hrs
36hrs
48hrs
Control
mLIGHT

b.

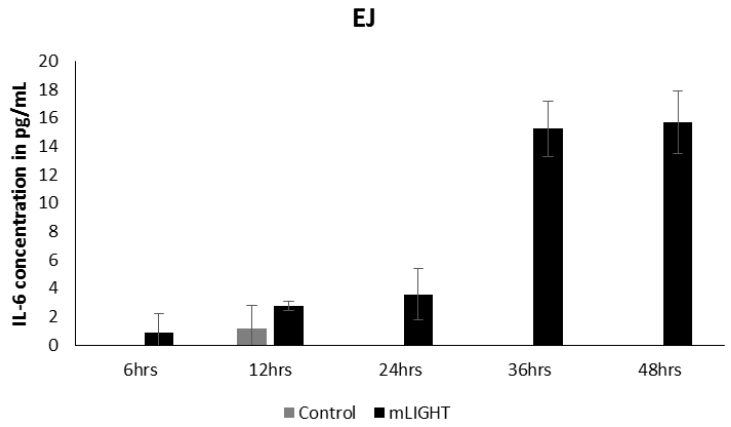
EJ
IL-6 concentration in pg/mL
20
18
16
14
12
10
8
6
4
2
0
6hrs
12hrs
24hrs
36hrs
48hrs
Control
mLIGHT

c.

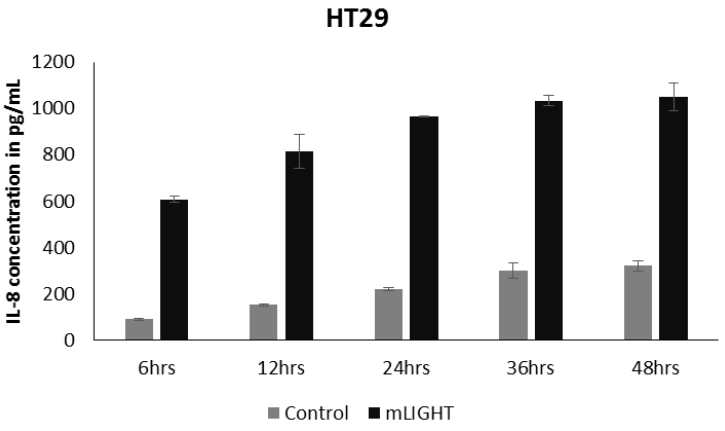
HT29
IL-8 concentration in pg/mL
1200
1000
800
600
400
200
0
6hrs
12hrs
24hrs
36hrs
48hrs
Control
mLIGHT

d.

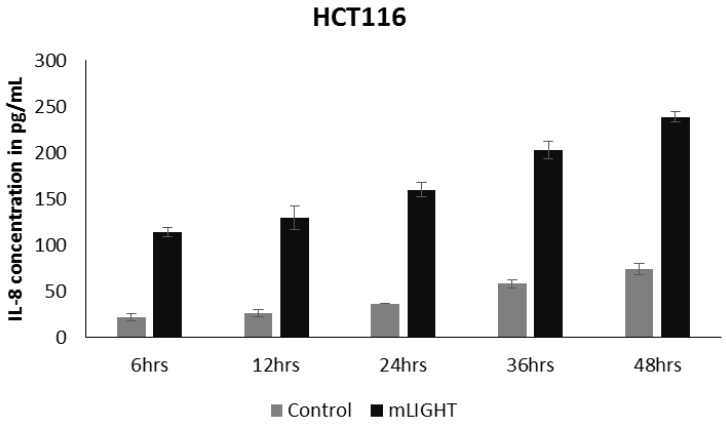
HCT116
IL-8 concentration in pg/mL
300
250
200
150
100
50
0
6hrs
12hrs
24hrs
36hrs
48hrs
Control
mLIGHT

e.

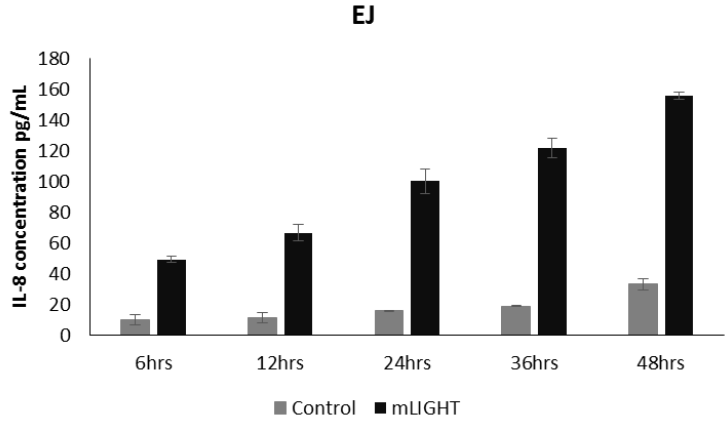
EJ
IL-8 concentration pg/mL
180
160
140
120
100
80
60
40
20
0
6hrs
12hrs
24hrs
36hrs
48hrs
Control
mLIGHT

f.

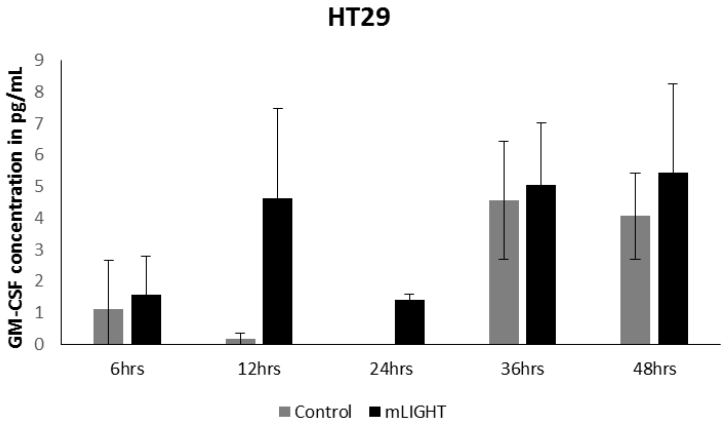

g.

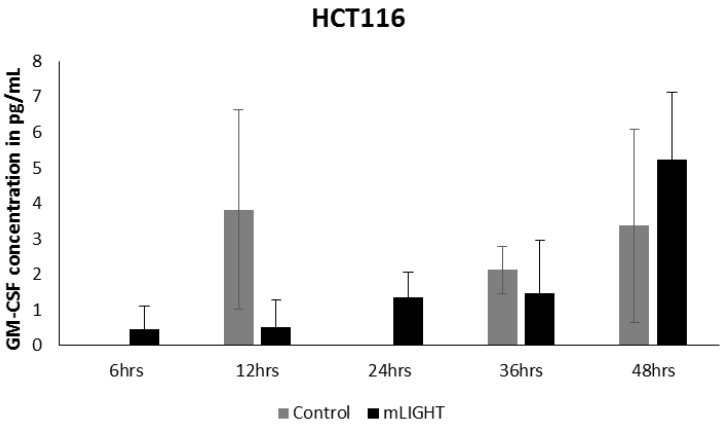

h.

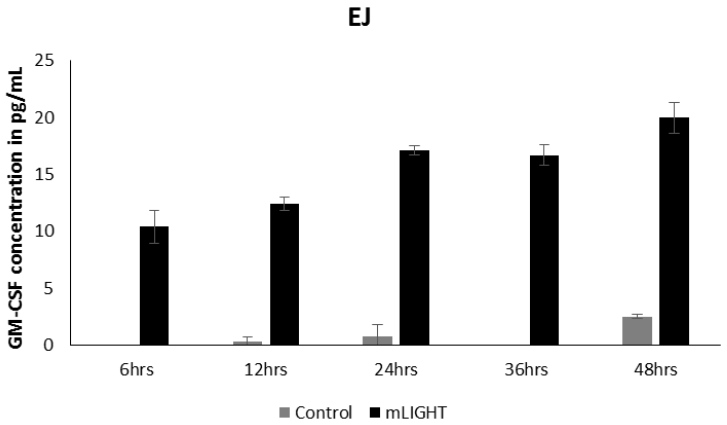

Figure 4.10. mLIGHT-mediated secretion of pro-inflammatory cytokines in carcinoma cells

HT29, HCT116 and EJ cells were co-cultured with MMC-treated control (NT-L) or mLIGHT-L cells for 6, 12, 24, 36 and 48hrs. Culture supernatants were collected at the indicated time points and secretion of IL-6, -8 and GM-CSF were assessed using cytokine specific ELISAs by a FLUOstar OPTIMA (BMG Labtech) plate reader. Data are represented as mean values ±S.D cytokine concentrations (pg/mL) for 2 replicates. a and b show IL-6 results for HT29 and EJ cells, c, d and e show results of IL-8 for HT29, HCT116 and EJ cells, respectively. f, g and h show GM-CSF results for HT29, HCT116 and EJ cells.

Summary

- Culture-medium adapted mLIGHT-L cells and the original mLIGHT-L cells showed similar levels of mLIGHT expression, whereas control (NT-L) cells were negative for LIGHT expression as determined by flow cytometry.

- Cell viability experiments demonstrated that control (NT-L) and mLIGHT-L cells were efficiently and optimally growth-arrested following MMC treatment using concentration 15µg/mL.

- MMC treatment had no effect on LIGHT expression in mLIGHT-L cells tested by flow cytometry.

- Using the *in vitro* co-culture system for mLIGHT delivery:

  a. CytoTox-Glo death detection assays demonstrated that mLIGHT, in the absence of IFN-γ, triggered extensive cell death in HT29, HCTT16 and EJ cells, whilst RT112 cells showed moderate level of cell death (within less than 72hrs), but SW480 cells appeared relatively resistant to mLIGHT.

  b. SensoLyte caspase-3/7 detection assays demonstrated that mLIGHT triggered significant activation of caspase-3/7 in HT29, HCT116, RT112 and EJ cells but not in SW480 cells and these observations are in agreement with the results of the CytoTox-Glo assays.

  c. DNA fragmentation experiments showed that mLIGHT caused significant levels of DNA fragmentation in HCT116 cells and low levels of DNA fragmentation in HT29 and EJ cells.

  d. LT receptors ligation by mLIGHT resulted in significant induction of IL-8 and GM-CSF secretion in HT29, HCT116 and EJ cells.

- Normal (NHU) epithelial cells were positive for LTβR and HVEM expression as determined by flow cytometry.

- Unlike to the pro-apoptotic effects of mLIGHT on carcinoma cells, mLIGHT ligation was cyto-protective in normal (NHU) cells.

- The findings in this chapter highlighted the importance of signal quality (strength) in determining cellular functional outcome, and that mLIGHT-mediated death is tumour cell-specific.

Chapter 5

Investigations on the regulation and functional role of intracellular signalling proteins involved in LTβR and HVEM-associated signal transduction pathways

5.1 Introduction

LTβR and HVEM are members of the non-classical death receptor TNFR subfamily and mediate their intracellular pathways via TRAF recruitment, following ligand-receptor binding and activation (Dempsey et al., 2003; Xie, 2013). In response to extracellular stimuli (e.g. growth factors or cytokines) intracellular cascades are activated and TRAF proteins are recruited and relocated to membrane lipid rafts (section 1.8.1). TRAF recruitment triggers the activation of signalling events such as MAPKs, ERK1/2, JNK and p38 (section 1.8.2), transcription factors (TFs) AP-1 and NF-κB (section 1.8.3) and may also involve ROS production, which all can ultimately control and regulate cellular processes ranging from cell survival to cell death (Albarbar et al., 2015; Bishop et al., 2007; Kyriakis and Avruch, 2012; Roux and Blenis, 2004; Xie, 2013). As the precise regulation and/or roles of the TRAF adaptor proteins and MAPK in LTβR/HVEM signalling remain relatively under-investigated, the specific aims of the work described in this chapter were to:

- optimise immunoblotting techniques for the detection of intracellular proteins associated with LTβR and HVEM signalling.

- detect TRAF1, 2, 3, 5 and 6 expression activation following LTβR and HVEM signalling triggered by mLIGHT using immunoblotting and by utilising human protein-specific antibodies for TRAFs.

- perform immunoblotting to investigate TRAF1 and 3 regulation following LTβR and HVEM signalling by soluble agonists versus mLIGHT.

- employ immunoblotting to detect LT receptor-mediated ERK1/2, JNK and p38 expression/activation and use specific pharmacological inhibitors for ERK1/2 (U0126), JNK (SP600125) and p38 (SB202190) to investigate the functional role of these MAPKs in LTβR/HVEM death triggered by mLIGHT using CytoTox-Glo assays.

- use specific pharmacological inhibitors to determine whether TFs NF-κB and JNK/AP-1 are critical in LTβR/HVEM-mediated death as determined by CytoTox-Glo death detection assays.

5.2 Optimisation of immunoblotting techniques for detection of protein expression in epithelial and non-epithelial cultured cells

Due to the experimental challenges that the co-culture experiments pose when determining epithelial cell protein expression by immunoblotting (Western blotting) (see subsequent section), preliminary experiments were initially performed for detection of house-keeping protein expression for the selection of appropriate loading control proteins for co-culture-derived lysates. It is well-documented that the house-keeping protein β-actin expressed in most cell types (including epithelial cells and fibroblasts), as a part of the cell cytoskeleton as well as being important in controlling other housekeeping functions (i.e., development of cell shape and cell division) (Hofmann, 2009; Hofmann and de Lanerolle, 2006). β-actin has been one of the most commonly used loading controls in laboratory techniques to normalise protein expression as it is believed to have constant expression levels in different cells. By contrast, cytokeratins (CKs) are epithelial cell-specific protein (e.g. CK8 and CK18) and are expressed by epithelial cells but not fibroblasts (Moll et al., 1982a; Moll et al., 1982b).

At a first step of this optimisation, CK8 and CK18 expression was examined in lysates from cultured epithelial and fibroblast cells alone. For CK detection, immunoblotting was performed using initially an antibody detecting both CK8 and 18 isoforms to confirm specificity in epithelial cells versus fibroblasts, whereas equal protein loading was confirmed in all cell lines using a β-actin-specific antibody. As shown in Figure 5.1, the expression of both CK8 and 18 was naturally detectable in epithelial cells RT4, SW480 and HT29 cells, whilst other cells lines, such as CRC cell line (HCT116), UCC (RT112) and transfected CRC cell line SW480 with CD40 (SW480CD40) were detectable for CK8 but not CK18. CK8 or 18 expression was absent in fibroblast cell lines 3T3Neo and 3T3CD40L, whilst little CK expression was detectable with this antibody in EJ cells, which is in agreement with the highly mesenchymal nature of EJ cells (Crallan et al., 2006). Equal loading was confirmed by β-actin detection.

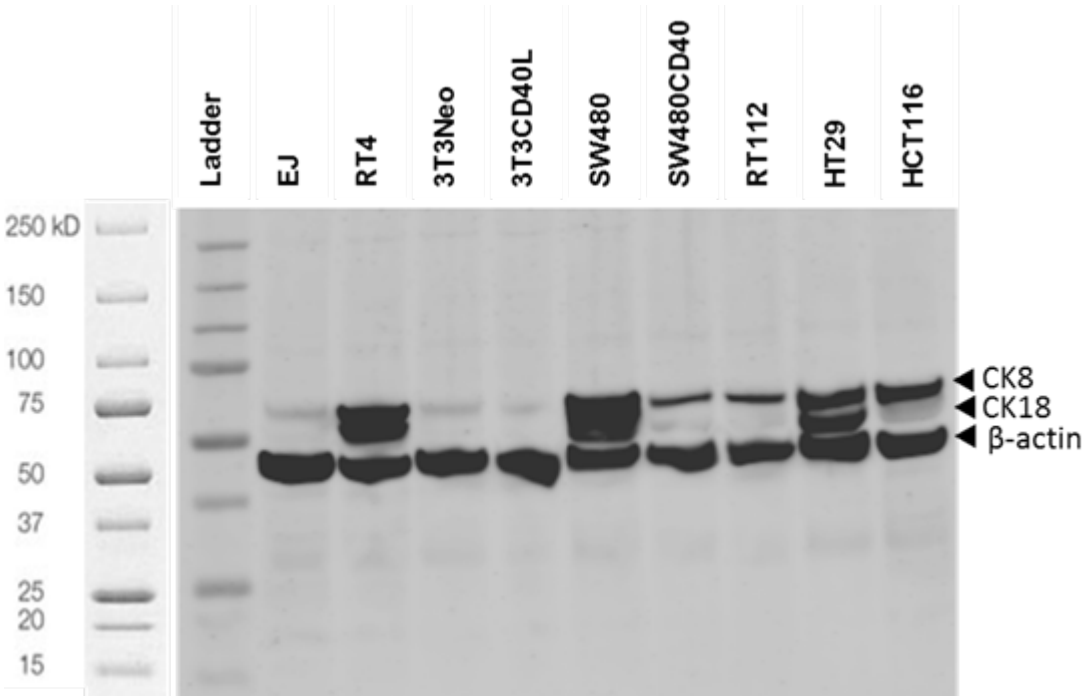

Figure 5.1. Detection of CK8 and CK18 expression in cell lines of epithelial and mesenchymal (fibroblast) origins

20µg of cell lysates from various cells lines as indicated were loaded per track and separated by SDS-PAGE using 4-12% (w/v) Bis-Tris gel and then transferred onto a PVDF membrane. The PVDF membrane was probed overnight with monoclonal anti-CK8-18 (Zym5.2) in TBS/Tween 0.1% (v/v) (1:1000 dilution) and then the membrane was immunoblotted with primary monoclonal antibody β-actin (1:25,000 dilution) in TBS/Tween 0.1% (v/v). The membrane was incubated with goat anti-mouse IgG Alexa 680 antibody (1:10,000) in TBS/Tween 0.1%. Antibody binding was visualised at channel 700nm using an Odyssey™ Infra-red Imaging system (Li-Cor). The expected molecular weight of CK8, 18 and β-actin were 52.5, 50 and 42kDa, respectively.

As only very little detectable CK expression was evident for the UCC line EJ and this may be because the monoclonal anti-CK8-18 (Zym5.2) used was not sensitive for detection of CK8-18 on EJ cells, immunoblotting experiments were performed using different human-specific antibodies against CK8/18 to a) detect CK8/18 expression in EJ cells and b) confirm lack of CK expression in NT-L (control) and mLIGHT cells (to be used in co-culture experiments) and the HCT116 line (served as a positive control). As shown in Figure 5.2, EJ cells exhibited detectable CK18 expression but not CK8 whereas both CK8 and 18 were absent in fibroblast cells NT-L and mLIGHT-L cells. HCT116 cells showed high levels of CK8 and CK18 expression.

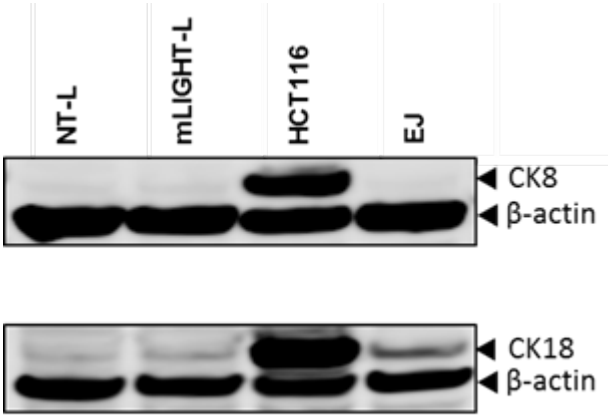

Figure 5.2. Optimised detection of CK expression in effector and target cell lines

20µg of cell lysates from control (NT-L), mLIGHT-L, HCT116, and EJ cells were loaded per track and separated by SDS-PAGE using 4-12% (w/v) Bis-Tris gels and then transferred onto a PVDF membrane. Then PVDF membrane was probed with the primary monoclonal antibody anti-CK8 (C51) or anti-CK18 (CY-90) in TBS/Tween 0.1% (v/v) (1:1000 dilution). Membranes were immunoblotted with primary monoclonal antibody β-actin (1:25,000 dilution) in TBS/Tween 0.1% (v/v). Then membranes were incubated with secondary antibody goat anti-mouse IgG Alexa 680 in TBS/Tween 0.1% (v/v) (1:10,000). Antibody binding was visualised at channel 700nm using an Odyssey™ Infra-red Imaging system (Li-Cor). The expected molecular weight of CK8, 18 and β-actin were 52.5, 50 and 42kDa, respectively.

5.3 Immunoblotting methodologies for correct and sensitive detection of epithelial proteins in lysates derived following co-culture experiments

The use of the co-culture system for LT receptor activation in epithelial (target cancer) cells poses experimental limitations in terms of using appropriate loading controls in immunoblotting experiments, in comparison to experiments involving protein detection in epithelial cells alone (e.g. treated with soluble agonists). The optimisation experiments described in the previous section, established the methods for the detection of total (β-actin) and epithelial cell-specific markers (CK8 and 18). CK8 and 18 were used as a loading control for immunoblotting and densitometry-based normalisation and adjustment of loading. This was to ensure that when lysates were loaded for gel electrophoresis (and subsequent blotting), the equivalent protein content of target cells from co-cultures of both target/control (NT-L) and target/mLIGHT-L cells was appropriately assessed, as also described previously (Bugajska et al., 2002; Georgopoulos et al., 2006). In particular, for all co-culture experiments, densitometry was initially used to quantify band intensity for CK8 (for HT29 and HCT116) or CK18 (for EJ cells) by the Li-Cor Odyssey analysis software and correction based on CK8 or CK18 band intensity was performed. Following band intensity-based normalisation of lysates (Figure 5.3a), subsequent immunoblotting experiments were performed with equal protein from epithelial cells ensured, as shown in Figure 5.3b where representative data are provided.

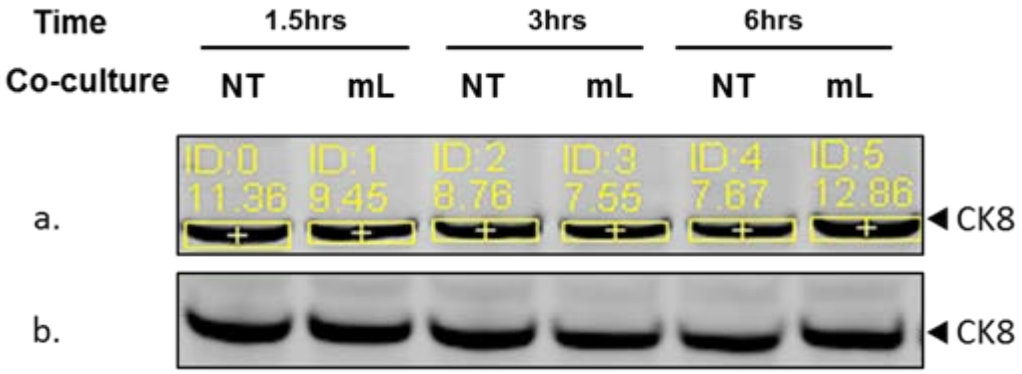

Figure 5.3. An example of densitometry analysis for protein expression correction based on CK8 band intensities values

40µg of cell lysates from HCT116 co-cultures with control (NT) and mLIGHT-L (mL) cells were loaded per track and separated by SDS-PAGE using 4-12% (w/v) Bis-Tris gels and then transferred onto a PVDF membrane. Then PVDF membrane was probed with primary anti-CK8 in TBS/Tween 0.1% (v/v) (1:1000 dilution). The membrane was then incubated with goat anti-mouse IgG Alexa 680 antibody in TBS/Tween 0.1% (v/v) (1:10,000 dilution). Antibody binding was visualised at 700nm using an Odyssey™ Infra-red Imaging system (Li-Cor). a, results from "first run" immunoblotting experiment with quantification of band intensities for CK8 expression (before loading correction). b, "second run" immunoblotting experiment following densitometry analysis (after loading correction).

5.4 Differential regulation of TRAFs following LTβR and HVEM signalling

The TRAF adaptor proteins play critical roles in the intracellular signalling pathways triggered by members of the TNFR family. Studies demonstrated that TRAF1 interacts indirectly with TNFRI (via TRADD) and forms a complex with TRAF2 to trigger the activation of MAPK and TFs (Hehlgans and Pfeffer, 2005). TRAF2 on the other hand was reported to regulate cell survival by the activation of MAPK and NF-κB (Arch et al., 1998; Park et al., 2000). TRAF3 is an important and multifaceted regulator of TNFRSF signalling, and studies have previously demonstrated that TRAF3 contains a site on its C-terminal cytoplasmic domain that can interact with TRAF1, 2 and 5, and mediates EBV and induced B cell proliferation and the activation of NF-κB (Izumi et al., 1999). Previous studies reported that TRAF3 recruitment is important in cell death triggered by the activation of CD40 and LTβR (Eliopoulos et al., 1996; Force et al., 1997; Georgopoulos et al., 2006; Rooney et al., 2000; VanArsdale et al., 1997). However, TRAF5 was discovered as an adaptor protein that can bind to CD40 and LTβR (Ishida et al., 1996a; Nakano et al., 1996), and it was reported to be implicated in NF-κB activation following CD27 and CD30 signalling (Aizawa et al., 1997; Akiba et al., 1998). Similarly to TRAF5, TRAF6 was reported to activate NF-κB, JNK and p38 when it is overexpressed (Song et al., 1997) and other studies demonstrated that TRAF6 can interact with some of TNFR members such as CD40, RANK, TNFRII and NGFR (Darnay et al., 1999; Galibert et al., 1998; Ishida et al., 1996b; Khursigara et al., 1999; Tsukamoto et al., 1999; Wong et al., 1998).

Therefore, to understand the proximal events of LT receptor signalling, this study screened for the expression (and its regulation) of cytosolic TRAF proteins TRAF1, 2, 3, 5 and 6 following LTβR and HVEM signalling by immunoblotting using human-specific antibodies. As TRAF1 and 3 have been reported to be crucial in transcriptional mechanisms and induction of cell death, respectively (Georgopoulos et al., 2006), TRAF1 and 3 expression in particular were examined following the activation of LTβR and HVEM by soluble agonists versus mLIGHT. In some experiments, positive controls have been used as described in figure legends.

Based on the observations in Chapters 3 and 4 that HT29, HCT116 and EJ cells showed LT receptor-mediated death at 72hrs and 24hrs after activation with soluble agonists and mLIGHT treatment, respectively, and as TRAF recruitment represents an early event in TNFRSF signalling, TRAF expression was investigated following cell treatment with soluble agonists and as early as 1.5, 3, and 6hrs following treatment with mLIGHT. The results showed that HT29 and HCT116 cells showed some level of TRAF1 upregulation following LIGHT and/or combinatorial LIGHT/IFN-γ treatment, whereas EJ cells showed a massive induction of TRAF1 after LIGHT/IFN-γ treatment (Figure 5.4a). Importantly, treatment with mLIGHT, although it did not lead to a detectable increase in HT29 cells, it caused a dramatic, and time-dependent induction of TRAF1 levels in both HCT116 and EJ cells (Figure 5.4b).

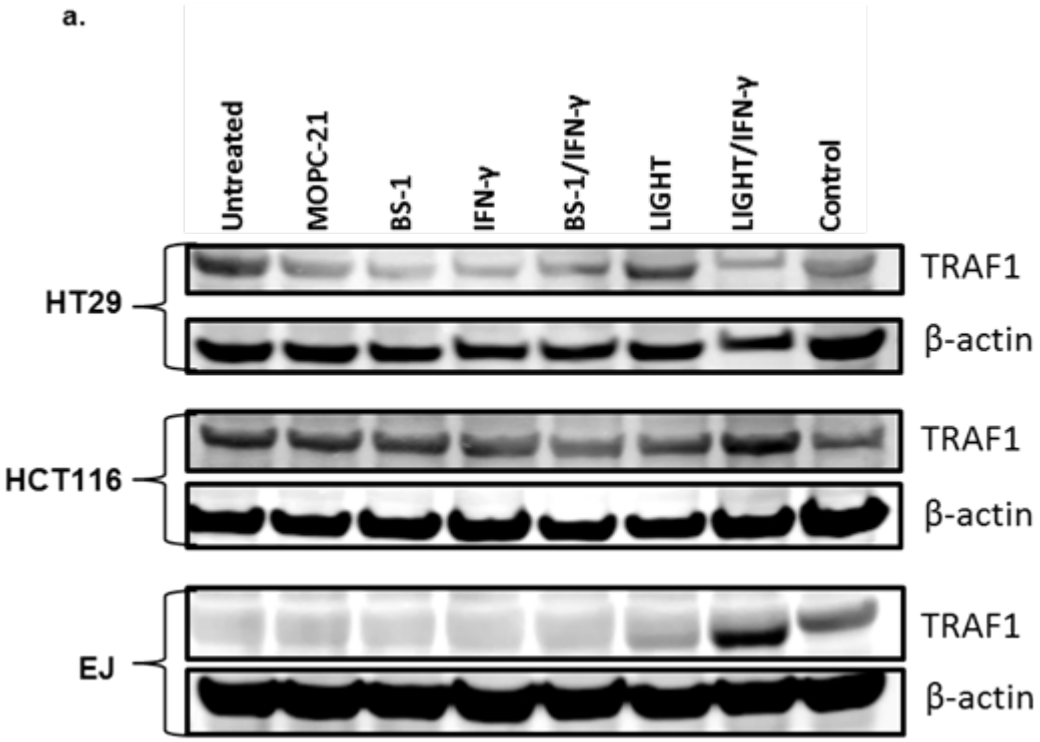

b.

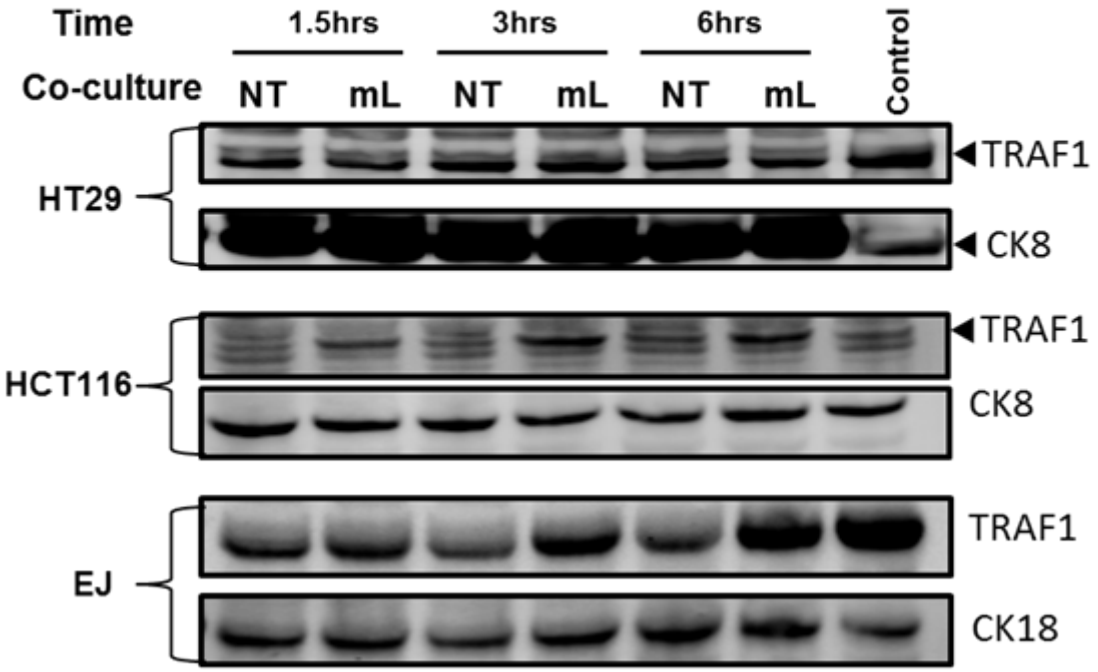

Figure 5.4. TRAF1 expression following LTβR and HVEM activation in carcinoma cells after receptor activation by soluble receptor agonists *versus* mLIGHT

a, HT29, HCT116 and EJ cells were seeded in 10cm^2 culture dishes and treated with control antibody (MOPC-21 – at conc. 10μg/mL), agonistic antibody (BS-1 – at conc. 30μg/mL), IFN-γ (at conc. 180U/mL), LIGHT (at conc. 1μg/mL) in the absence or presence of IFN-γ and incubated for 48hrs. b, HT29, HCT116 and EJ cells were co-cultured at cell density 3x10^6 with MMC-treated control (NT) or mLIGHT-L cells (mL) at cell density 3.5x10^6 in 10cm^2 culture dishes and incubated for the indicated times. 20μg of treated cells or 40μg of co-cultured cells of whole cell lysates were loaded per track and separated under denaturing conditions by SDS-PAGE using 4-12% (w/v) Bis-Tris gels and then transferred onto a PVDF membrane. The membranes were probed with primary polyclonal antibody anti-TRAF1 in TBS/Tween 0.1% (v/v) (1:250 dilution). Then membranes were immunoblotted with primary monoclonal antibody β-actin (1:25,000 dilution) in TBS/Tween 0.1% for treated cells with soluble agonist or membranes were probed with CK8 (for H29 and HCT116 cells) or CK18 (for EJ cells) (1:1000 dilution) for co-cultured cells. Then incubated for one hour with secondary antibody goat anti-rabbit IgG IRDye 800 (1:10,000 dilution) for TRAF1 detection or incubated with secondary antibody goat anti-mouse IgG Alexa 680 in TBS/Tween 0.1% (v/v) (1:10,000) for β-actin, CK8 and 18 detection. Antibody binding was visualised using an Odyssey^{TM} Infra-red Imaging system (Li-Cor). Positive control represents lysates from co-cultures of mCD40L with HCT116 cells for TRAF1 induction. The expected molecular weight of TRAF1 was 52kDa.

Interestingly, the pattern of regulation for TRAF2 was different, with TRAF2 expression being downregulated following treatment of HT29 cells with mLIGHT in comparison to control. A similar trend in TRAF2 level regulation was observed in HCT116 and EJ cells after treatment with mLIGHT (Figure 5.5).

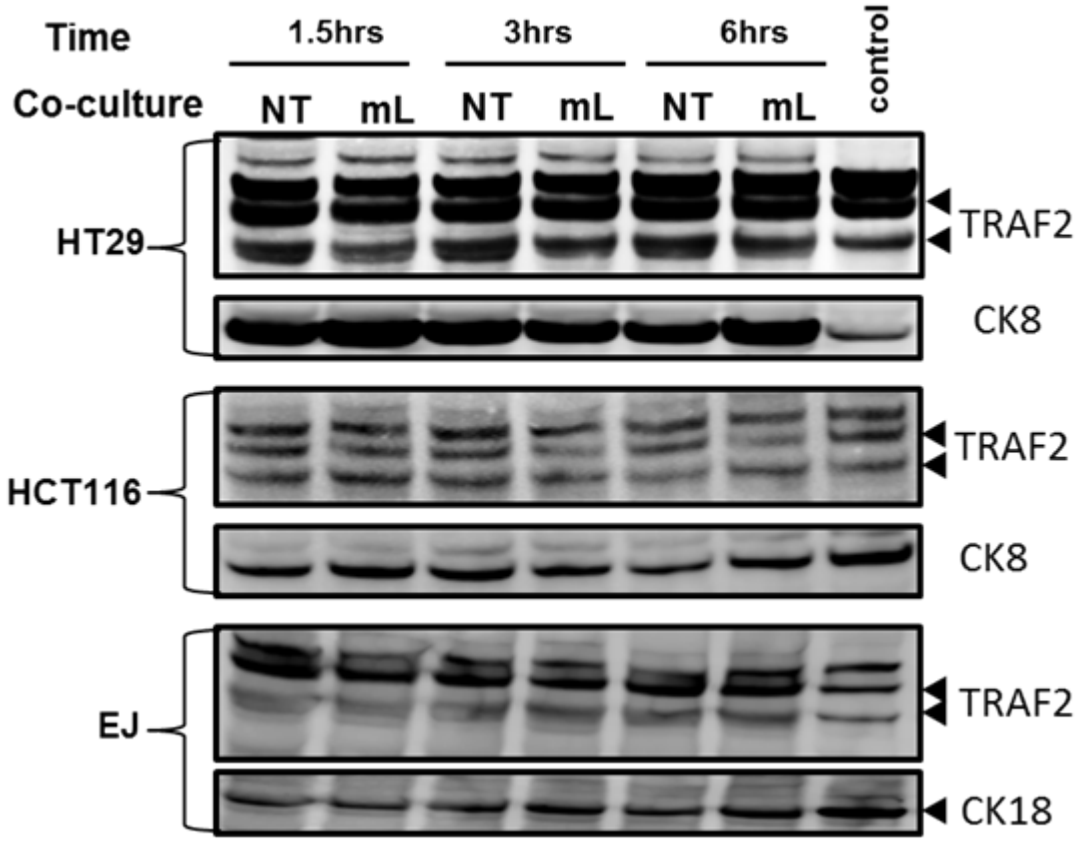

Figure 5.5. TRAF2 expression following LTβR and HVEM activation in carcinoma cells by mLIGHT

HT29, HCT116 and EJ cells were co-cultured in 10cm^2 culture dishes at cell density 3x10^6 with MMC-treated control (NT) or mLIGHT-L cells (mL) at cell density 3.5x10^6 for different time points 1.5, 3 and 6hrs, as indicated in figure. 40µg of whole cell lysates were loaded per track and separated under denaturing conditions by SDS-PAGE using 4-12% (w/v) Bis-Tris gels and then transferred onto a PVDF membrane. Membranes were probed with primary polyclonal antibody anti-TRAF2 in TBS/Tween 0.1% (v/v) (1:250 dilution) and then membranes were incubated with primary monoclonal antibody CK8 (for H29 and HCT116 cells) or CK18 (for EJ cells) (1:1000 dilution). Membranes were incubated with secondary antibody goat anti-rabbit IgG IRDye 800 (1:10,000 dilution) for TRAF2 detection and membranes were probed with secondary antibody goat anti-mouse 680 (1:10,000 dilution) for CK8 and 18 detection. Antibody binding was visualised using an Odyssey^{TM} Infra-red Imaging system (Li-Cor). Positive control represents lysates from co-cultures of 3T3Neo with HCT116 cells for TRAF2 induction. The expected molecular weight of TRAF2 was 50kDa.

TRAF3 expression was detected following treatment with soluble receptor agonists and mLIGHT. Treatment with LIGHT and combination of LIGHT/IFN-γ caused a massive induction of TRAF3 expression in EJ cells but there was no TRAF3 expression observed in HT29 and HCT116 cells (Figure 5.6a). Importantly, however, treatment with mLIGHT cells in HT29 cells caused detectable TRAF3 at 1.5, 3 and 6hrs, whereas there was moderate and strong upregulation of TRAF3 in HCT116 and EJ cells, respectively, as early as 1.5hrs post-ligation (Figure 5.6b).

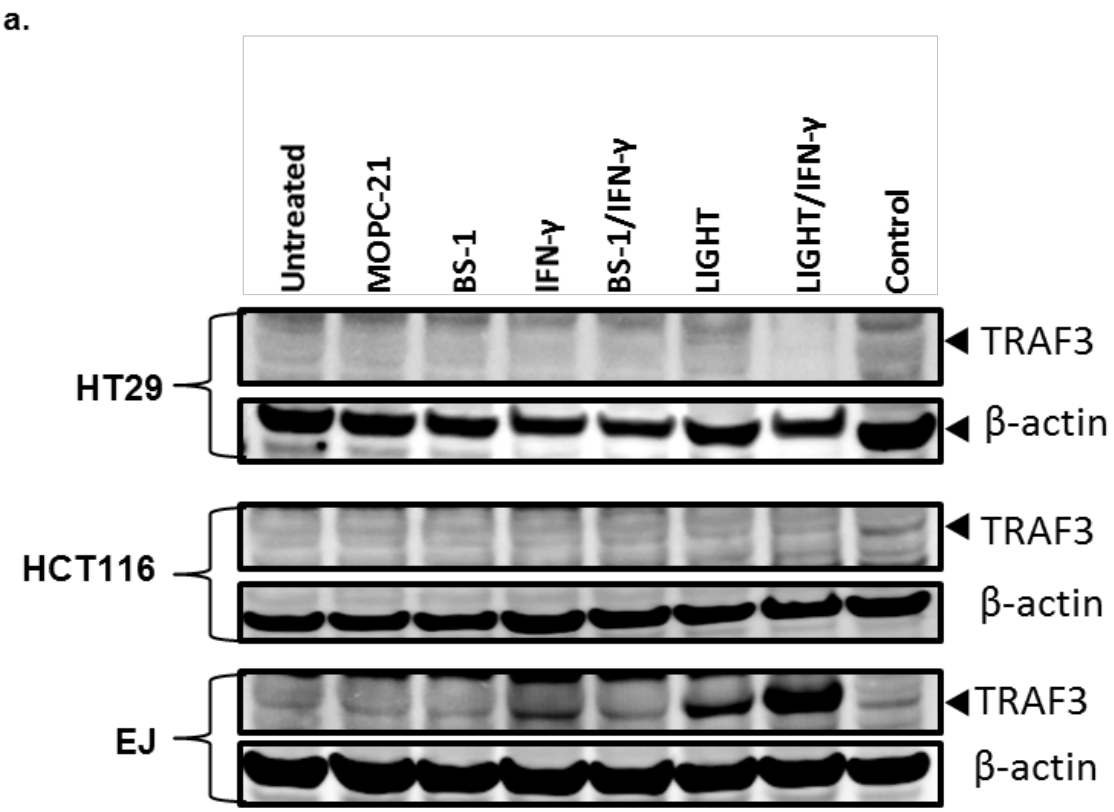

b.

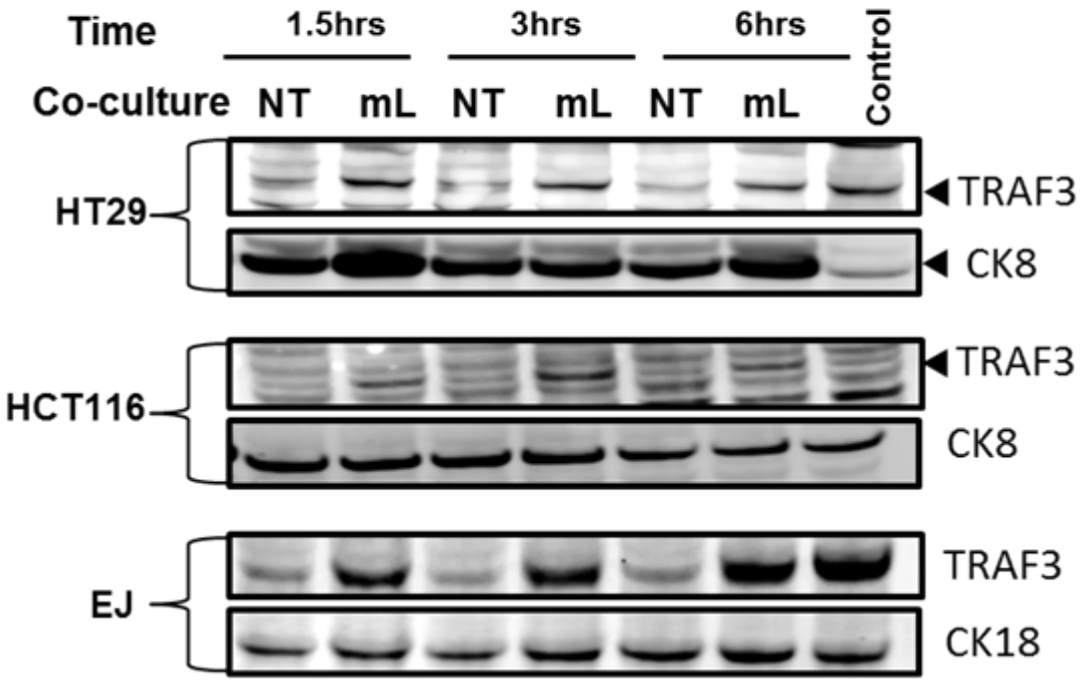

Figure 5.6. TRAF3 expression following LTβR and HVEM activation in carcinoma cells after receptor activation by soluble receptor agonists *versus* mLIGHT

a, HT29, HCT116 and EJ cells were seeded in 10cm^2 culture dishes and treated with control antibody (MOPC-21 – at conc. 10μg/mL), agonistic antibody (BS-1 – at conc. 30μg/mL), IFN-γ (at conc. 180U/mL), LIGHT (at conc. 1μg/mL) in the absence or presence of IFN-γ and incubated for 48hrs. b, HT29, HCT116 and EJ cells were co-cultured at cell density 3x10^6 with MMC-treated control (NT) or mLIGHT-L cells (mL) at cell density 3.5x10^6 in 10cm^2 culture dishes and incubated for various time points 1.5, 3 and 6hrs. 20μg of treated cells or 40μg of co-cultured cells of whole cell lysates were loaded per track and separated under denaturing conditions by SDS-PAGE using 4-12% (w/v) Bis-Tris gels and then transferred onto a PVDF membrane. The membranes were probed with primary polyclonal antibody anti-TRAF3 in TBS/Tween 0.1% (v/v) (1:250 dilution). Then membranes were incubated with primary monoclonal antibody β-actin (1:25,000 dilution) for treated cells or CK8 (for H29 and HCT116 cells) or CK18 (for EJ cells) co-cultured cells (1:1000 dilution). Membranes were incubated with secondary antibody goat anti-rabbit IgG IRDye 800 (1:10,000 dilution) for TRAF3 detection and membranes were probed with secondary antibody goat anti-mouse 680 (1:10,000 dilution) for β-actin, CK8 and 18 detection. Antibody binding was visualised using an Odyssey^{TM} Infra-red Imaging system (Li-Cor). Positive control represents lysates from co-cultures of mCD40L with HCT116 cells for TRAF3 induction. The expected molecular weight of TRAF3 was 50kDa.

Although TRAF5 basal levels were detectable in 2/3 of the cell lines tested (HT29 and EJ), the level of TRAF5 protein expression was relatively unchanged in HT29 and EJ following treatment with mLIGHT, whereas TRAF5 expression was undetectable in HCT116 cells (Figure 5.7). No TRAF6 expression was detected in HT29, HCT116 and EJ cells following treatment with mLIGHT, although TRAF6 expression was detected in the positive control (Figure 5.8), which represents CD40-mediated TRAF6 upregulation by mCD40L (Mohamed and Georgopoulos, unpublished observations).

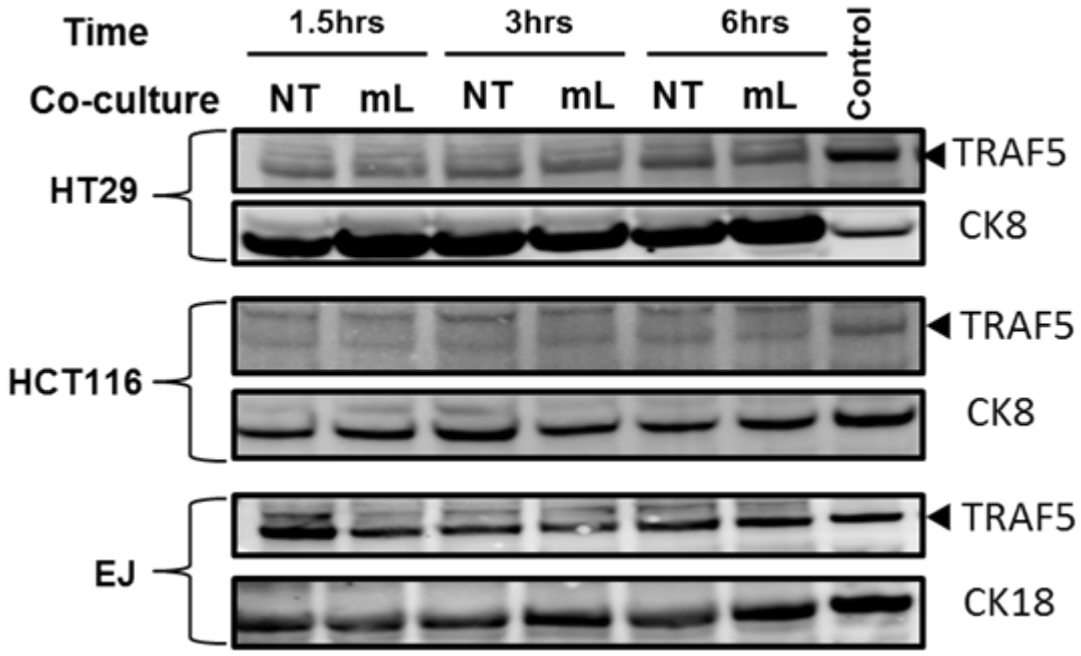

Figure 5.7. TRAF5 expression following LTβR and HVEM activation in carcinoma cells by mLIGHT

HT29, HCT116 and EJ cells were co-cultured at cell density $3x10^6$ with MMC-treated control (NT) or mLIGHT-L cells (mL) at cell density $3.5x10^6$ in $10cm^2$ culture dishes and incubated for different time points 1.5, 3 and 6hrs, as indicated. 40µg of whole cell lysates were loaded per track and separated under denaturing conditions by SDS-PAGE using 4-12% (w/v) Bis-Tris gels and then transferred onto a PVDF membrane. The membranes were probed with primary polyclonal antibody anti-TRAF5 in TBS/Tween 0.1% (v/v) (1:250 dilution). Membranes were incubated with primary monoclonal antibody CK8 (for H29 and HCT116 cells) or CK18 (for EJ cells) (1:1000 dilution). Membranes were incubated with secondary antibody goat anti-rabbit IgG IRDye 800 (1:10,000 dilution) for TRAF5 detection or membranes were probed with secondary antibody goat anti-mouse 680 (1:10,000 dilution) for CK8 and 18 detection. Antibody binding was visualised using an Odyssey™ Infra-red Imaging system (Li-Cor). Positive control represents lysates from co-cultures of 3T3Neo with HCT116 cells for TRAF5 induction. The expected molecular weight of TRAF5 was 55kDa.

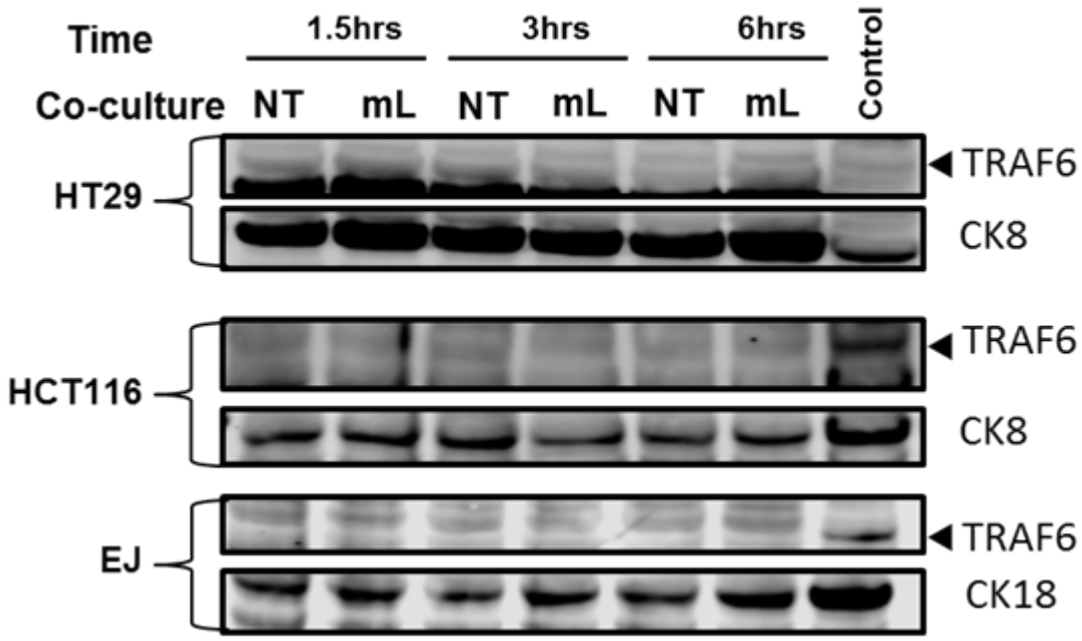

Figure 5.8. TRAF6 expression following LTβR and HVEM activation in carcinoma cells by mLIGHT

HT29, HCT116 and EJ cells were co-cultured in 10cm^2 culture dishes at cell density 3x10^6 with MMC-treated control (NT) or mLIGHT-L cells (mL) at cell density 3.5x10^6 and incubated for different time points 1.5, 3 and 6hrs, as indicated. 40µg of whole cell lysates were loaded per track and separated under denaturing conditions by SDS-PAGE using 4-12% (w/v) Bis-Tris gels and then transferred onto a PVDF membrane. The membranes were probed with primary monoclonal antibody anti-TRAF6 in TBS/Tween 0.1% (v/v) (1:250 dilution). Then membranes were incubated with primary monoclonal antibody CK8 (for H29 and HCT116 cells) or CK18 (for EJ cells) (1:1000 dilution). Then membranes were probed with secondary antibody goat anti-mouse 680 (1:10,000 dilution) for TRAF6, CK8 and 18 detection. Antibody binding was visualised using an Odyssey™ Infra-red Imaging system (Li-Cor). Positive control represents lysates from co-cultures of mCD40L with HCT116 cells for TRAF6 induction. The expected molecular weight of TRAF6 was 50kDa.

5.5 The role of MAPKs in LTβR and HVEM signalling

The main MAPKs identified in mammals include a) ERKs, b) JNKs, c) p38 and d) ERKs 3, 4 and 5 (Roux and Blenis, 2004) (as discussed in detail in section 1.8.2). The majority of studies that have reported on ERK1/2 function indicate that these MAPKs are mainly inducers of cell proliferation (Chang and Karin, 2001; Kyriakis and Avruch, 2012). However, other studies have implicated ERK1/2 in loss of proliferation and/or cell death responses, for instance it has been demonstrated that HeLa cells treatment with cisplatin can activate ERK (Wang et al., 2000), and inhibition of ERK in renal cell lines and primary cultures of renal proximal tubular cells stimulated their survival (Kim et al., 2005; Nowak et al., 2004). JNK can have multifaceted roles in cell fate but in many cases represents a strong pro-apoptotic mediator. For instance, JNK is activated in cell death responses to chemotherapy drugs (Hayakawa et al., 2004; Potapova et al., 2001). Furthermore, the ligation of RANK in osteoclast precursor cells and CD40 in carcinoma cells with cognate ligand RANKL and CD40L, respectively, contribute to cell death associated with JNK activation (Boyle et al., 2003; Eliopoulos et al., 2000; Elmetwali et al., 2010). Studies also have shown that the activation of LTβR and HVEM by overexpression leads to JNK activation (Chang et al., 2002; Hsu et al., 1997; Marsters et al., 1997b).

p38 is also a member of the MAPK family and studies reported that p38 can play anti-apoptotic and pro-apoptotic roles and this is depending on cell type as well as the stimuli. For instance, overexpression of the active form of the p38 inhibits cardiac myocytes from β-adrenergic receptor-mediated apoptosis (Zechner et al., 1998). Moreover, early activation of p38 protects Kyme cells from TNF-α-mediated apoptosis (Roulston et al., 1998). With a role of p38 in pro-apoptotic responses, studies demonstrated that NGF withdrawal and Fas ligation induced p38 activation (Juo et al., 1997; Kummer et al., 1997; Xia et al., 1995). Studies reported that p38 activation is a mediator in cell apoptosis of neurons (De Zutter and Davis, 2001), others demonstrated that p38 activates cell death in rat fetal brown adipocytes following stimulation with TNF-α (Valladares et al., 2000), and TRAIL-mediated cell death via ROS-activated p38 followed by caspase activation in HeLa cells (Lee et al., 2002).

As TRAF protein recruitment triggers the activation of MAPK cascades (Bishop, 2004; Bishop et al., 2007; Ichijo, 1999) and, as shown above, TRAF1 and 3 are induced as early as 1.5hrs (and remained upregulated at 3 and 6hrs) following treatment of HT29, HCT116 and EJ cells with mLIGHT, the activation (in the form of phosphorylation) of ERK1/2, JNK and p38 was examined at 6, 12 and 24hrs following LTβR and HVEM ligation with mLIGHT by immunoblotting using human protein-specific antibodies. Moreover, to determine the possible functional involvement of these MAPKs and downstream of TFs in LT receptor signalling, MAPK- and TF-specific pharmacological inhibitors (for JNK, MEK/ERK and p38, as well as inhibitors for NF-κB and AP-1 – see Appendix V for MAPK inhibitors titrations) were used and their effects in LTβR/HVEM-mediated activation by mLIGHT were assessed using CytoTox-Glo death detection assays.

Following treatment with mLIGHT, the immunoblotting results demonstrated that mLIGHT treatment did not appear to cause an obvious activation (phosphorylation) of ERK expression in HT29, HCT116 and EJ cells as shown in Figure 5.9. However, results from functional inhibition experiments showed that mLIGHT-mediated death was significantly abolished in a dose-dependent fashion by the inhibitor of MEK/ERK U0126 in HT29, HCT116 and EJ cells (Figure 5.10).

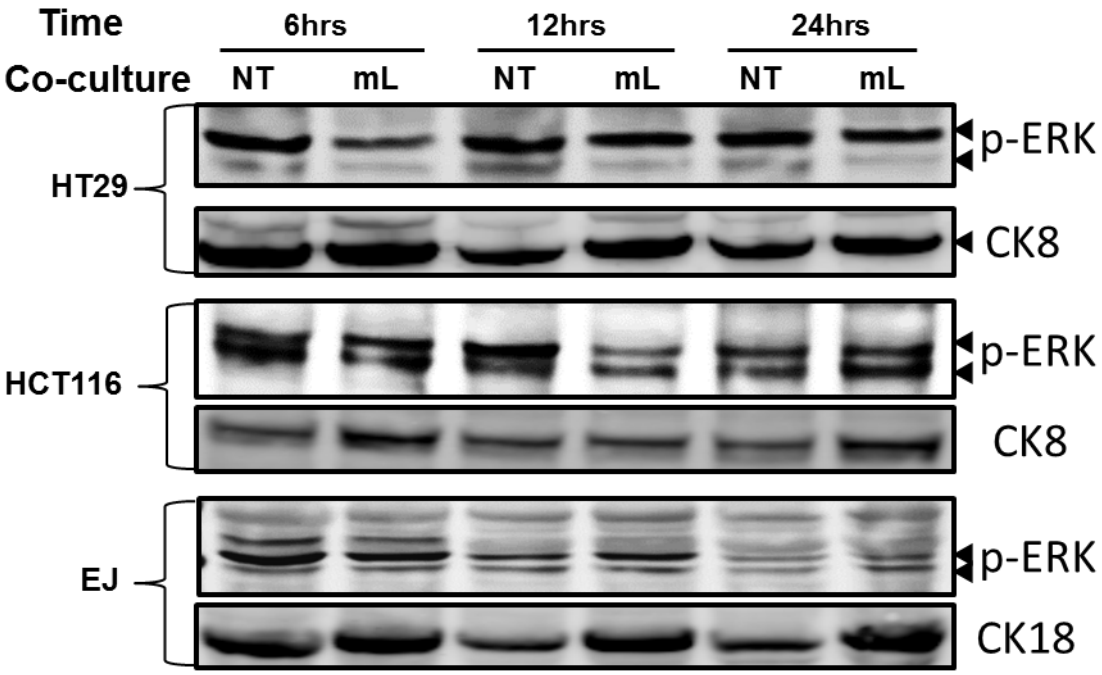

Figure 5.9. ERK1/2 expression following LTβR and HVEM activation in carcinoma cells by mLIGHT

HT29, HCT116 and EJ cells were co-cultured at cell density $3x10^6$ with MMC-treated control (NT) or mLIGHT-L cells at cell density $3.5x10^6$ in $10cm^2$ culture dishes and incubated for time points 6, 12 and 24hrs. 40µg of whole cell lysates were loaded per track and separated under denaturing conditions by SDS-PAGE using 4-12% (w/v) Bis-Tris gels and then transferred onto a PVDF membrane. The membranes were probed with primary monoclonal antibody anti-phospho-ERK1/2 in TBS/Tween 0.1% (v/v) (1:1000 dilution) with 5% w/v non-fat dry milk. Membranes were incubated with primary monoclonal antibody CK8 (for H29 and HCT116 cells) or CK18 (for EJ cells) (1:1000 dilution). Then membranes were incubated with secondary antibody goat anti-mouse 680 (1:10,000 dilution) for p-ERK1/2, CK8 and 18 detection. Antibody binding was visualised using an Odyssey™ Infra-red Imaging system (Li-Cor). Top and bottom black solid triangle indicate activated ERK (p-ERK) isoforms: p-ERK1 and p-ERK2 at molecular weight 44kDa and 42kDa, respectively.

a.

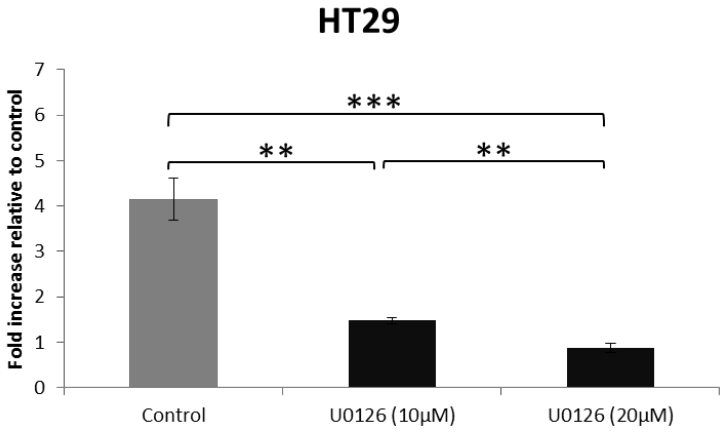

b.

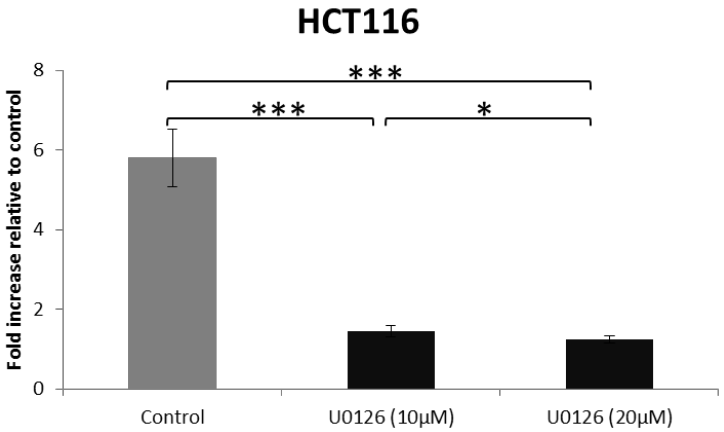

c.

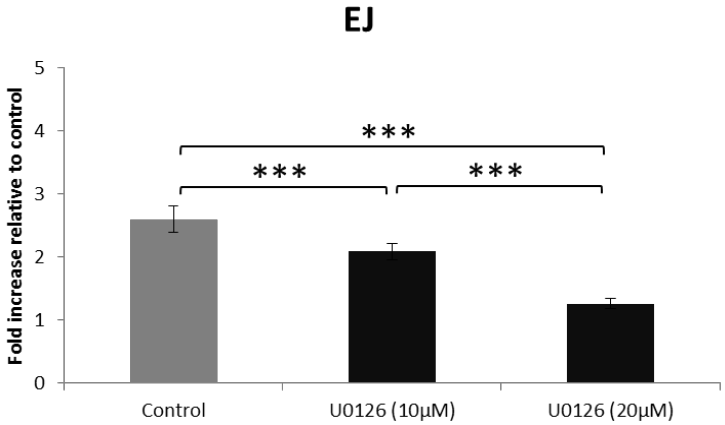

Figure 5.10. Effects of the MEK/ERK inhibitor U0126 on mLIGHT-mediated cell death

HT29, HCT116 and EJ were co-cultured at density $1.6x10^4$ cells/well with MMC-treated control (NT-L) or mLIGHT-L cells at cell density $2x10^4$ cells/well in 96-well plates, in the absence (control) or presence of MEK inhibitor (U0126) at concentrations 10 and 20µM, and solvent control (DMSO) was included. Cells were incubated for 72hrs at 37ºC and 5% CO_2. 50µL of prepared CytoTox-Glo reagents was added to wells and luminescence was measured by a FLUOstar OPTIMA (BMG Labtech) plate reader. Fold increase relative to control was generated from background corrected data as detailed in section 2.13.2 and as described in Figure 4.4. a, b and c show HT29, HCT116 and EJ cells, respectively. Data are represented as mean values of 4-5 replicates ±S.D. Stats: ns. non-significant; *, $p < 0.05$; **, $p < 0.01$; ***, $p < 0.001$, paired student t-test for co-cultured HT29, HCT116 or EJ cells with mLIGHT-L cells vs co-cultured cells with mLIGHT plus U0126, as indicated.

The immunoblotting results of JNK showed that there was no significant activation of JNK expression in HT29, HCT116 and EJ cells following mLIGHT treatment (Figure 5.11). When JNK function was blocked by pharmacological inhibition using the highly specific JNK inhibitor SP600125, strikingly JNK blockade enhanced death in HT29 cells, yet it significantly attenuated death in HCT116 and EJ cells after LT receptor ligation by mLIGHT (Figure 5.12).

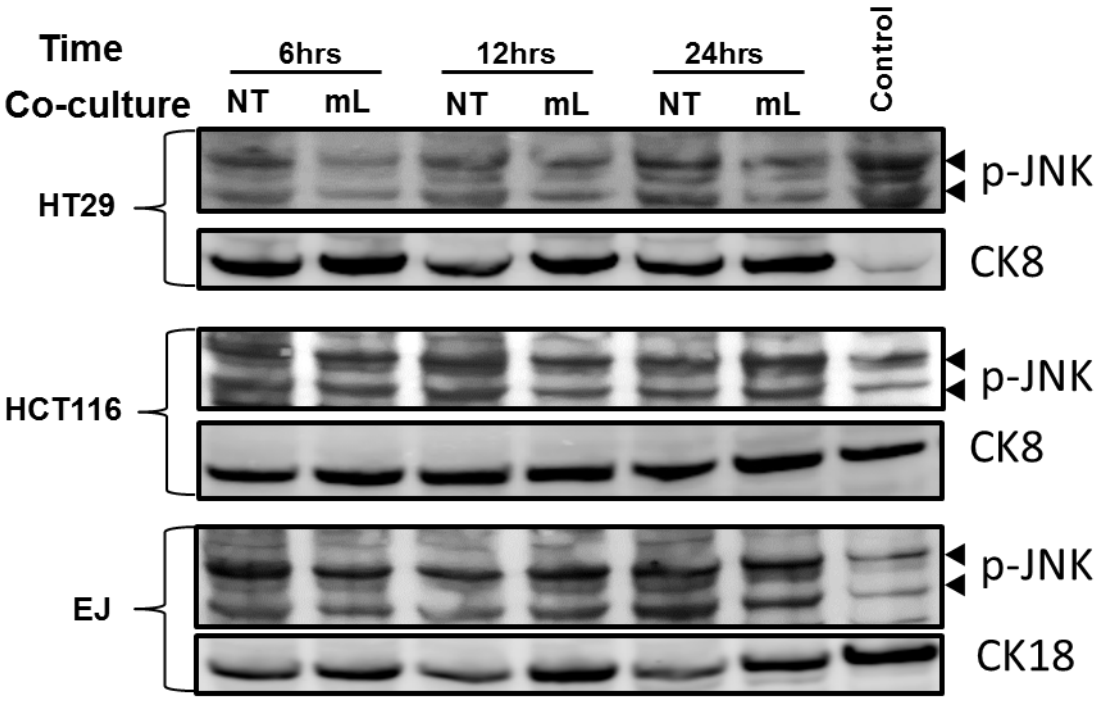

Figure 5.11. JNK expression following LTβR and HVEM activation in carcinoma cells by mLIGHT

HT29, HCT116 and EJ cells were co-cultured at cell density $3x10^6$ with MMC-treated control (NT) or mLIGHT-L cells (mL) at cell density $3.5x10^6$ in $10cm^2$ culture dishes and incubated for time points 6, 12 and 24hrs. 40µg of whole cell lysates were loaded per track and separated under denaturing conditions by SDS-PAGE using 4-12% (w/v) Bis-Tris gels and then transferred onto a PVDF membrane. The membranes were probed with primary monoclonal antibody anti-phospho-JNK in TBS/Tween 0.1% (v/v) (1:1000 dilution) with 5% w/v non-fat dry milk. Membranes were incubated with primary monoclonal antibody CK8 (for H29 and HCT116 cells) or CK18 (for EJ cells). Then incubated with secondary antibody goat anti-mouse 680 (1:10,000 dilution) for p-JNK, CK8 and 18 detection. Antibody binding was visualised using an Odyssey™ Infra-red Imaging system (Li-Cor). Positive control represents lysates from co-cultures of mCD40L with HCT116 cells for phospho-JNK induction. Top and bottom black solid triangle indicate activated JNK (p-JNK) isoforms: short isoform and long isoform at molecular weight 46kDa and 54kDa, respectively.

a.

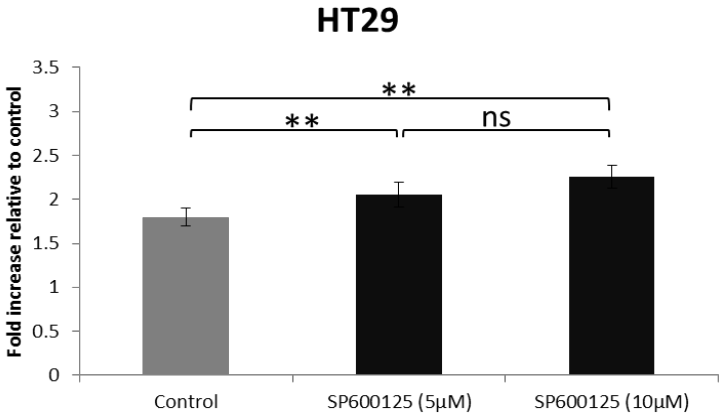

b.

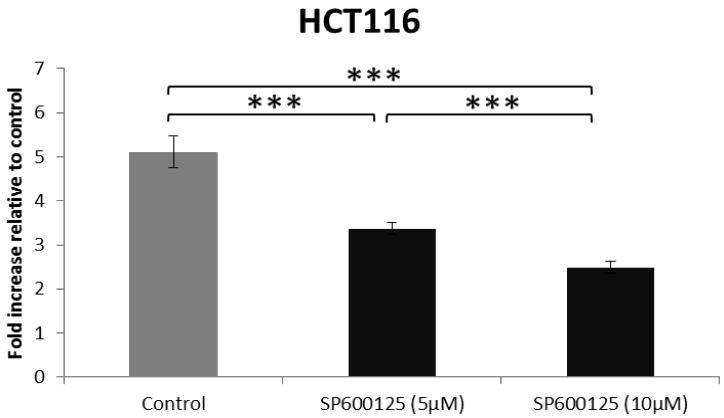

c.

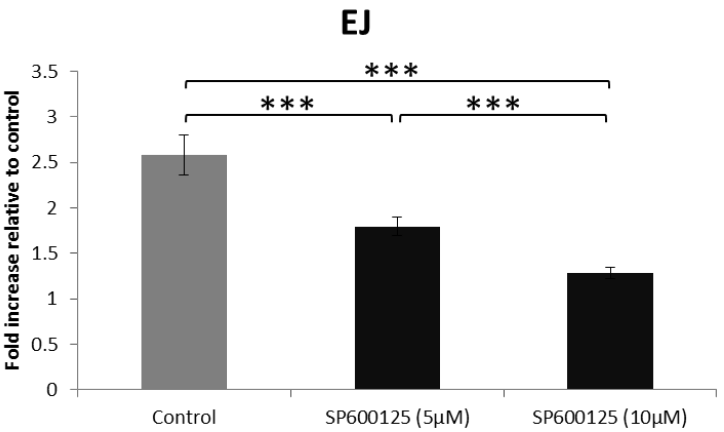

Figure 5.12. Effects of the JNK inhibitor SP600125 on mLIGHT-mediated cell death

HT29, HCT116 and EJ were co-cultured at density 1.6x10^4 cells/well with MMC-treated control (NT-L) or mLIGHT-L cells at cell density 2x10^4 cells/well in 96-well plates, in the absence (control) or presence of JNK inhibitor (SP600125) at concentrations 5 and 10µM, solvent control was included DMSO. Cells were incubated for 72hrs at 37ºC and 5% CO_2. 50µL of prepared CytoTox-Glo was added to wells and luminescence was measured by a FLUOstar OPTIMA (BMG Labtech) plate reader. Fold increase relative to control was generated from background corrected data as detailed in section 2.13.2 and as described in Figure 4.4. a, b and c show HT29, HCT116 and EJ cells, respectively. Data are represented as mean values of 5-6 replicates ±S.D. Stat: ns. non-significant; *, $p < 0.05$; **, $p < 0.01$; ***, $p < 0.001$, paired student t-test for co-cultured HT29, HCT116 or EJ cells with mLIGHT-L cells vs co-cultured cells with mLIGHT plus SP600125, as indicated.

Immunoblotting for p38 activation showed that the expression of phospho-p38 level appeared unchanged in HT29 and EJ cells following treatment with mLIGHT; by contrast, HCT116 showed a significant induction of phospho-p38 at 24hrs (Figure 5.13). Interestingly, p38 blockade using the inhibitor SB202190 significantly but only partially attenuated mLIGHT-mediated cell death in HT29, HCT116 and EJ cells (Figure 5.14).

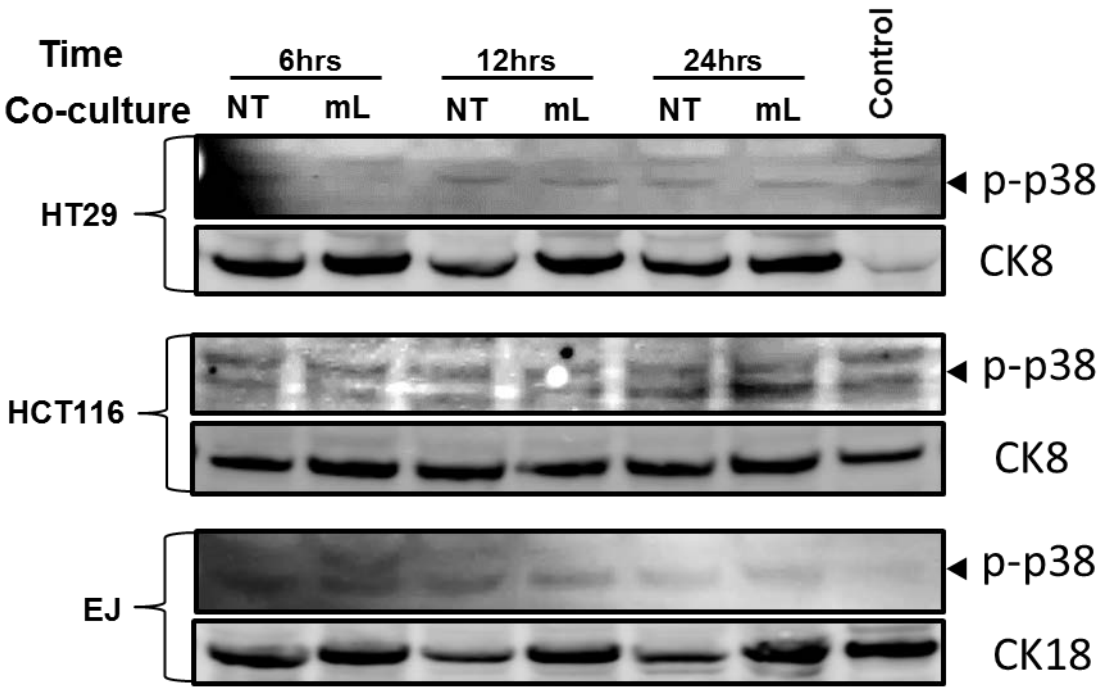

Figure 5.13. p38 expression following LTβR and HVEM activation in carcinoma cells by mLIGHT

HT29, HCT116 and EJ cells were co-cultured at cell density $3x10^6$ with MMC-treated control (NT) or mLIGHT-L cells (mL) at cell density $3.5x10^6$ in $10cm^2$ culture dishes and incubated for time points 6, 12 and 24hrs. 40µg of whole cell lysates were loaded per track and separated under denaturing conditions by SDS-PAGE using 4-12% (w/v) Bis-Tris gels and then transferred onto a PVDF membrane. The membranes were probed with primary polyclonal antibody anti-phospho-p38 in TBS/Tween 0.1% (v/v) (1:1000 dilution) in 5% w/v BSA. Membranes were incubated with primary monoclonal antibody CK8 (for H29 and HCT116 cells) or CK18 (for EJ cells). Then incubated with secondary antibody goat anti-rabbit 800 (1:10,000 dilution) for p38 detection and were probed with secondary antibody goat anti-mouse 680 (1:10,000 dilution) for CK8 and 18 detection. Antibody binding was visualised using an Odyssey™ Infra-red Imaging system (Li-Cor). Positive control represents lysates from co-cultures of mCD40L with HCT116 cells for phospho-p38 induction. The expected molecular weight of activated p38 was 43kDa.

a.

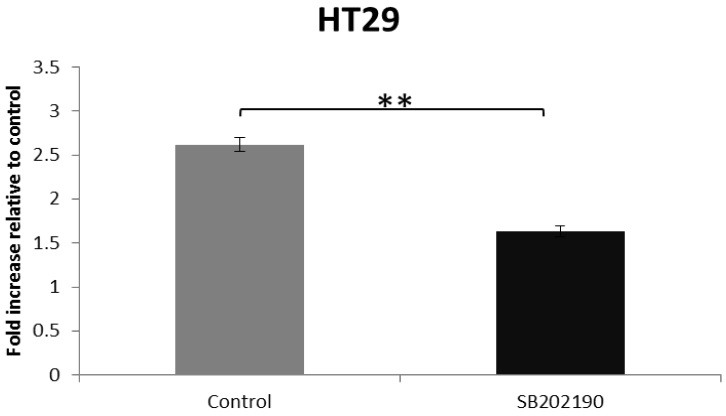

b.

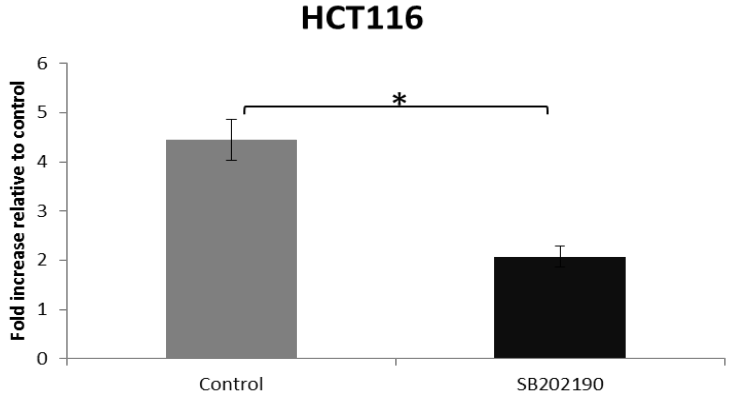

c.

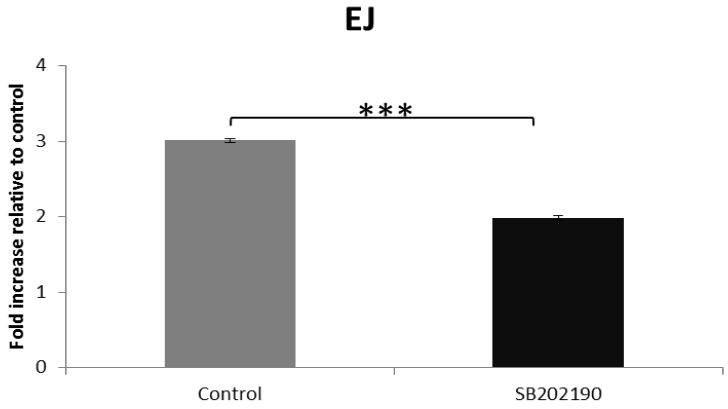

Figure 5.14. Effects of the p38 inhibitor SB202190 on mLIGHT-mediated cell death

HT29, HCT116 and EJ were co-cultured at density $1.6x10^4$ cells/well with MMC-treated control (NT-L) or mLIGHT-L cells at cell density $2x10^4$ cells/well in 96-well plates, in the absence or absence of p38 inhibitor (SB202190) at concentration 25μM, solvent control was included DMSO. Cells were incubated for 72hrs at 37ºC and 5% CO_2. 50μL of prepared CytoTox-Glo was added to wells and luminescence was measured by a FLUOstar OPTIMA (BMG Labtech) plate reader. Fold increase relative to control was generated from background corrected data as detailed in section 2.13.2 and as described in Figure 4.4. Data are represented as mean values of 5 replicates ±S.D. a, b and c show HT29, HCT116 and EJ cells, respectively. Stats: ns. non-significant; *, $p < 0.05$; **, $p < 0.01$; ***, $p < 0.001$, paired student t-test for co-cultured HT29, HCT116 or EJ cells with mLIGHT-L cells vs co-cultured cells with mLIGHT plus SB202190, as indicated.

As MAPK signalling leads to the activation of TFs NF-κB and AP-1, the functional roles of NF-κB and AP-1 in LTβR and HVEM signalling were also investigated using well-characterised pharmacological inhibitors of NF-κB (NF-κB Activation Inhibitor III) and AP-1 (NDGA). Results from CytoTox-Glo death detection assays revealed that inhibition of NF-κB activity partially reduced mLIGHT-mediated death in HT29 and HCT116 cells, whereas it potentiated death EJ cells (Figure 5.15).

On the other hand, AP-1 inhibition partially of fully blocked death in HCT116 and EJ cells, respectively; by contrast (and in agreement with the JNK blockade results using SP600125), AP-1 blockade did not cause any statistically significant effect in mLIGHT-mediated death in HT29 cells (Figure 5.15).

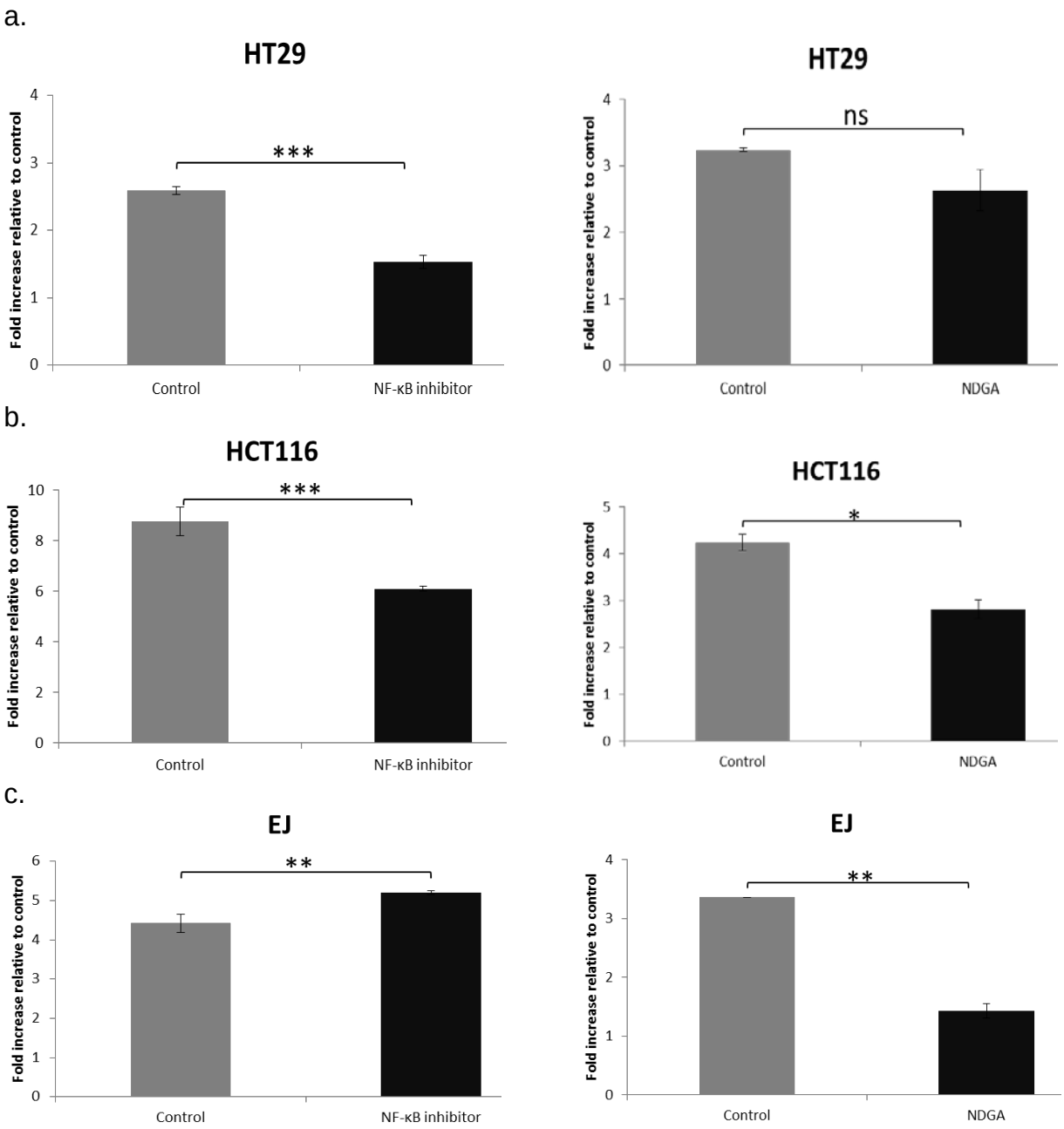

Figure 5.15. Effects of NF-κB/NDGA on mLIGHT-mediated cell death

HT29, HCT116 and EJ were co-cultured at density 1.6x10^4 cells/well with MMC-treated control (NT-L) or mLIGHT-L cells at cell density 2x10^4 cells/well in 96-well plates, in the absence or presence of NF-κB inhibitor (NF-κB Activation Inhibitor III) or AP-1 inhibitor (NDGA) at concentration 5μM and 25μM, respectively. Solvent control (DMSO) was included. Cells were incubated for 72hrs at 37ºC and 5% CO_2. 50μL of prepared CytoTox-Glo was added to wells and luminescence was measured by a FLUOstar OPTIMA (BMG Labtech) plate reader. Fold increase relative to control was generated from background corrected data as detailed in section 2.13.2 and as described in Figure 4.4. Data are represented as mean values of 3-5 replicates ±S.D. a, b and c, show HT29, HCT116 and EJ cells treated with NF-κB inhibitor (left figures) and HT29, HCT116 and EJ cells treated with NDGA (right figures). Stats: ns. non-significant; *, $p < 0.05$; **, $p < 0.01$; ***, $p < 0.001$, paired student t-test for co-cultured HT29, HCT116 or EJ cells with mLIGHT-L cells vs co-cultured cells with mLIGHT plus NF-κB inhibitor or NDGA, as indicated.

Summary

- In this chapter this study provided evidence for the first time that LIGHT and/or combinatorial LIGHT/IFN-γ treatment caused stabilisation and some degree of upregulation in TRAF1 expression in CRC (HCT116 and HT29) and UCC (EJ) cells, respectively. By contrast, mLIGHT treatment induced a dramatic activation of TRAF1 in some CRC (HCT116) and UCC (EJ) whereas no significant TRAF1 induction was observed in HT29 cells.

- Western blotting results demonstrated that treatment with mLIGHT downregulated TRAF2 expression in HT29 cells, it caused slight reduction in TRAF2 levels in HCT116 cells, whereas little change in TRAF2 levels was observed in EJ cells.

- UCC cells showed a massive induction of TRAF3 expression in response to soluble LIGHT and combinatorial LIGHT/IFN-γ treatment, whereas no TRAF3 was detected in CRC cells. However, TRAF3 regulation by mLIGHT treatment was different, as TRAF3 was upregulated in all cell lines as early as 1.5hrs post-ligation, showing similar observations with TRAF1 data.

- Despite the presence of basal TRAF5 expression in all cell lines tested, mLIGHT treatment caused little detectable effects in TRAF5 levels (very little TRAF5 expression was detectable in HCT116). TRAF6 expression was not detected in any of the cell lines with or without treatment with mLIGHT.

- The investigations in MAPK expression levels following mLIGHT-mediated LT receptor ligation showed little detectable differences in phospho-ERK, -JNK or -p38 in CRC and UCC cells, with the sole exception HCT116 cells which showed a significant activation of phospho-p38 in response to mLIGHT.

- However, when functional inhibition experiments were performed to define any functional role for these MAPKs in mLIGHT-mediated death, it was shown that:

  a. inhibition of MEK/ERK and JNK dose-dependently and significantly abrogated mLIGHT-mediated death in HCT116 and EJ cells, whereas JNK inhibitor potentiated death of HT29 cells.

  b. p38 inhibition significantly attenuated, but not fully, mLIGHT-mediated cell death in CRC and UCC cells.

  c. the NF-κB inhibitor partially reduced death of CRC cells and potentiated death of UCC (EJ) cells in response to mLIGHT.

  d. inhibition of AP-1 partially blocked death in HCT116 and EJ cells (but not in HT29 cells) following mLIGHT treatment.

- The results have provided evidence that mLIGHT, but not soluble receptor agonists, triggered not only extensive cell death but also induced rapid TRAF1 and TRAF3 signalling; this is the first time this has been demonstrated on carcinoma cells of CRC and UCC origins.

- Moreover, it appears that mLIGHT-mediated cell death involves a number of MAPKs (such as ERK, JNK and p38); however, clearly the involvement of these MAPKs (and downstream TFs), appears to be cell type specific, as significantly different observation were made in HT29 versus HCT116 and EJ cells.

- These findings not only provide a better understanding of the mechanisms of LT receptor-mediated death in carcinoma cells but also raise a significant argument against the suitability of HT29 cells as a model for the study of the effects of the LT system in carcinoma cells.

Chapter 6

Investigations into the molecular nature of mLIGHT-mediated apoptosis: the role of Reactive Oxygen Species (ROS), the mitochondrial pathway, and the caspases in cell death

6.1 Introduction

Reactive oxygen species (ROS) are normally produced in mammalian cells and are chemically highly reactive, which can in turn lead to modification of lipids, protein oxidation and degradation (Kathiria et al., 2012; Kobayashi and Suda, 2012; MatÉs et al., 1999). Cells can generate ROS under physiological conditions as by-products from two sources: a) the mitochondrial electron transport chain and b) by the action of the NADPH oxidase (NOX) complex and peroxidases (from several cellular components such as cell membrane and endoplasmic reticulum) (Dickinson and Chang, 2011; Lennicke et al., 2015; Turrens, 2003). ROS include: a) superoxide anion radicals (O_2–), and b) singlet O_2, which are mainly produced by the mitochondrial respiratory chain, c) hydrogen peroxide (H_2O_2), which can be produced directly from action of oxidases or indirectly from the dismutation of O_2-, and d) hydroxyl radicals (-OH), which are highly reactive species that can change purine and pyrimidine bases of DNA and lead to DNA damage (Matés et al., 2010; Matés et al., 2012).

Cellular ROS balance is controlled by the antioxidant system, which includes endogenous antioxidant enzymes (such as superoxide dismutase (SOD), catalase, glutathione peroxidase (GPx), and glutathione (GSH)). The antioxidant system is regulated through genes such as Ref-1, Nrf-2 and Thioredoxin (Trx), and the antioxidant system scavenges ROS to prevent cellular oxidative damage (Fruehauf and Meyskens, 2007; Poljsak et al., 2013). The level of ROS has an impact on cell fate; low or moderate ROS most likely promotes cell growth and survival (Dunnill et al., 2015; Hamanaka and Chandel, 2010), whereas cells under stress show increased ROS levels (e.g. following chemotherapy or UV exposure) and ultimately high ROS levels cause cytotoxicity, apoptosis and probably necrosis (Ambrosone, 2000; Halliwell, 2007; Hoeijmakers, 2009; Lee et al., 2011; Phillips et al., 2006; Szatrowski and Nathan, 1991; Yee et al., 2014). Previous studies demonstrated that some members of TNFR use ROS, which is induced as a result of the interaction of TRAF with NADPH oxidases (Matés et al., 2012). For instance CD40 activation produced ROS via 5-lipoxygenase pathway and a TRAF3-NADPH oxidase association (Aggarwal, 2004; Dickinson and Chang, 2011). Moreover, it was demonstrated that CD40 ligation in B-cells leads to the production of oxidative stress, ROS and triggers NF-κB and JNK activation (Ha and Lee, 2004; Ha et al., 2011).

It has been reported that ROS play a crucial role in the activation of stress-activated mitogen-activated protein kinase kinase kinase (MAPKKK) signalling pathway, such as ASK1 and the release and auto-phosphorylation of Trx (redox-sensing protein and an inhibitor for ASK1) was shown to associate with ASK1 (Gotoh and Cooper, 1998; Liu and Min, 2002; Saitoh et al., 1998). Studies demonstrated that LTβR and TNF-α signal transduction was triggered by the activation of ASK1 through the production of ROS (Chen et al., 2003; Gotoh and Cooper, 1998). This was previously explained as ROS activates ASK1 by preventing ASK1 and Trx association and this leads to form complex of binding TRAF2 and ASK1 (Liu and Min, 2002). These events may trigger cell death which is mediated by two main pathways: extrinsic and intrinsic and these pathways are associated with activation of specific caspases (as discussed in detail in Chapter 1 section 1.3). It is well-documented that caspase-8 is activated and involved within the extrinsic pathway, while apoptosis that is triggered by the intrinsic pathway activates caspase-9 (Fulda and Debatin, 2006; Zimmermann and Green, 2001).

Previous study on the mechanism of CD40-mediated apoptosis demonstrated that CD40 ligation by mCD40L in bladder carcinoma cells triggers apoptosis via the activation of caspase-9, but not caspase-8 (Georgopoulos et al., 2006). Studies on LT receptors demonstrated that activation of LTβR in epithelial cells by agonistic antibody (BS-1) induces the activation of caspase -8 and -3 and cytochrome c release in multidrug-resistant counterpart of human sarcoma cell line (MES-SA/Dx5), which may indicate that the activation of LTβR mediates cell death via caspase-dependent mitochondria-mediated apoptosis (Hu et al., 2013). A previous study reported that HVEM activation on a lymphoid malignancy by LIGHT or anti-HVEM (mAb) induced caspase activation, decrease in mitochondrial membrane potential, upregulation of the pro-apoptotic protein Bax, also a role of TRAIL and induced endogenous TNF-α production and TNF-α enhanced HVEM-mediated cell death (Pasero et al., 2009b).

Cells initiate mitochondrial apoptosis signalling via the involvement of the pro-apoptotic Bcl-2 protein activation with three BH domains (e.g. Bak and Bax) that trigger mitochondrial outer membrane permeabilisation (MOMP) (Fesik, 2000; Hengartner, 2000). This results in cytochrome c and other proteins release into the cytosol and initiate caspase activation in the cell leading ultimately to cell death (Nechushtan et al., 2001; Todt et al., 2015; Wolter et al., 1997). Bax is believed to form a supramolecular opening or pores for the MOMP alone or with the help of Bak or the active form of Bid, truncated Bid (tBid) (Kuwana et al., 2002; Li et al., 1998; Luo et al., 1998). Bax and Bak are present in the cytosol of healthy cells, and the relocalisation of Bax from cytosol to mitochondria to facilitate MOMP is essential for triggering cell death (Todt et al., 2015; Wolter et al., 1997), Bax retaining in cytosol, MOMP and cell death are found to be inhibited (Cheng et al., 2001; Wei et al., 2001; Zong et al., 2001).

The aims of the work presented in this chapter were to:

- detect ROS production during LTβR/HVEM death by mLIGHT-mediated signalling using ROS-Glo assays.

- perform functional inhibition experiments using the antioxidant NAC and to determine whether ROS release is critical in LTβR/HVEM-mediated death triggered by mLIGHT as determined by CytoTox-Glo death detection assays.

- perform immunoblotting to investigate the activation of NOX subunit (p40phox) and to use a pharmacological inhibitor for NOX (DPI) to determine whether NOX is involved in LTβR/HVEM death signalling triggered by mLIGHT as determined by CytoTox-Glo assays.

- investigate the activation of ASK1 and Thioredoxin expression in LTβR/HVEM-mediated cell death by mLIGHT using immunoblotting and human protein-specific antibodies for ASK1 and Thioredoxin.

- use biochemical inhibitors for caspases (pan caspase z-VAD), caspase-3 and -7 (Z-DEVD-FMK), -8 (Z-IETD-FMK), -9 (Z-LEHD-FMK) and -10 (Z-AEVD-FMK) to determine whether caspases are critical in LTβR/HVEM-mediated death triggered by mLIGHT using CytoTox-Glo death detection assays.

- investigate the regulation of pro-apoptotic mitochondrial pathway-related proteins Bak and Bax in LTβR/HVEM-mediated death triggered by soluble agonists versus mLIGHT treatment, using immunoblotting techniques and by utilising human protein-specific antibodies for Bak and Bax.

- optimise transfection techniques for using small interfering RNA (siRNA) to knockdown LT receptors expression to determine whether LT receptors (LTβR and HVEM) signal independently, cooperatively or in an antagonistic fashion in determining cell fate in the context of mLIGHT treatment.

6.2 Detection of ROS production

For ROS detection, two assays were used to measure ROS levels following mLIGHT treatment: CM-H_2DCFDA and ROS-Glo (section 2.14). A series of experiments were performed to measure ROS levels following co-culture of effector (NT-L and mLIGHT-L) cells with target carcinoma cells using CM-H_2DCFDA (section 2.14.1). CM-H_2DCFDA assay did not prove effective in detecting ROS in cells and due to time constraints near the end of the experimental work it was not possible to sufficiently optimise it, so the ROS-Glo assay was performed instead.

ROS-Glo is designed to measure H_2O_2 levels, as most cellular ROS are converted to H_2O_2 and have the longest half-life of all ROS in cultured cells. The ROS-Glo assay is convenient and does not involve medium aspiration and washing steps as does the CM-H_2DCFDA assay. In these assays the CRC and UCC lines HCT116 and EJ cells were selected as representative cell lines to measure ROS levels. Tests involved co-cultures of HCT116 and EJ cells with control (NT-L) and mLIGHT-L cells, whilst EJ cells treated with H_2O_2 served as the positive control. Unlike the CytoTox-Glo and caspase detection assays, no “cells alone” background control subtractions were necessary in this assay as only target cells were treated with the H_2O_2 detection substrate (ROS-Glo is detailed in section 2.14.2). Data were presented as Relative Luminescence Unit (RLU) as shown in Figure 6.1.

The results showed that mLIGHT induced a significant and rapid production of ROS levels in HCT116 and EJ cells at 3hrs post receptor ligation compared with controls (Figure 6.1). Treated EJ cells with H_2O_2 showed high levels of ROS production.

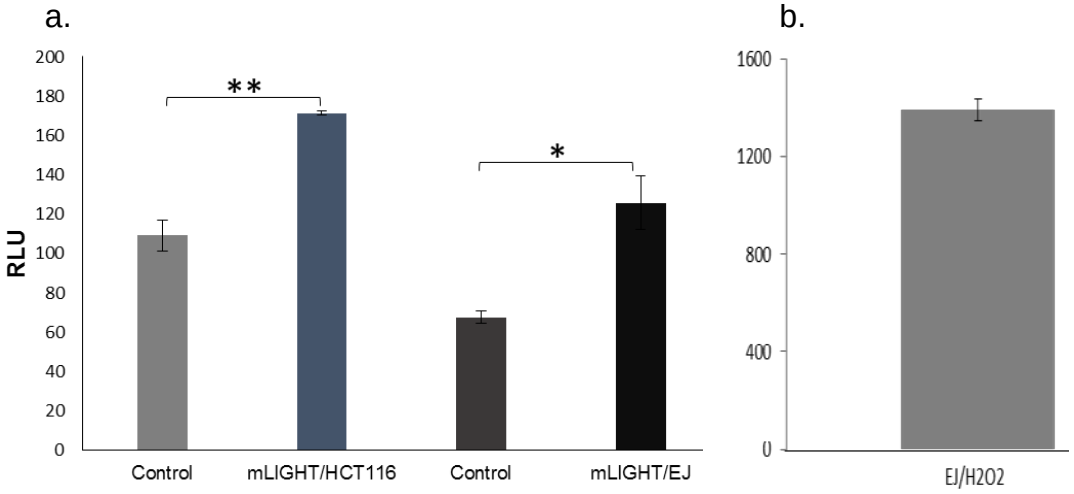

Figure 6.1. Measurement of ROS induction in carcinoma cells following mLIGHT treatment

HCT116 and EJ were pretreated with H_2O_2 substrate for 30mins and cells were co-cultured with control (NT-L) or mLIGHT-L cells in 96-well plates. Cells were incubated for 3hrs at 37ºC and 5% (v/v) CO_2. 100µL of prepared ROS-Glo Detection Solution was added to the wells and relative luminescence unit (RLU) was determined by a FLUOstar OPTIMA (BMG Labtech) plate reader. The intensity of the RLU signal is proportional to H_2O_2 level which corresponds to ROS production in cells (as described in section 2.14.2). a, data of HCT116 and EJ cells. b, ROS positive control data (EJ cells was treated with H_2O_2). Data are represented as mean values of 3 replicates ±S.D. Stats: ns. non-significant; *, $p < 0.05$; **, $p < 0.01$, paired student t-test for co-cultured HCT116 or EJ cells with control cells vs co-cultured cells with mLIGHT-L cells, as indicated.

6.3 Effects of the ROS scavenger and antioxidant NAC on mLIGHT-mediated cell death

Based on the finding that the aforementioned cells released ROS following LTβR and HVEM ligation with mLIGHT and to demonstrate the functional involvement of ROS in mLIGHT-induced cell death, the antioxidant N-acetyl L-cysteine (NAC) was used. The L-NAC is a precursor form metabolised to cysteine and then to GSH, which functions as an antioxidant that can prevent damage to important cellular components caused by ROS (De Vries and De Flora, 1993).

Following initial pre-titration experiments, it was observed that NAC was cytotoxic when it was added to cultures at high concentrations (5mM and above), compared with control. Treatment of cells with 1.25mM of NAC appeared to be the optimal concentration (see Appendix VI). Therefore, the concentration of 1.25mM was selected and used in co-culture experiments as presented in Figure 6.2. Cells were pre-treated with NAC for two time points 1hr and 3hrs and then cells were co-cultured with control (NT-L) or mLIGHT-L cells for 72hrs and the CytoTox-Glo assay was performed. Data were presented as fold increase relative to control and calculated using the parameters and equations as described in section 2.13.2.

The addition of NAC without pre-treatment showed no significant effects on mLIGHT-mediated cell death in HT29, HCT116 and EJ cells (data not shown). Interestingly, when NAC pre-treatment was performed, in particular for 3hrs, it did partially inhibit death of HT29, HCT116 and EJ cells in response to mLIGHT treatment (Figure 6.2)

a.

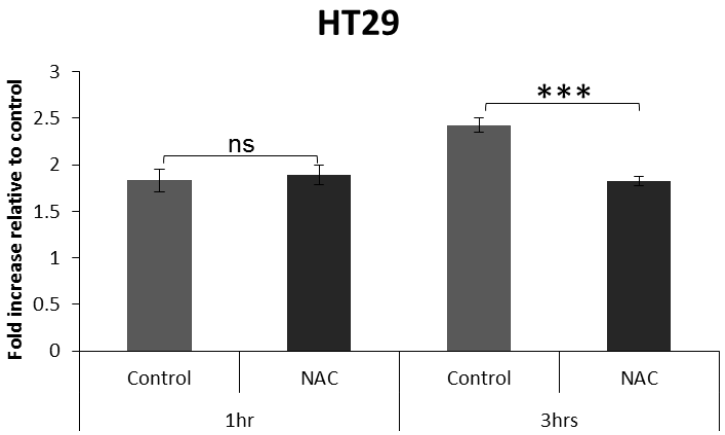

b.

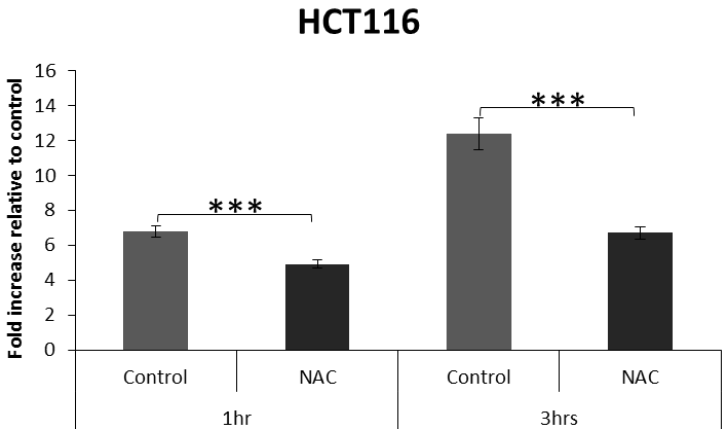

c.

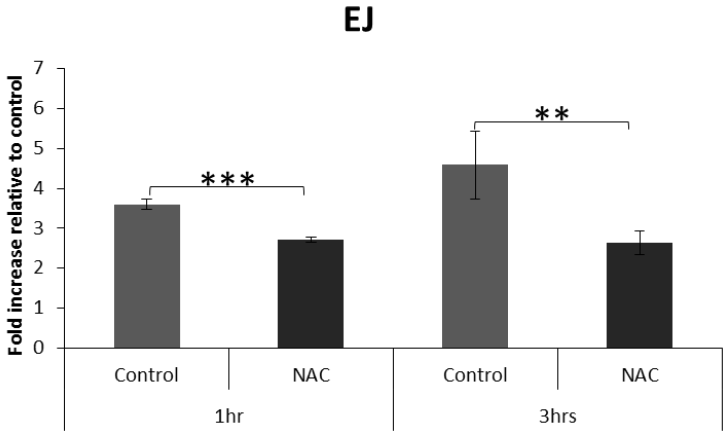

Figure 6.2. Effects of the antioxidant NAC on mLIGHT-mediated cell death

HT29, HCT116 and EJ were pre-treated with NAC for 1 and 3hrs at concentration 1.25mM. HT29, HCT116 and EJ were co-cultured at cell density $1.6x10^4$ cells/well with MMC-treated control (NT-L) or mLIGHT-L cells at cell density $2x10^4$ cells/well in 96-well plates, in the absence or presence of NAC. Cells were incubated for 72hrs at 37ºC and 5% (v/v) CO_2. 50µL of prepared CytoTox-Glo reagents were added to wells and luminescence was measured by a FLUOstar OPTIMA (BMG Labtech) plate reader. Fold increase relative to control was generated from background corrected data as detailed in section 2.13.2 and as described in Figure 4.4. Data are represented as mean values of 5 replicates ±S.D. a, b and c show HT29, HCT116 and EJ cells. Stats: ns. non-significant; *, $p < 0.05$; **, $p < 0.01$; $p < 0.001$; ***, paired student t-test for co-cultured HT29, HCT116 or EJ cells with mLIGHT-L cells vs co-cultured cells with mLIGHT plus NAC, as indicated.

6.4 The role of NOX in ROS production following LTβR/HVEM signalling

The NOX enzyme complex can play a role in cellular ROS production, and in the context of the TNFR family and CD40 in particular it was reported that CD40 can generate ROS in malignant B-cells through the association of TRAF3 and the NOX subunit phospho-p40phox (Ha and Lee, 2004). This study showed in chapter 5 (Figure 5.6) that mLIGHT in particular induced rapid and significant induction of TRAF3 and it showed in chapter 6 (Figure 6.2) that the antioxidant NAC inhibited cell death in CRC and UCC cells, indicating possible ROS involvement in cell death. Therefore, the involvement of NOX in ROS production was investigated. As there is a possible link between TRAF3 and NOX activation, the activation of p40phox was examined at time points 6, 12 and 24hrs following LTβR and HVEM activation by mLIGHT by immunoblotting as shown in Figure 6.3. The results showed that mLIGHT caused little detectable effects in phospho-p40phox expression in HT29. By contrast there was some level of activation in EJ cells by 12 hours following mLIGHT treatment and more dramatically there was a significant induction of p40phox in HCT116 cells at 24hrs post-ligation (Figure 6.3).

Following the investigation of p40phox activation (by measuring its phosphorylation), inhibition experiments were performed to examine whether the activation of p40phox was of functional importance in LTβR/HVEM signalling by mLIGHT. For this purpose, the inhibitor diphenyleneiodonium chloride (DPI) (an inhibitor for the NOX enzyme complex) was used. DPI is a chemical compound specifically inhibiting NOS2, NOS3 and NADPH oxidase. DPI was used to inhibit ROS sourced from NOX (Li et al., 2003). Cells were pre-titrated with various concentrations of DPI to select the optimal concentration. According to the obtained results, cells were very sensitive to DPI, and that even low concentrations appeared toxic to all cells. However, doses of 0.01562 and 0.03125μM were well tolerated by HT29, HCT116 and EJ cells (Appendix VII). Therefore, HT29, HCT116 and EJ cells were co-cultured with control (NT-L) or mLIGHT-L cells in the absence or presence of DPI at two concentrations: 0.01562 and 0.03125μM and the effects of DPI on cell death triggered by mLIGHT treatment was tested and data was presented as fold increase relative to control. The results showed that NOX blockade enhanced death in HT29, HCT116 and EJ cells after LT receptor ligation by mLIGHT (Figure 6.4).

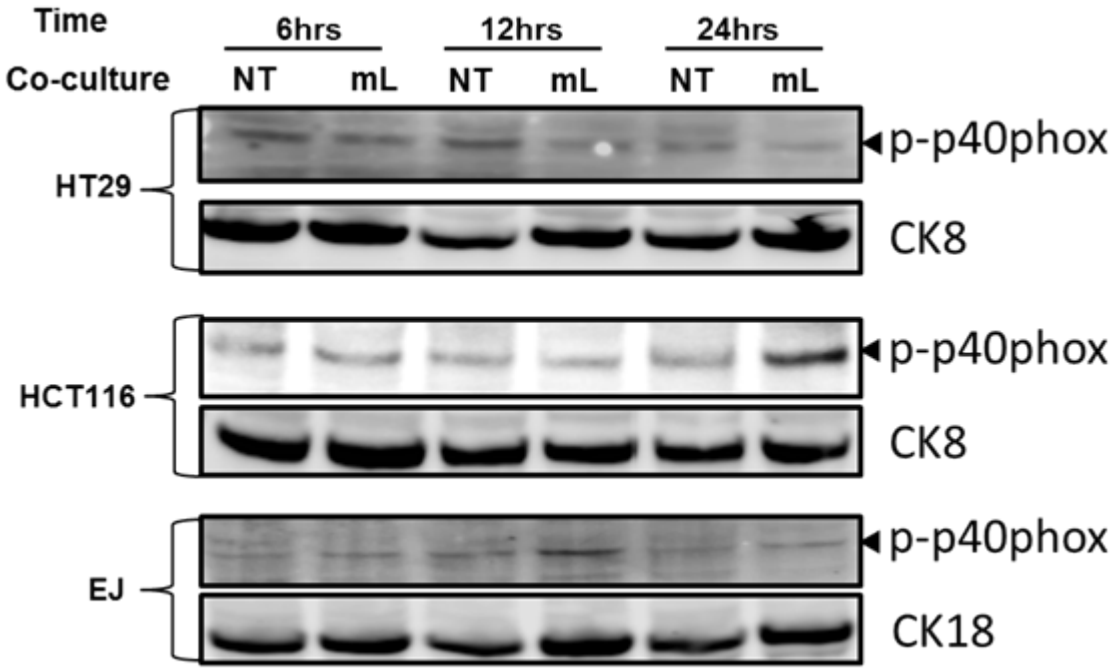

Figure 6.3. p40phox expression following LTβR and HVEM activation in carcinoma cells by mLIGHT

HT29, HCT116 and EJ cells were co-cultured at cell density $3x10^6$ with MMC-treated control (NT) or mLIGHT-L cells (mL) cells at cell density $3.5x10^6$ in $10cm^2$ culture dishes and incubated for time points 6, 12 and 24hrs. 40µg of whole lysates were separated under denaturing conditions by SDS-PAGE using 4-12% (w/v) Bis-Tris gels and then transferred onto a PVDF membrane. The membranes were probed with primary polyclonal antibody anti-phospho-p40phox in TBS/Tween 0.1% (v/v) (1:1000 dilution) with 5% (w/v) BSA and then incubated with primary monoclonal antibody CK8 (for H29 and HCT116 cells) or CK18 (for EJ cells). Then membranes were incubated with secondary antibody goat anti-rabbit 800 (1:10,000 dilution) for p-p40phox detection or were probed with secondary antibody goat anti-mouse 680 (1:10,000 dilution) for CK8 and 18 detection. Antibody binding was visualised using an Odyssey™ Infra-red Imaging system (Li-Cor). The expected molecular weight of activated p40phox (p-p40phox) was 40kDa.

a.

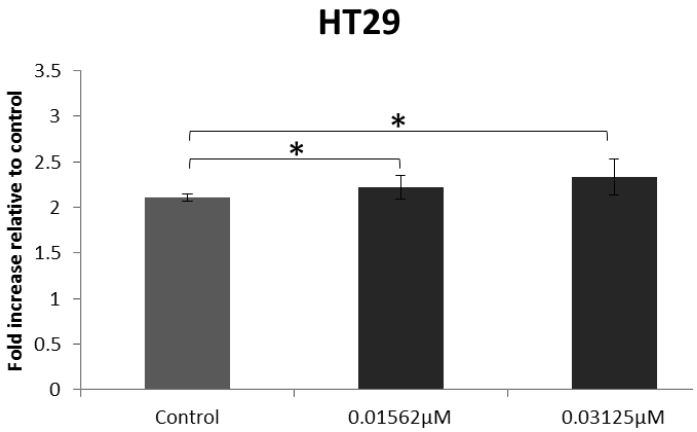

b.

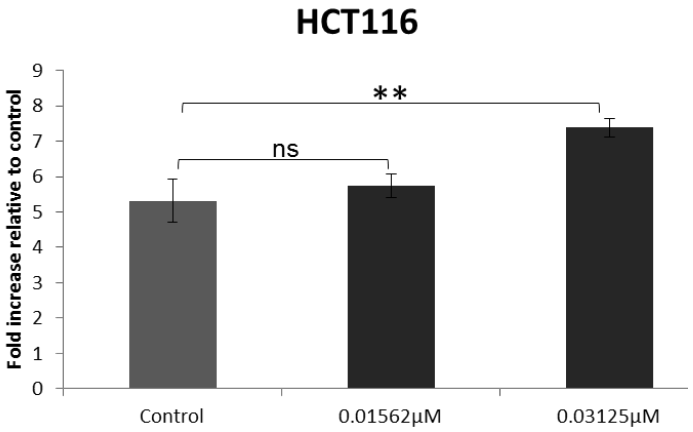

c.

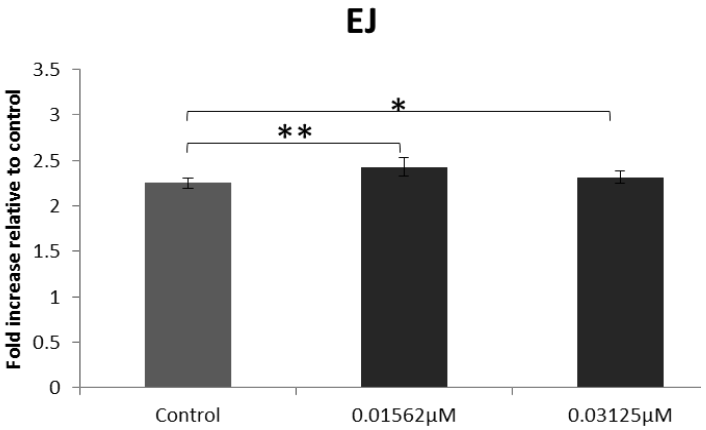

Figure 6.4. Effects of the NOX inhibitor DPI on mLIGHT-mediated cell death

HT29, HCT116 and EJ were co-cultured at density $1.6x10^4$ cells/well with MMC-treated control (NT-L) or mLIGHT-L cells at cell density $2x10^4$ cells/well in 96-well plates. DPI was added to co-cultures at two concentrations 0.01562 and 0.03125µM, as indicated, and then cells were incubated for 72hrs at 37ºC and 5% (v/v) CO_2. 50µL of prepared CytoTox-Glo reagents were added to wells and luminescence was measured by a FLUOstar OPTIMA (BMG Labtech) plate reader. Fold increase relative to control was generated from background corrected data as detailed in section 2.13.2 and as described in Figure 4.4. Data are represented as mean values of 5 replicates ±S.D. a, b and c show HT29, HCT116 and EJ cells, respectively. Stats: ns. non-significant; *, $p < 0.05$; **, $p < 0.01$, paired student t-test for co-cultured HT29, HCT116 or EJ cells with mLIGHT-L cells vs co-cultured cells with mLIGHT plus DPI, as indicated.

6.5 Effects of LTβR/HVEM signalling on ASK1 and Trx expression

The activation of ASK1 and Trx were investigated at various times 6, 12 and 24hrs following ligation with mLIGHT, using immunoblotting and by utilising human protein-specific antibodies for ASK1 and Trx. The immunoblotting results showed that HT29 cells showed no detectable of phospho-ASK1, whereas HCT116 cells showed some activation of ASK1 at 24hrs and it appeared that the pattern level of phospho-ASK1 in EJ cells was relatively unchanged, following mLIGHT treatment as shown in Figure 6.5.

On the other hand, interestingly, Trx expression basal levels were detectable in all cell lines tested HT29, HCT116 and EJ cells, and in agreement with previous observations in our laboratory (Dunnill and Georgopoulos, manuscript in preparation), Trx levels progressively increased in cultured cells following seeding. Strikingly, mLIGHT induced down-regulation of Trx in all cell lines by 6-12 hours post receptor ligation, although the exact pattern (and timing) differed between different cell lines (Figure 6.6).

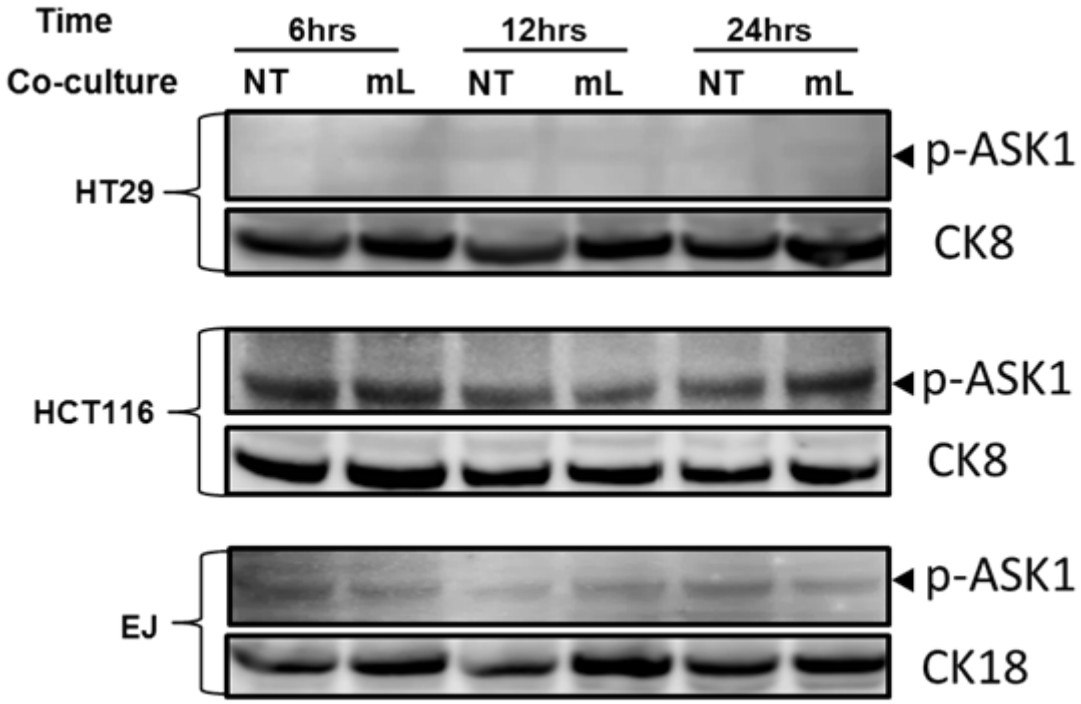

Figure 6.5. ASK1 expression following LTβR and HVEM activation in carcinoma cells by mLIGHT

HT29, HCT116 and EJ cells were co-cultured at cell density $3x10^6$ with MMC-treated control (NT) or mLIGHT-L cells (mL) cells at cell density $3.5x10^6$ in $10cm^2$ culture dishes and incubated for time points 6, 12 and 24hrs. 40µg of whole lysates were separated under denaturing conditions by SDS-PAGE using 4-12% (w/v) Bis-Tris gels and then transferred onto a PVDF membrane. The membranes were probed with primary polyclonal antibody anti-phospho-ASK1 in TBS/Tween 0.1% (v/v) (1:1000 dilution) with 5% (w/v) BSA and then with primary monoclonal antibody CK8 (for H29 and HCT116 cells) or CK18 (for EJ cells). Membranes were probed with secondary antibody goat anti-rabbit 800 (1:10,000 dilution) for ASK1 detection and membranes were probed with secondary antibody goat anti-mouse 680 (1:10,000 dilution) for CK8 and 18 detection. Antibody binding was visualised using an Odyssey™ Infra-red Imaging system (Li-Cor). The expected molecular weight of activated ASK1 (p-ASK1) was 50kDa.

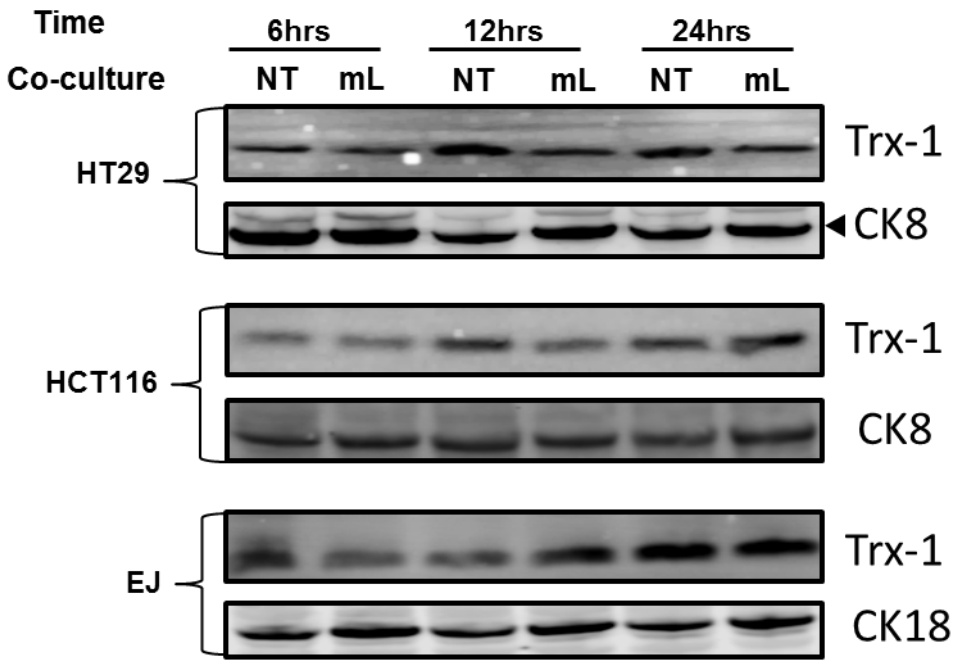

Figure 6.6. Trx-1 expression following LTβR and HVEM activation in carcinoma cells by mLIGHT

HT29, HCT116 and EJ cells were co-cultured at cell density $3x10^6$ with MMC-treated control (NT) or mLIGHT-L cells (mL) cells at cell density $3.5x10^6$ in $10cm^2$ culture dishes and incubated for time points 6, 12 and 24hrs. 40µg of whole lysates were separated under denaturing conditions by SDS-PAGE using 4-12% (w/v) Bis-Tris gels and then transferred onto a PVDF membrane. The membranes were probed with primary polyclonal antibody anti-Thioredoxin-1 in TBS/Tween 0.1% (v/v) (1:1000 dilution) with 5% (w/v) BSA and then with primary monoclonal antibody CK8 (for H29 and HCT116 cells) or CK18 (for EJ cells). Membranes were probed with secondary antibody goat anti-rabbit 800 (1:10,000 dilution) for Trx-1 detection and were probed with secondary antibody goat anti-mouse 680 (1:10,000 dilution) for CK8 and 18 detection. Antibody binding was visualised using an Odyssey™ Infra-red Imaging system (Li-Cor). The expected molecular weight of Trx-1 was 12kDa.

6.6 The role of caspases in LTβR/HVEM signalling

Functional inhibition experiments were also performed to determine the role of specific caspases in mLIGHT-mediated apoptosis and to understand whether the extrinsic or intrinsic pathways were involved in cell death. First, using a generic biochemical caspase inhibitor, the pan-caspase inhibitor z-VAD to determine whether cell death was caspase dependent. The results showed that the addition of pan-caspase z-VAD increased death of HT29 and EJ cells following ligation with mLIGHT, whereas z-VAD partially blocked HCT116 death in response to mLIGHT treatment compared with controls (Figure 6.7).

As only HCT116 cells death was blocked by z-VAD treatment, thus indicating a caspase-dependent apoptotic pathway in these cells (and non caspase-dependent, and possibly non-apoptotic/necrotic pathways in the other cell lines), further investigations were performed to determine which death pathway was utilised, extrinsic or intrinsic. Therefore, biochemical caspase inhibitors used specific for caspase-3 and -7 (Z-DEVD-FMK), -8 (Z-IETD-FMK), -9 (Z-LEHD-FMK), -10 (Z-AEVD-FMK) alongside z-VAD (used as a control). Caspase inhibitors were added to co-cultured cells and their effects were determined using CytoTox-Glo. Data were presented as fold increase relative to control and calculated using the parameters and equations as described in section 2.13.2. As shown in Figure 6.8, it was observed that treatment with caspase-3 inhibitor (Z-DEVD-FMK), and -8 inhibitor (Z-IETD-FMK) had some reduction effects on HCT116 death triggered by mLIGHT, whereas, interestingly, inhibition of caspase-9 and -10 increased death of HCT116 (Figure 6.8).

a.

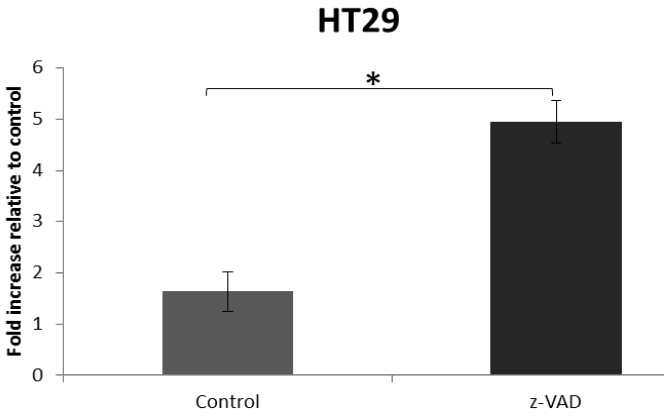

b.

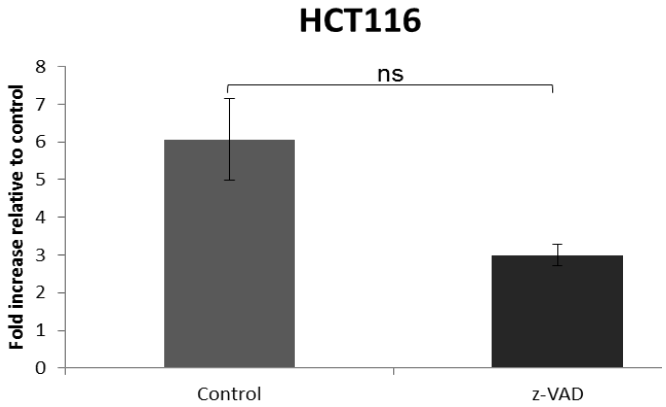

c.

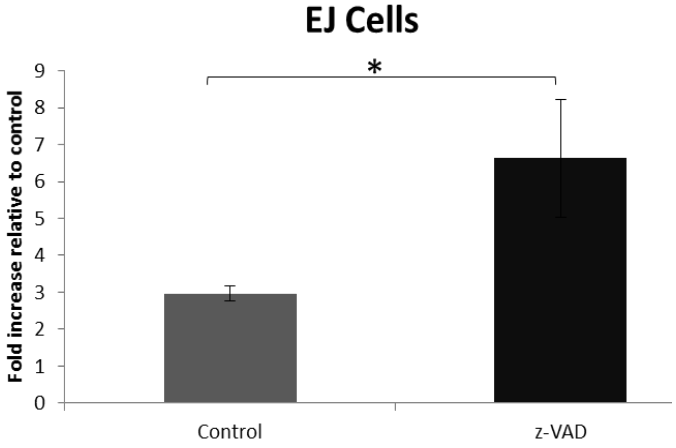

Figure 6.7. Effects of the pan-caspase inhibitor z-VAD on mLIGHT-mediated cell death

HT29, HCT116 and EJ were co-cultured at density 1.6x10^4 cells/well with MMC-treated control (NT-L) or mLIGHT-L cells at cell density 2x10^4 cells/well in 96-well plates. z-VAD was added to co-cultures at concentration 100μM and then cells were incubated for 72hrs at 37ºC and 5% (v/v) CO_2. 50μL of prepared CytoTox-Glo reagent was added to wells and luminescence was measured by a FLUOstar OPTIMA (BMG Labtech) plate reader. Fold increase relative to control was generated from background corrected data as detailed in section 2.13.2 and as described in Figure 4.4. a, b and c show HT29, HCT116 and EJ cells. Bars correspond to mean values of 3 replicates ±S.D. Stats: ns. non-significant; *, $p < 0.05$, paired student t-test for co-cultured HT29, HCT116 or EJ cells with mLIGHT-L cells vs co-cultured cells with mLIGHT plus z-VAD, as indicated.

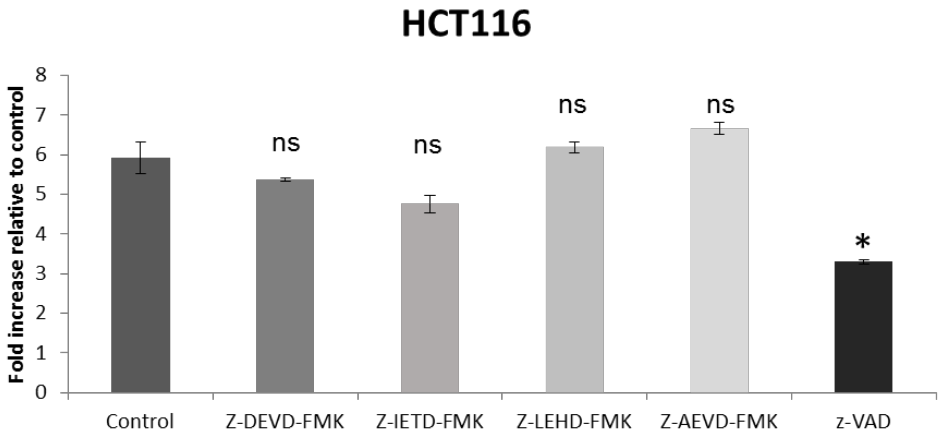

Figure 6.8. Effects of caspase -3, -8, -9, -10 and z-VAD inhibitors on mLIGHT-mediated cell death

HCT116 cells were co-cultured at density $1.6x10^4$ cells/well with MMC-treated control (NT-L) or mLIGHT-L cells at cell density $2x10^4$ cells/well in 96-well plates. Caspase inhibitors were added, caspase-3 (Z-DEVD-FMK), -8 (Z-IETD-FMK), -9 (Z-LEHD-FMK), -10 (Z-AEVD-FMK) and pan caspases inhibitor (z-VAD) at concentration 100μM and incubated for 72hrs at 37ºC and 5% (v/v) CO_2. 50μL of prepared CytoTox-Glo reagent was added to wells and luminescence was measured by a FLUOstar OPTIMA (BMG Labtech) plate reader. Fold increase relative to control was generated from background corrected data as detailed in section 2.13.2 and as described in Figure 4.4. Bars correspond to mean values of 3 replicates ±S.D. Stats: ns. non-significant, *, $p < 0.05$, paired student t-test for co-cultured HCT116 with mLIGHT-L cells vs co-cultured cells with mLIGHT plus caspase inhibitors, as indicated.

6.7 Regulation of pro-apoptotic proteins in LTβR/HVEM signalling

Previous studies demonstrated that CD40 activation induced Bak and Bax expression in epithelial carcinoma cell lines (Bugajska et al., 2002). More recent work in our laboratory has shown that mCD40L induced MOMP in both UCC and CRC cells (Dunnill et al, under review) and release of cytochrome c in parallel with translocation of Bax/Bak to the mitochondria (Mohamed and Georgopoulos, unpublished observations). Activation of LTβR and HVEM in the breast cancer cell line MDA-MB-231 and CRC cells HT29 with LIGHT/IFN-γ treatment led to the upregulation of Bak and downregulation of Bax and associated with the activation of caspases-3, -6, -7, -8 and -9 and DNA fragmentation factor (DFF45) (Zhang, 2004; Zhang et al., 2004; Zhang et al., 1996). To better understand the involvement of Bak and Bax in LTβR/HVEM signalling triggered by soluble agonists versus mLIGHT in epithelial cells, the expression of Bak (Figure 6.9) and Bax (Figure 6.10) was investigated following cell treatment with soluble agonists and at 6, 12, 24 and 48hrs following mLIGHT, using immunoblotting techniques and by utilising human protein-specific antibodies for Bak and Bax detection.

The immunoblotting data showed that soluble agonists treatment did not cause any significant changes in Bak expression in HT29 and EJ cells. Little Bak expression was detected in HCT116 cells following treatment with soluble agonists (Figure 6.9a). Similarly, no significant / noticeable changes in Bak expression were observed following mLIGHT treatment in the cell lines tested (Figure 6.9b), although Bak expression was detected in the positive control (which represents HaCaTa cells treated with cyclophosphamide (4-OH-CP) (Al-Tameemi and Georgopoulos, unpublished observations).

On the other hand, Bax expression was detectable in treated HT29, HCT116 and EJ cells with soluble agonists, and the level of Bax expression was relatively unchanged in HT29, HCT116 and EJ cells following soluble agonist treatment (Figure 6.10a), although strangely treatment HT29 and HCT116 cells with LIGHT/IFN-γ led to downregulation of Bax expression. mLIGHT caused no noticeable Bax expression changes, whilst Bax was undetectable in HCT116 cells following co-cultures (Figure 6.10b) although it was detectable in experiments involving treatments with soluble agonists (Figure 6.10a). The positive control, which represents HaCaTa cells treated

with cyclophosphamide (4-OH-CP) (Al-Tameemi and Georgopoulos, unpublished observations) showed a significant induction of Bax expression.

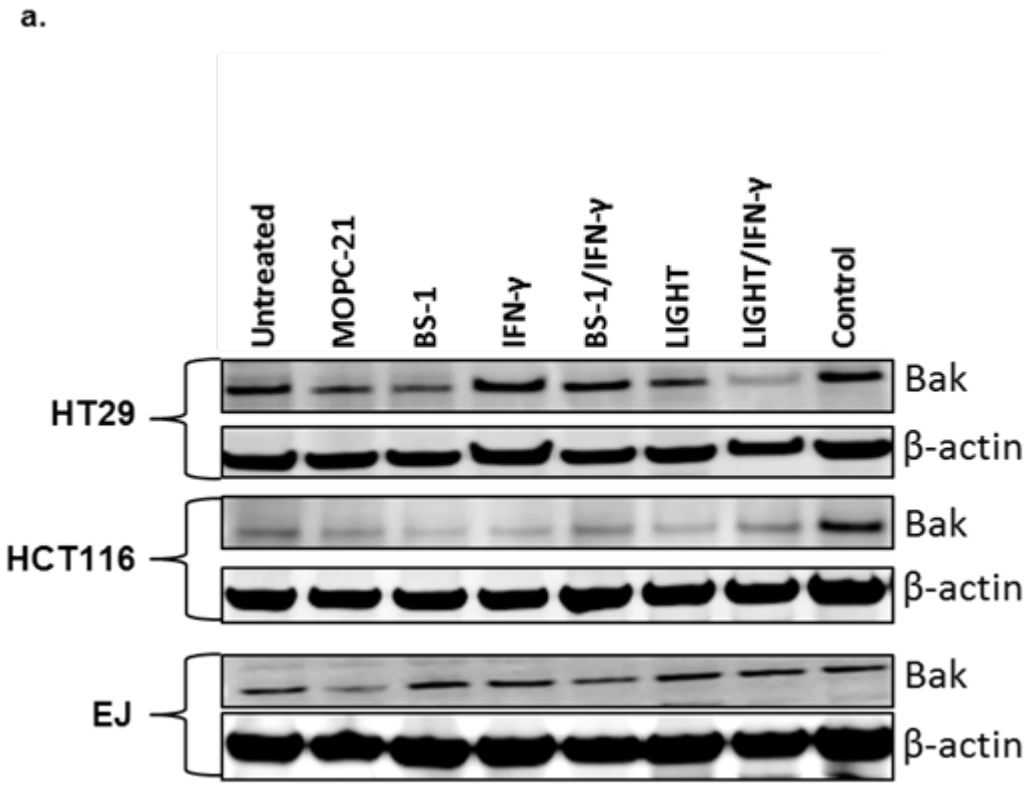

b.

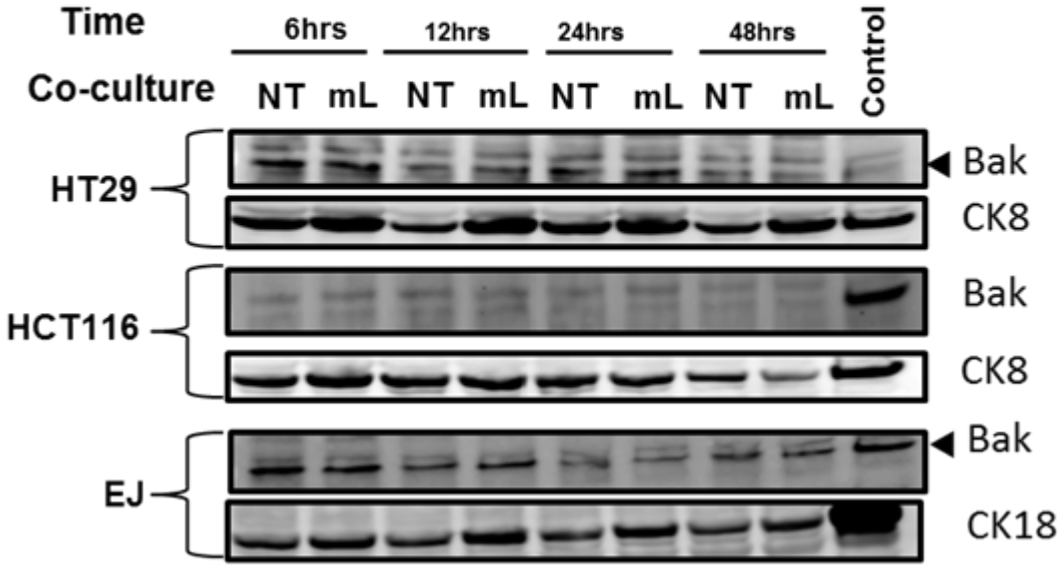

Figure 6.9. Bak expression following LTβR and HVEM activation in carcinoma cells after receptor activation by soluble receptor agonists *versus* mLIGHT

a), HT29, HCT116 and EJ cells were seeded in 10cm^2 culture dishes and treated either with control antibody (MOPC-21 – at conc. 10μg/mL), agonistic antibody (BS-1 – at conc. 30μg/mL), IFN-γ (at conc. 180U/mL), LIGHT (at conc. 1μg/mL) or in the absence or presence of IFN-γ, and incubated for 48hrs. b), HT29, HCT116 and EJ cells were co-cultured at cell density 3x10^6 with MMC-treated control (NT) or mLIGHT-L cells (mL) cells at cell density 3.5x10^6 in 10cm^2 culture dishes and incubated for time points 6, 12, 24 and 48hrs. Cells were lysed using 2x SDS-lysis buffer and protein concentration was determined. 20μg of treated cells or 40μg of co-cultured cells of whole lysates were separated under denaturing conditions by SDS-PAGE using 4 -12% (w/v) Bis-Tris gels and then transferred onto a PVDF membrane. The membranes were probed with primary polyclonal antibody anti-Bak in TBS/Tween 0.1% (v/v) (1:500 dilution) and then incubated with primary monoclonal antibody β-actin (1:25,000 dilution) for treated cells (a) or CK8 and 18 for co-cultured cells (b). Membranes were with secondary antibody goat anti-rabbit IgG IRDye 800 (1:10,000 dilution) for Bak detection or were incubated with secondary antibody goat anti-mouse 680 (1:10,000 dilution) for CK8 and CK18 detection. Antibody binding was visualised using an Odyssey^{TM} Infra-red Imaging system (Li-Cor). Control represents lysates from HaCaTa cells treated with cyclophosphamide (4-OH-CP). The expected molecular weight of Bak was 28kDa.

a.

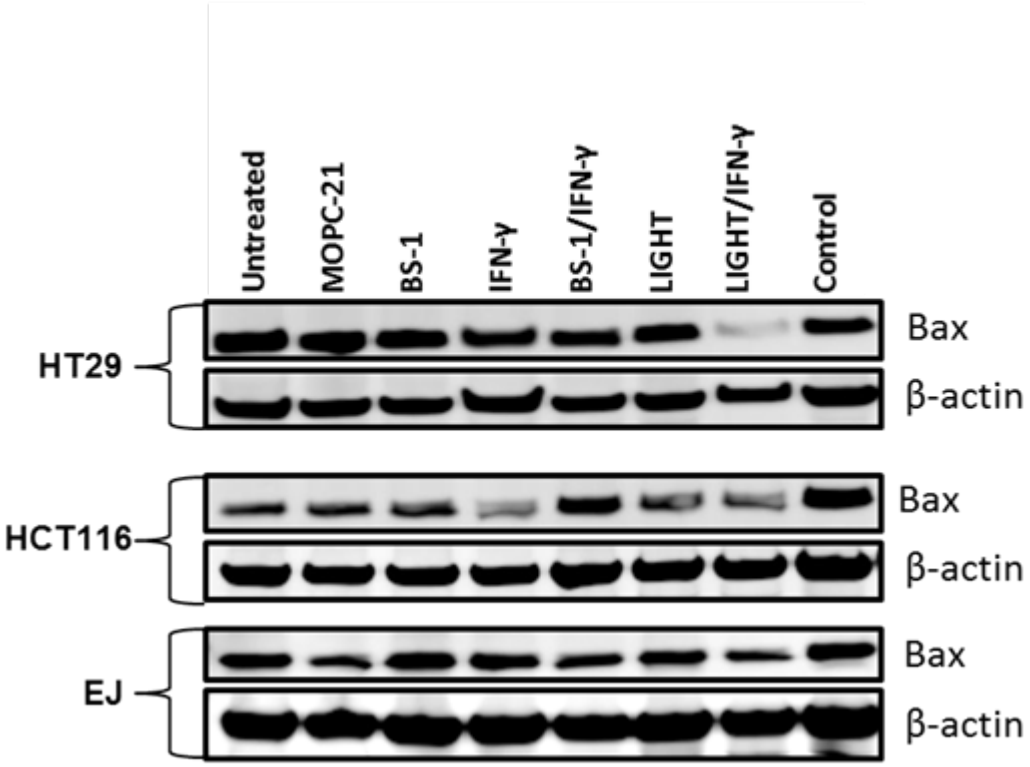
Untreated
MOPC-21
BS-1
IFN-γ
BS-1/IFN-γ
LIGHT
LIGHT/IFN-γ
Control
HT29
Bax
β-actin
HCT116
Bax
β-actin
EJ
Bax
β-actin

b.

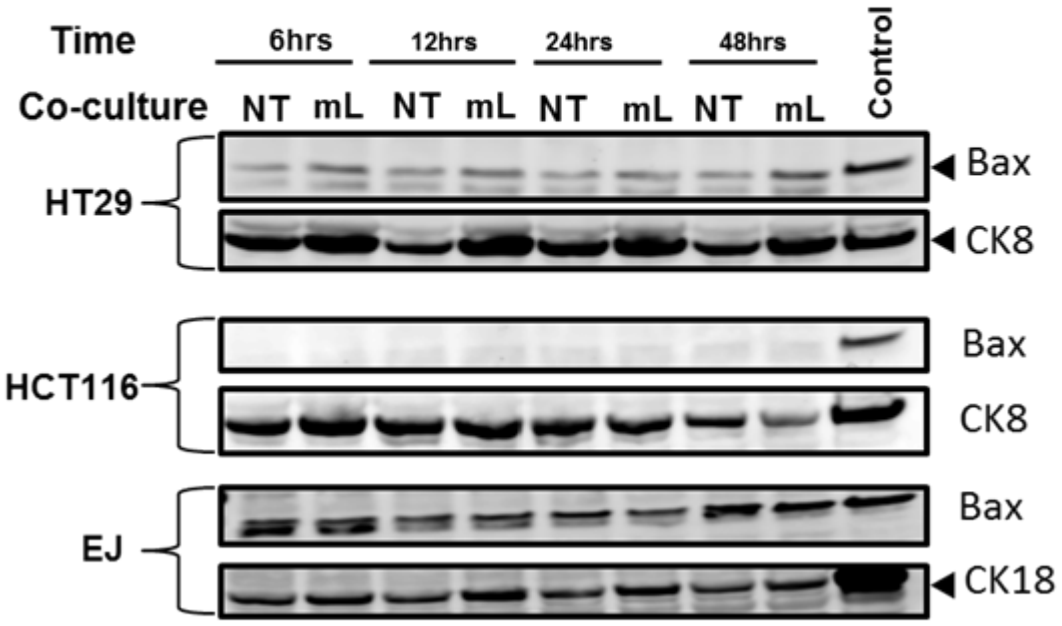

Figure 6.10. Bax expression following LTβR and HVEM activation in carcinoma cells after receptor activation by soluble receptor agonists *versus* mLIGHT

a) HT29, HCT116 and EJ cells were seeded and treated either with control antibody (MOPC-21 – at conc. 10μg/mL), agonistic antibody (BS-1 – at conc. 30μg/mL), IFN-γ (at conc. 180U/mL), LIGHT (at conc. 1μg/mL) in the absence or presence IFN-γ and incubated for 48hrs. HT29, HCT116 and EJ cells were seeded in 10cm^2 culture dishes and either treated with the indicated treatment as shown in (a) and incubated for 48hrs. b) HT29, HCT116 and EJ cells were co-cultured at cell density 3x10^6 with MMC-treated control (NT) or mLIGHT-L cells (mL) cells at cell density 3.5x10^6 in 10cm^2 culture dishes and incubated for time points 6, 12, 24 and 48hrs. Cells were lysed using 2x SDS-lysis buffer and protein concentration was determined. 20μg of treated cells or 40μg of co-cultured cells of whole lysates were separated under denaturing conditions by SDS-PAGE using 4 -12% (w/v) Bis-Tris gels and then transferred onto a PVDF membrane. The membranes were probed with primary monoclonal antibody anti-Bax in TBS/Tween 0.1% (v/v) (1:500 dilution) and then incubated with primary monoclonal antibody β-actin (1:25,000 dilution) for treated cells (a) or CK8 or 18 co-cultured cells (b). Then membranes were probed with secondary antibody goat anti-mouse 680 (1:10,000 dilution) for Bax and CK8 and 18 detection. Antibody binding was visualised using an Odyssey^{TM} Infra-red Imaging system (Li-Cor). Control represents lysates from HaCaTa cells treated with cyclophosphamide (4-OH-CP). The expected molecular weight of Bax was 21kDa.

6.8 Effects of LT receptor knockdown on mLIGHT-mediated cell death

LIGHT interacts with two membrane receptors LTβR and HVEM and one soluble receptor DcR3 (as discussed in detail in Chapter 1 section 1.11.3). This work has showed for the first time that mLIGHT triggered extensive cell death in HT29, HCT116 and EJ cells, yet it remains unknown whether these receptors signal cooperatively, independently or in an antagonistic fashion in determining cell fate in the context of mLIGHT signalling. Some studies have previously investigated the roles of LTβR and HVEM in cell death using different agonist formats; for instance, previous studies have demonstrated that the presence and activation of both LTβR and HVEM by soluble LIGHT are important to induce cell death (Zhai et al., 1998). However, a study by Rooney and colleagues (2000) reported that LTβR activation by soluble mutant LIGHT (LIGHT-R228E discriminates between two receptors and interacts with LTβR) is sufficient to trigger cell death but this was only shown in the HT29.14S cell line (which is a clone of the HT29 cells).

In this work, transfection experiments were performed to exploit RNA interference (RNAi) and LT receptor specific small interfering RNAs (siRNAs) to knockdown expression of LTβR and HVEM proteins in HT29, HCT116 and EJ cells as detailed in Materials and Methods (section 2.10). To assess whether successful knockdown for LTβR and HVEM was achieved, transfection experiments were performed several times with HT29, HCT116 and EJ cells which had been treated with LTβR or HVEM-specific siRNA (LTβR or HVEM siRNA) prior to LT receptor activation. As a first step, a series of optimisations were performed to determine the best conditions that would provide a good protein knockdown (e.g. siRNA amount and incubation time of transfection) whilst maintaining levels of cell death, i.e. within a period and using conditions where death was sufficiently detectable using the co-culture system (see modified protocol for siRNA delivery as described in section 2.10.5). Receptor expression following knockdown was determined by flow cytometry. A treatment with 100nM siRNA LTβR or HVEM was used and could reduce cell surface expression compared with non-specific siRNA (referred to as Con siRNA).

As shown in Figure 6.11, the flow cytometry results showed that transfection with siRNA against LTβR and HVEM expression reduced in overall LTβR and HVEM cell surface expression of cell lines tested (HT29, HCT116 and EJ) following treatment with LTβR or HVEM siRNA. Based on this partially successful knockdown for LTβR and HVEM (LTβR-KD and HVEM-KD) with siRNA, the effect of LTβR and HVEM knockdown on mLIGHT apoptosis was investigated using CytoTox-Glo death detection assays and data were presented as fold increase relative to control (calculated using the parameters and equations detailed in section 2.13.2). The results showed that transfection with LTβR siRNA (LTβR-KD) has no effect on mLIGHT-mediated death in HT29 and EJ cells, yet it caused statistically significant reduction in death of HCT116 cells triggered by mLIGHT. When HVEM transfection was performed using HVEM siRNA (HVEM-KD), it caused some increase in cell death levels in all cell lines tested which reached statistical significance (Figure 6.12).

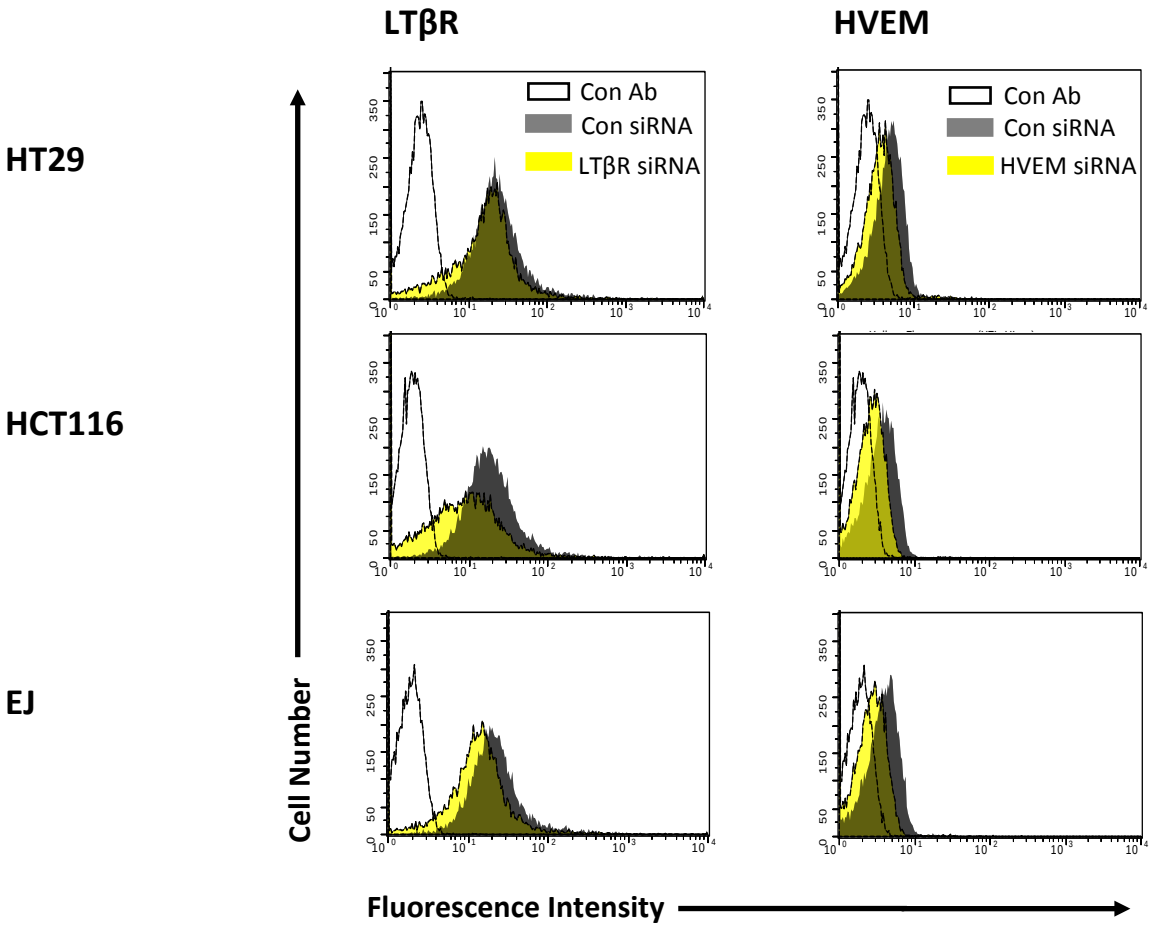

Figure 6.11. LTβR and HVEM cell surface expression knockdown by siRNA

HT29, HCT116 and EJ cells were transfected with LTβR or HVEM Accell Human SMARTpool siRNA or an irrelevant siRNA (control) in KSFM medium and incubated for 24hrs. KSFM and transfection reagents were replaced with DR 5% medium and incubated for 48hrs. Cells were harvested and labelled with anti-LTβR or HVEM or isotype control antibody PE-conjugated for 20-30mins. Cells were then washed and re-suspended in FACS buffer. Samples were acquired on an EasyCyte Guava flow cytometer and data analysed using InCyte2.6 Guava software (Millipore). The open histograms represent the fluorescence of cells labelled with isotype-matched control mAb of irrelevant specificity (Con Ab). The filled grey and yellow histograms represent specific LTβR-PE or HVEM-PE conjugated mAb. Grey and yellow histograms show the expression of LTβR or HVEM for control cells (Con siRNA) and transfected cells LTβR siRNA (LTβR-KD) or HVEM siRNA (HVEM-KD), respectively.

a.

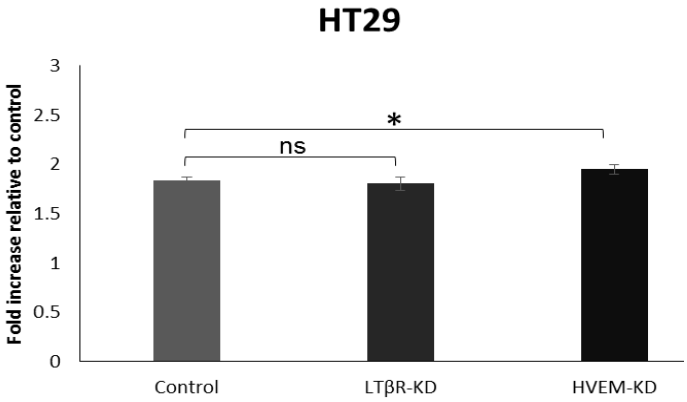

b.

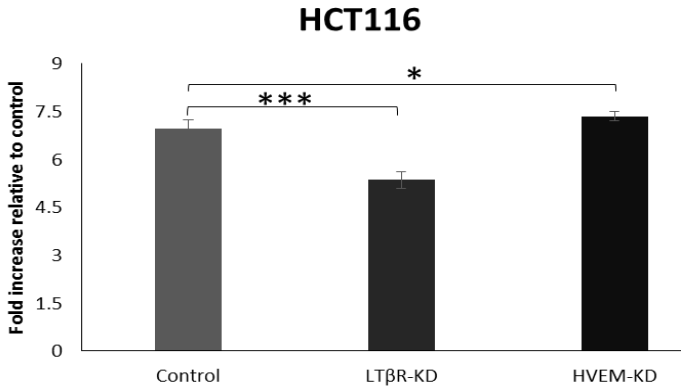

c.

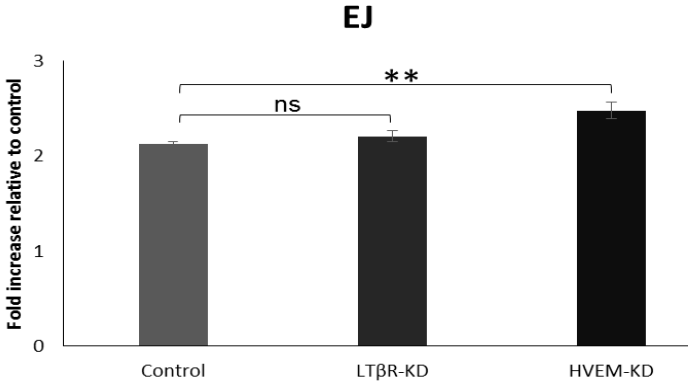

Figure 6.12. Effects of LTβR and HVEM knockdown on mLIGHT-induced cell death

HT29, HCT116 and EJ were transfected with LTβR or HVEM Accell Human SMARTpool siRNA or an irrelevant siRNA (control) for 24hrs at concentration 100nM in KSFM medium. HT29, HCT116 and EJ were harvested and co-cultured at density $1.6x10^4$ cells/well with MMC-treated control (NT-L) or mLIGHT-L cells at cell density $2x10^4$ cells/well in 96-well plates, and incubated at 37°C in 5% (v/v) CO_2 for 72hrs. 50µL of prepared CytoTox-Glo reagent was added to wells and luminescence was determined by a FLUOstar OPTIMA (BMG Labtech) plate reader. Fold increase relative to control was generated from background corrected data as detailed in section 2.13.2 and as described in Figure 4.4. Data are represented as mean values of 4-5 replicates ±S.D. a, b and c, show HT29, HCT116 and EJ cells, respectively. Stats: ns. non-significant; *, $p < 0.05$; **, $p < 0.01$, $p < 0.001$; ***, paired student t-test for HT29, HCT116 or EJ vs LTβR-KD and HVEM-KD cells.

Summary

- In this chapter, this work has provided evidence for the first time that mLIGHT triggered rapid production of ROS in cell lines tested (HCT116 and EJ cells), ROS production was observed at 3hrs following receptor post ligation with mLIGHT.

- Pre-treatment of cells with the ROS scavenger NAC caused statistically significant inhibition in mLIGHT-mediated cell death in CRC and UCC cells.

- Western blotting results demonstrated that CRC and UCC cells showed detectable phospho-p40phox expression in response to mLIGHT. However, cell death of CRC and UCC was not affected by the addition of inhibitor DPI in response to mLIGHT.

- The investigations in the activation of ASK1 expression levels following ligation with mLIGHT demonstrated that only HCT116 cells showed phospho-ASK1 at 24hrs (HT29 cells showed no detectable activation in ASK-1) and the expression of phospho-ASK-1 level was unchanged in EJ cells.

- Trx-1 expression was detected in CRC and UCC cells, which increased during culture, and interestingly there was downregulation of Trx-1 expression in CRC and UCC cells by 6-12 hours post receptor ligation, although the pattern and the timing differed between CRC and UCC cells.

- Incubation of CRC and UCC cells with the caspase inhibitor z-VAD potentiated death in HT29 and EJ cells yet partially blocked death in HCT116 cells in response to mLIGHT. As caspase activation was involved in HCT116 death, the inhibition of caspase-8 partially reduced mLIGHT-mediated death in HCT116 cells.

- Despite the presence of basal Bak and Bax expression in all cell lines tested, after treatment with soluble agonists, Bak expression was detected in CRC (little Bak was detectable in HCTT16 cells) and UCC cells. mLIGHT caused no significant changes in Bak expression in CRC and UCC cells.

- The level of Bax expression was relatively unchanged in CRC and UCC cells in response to soluble agonist treatment, however, CRC cells showed downregulation of Bax expression with combinatorial treatment LIGHT/IFN-γ. Similarly, mLIGHT caused no noticeable Bax expression changes in CRC and UCC cells (Bax was undetectable in HCT116 cells).

- Knockdown experiments to reduce expression of LTβR and HVEM proteins in CRC and UCC cells, showed that LTβR-KD caused reduction in cell death only in HCT116 cells in response to mLIGHT. HVEM-KD caused statistically significant increase in mLIGHT-mediated cell death in CRC and UCC cells.

- The results have provided a mechanistic insight into mLIGHT killing in CRC and UCC, it appears that mLIGHT-mediated cell death involves ROS production, the activation of p40phox in CRC and UCC cells. This study also demonstrated that mLIGHT-induced cell death was partially dependent on caspase activation in HCT116 cells; by contrast death was non caspase-dependent in HT29 and EJ cells, in fact caspase-inhibition potentiated death in these cells.

Chapter 7

General Discussion

7.1 General perspective

LT receptors, LTβR and HVEM, and their cognate ligand (LIGHT) belong to the TNFSF. LTβR and HVEM-mediated signalling plays roles in regulating cell fate both in the immune system and in non-lymphoid tissues. Although LTβR and HVEM comprise no intrinsic 'death' domain (DD) *per se* (hence they are referred to as non-death domain-containing TNFRs), there is evidence that they do have the ability to transmit death (apoptotic) signals through the recruitment of TRAF adaptor proteins; thus they share similarities to other TNFR members, in particular with CD40 (Albarbar et al., 2015; Georgopoulos et al., 2006; Georgopoulos et al., 2007). The absence of a classical DD inherently confers a higher level of intracellular signalling complexity and, combined with the fact that the LT system comprises two receptors, understanding the pathways involved in LTβR and HVEM-mediated cell death in carcinoma cells has been more challenging.

Few studies have focused on the specific activation of LTβR and/or HVEM by soluble agonists and showed that the activation of LTβR by agonistic antibody BS-1 induced growth inhibition in HT29 cells, whereas a study showed that the activation of HVEM on chronic lymphocytic leukaemia (CLL) by anti-HVEM mAb induced an increase in the level of pro-apoptotic genes and chemokine IL-8 secretion. Moreover, activation of LTβR and HVEM by combinatorial treatment with LIGHT and IFN-γ dramatically enhanced cell death in limited tumour cells including HT29 cells (Chang et al., 2004; Hu et al., 2013; Pasero et al., 2009b; Zhai et al., 1998). These reports have indicated that the soluble LT agonists alone are weakly (if at all) pro-apoptotic. It appears that LT soluble agonists require IFN-γ to induce cell death. Equally importantly, most of these studies have used a limited type of cells to demonstrate these effects (Albarbar et al., 2015), with the majority of studies utilising HT29 or HT29-specific sublines of this cell line.

The aim of the present work was to investigate the effects of LT soluble agonists using a panel of carcinoma cell lines that have been extensively characterised for their responses to pro-apoptotic signals triggered by the TNFSF (Bugajska et al., 2002; Georgopoulos et al., 2006; Georgopoulos et al., 2007; Hill et al., 2008; Steele et al.,

2006) and to deliver, for the first time, membrane-presented LIGHT ligand (mLIGHT) to activate LTβR and HVEM. Because of the close similarities between the LT receptors and CD40, this study focused on well-characterised carcinoma cells for their responses to CD40, such as HCT116 and EJ cells, and then compared them to the widely used HT29 cells to investigate the differences in pro-apoptotic potential between soluble agonists and mLIGHT. To perform this experimentally, the activation of LT receptors was achieved by three methods: a) agonistic antibody BS-1 for LTβR activation, b) soluble recombinant LIGHT and c) mLIGHT delivered to epithelial cells by co-culture with third-party cells (L cells engineered to express membrane LIGHT on their surface) to trigger the activation of LTβR and HVEM.

Following initial flow cytometry-based receptor expression studies and systematic assessment of the effects of soluble LT agonists in carcinoma cells, the work involved extensive optimisation for the establishment of a robust and reproducible co-culture system for the delivery of mLIGHT to epithelial (normal and malignant) cells. Upon successful optimisation, the work permitted for the first time the assessment of the pro-apoptotic effects of LTβR and HVEM via a number of assays, as well as detection of intracellular signalling mediators and their potential involvement in cell death. This work has identified intracellular proteins and their potential functional roles in LTβR/HVEM-mediated death signalling triggered by mLIGHT, and these observations are discussed in detail in subsequent sections.

7.2 LT receptor expression on carcinoma and normal cells and its regulation by pro-inflammatory cytokines

One interesting characteristic of LT receptors is that expression is not restricted only to normal cells and particularly immunocytes, but it is also expressed in both mice and humans in certain malignant cell types of lymphoid and non-lymphoid origins, such solid tumours (e.g. colorectal carcinoma) (Hu et al., 2013; Lukashev et al., 2006; Pasero et al., 2009a; Pasero et al., 2009b). This work examined the expression of LTβR and HVEM in epithelial tumours of different origins including CRC (HT29, SW480 and HCT116) and UCC cells (RT4, RT112 and EJ) as well as in normal human urothelial

cells (NHU). This work has provided evidence (Figure 3.2) that all the tested cells expressed both LTβR and HVEM receptors thus the data offered additional evidence that LTβR and HVEM are not restricted only to lymphoid malignancies but can be also detected in epithelial tumours, as well as normal (NHU) cells. As shown in Chapter 3 (Figure 3.2), the presence of LT receptor on the CRC and UCC cells allowed investigations on the effects of pro-inflammatory cytokines (IFN-γ and TNF-α) on the regulation of LTβR and HVEM expression alongside with the detection of other TNFRs (e.g. TNFRI, TNFRII and CD40) and ICAM-1 expression. The rationale for this part of the work was that it was of interest to determine whether a pro-inflammatory cytokine milieu could regulate LT receptor expression.

The pro-inflammatory cytokine IFN-γ is usually classified as a growth inhibitor as well as a growth factor for many types of cells (Schroder et al., 2004). On one hand, IFN-γ can be a growth inhibitor as it induces the activation of signal transducer activator of transcription 1 (Stat1) and interferon regulatory factor-1 (IRF-1) (Asao and Fu, 2000). Stat1 is a class of transcription factor which can play an essential role in cell differentiation, cell cycle and cell death (Asao and Fu, 2000), whilst IRF-1 functions to regulate the expression of target genes by binding to an interferon stimulated response element (ISRE) in their promoters (Asao and Fu, 2000). The activation of Stat1 and IRF-1 expression has been reported to be implicated in the inhibition of cell proliferation (Chin et al., 1997; Sato et al., 1998). IFN-γ, on the other hand, can stimulate cell growth once the Stat1 is inhibited or cells lack Stat1 expression (Bromberg et al., 1996). It is reported that IFN-γ is a strong inducer for Stat1 activation and therefore under these conditions IFN-γ acts as a growth inhibitor (Bromberg et al., 1996; Schroder et al., 2004). Given the complexity of IFN-γ regulation, it is likely that IFN-γ treatment regulates the expression of target genes and this may have an effect on upregulation, downregulation or the induction of protein expression on cell surface. As shown in Chapter 3 (Figure 3.2), cell treatment with IFN-γ overall led to an increase in LTβR expression in RT112 cells and also HVEM expression in HT29, SW480, HCT116, RT4, RT112 and EJ cells compared with controls. Moreover, IFN-γ treatment upregulated CD40 expression in EJ and HCT116 cells and this is supported by previous studies by our group (Georgopoulos et al., 2007). As IFN-γ may trigger direct cell growth regulatory

signalling and have an effect on LT receptor expression, it was interesting to investigate the effects of IFN-γ in combination with LT soluble agonists on cell growth, as IFN-γ may play an important role in enhancing the cytotoxic activity of LT soluble agonists by known mechanisms (as discussed above) or by unknown mechanisms which need to be further investigated.

TNF-α was also used in such cell treatment and to determine any effects on LT receptor expression. TNF-α is a member of TNFLs and it can bind two receptors: death receptor (TNFR-I) and non-death receptor (TNFR-II) (Cabal-Hierro and Lazo, 2012) (as discussed in detail in Chapter 1 section 1.7.1 and 1.9). As shown in Chapter 3 (Figure 3.2), cell treatment with TNF-α upregulated LTβR expression in RT4 and HCTT16 cells and also HVEM expression in HT29, HCT116 and EJ cells. In terms to the biological effects of TNF-α on cell signalling whether cell survival or cell death, studies demonstrated that TNF-α acted as an inducer of apoptotic cell death during the maturation of mice thymocytes (Giroir et al., 1992; Hernandez-Caselles and Stutman, 1993). *In vitro*, TNF-α has either growth inhibitory or cytotoxic effects in some normal cell types and human tumour cells, but in most cases tumour cell lines are sensitive to TNF-α particularly when the protein synthesis is inhibited by CHX (Meager, 1991; Porter, 1990; Ruggiero et al., 1987). TNF-α can induce both necrotic and apoptotic cell death in mouse fibroblasts *in vitro* and *in vivo* (Kamata et al., 2005) and under some circumstances accumulating evidence suggest that it can induce a characteristic type of death known as necroptosis (Vandenabeele et al., 2010). In particular, recombinant TNF-α causes growth inhibition or cytotoxicity in a number of cell lines of human and murine origin such as human carcinoma cell lines ME-180 (cervical) and murine fibroblasts (L929); interestingly, not all cells respond to TNF-α by apoptosis as reviewed extensively elsewhere (Albarbar et al., 2015). Consistent with this and as shown in Chapter 3 (Figure 3.3), TNF-α showed inhibitory effects on cell growth of RT4 and RT112 cells. However, TNF-α treatment promoted cell growth or had no effects on cell growth of HT29, SW480, HCT116 and EJ cells and this is in agreement with a previous study demonstrating that there are some carcinoma cell types of UCC where TNF-α can be growth-promoting (Bugajska et al., 2002). In support of this and others, there are other studies demonstrating that normal skin (Detroit 551) and lung fibroblasts (WI-38)

were resistant and TNF-α treatment stimulated their growth (Fransen et al., 1986; Haranaka and Satomi, 1981; Sugarman et al., 1985). These opposing signals described for TNF-α, are attributed to its ability to bind to different receptors TNFR-I and/or TNFR-II and leading to different complexes following receptor activation (Cabal-Hierro and Lazo, 2012). TNF-α engagement of TNFRI triggers responses which may be cell proliferation, apoptosis or necroptosis (Andera, 2009; Gommerman and Summers deLuca, 2011; Micheau and Tschopp, 2003; Nagata, 1997), whereas binding to TNFR-II results in anti-apoptotic signalling outcomes by involving TRAF2 localisation and degradation and can also induce a slow apoptotic cell death (Grell et al., 1995; Rauert et al., 2010; Rodríguez et al., 2011). Although in Chapter 3 (section 3.2) the effects of TNF-α and IFN-γ were tested in the context of LT receptor expression, only the role IFN-γ in the context of LT receptor signalling was examined further (in subsequent Results chapters – section 7.3.1). The influence of TNF-α in the context of LT receptor signalling (via LIGHT) should be the subject of future experimental work, in order to determine any potential cell type-dependent effects and/or any context-specificity.

7.3 Insights into the activation of LTβR and HVEM using various agonist formats

It is well documented, yet often its importance is largely understated in the literature, that the ability of some TNFR members to cause cell proliferation/differentiation or lead to cell death (apoptosis) depends on signal “quality” as determined by the nature of the agonist used. i.e. whether the agonist is delivered in soluble or membrane-bound form; it may also depend on tumour type- and the cellular context (Albarbar et al., 2015). In this study, in order to address these questions, LT soluble agonists used were anti-LTβR Ab (BS-1) and soluble recombinant LIGHT and their effects compared to membrane ligand (mLIGHT).

7.3.1 Soluble LT agonists are weakly pro-apoptotic in carcinoma cells

A study by Lukashev et al. demonstrated that agonistic anti-LTβR antibody CBE11 (multivalent, pentameric antibody) can reduce the growth of colon and cervical tumours *in vivo* (Lukashev et al., 2006), and more recently Hu et al. (2013) showed that BS-1 induced growth inhibition as well as NF-κB activation in colon carcinoma cell lines HT29, CT26, mammary carcinoma 4T1 and soft-tissue sarcoma CMS4 cell lines. The latter study also demonstrated that BS-1 triggered the activation of caspase-8 and -3 as well as release of cytochrome c in tumour cells, thus providing evidence that growth inhibition of these tumour cells could be partially driven by a caspase-dependent death mechanism (Hu et al., 2013). The aforementioned study also reported that the activation of LTβR using a different monoclonal anti-LTβR antibody (ACH6) suppressed colon carcinoma metastasis *in vivo* (Hu et al., 2013). These findings are supported by previous work demonstrating that anti-LTβR (mAb) caused cell death *in vitro* for number of cell lines (Browning et al., 1996).

Studies on LTβR activation by agonistic antibody are relatively limited, and this has been tested on limited number of cell lines, whilst most importantly often the effects of these agonists are tested by means of detection of total cells biomass (MTT-based assays) and not using assays formally detecting cell death (apoptosis and/or necrosis). It was therefore interesting to determine if similar effects could be triggered via LTβR on a panel of carcinoma cells characterised by our group for their responses to CD40 (HCT116 and EJ cells) and additional cell lines SW480 and RT112, and to compare them to widely used HT29. As shown in Chapter 3 (Figure 3.4), cell treatment with BS-1 alone had no effect on the cell growth of HT29, SW480, HCT116, RT112 and EJ cells, but it showed some growth inhibition when BS-1 was combined with IFN-γ (which synergised the BS-1 toxicity). This effect was particularly noticeable on the growth of HT29 and RT112 cells. SW480 cells showed no detectable response to either the cytotoxic activity of BS-1 or co-treatment with IFN-γ; this observation is in agreement with a previous study which reported that SW480 cells are resistant to the cytotoxic effects of LTβR agonistic antibody (Lukashev et al., 2006). The present study also used BS-1 treatment with the protein synthesis inhibitor CHX (Figure 3.5). The use of CHX

was reported to sensitise agonistic Fas mAb (APO-1), TNF-α and soluble CD40 agonist treatment in carcinoma cells (Bugajska et al., 2002; Chinnaiyan et al., 1995; Eliopoulos et al., 2000; Eliopoulos et al., 1996; Miura et al., 1995). Because of its ability to block protein synthesis, CHX is expected to block the function of anti-apoptotic proteins Bcl-2, which in turn enhances the cytotoxic activity of soluble agonists. Our findings demonstrated that CHX only sensitised HCT116 and EJ cells to BS-1.

Importantly, this study demonstrated that treatment with BS-1 alone was not cytotoxic in HT29 cells (and the other cell lines tested), and this is in contrast with previous studies demonstrating that BS-1 was cytotoxic on HT29 cells (Browning et al., 1996; Hu et al., 2013). Despite systematic attempts to do so, this study could not reproduce some of the previously published data. In fact, we could only partially demonstrate some (though small) level of loss of cell biomass by adjusting both cell density (cell number/well) or the timing of addition of soluble agonists (this was investigated as part of this study as well as additional studies in our laboratory). Only when a much smaller cell number was seeded (<5,000/well) and LT agonist was added whilst cells were attaching to their substratum, was detectable growth inhibition observed. Of note also, all cell lines routinely cultured in our laboratory are maintained in antibiotic-free medium, and we have unpublished evidence that the presence of antibiotics induces low level of stress that can enhance weakly pro-apoptotic insults (Dunnill and Georgopoulos, unpublished). Interestingly, the Hu et al. (2013) study demonstrated that BS-1 can induce both growth inhibition and growth promotion (via NF-κB activation) in human CRC and other cells, and the present data suggest that growth promotion by BS-1 is evident in CRC and UCC cells (e.g. in EJ cells). It is also worth mentioning that two previous studies reported that activation of LTβR in transfected tumour cell lines to express LTβR leads to cell growth (Fujiwara et al., 2005; Hehlgans et al., 2002).

Activation of LTβR may be insufficient to induce cell death in CRC and UCC cells and activation of both LTβR and HVEM may be needed to trigger cell death; this is supported by a previous study demonstrating that activation of LTβR and HVEM is necessary to induce cell death in HT29 cells (Zhai et al., 1998), which contradicts findings by Browning and colleagues. For this purpose, our study initially activated both

LTβR and HVEM using the recombinant trimeric ligand LIGHT. LIGHT is the ligand for LTβR and HVEM and also has the property of binding to DcR3 which functions to neutralise LIGHT and LTβR/HVEM interactions (Yu et al., 1999). Previous studies showed that HT29 cells were sensitive to LIGHT treatment (Zhai et al., 1998; Zhang et al., 2004). This study observed (Figure 3.6) that a) unlike BS-1, recombinant LIGHT was clearly and significantly growth inhibitory in most lines tested and b) the combination of LIGHT with IFN-γ was more effective than LIGHT treatment alone in reducing carcinoma cell viability, particularly in HT29 cells; to an extent, similar effects were observed in HCT116 and RT112 cells with little effects in EJ. These findings concord with those observed previously in HT29 cells (Zhai et al., 1998; Zhang et al., 2004). Importantly and as shown in Figure 3.7, LIGHT in combination with IFN-γ can trigger growth inhibition only in HT29 cells (and to a smaller extent in RT112 cells), which suggest a necessity for LIGHT/IFN-γ synergy to induce loss of viability. By contrast the same treatment showed cytoprotection or little growth inhibition in the other cell lines tested (SW480, HCT116 and EJ). This is a significant observation as it is suggestive of a possible effect that is specific or idiosyncratic for HT29 cells (Figure 3.7). As discussed above (section 7.2), IFN-γ is a pleiotropic cytokine and can play dual roles; it can inhibit and stimulate cell growth (Asao and Fu, 2000). It was reported that IFN-γ can induce cell death through induction of several genes/protein molecules, by upregulation of Fas and TNF-α receptor expression, and also via ROS production (Cassatella et al., 1990; Schroder et al., 2004; Spanaus et al., 1998; Spets et al., 1998; Tsujimoto et al., 1986; Xu et al., 1998; Zheng et al., 2002), as well as by other poorly defined mechanisms (Schroder et al., 2004). Zhang and colleagues reported that LIGHT/IFN-γ did not induce cell death in STAT1 deficient fibrosarcoma cells U3A, yet by contrast, cell death was induced in STAT1 knock-in cells U3A1-1. These studies are consistent with a study demonstrating that the STAT signalling pathway plays a critical role in triggering cell death (Chin et al., 1997). Previous work had shown that based on RNA found that IFN-γ upregulated caspases in HT29 cells and leading cell death (Ossina et al., 1997). Although IFN-γ can potentiate the cytotoxic effects of BS-1 in HT29 cells and LIGHT on many of the CRC and UCC cells, the exact mechanism by IFN-γ crosstalks or synergies with soluble agonist to induce or inhibit cell death remains unknown. As the analysis of the molecular

mechanism underlying IFN-γ was not within the scope of this work, however, future work should investigate the effects of IFN-γ alone and in combination with LT soluble agonists on the upregulation of death receptors/ligands, ROS levels, caspase activation and Bcl-2 family members for the respective tested cell lines. This work also showed (Figure 3.8) that LIGHT combined with CHX (to inhibit the cell survival machinery and allow the death-signalling pathway) was cytotoxic only on carcinoma cells HCT116 and EJ and less cytotoxic on the other cells, these observations are in agreement with the data from BS-1/CHX treatment (as discussed above). The findings are also supportive of previous studies demonstrating that combination of soluble CD40 agonist with CHX dramatically enhanced the anti-proliferative properties of CD40 ligation in various types of carcinoma cells (Bugajska et al., 2002; Eliopoulos et al., 2000; Georgopoulos et al., 2007; Ghamande et al., 2001; Hess and Engelmann, 1996; Melichar et al., 2007). This work showed that only EJ and HCT116 cells, but not others, were sensitive to combined LT soluble agonists with CHX; it is tempting to speculate the exact mechanism signalling of CHX treatment combined with LT soluble agonists on cell growth in our system. It is possible that CHX may synthesis of anti-apoptotic proteins or reverse BS-1 and LIGHT resistance by influencing post-translational modifications of proteins such as c-FLIP, as previously shown in group of B cell lines when were treated with Fas and CD40L (Irmler et al., 1997; Sato et al., 1995b). Our observations are interesting and future studies should investigate the mechanism of LT soluble agonists combined with CHX and the involvement and interactions of multi-protein complex between the receptor and c-FLIP. Overall, our data from the MTS (biomass detection) assays indicated that activation of LTβR and HVEM with the combinatorial treatment LIGHT/IFN-γ (but not LTβR agonist BS-1 with or without IFN-γ) is cytotoxic in tumour cells. The findings also indicate that although LIGHT is superior than BS-1, the induction of more significant cytotoxicity requires combination with another ‘insult’ (IFN-γ).

However, the MTS assay strictly detects effects of cell viability but does not measure cell death and therefore other assays were employed (e.g. cell death detection assays (CytoTox-Glo)) (Kroemer et al., 2009; Martinez et al., 2010). As shown in Chapter 3 (Figure 3.10), activation of both receptors by LIGHT/IFN-γ treatment induced significant cell death in HT29, HCT116 and RT112 cells, yet EJ cells showed little if any cell death

in response to LIGHT/IFN-γ. Interestingly, the amount of death triggered in RT112 cells by LIGHT/IFN-γ was much less than that triggered by BS-1/IFN-γ (Figure 3.9). In agreement with the MTS data, SW480 cells were relatively resistant to both combinatorial treatments BS-1/IFN-γ and LIGHT/IFN-γ and this had been supported by two previous studies. In one study, SW480 cells are resistant to the cytotoxic activity of agonistic anti-LTβR (Lukashev et al., 2006). In a second report, SW480 cells did not respond to the cytotoxic effects of LIGHT treatment due to SW480 cells releasing DcR3 (which antagonises LIGHT and LTβR/HVEM interactions) and thus inhibiting cell death (Yu et al., 1999; Yu et al., 2013).

7.3.2 mLIGHT is a potent pro-apoptotic in carcinoma cells

The findings discussed above indicated that LT soluble agonists are not cytotoxic in the absence of IFN-γ and suggested that the signals of LT soluble agonists are weak as they may not trigger adequate receptor cross-linking as previously reported with some TNFR members (Bugajska et al., 2002; Holler et al., 2003). In this regard, this study delivered for the first time a membrane signal in the form of membrane-bound LIGHT (mLIGHT) to trigger activation of both LT receptors. One fundamental property of the TNFR signalling is related to “signal quality” (i.e. the degree of receptor cross-linking), which determines the outcome of receptor ligation (Albarbar et al., 2015; Fernandes et al., 2016; Georgopoulos et al., 2007). In support of this, several previous studies have demonstrated that there are differences in receptor activation potential and triggering cell signalling between the soluble and membrane-bound forms, which have been described for some common TNFR members. For instance, cross-linking with membrane-bound ligands of Fas, TRAIL, TNF-α or CD40 induced higher cytotoxicity than soluble ligand in certain tumour cell lines in comparison to their soluble forms (Ardestani et al., 2013a; Bugajska et al., 2002; Engels et al., 2005; Georgopoulos et al., 2007; Schneider et al., 1998; Suda et al., 1997; Wajant et al., 2001b; Zapata et al., 2001). Consistent with this and as shown in Chapter 4 (Figure 4.4), this study showed for the first time that mLIGHT induced extensive cell death in HT29, HCT116 and EJ cells and moderate cell death in RT112 cells, whereas SW480 cells appeared relatively resistant to mLIGHT (although some small level of death was observed). By contrast,

strikingly, mLIGHT was a cyto-protective signal in normal human urothelial (NHU) cells (Figure 4.9). Therefore mLIGHT demonstrates a) strong similarities to the effects of the CD40 system in normal and malignant epithelial cells (Bugajska et al., 2002; Georgopoulos et al., 2006) and b) a clear parallel with the situation *in vivo* whereby binding with LIGHT functions as a co-stimulatory signal for some normal immune cells (Granger and Rickert, 2003; Holmes et al., 2014). Overall, our data indicate that LTβR and HVEM expression is functional, as LTβR/HVEM ligation by mLIGHT induced extensive cell death in most CRC and UCC cells. SW480 cells showed relative resistance to mLIGHT and this is in agreement with the data of LT soluble agonists (above) and LIGHT delivered in membrane-bound form caused extensive death in carcinoma cells, whereas LT soluble agonists BS-1 and LIGHT were non-apoptotic and/or required IFN-γ to trigger cell death. Our data also have provided evidence that cell death susceptibility is clearly dependent on signal quality as well as that mLIGHT-mediated death is tumour cell-specific (it did not cause death in NHU cells).

mLIGHT induced caspase-3/7 activation in HT29, HCT116, RT112 and EJ cells, whereas SW480 cells showed no activation in caspase-3/7 and this is in agreement with cell death detection assay (CytoTox-Glo) data which demonstrated that SW480 cells did not undergo cell death (Figure 4.5). In combination, the CytoTox-Glo and Anaspec caspase detection assays permitted measurement of different components of cell death, indicating that mLIGHT induces extensive cell death which is associated with effector caspase-3/7 activity in HT29, HCT116, RT112 and EJ cells, in contrast to SW480 cells that were resistant. The differential responses of RT112 to soluble LT agonist plus IFN-γ *versus* mLIGHT, as well as the overall resistance of SW480 cells to either signal are extremely interesting observations that merit further investigation by future studies.

In addition to cell death and caspase-3/7 activation triggered by mLIGHT in HT29, HCT116 and EJ cells, this study also found that (Figure 4.6) mLIGHT caused significant levels in DNA fragmentation in HCT116 cells. However, relatively little DNA fragmentation was detected in HT29 and EJ cells. As DNA fragmentation is a marker for classically apoptotic cell death, these findings indicated that HCT116 death was apoptotic but raised the possibility that death observed in HT29 and EJ cells might show

necrotic features as well. In line with this possibility, a previous report demonstrated that death triggered by the LT system may display both apoptotic and non-apoptotic features (Wilson and Browning, 2002), whilst more generally in the TNFR family, receptor activation does not always induce DNA fragmentation when cell death induced also displays non-apoptotic features, as has been shown for the TRAIL-R system in particular ((Steele et al., 2006) and references therein). In support of this, Wallach et al. (1999) have demonstrated that a mixture of cell death features were observed following LTβR activation and this depends on cell type. For instance, apoptosis was observed in the fibroblastoid line WEHI164, whereas a mixed type of cell death (apoptosis and necrosis) was detected in HT29 cells. Collectively, apoptotic and necrotic cell death triggered by mLIGHT appeared to exist in a cell-type dependent manner.

The study also observed increased cytokine secretion in response to mLIGHT, in particular induction of pro-inflammatory cytokines IL-6, IL-8 and GM-CSF in CRC and UCC cells (although HCT116 cells showed no detectable IL-6 secretion). IL-6 is a pleiotropic cytokine that plays critical roles in the acute phase reaction, inflammation, haematopoiesis and bone metabolism (Mansell and Jenkins, 2013). mLIGHT induced marked secretion of IL-8 in all cell lines tested HT29, HCT116 and EJ cells (Chapter 4 – Figure 4.10). IL-8 is an inflammatory chemokine (CXCL8) which is chemoattractant of neutrophil and lymphocytes in a variety of inflammatory diseases (Belperio et al., 2000). A previous study demonstrated that the activation of LTβR activation with anti-LTβR (mAb) induced IL-8 and RANTES secretion in A375 cells and similar observations were made when membrane-bound LTβ and LTαβ (ligands for LTβR) were investigated (Degli-Esposti et al., 1997b). Moreover, a study reported that treatment of HT29 cells with TNF-α (a non-classical activator of the LT system) and Fas induced IL-8 secretion (Abreu-Martin et al., 1995). Significantly, mLIGHT also caused GM-CSF secretion in HT29, HCT116 and EJ cells. GM-CSF is a pleiotropic cytokine and functions to maintain the generation of immune responses and it has been demonstrated that the secretion of GM-CSF *in vivo* chemo-attracts mononuclear cells, dendritic cells and macrophages, which ultimately lead to macrophage-mediated tumour cell cytolysis (Shinohara et al., 2000). These observations are in agreement with a previous study showing that the activation of CD40 by mCD40L caused IL-8 and GM-CSF secretion in some carcinoma

cell lines of CRC and UCC cells (Georgopoulos et al., 2007). Moreover, previous reports demonstrated that the secretion of IL-8 and GM-CSF is dependent on NF-κB and AP-1 activation in normal and malignant epithelial cells, respectively (Cagnoni et al., 2004; Gallagher et al., 2002; Gelbmann et al., 2003; Schwabe et al., 2001). It is attempting to speculate the relationship between IL-8 and GM-CSF secretion and NF-κB and AP-1 activation in our system, but it would be necessary for future work to explore the mechanisms underlying mLIGHT-mediated cytokine secretion in CRC and UCC cells.

7.4 Regulation of TRAF adaptor proteins in LTβR/HVEM death signalling

TNFRs are activated by ligand-induced trimerisation and oligomerisation through the interaction of receptor CRD domains, which typically leads to receptor aggregation and at the molecular level the subsequent recruitment of cytosolic TRAF adaptor proteins (TRAF1-3, 5, and 6) to the TNFR cytoplasmic tail (Fernandes et al., 2016; Rauert et al., 2010; Wyzgol et al., 2009). TRAF1 can interact indirectly with TNFR-II, and directly with some other TNFR members, such as CD30 (Lee et al., 1996) and HVEM (Marsters et al., 1997b) and others (Bradley and Pober, 2001). TRAF1 was reported to regulate transcriptional activation (Leo et al., 1999; Schwenzer et al., 1999). Marsters and colleagues reported that TRAF1 binds to HVEM following its activation in some epithelial cells (Marsters et al., 1997b). As shown in Chapter 5 (Figure 5.4), this work showed that there was some degree of upregulation in TRAF1 expression in CRC and UCC cells, following LIGHT and/or combinatorial treatment with LIGHT/IFN-γ. mLIGHT induced marked upregulation of TRAF1 in HCT116 and EJ cells but no significant TRAF1 induction was observed in HT29 cells. These observations share similarities to previous studies on CD40 where TRAF1 was induced and indirectly recruited via interactions with TRAF2 (Pullen et al., 1999a; Pullen et al., 1998; Pullen et al., 1999b). On the other hand, TRAF2 functions as an inducer, but TRAF3 (discussed below) acts as an inhibitor of NF-κB (Hostager et al., 2003). It has been shown that TRAF2 recruitment and association with CD40 leads to the activation of pro-inflammatory signalling pathways (Mukundan et al., 2004), whereas TRAF2 is found to mediate the activation of NF-κB following LTβR signalling (Luftig et al., 2001). Other studies demonstrated that HVEM is

likely to recruit TRAF2 and TRAF5 which are key mediators for the activation of NF-κB as well as AP-1 (Kim, 2005; Kuai et al., 2003). In this work, it appeared that TRAF2 expression (Figure 5.5) was downregulated in HT29 cells, and HCT116 and EJ cells showed little changes in TRAF2 levels in response to mLIGHT.

TRAF3, on the other hand, often acts as a negative regulator of NF-κB activation and studies demonstrated that TRAF3 activation is associated with cell death in HT29 cells and in human embryonic kidney (HEK293T) cells (Force et al., 1997; Sanjo et al., 2010; VanArsdale et al., 1997). This study for the first time demonstrated in Chapter 5 (Figure 5.6) that marked induction of TRAF3 expression was observed in UCC cells following LIGHT and/or combinatorial treatment LIGHT/IFN-γ, whereas CRC cells showed no detectable TRAF3 expression. Importantly, mLIGHT caused TRAF3 upregulation in CRC and UCC cells as early as 1.5hrs post-ligation. Therefore, it appears that as extensive cell death is triggered, TRAF2 and TRAF3 may be competing and thus TRAF3 is upregulated and TRAF2 degraded, as has previously been reported following CD40 ligation by mCD40L (Georgopoulos et al., 2006) and in line with findings reporting CD40-mediated TRAF2 degradation in B cell lines (Brown et al., 2002). Critically, killing by mLIGHT occurs without co-treatment with IFN-γ or CHX and triggered TRAF1 and TRAF3 upregulation, whereas LT soluble agonist treatment did not cause any detectable death and entrained the apoptotic pathway only if both LTβR and HVEM expression were activated by combinatorial LIGHT/IFN-γ treatment and caused TRAF1 and 3 upregulation only in UCC cells. These findings have provided direct evidence that the degree of receptor cross-linking determines TRAF adaptor protein regulation in LTβR/HVEM death signalling, thus showing parallels with other TNFR members (e.g. CD40) by our group and others (Georgopoulos et al., 2006; Hauer et al., 2005). The current data are in agreement with previous studies reporting that HT29 death is TRAF3-dependent (Rooney et al., 2000). This is also consistent with previous findings that the LTβR-mediated signalling in a number of cell lines is transduced by TRAF3 and TRAF5 recruitment and ROS production (discussed in more detail below) (Chen et al., 2003). What is interesting about the TRAF3 expression observation is that it was detected at an approximately 50kDa protein despite its full length being reported as 65kDa. This observation is interesting yet in agreement with studies in CRC (Mohamed and

Georgopoulos, manuscript in preparation) and UCC (Dunnill et al, manuscript under review). This is a novel observation in the context of the LT system but adds to the similarities with CD40 signalling. It has previously been reported that TRAF3 protein has several splice variants that can produce different isoforms (Gamper et al., 2001; Van Eyndhoven et al., 1999).

Previous studies have demonstrated that recruitment of TRAF5 via CD40 mediated the activation of NF-κB (Ishida et al., 1996a) and later findings reported that TRAF5 forms heterodimers with TRAF3 and contributes to NF-κB activation (Leo et al., 1999). Moreover, it has been reported that TRAF6 can induce cell death via caspase-dependent pathways, which is mediated by the interaction of the RING domain of TRAF6 with caspases (He et al., 2006). It has been shown that targeting TRAF6 following the activation of CD40 by CD40L leads to the inhibition of NF-κB, p38, JNK and Akt activation (Davies et al., 2005a; Davies et al., 2005b). In this work, mLIGHT caused little detectable effects in TRAF5 levels in CRC (very little TRAF5 expression was detected in HCT116) and UCC (Figure 5.7). TRAF6 expression was not detected in any of CRC and UCC lines treated with mLIGHT (Figure 5.8). It appeared that TRAF5 and TRAF6 expression may not be as important as TRAF1, 2 and 3 in cell death of CRC and UCC cells triggered by mLIGHT. This is in line with previous findings in CD40 signalling in our laboratory (Dunnill et al, under review).

Overall, the findings presented in this study revealed that cross-linking with mLIGHT-induced not only extensive cell death but it also induced early activation of TRAF1 and TRAF3 expression (and TRAF2 downregulation in HT29 cells). It appeared that recruitment of TRAF3 may inhibit TRAF2/5 activation by downregulation (this inactivates NF-κB pathway) and allow for the death pathway to take place, and this mechanism shares similarities with reported mechanism of CD40-mediated cell death (Georgopoulos et al., 2006; Hauer et al., 2005). It should, however, be noted that to demonstrate these hypotheses it would be necessary to perform functional assays (in the form of siRNA-mediated knockdown) to confirm the actual functional involvement of molecules like TRAF1 and particularly TRAF3 in mLIGHT-mediated death. Finally, the induction of TRAF3 mediated cell death is possibly mediated by lipid raft formation

(Dadgostar and Cheng, 2000) and this process may be dependent on and crosstalk with other molecules (e.g. ROS)-mediated receptor clustering (via acid sphingomyelinase activation and ceramide production) (Zhang et al., 2006).

Future work should further probe the exact mechanism of regulation of TRAF1 and TRAF3 (i.e. whether regulation is at the transcriptional and/or post-transcriptional level) in LTβR/HVEM death signalling by performing such as investigating the precise role of these TRAFs by RNAi (as described above).

7.5 The roles of MAPKs and TFs in pro-apoptotic LTβR/HVEM signalling

MAPKs are intracellular signalling molecules that regulate a number of cellular activities (e.g. cell differentiation, cell survival and cell death) and are divided into subgroups: ERK1/2, JNK and p38 (Mebratu and Tesfaigzi, 2009). In the context of cell death induction, studies demonstrated that ERK1/2 can phosphorylate BH3-proteins Bim and Bad to reduce cell sensitivity to death and thus lead to cell growth promotion and this is entirely dependent on the cell and stimuli types (Hübner et al., 2008; Ley et al., 2003; Ley et al., 2004; Zha et al., 1996a). In this work, we could not sensitively detect activation (phosphorylation) by immunoblotting, so functional inhibition experiments were performed to demonstrate the functional role of MAPKs in mLIGHT-mediated cell death. This work found in Chapter 5 (Figure 5.9) that mLIGHT caused little detectable differences in phospho-ERK in CRC and UCC cells, yet interestingly, inhibition of MEK/ERK significantly abrogated mLIGHT-mediated death in CRC and UCC cells (Figure 5.10). Consistent with this ERK1/2 observation, previous studies demonstrated that ERK1/2 is implicated in cell death responses of HeLa cells treated with cisplatin (Wang et al., 2000), and inhibition of ERK1/2 in renal cell lines and primary cultures of renal proximal tubular cells stimulated their survival (Kim et al., 2005; Nowak et al., 2004). Although the overall levels of p-ERK are not altered, future studies (immunofluorescence microscopy) should investigate whether p-ERK translocates to the nucleus. Nevertheless, the pharmacological inhibition studies clearly suggest that ERK1/2 regulates mLIGHT-mediated cell death in CRC and UCC cells. This observation

is in contrast to findings by our group in the CD40 system, where ERK is not involved in mCD40L-mediated apoptosis (Georgopoulos et al., 2006).

JNK is MAPK that is intimately associated with the induction of apoptosis (Davis, 2000; Green and Kroemer, 2004). Previous studies reported that JNK is activated in response to chemotherapy drugs (Hayakawa et al., 2004; Potapova et al., 2001), whilst in the context of the TNFR family, it has been shown that CD40 signalling in carcinoma cells triggered JNK activation (Eliopoulos et al., 2000; Elmetwali et al., 2010). Moreover, Georgopoulos and colleagues (2006) reported that JNK activation plays a role in cell death via the cooperation and regulation of pro-apoptotic proteins of Bcl-2 leading to intrinsic cell death (mitochondrial pathway). The activation of the stress kinase p38, plays a critical role in cell death of rat fetal brown adipocytes triggered by TNF-α treatment (Valladares et al., 2000). Furthermore, studies by our group demonstrated that CD40-mediated apoptosis activated p38 and blocking the function of p38 attenuated death in CRC cells (Mohammed and Georgopoulos, manuscript in preparation). Consistent with the role of JNK and p38 in cell death, this study showed that some detectable differences in phospho-JNK and -p38 in CRC (HCT116 cells showed a significant activation of phospho-p38 in response to mLIGHT) and UCC cells. The inhibition of JNK partially blocked death in HCT116 and EJ cells, yet, strikingly, JNK inhibitor potentiated death of HT29 cells. The blockade of p38 significantly reduced mLIGHT-mediated cell death in CRC and UCC cells (Figure 5.11 – 5.14). The present work suggests that activation of MAPKs ERK1/2, JNK and p38 closely regulates mLIGHT-mediated cell death in CRC and UCC cells, although further experiments would be required to clarify their exact functional roles.

As the role of MAPKs is to activate downstream ubiquitous TFs and in particular NF-κB and AP-1, this work examined the functional role of these TFs in mLIGHT-mediated death using specific inhibitors. NF-κB plays an anti-apoptotic role in TNF-α stimulation and JNK activation is found to be required for TNF-α-induced apoptosis (De Smaele et al., 2001; Deng et al., 2003; Javelaud and BesancËon, 2001; Tang et al., 2001). NF-κB can modulate the activity of c-Fos and AP-1 (Fujioka et al., 2004), whereas other studies reported that NF-κB has the capability to inhibit JNK activation (De Smaele et al., 2001;

Papa et al., 2004; Park et al., 2004; Tang et al., 2001). Previous studies have demonstrated that overexpression of HVEM in HEK293 cells leads to the activation of NF-κB and AP-1 as a result of TRAF2 and TRAF5 recruitment (Hsu et al., 1997; Marsters et al., 1997b). As shown in Chapter 5 (Figure 5.15), NF-κB inhibition partially reduced death in CRC cells and potentiated death in UCC cells, whereas inhibition of AP-1 partially blocked death in HCT116 and EJ cells (but not in HT29 cells) following the ligation with mLIGHT.

Our data have provided the first demonstration of a direct role for JNK/AP-1 in the LTβR/HVEM death signalling in CRC and UCC cells, observations showing some similarity to those from studies reporting a role for JNK/AP-1 in CD40-induced cell death in other model systems (Afford et al., 2001; Choudhury et al., 2003; Georgopoulos et al., 2006). Overall, these data offer evidence for the first time that mLIGHT-mediated cell death involves a number of MAPKs (e.g. ERK, JNK and p38) and downstream NF-κB and AP-1 and these events may be triggered via a TRAF3-dependent mechanism in malignant epithelial cells (Force et al., 1997). It, however, remains unknown how the same signal can be so cell type- and context-specific, as significantly different observations were made in the widely used HT29 versus HCT116 and EJ cell lines, and functionally mLIGHT is non-apoptotic in normal cells.

7.6 The role of ROS and NOX in mLIGHT-mediated cell death

ROS represent a critical upstream component in the activation of MAPKs and TFs (NF-κB and AP-1) and caspases in TNFR-induced responses (Kamata et al., 2005; Zhang and Chen, 2004). For instance, ROS regulate TNF-α-induced apoptosis and/or necrosis (Crompton, 1999; Sakon et al., 2003). Moreover, activation of CD40 by soluble CD40L triggers ROS production in B-cells and hepatocytes through the activation of NOX (Bhogal et al., 2012; Ha and Lee, 2004). There is accumulating evidence on the role of ROS in TNFRs-induced cell death and ROS-induced death is overall increasingly attracting attention in the context of the TNFRSF signalling. As shown in Chapter 6 (Figure 6.1), ROS production was rapidly induced in HCT116 and EJ cells within 3hrs post receptor ligation by mLIGHT. The data suggested that mLIGHT induced oxidative stress, a finding in agreement with studies by Chen and colleagues demonstrating that LIGHT/IFN-γ drives ROS-dependent cell death in the human hepatoma cell line Hep3BT2 (Chen et al., 2000; Chen et al., 2003). Importantly, ROS induction is critical in mLIGHT-mediated death as the antioxidant NAC inhibited death in CRC and UCC cells in response to mLIGHT (Figure 6.2).

It has been shown that the activation of CD40 can generate ROS in a malignant B-cells through the association of TRAF3 and the activation of NOX subunit p40phox (Ha and Lee, 2004). Moreover, our group has recently demonstrated that CD40-mediated apoptosis in UCC (Dunnill et al, manuscript under review) and CRC cells (Mohamed and Georgopoulos, manuscript in preparation) involves rapid, TRAF3-dependent induction of ROS in a NOX-dependent fashion. Although there was little activation in p40phox in HT29 cells, activation in p40phox was detected in HCT116 and EJ cells at 24 and 12hrs, respectively, in response to mLIGHT (Figure 6.3). As mentioned above there is a link between TRAF3 and p40phox activation, thus the findings of this work indicated that mLIGHT may induce cell death via TRAF3-dependent phospho-p40phox in CRC and UCC. Paradoxically, however, when the NOX inhibitor DPI was used, DPI treatment had no effects in mLIGHT-mediated cell death in CRC and UCC cells (Figure 6.4). It is possible that because the NOX enzyme complex has several subunits and DPI may have an effect on other, less well-characterised NOX subunits which should be further

investigated in future. Future work should investigate the exact functional role of NOX subunits in context of mLIGHT-mediated cell death, and this may be by using shRNA knockdowns. Of note, although this study has provided evidence that mLIGHT may trigger a novel TRAF3-MAPKs-p40phox pathway, which triggers ROS for the activation of cell death, this applies to well characterised cell lines, such as HCT116 and EJ cells, but does not appear to be functional in HT29 cells.

7.7 Regulation of ASK1 and Thioredoxin in mLIGHT-mediated cell death

ASK1 phosphorylates MKK4/7 which then activates JNK and also phosphorylates MKK3/6 resulting in p38 activation (Cargnello and Roux, 2011). ASK1 plays a critical role in cell death and it has been demonstrated that kinase-inactive mutant ASK1 inhibits cell death triggered by TNF-α, Fas, anti-cancer drugs, or the withdrawal of neurotrophic factors (Chang et al., 1998; Chen et al., 1999; Ichijo et al., 1997; Kanamoto et al., 2000; Wang et al., 1999). TNF-α-mediated cell death can occur by activation of ASK1 through ROS production (Gotoh and Cooper, 1998). ROS indirectly activates ASK1 by preventing ASK1 and Thioredoxin (Trx) association via direct oxidation of Trx (Liu and Min, 2002). Similarly, Chen and colleagues (2003) demonstrated that LTβR can mediate cell death via ROS production, which in turn activates ASK1, which is dependent on TRAF3 recruitment.

In this work, HCT116 cells showed some ASK1 activation at 24hrs and the level of ASK1 activation in EJ cells was similar, in response to mLIGHT. However, HT29 cells were different as there was no detectable ASK1 activation in response to mLIGHT. An interesting observation with ASK1 related to its MW; this study showed that the activated (phosphorylated) ASK1 fragment was 50kDa as shown in Chapter 6 (Figure 6.5). It has previously been reported that ASK1 are cleaved to different fragments of MW 39, 50, 75, 110kDa in carcinoma cells but only following transfection (over-expression) is the full length 150kDa protein produced and detected (Stordal and Davey, 2008), which interestingly is consistent with recent observations in CD40-mediated apoptosis in UCC and CRC cells (Dunnill et al, under review), where phosphorylated ASK1 was observed

at 39kDa and 50kDa, respectively, during immunoblotting techniques. It remains to be confirmed however, whether the active isoform of ASK1 involved in LTβR/HVEM death signalling is the 50kDa one and future RNAi experiments can confirm this.

This work also investigated expression of Trx-1 following ligation with mLIGHT (Figure 6.6). Interestingly, it was found that although immediately after seeding CRC and UCC cells expressed low levels of Trx-1, the expression of this protein progressively increased steadily from 6hrs to 12 and 24hrs in untreated cells. It has been suggested that cells *in vitro* progressively increase Trx levels because Trx may protect from culture related stress, a suggestion based on evidence that the inhibition of Trx arrests the growth of carcinoma cells *in vivo* (Baker et al., 1997; Welsh et al., 2003). Strikingly, Trx-1 was downregulated in mLIGHT-treated CRC and UCC cells in comparison to controls, indicating that receptor ligation by mLIGHT actively down-regulates Trx-1 to permit ASK1 activation and subsequently cell death. These observations are strikingly consistent with very recent observations in CD40-mediated cell death (Dunnill et al, under review) demonstrating that Trx-1 levels progressively increased in UCC and CRC cultured cells following seeding and Trx-1 is actively downregulated by membrane-bound but not soluble CD40 agonists. Both the biological function of the detected ASK1 isoform and Trx-1 regulation in LTβR/HVEM death signalling remain unknown and merit further investigation by performing functional (shRNA knockdown) experiments.

Collectively, our findings suggested that LTβR/HVEM death signalling induced TRAF3, p40phox activation and ROS production, and caused the downregulation of Trx-1 expression leading to ASK1 activation in HCT116 and EJ cells (but not in HT29 cells).

7.8 Regulation of pro-apoptotic proteins and caspases by mLIGHT signalling

The activation of caspases is critical in classical apoptotic pathways and normally requires the Bcl-2 family pro-apoptotic Bax (and often Bak) to activate, in particular, caspase-9 (Davis, 2000; Lei and Davis, 2003). This study showed in Chapter 6 (Figure 6.7) that the inhibition of total caspase activity (using z-VAD) surprisingly potentiated death in HT29 and EJ cells, whereas z-VAD partially blocked death in HCT116 cells,

suggesting that caspases are partially involved in HCT116 cell death, yet death in HT29 and EJ cells is caspase-independent. Interestingly, these observations are in agreement with DNA fragmentation data which showed that there was little DNA fragmentation detected in HT29 and EJ cells, whereas high level of DNA fragmentation was detected in HCT116 cells. In support of this and others, Wilson and Browning (2002) demonstrated that death of HT29 cells triggered by the activation of a number of TNFR members (e.g. Fas, TRAIL, TNF, TWEAK and LTβ) was not blocked by z-VAD, thus indicating that death is mediated via a caspase-independent pathway. As death of HCT116 cells was shown to be caspase-dependent and this suggests possible involvement of known caspases (e.g. caspase-8, -9 and -10), further investigations were carried out. As shown in Chapter 6 (Figure 6.8), death of HCT116 was partially blocked using the specific inhibitors of caspase-3/7 and, interestingly, caspase-8. This indicated that mLIGHT-mediated cell death in HCT116 cells may involve the extrinsic pathway and be triggered via cross-talk with other TNFR and possibly death receptors, as is the case of CD40-mediated death in CRC cells, where death is partially dependent on cross-talk of CD40 with TRAIL (Mohamed and Georgopoulos, manuscript in preparation).

Bak and Bax are cytosolic proteins and are associated with induction of MOMP to trigger cell death (Nechushtan et al., 2001; Wolter et al., 1997). Previous studies demonstrated that LTβR/HVEM activation by LIGHT/IFN-γ in MDA-MB-231 and HT29 cells led to the upregulation of Bak, Bax and the activation of caspases-3, -6, -7, -8 and -9 (Zhang et al., 2004). This ultimately resulted in the activation of both poly ADP-ribose polymerase (PARP) and a DNA fragmentation factor (DFF45) (Zhang, 2004; Zhang et al., 2004; Zhang et al., 1996). Our laboratory has previously demonstrated the activation of Bak and Bax by mCD40L in UCC (Bugajska et al., 2002). This work showed in Chapter 6 (Figure 6.9) that, although Bak expression was detectable in CRC and UCC cells, neither soluble agonists nor mLIGHT caused significant changes in Bak expression in CRC and UCC cells. Surprisingly, Bax expression was relatively unchanged in UCC following soluble agonists treatment cells yet CRC cells showed downregulation of Bax expression following combinatorial treatment LIGHT/IFN-γ. mLIGHT caused no noticeable Bax expression changes in CRC and UCC cells, although Bax was

undetectable in HCT116 cells (Figure 6.10). There is also a possible explanation that the mechanism underlying mLIGHT killing may involve the JNK pathway.

It may be possible that although mLIGHT does not directly regulate the overall level (relative protein amount) of Bak and Bax in carcinoma cells, it might instead regulate the localisation of these pro-apoptotic mediators to the mitochondria. Therefore, it is critical that future studies investigate these possibilities and should involve immunofluorescence microscopy as well as cell fractionation experiments followed by immunoblotting to determine any such changes in Bak/Bax location. Collectively, our data have provided evidence that LTβR/HVEM-triggered death by mLIGHT is highly signal type-, cell type- and context dependent. Our findings also suggest that despite a plethora of signalling similarities between CD40 and the LT receptors, the two systems maintain a number of differences in terms of the precise nature of the death pathway triggered and in the way they entrain apoptotic (or non-apoptotic/necrotic) cell death.

7.9 LTβR and HVEM signal cooperatively in mLIGHT-induced cell death

As LIGHT can trigger signalling via both LTβR and HVEM receptors (Albarbar et al., 2015), it was important to examine whether these receptors act independently, cooperatively or in an antagonistic fashion when determining cell fate in the context of ligation by mLIGHT. In Chapter 6 (Figure 6.12), we attempted to examine the functional effects of LTβR and HVEM knockdown in mLIGHT killing. The results showed that knockdown of HVEM caused a very small increase in death in CRC and UCC cells, whereas LTβR knockdown showed no effect on cell death in HT29 and EJ cells yet it resulted in statistically significant reduction in death of HCT116 cells triggered by mLIGHT. It should be noted, however, that as the knockdown observed was transient, the results were difficult to interpret. Also, as it is possible that LTβR and HVEM signal cooperatively in inducing cell death, combination of siRNAs would be an appropriate strategy to examine this hypothesis. There is some evidence that activation of both LTβR and HVEM is important to induce cell death in tumour cell lines (HT29 cells) in response to LIGHT treatment (Zhai et al., 1998). By contrast, a study reported that

soluble mutated LIGHT (LIGHT-R228E – which is a mutated form of LIGHT that preferentially interacts with LTβR over HVEM) is sufficient to trigger cell death via LTβR in the HT29.14S cell line (a clone of the HT29 colon adenocarcinoma) that is sensitive to the pro-apoptotic activity of TNF-related ligands (Rooney et al., 2000). Another study demonstrated that activation of LTβR by membrane-bound LIGHT or mutant LIGHT (LIGHT-R228E) in the presence of IFN-γ induced high levels of chemokine secretion, with nothing reported about cell death induction (Bechill and Muller, 2014). In light of the unclear evidence (or even contradictory reports), and due to the relative inefficacy of knockdown observed (particularly in HT29) cells in our study, further experimentation would be required to understand which specific receptors are engaged by LIGHT and mLIGHT in our cells and to determine the exact role of each receptor in apoptosis. One appropriate approach would be the preparation of third party effector cells (L cell transfectants) expressing mutant LIGHT that preferentially interacts with LTβR over HVEM (the LIGHT-R228E mutant mentioned above), and study the effect of that in carcinoma cells. This would be important as it would address simultaneously the importance of an individual receptor (LTβR) in apoptosis whilst providing the signal in membrane-presented form. To perform this, our laboratory is currently in communication with Prof Carl Ware (Laboratory of Molecular Immunology, Sanford Burnham Discovery Institute, La Jolla, USA) for the preparation of an expression construct as published previously (Rooney et al., 2000) but adapted for expression in mammalian cells. In addition, using the new technology Clustered regularly interspaced short palindromic repeats (CRISPR) for LTβR and HVEM knockdown will be also ideal for future work for this purpose.

It should be noted that one of the limitations of our work relates to the Western blots experiments for co-cultures in terms of normalisation to housekeeping gene expression, although the normalisation has been performed for co-culture experiments; however, it was observed in some experiments differences in amounts loaded on gels. In this context, pharmacological inhibition experiments were performed for some essential mediators involved in mLIGHT-mediated cell death. This also could be improved in future by introducing other techniques such as immunofluorescence and immunoprecipitation assays. Regarding the controls and the specificities of antibodies

used in Western blotting experiments, controls are ideal for detection of proteins in our study, there are some experiments controls did not work for unknown reasons. It should be noted that antibodies used are specific for the proteins we investigated and this was demonstrated by our group (Dunnill et al, under review) and others (Bugajska et al., 2002; Georgopoulos et al., 2006). For publication purposes, controls (L cells alone) would be necessary and appropriate loading corrections to ensure equal loading has been confirmed. Also, further investigation could perhaps conceivable involve the immunoprecipitation assays.

7.10 Future directions

The role of the LT receptor and the ligand LIGHT in regulating cell fate in the immune system as well as in non-lymphoid tissues has been under extensive research in recent years. Moreover, the ability of several family members to induce death (mainly via apoptosis) represents a promising target for cancer therapy. Such efforts have focused mostly on death receptors such as TNFRI, Fas (CD95), and TRAIL-R due to their strong pro-apoptotic potential. However, lack of tumour cell-specificity represents an obstacle in such therapeutic strategies. The ability of tumour-specific death induction might instead be a feature of the non-classical death receptors, and the LT and CD40 systems might represent better such targets. However, as shown in this study, it appears that the interaction of LT receptor LTβR and HVEM with mLIGHT demonstrate more complex, cell-type and clearly context-specific capabilities, so it is essential that more studies delve further into the complexities of LT system signalling.

This complexity is evident at the signal transduction level as well as the level of receptor activation. For instance, there is clear difference between the ability of LT soluble agonists to trigger cell signalling when presented in a soluble versus membrane-bound form. LT soluble agonists lack cytotoxic potency when administrated as a single treatment (without synergism by co-treatment with IFN-γ), yet membrane-presented ligand mLIGHT caused extensive cell death. There is often a lack of consistency when it comes to the cell models used to study the functional role of LT receptor-ligand interactions. This may perhaps explain some of the inconsistencies evident in the literature, some of which we mentioned above. We believe that our work has for the first

time addressed some of these questions and provided some evidence for the underlying mechanisms of these differential responses. Future work should focus on understanding the complexity of the signalling cascades examined here. One fascinating prospect is to understand how the LT and CD40 receptors, though capable of recruiting similar (or identical) adaptor proteins and regulating their fate in similar fashion whilst showing similar requirement for effective cross-linking to induce strong enough death responses, can nevertheless engage cell death pathways that might differ in such signal- and cell-type fashion. How can the internal mediators engaged in HT29 and EJ cells differ yet death shows equally necrotic features? What is the mechanism of differential susceptibility in RT112 cells? How does HCT116 cell death differ? Another elegant experimental way to address these differences could involve construction of chimeric receptors comprising the extracellular domain of LT receptor but the cytoplasmic tail of CD40 and vice versa, as this could provide insights as to the molecular determinant of cell death type. Other questions also of interest include the investigation of the antioxidant pathways (excluding Trx), such as the Glutathione (GSH) pathway – is it regulated by LIGHT and how?

7.11 Conclusion

Using appropriate, well-characterised and robust epithelial cell models, this study has provided evidence for the first time that mLIGHT, in the absence of IFN-γ, is pro-apoptotic in carcinoma cells, but not in normal (NHU) cells. By contrast, this study showed the inability of LT soluble agonists to induce CRC and UCC cell death and their requirements for IFN-γ to kill HT29. Yet this combination did not kill other well-characterised carcinoma cell lines HCT116 and EJ cells. This study has also demonstrated that mLIGHT triggered 1) rapid TRAF signalling, 2) caspase-dependent and -independent pathways, 3) apoptotic and necrotic death features, and 4) ROS-dependent death. Thus, this study also identified for the first time the roles of MAPKs and ROS involvement in mLIGHT-mediated cell death. These findings have highlighted novel observations on the mechanism of cell death through LTβR/HVEM activation as well as the importance of the signal quality (strength) of ligand-receptor interactions in determining functional outcome and also demonstrated that mLIGHT is tumour cell-

specific. The new knowledge of the ability of mLIGHT signal to trigger extensive cell death in CRC and UCC cells has enhanced our understanding of the LTβR/HVEM death signalling pathway. Thus, these findings may allow for the design of better therapeutic strategies.

Appendix

Appendix I:

Stock solutions

1. EDTA preparation

Reagent	Volume or mass
Ethylenediaminetetraacetic acid (EDTA)	1g
Phosphate-buffered saline (PBS) (1x)	1000mL

The solution was mixed well and was then autoclaved.

2. SDS lysis buffer preparation for cell lysates

Reagent	Volume or mass
Glycerol	10mL
SDS	1g
Tris-HCl	6.25mL (stock conc. 1M) and pH 6.8
Sodium fluoride (NaF)	0.42g
Sodium pyrophosphate tetrabasic	0.446g
Sodium orthovandate (Na_3VO_4)	0.0184g

Up to total volume of 50mL of deionised water (dH_2O) and using magnetic heat block to and magnetic flea to dissolve all chemicals. SDS lysis buffer was then aliquoted and stored at -20°C.

Appendix II:

IFN-γ and CHX titrations

1. IFN-γ titration

a.

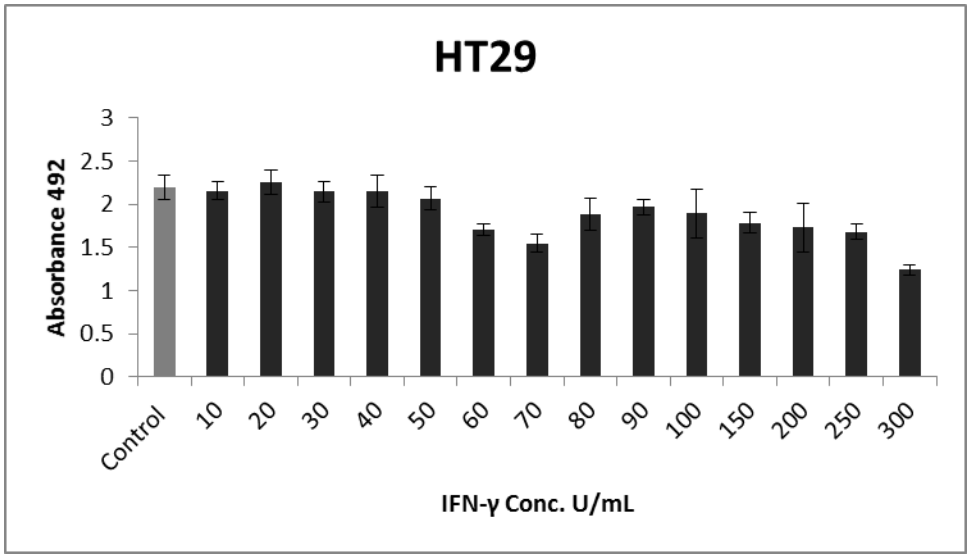

b.

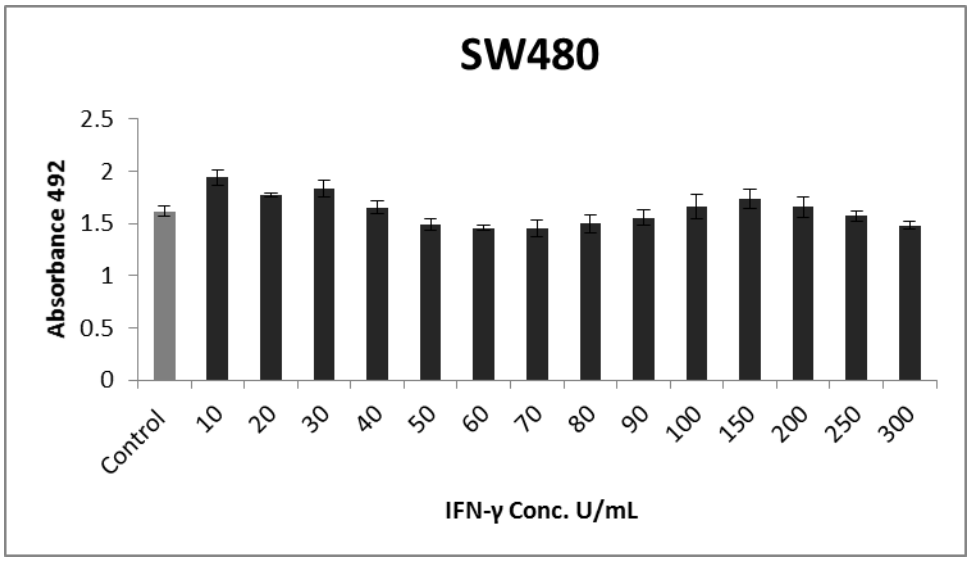

c.

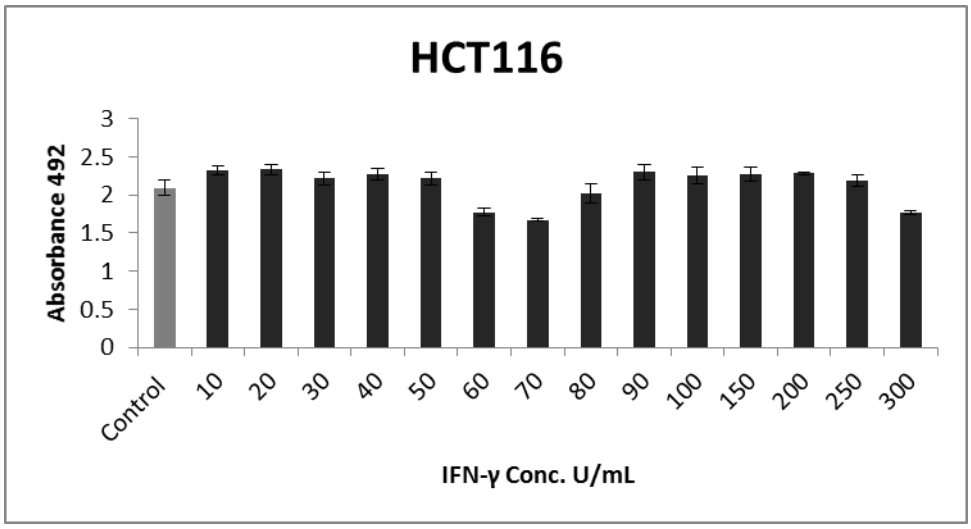
HCT116
Absorbance 492
3
2.5
2
1.5
1
0.5
0
Control
10
20
30
40
50
60
70
80
90
100
150
200
250
300
IFN-γ Conc. U/mL

d.

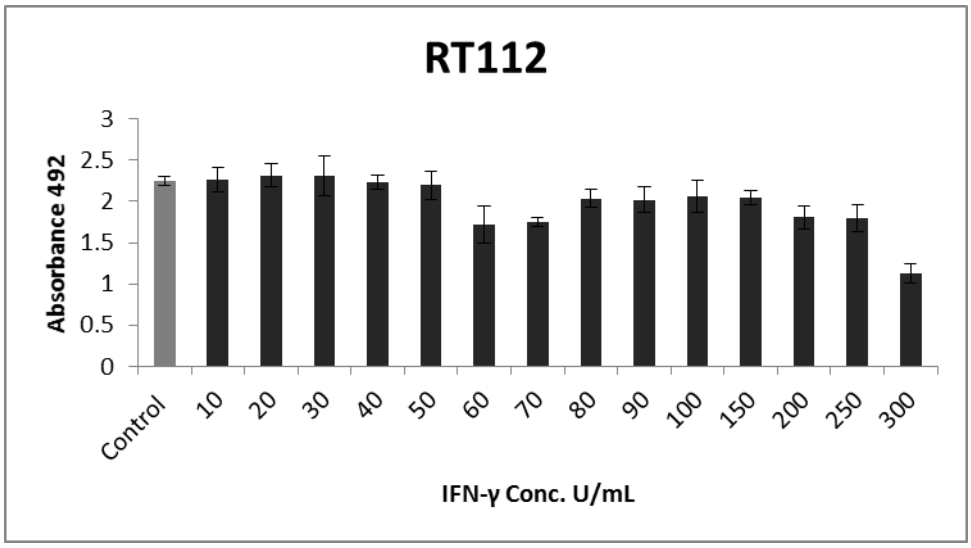
RT112
Absorbance 492
3
2.5
2
1.5
1
0.5
0
Control
10
20
30
40
50
60
70
80
90
100
150
200
250
300
IFN-γ Conc. U/mL

e.

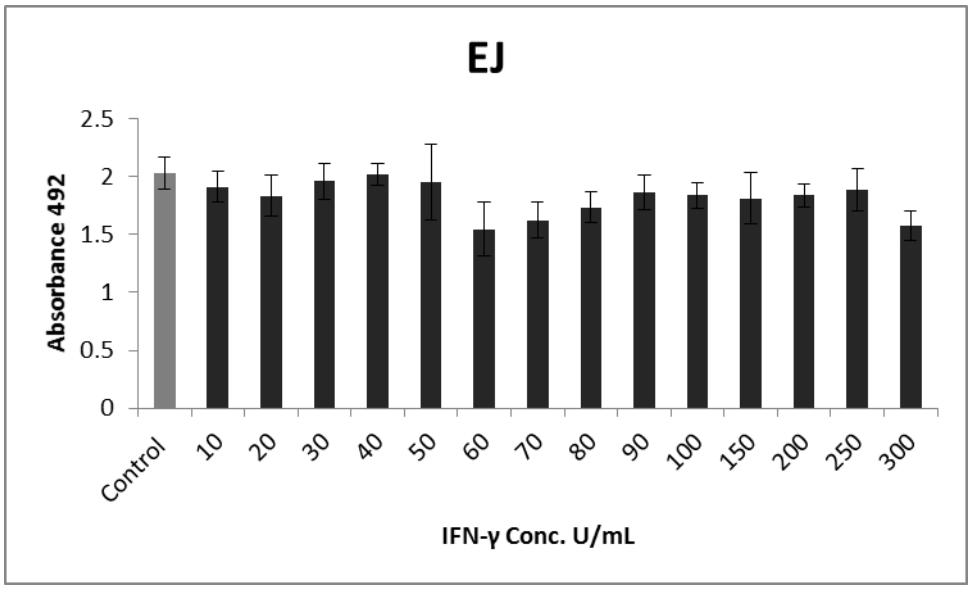

Effects of IFN-γ treatment on carcinoma cell viability

Cells of HT29, EJ, RT112, SW480 and HCT116 were plated in 96-well plates and treated with various concentrations of recombinant IFN-γ for 96hrs as indicated. 20µl of MTS solution was added to each well and incubated for approximately 4hrs. Cell viability was determined by a FLUOstar OPTIMA (BMG Labtech) plate reader at absorbance 492nm. Data are represented as mean values of 5-6 replicates ±S.D. a, b, c, d and e show HT29, SW480, HCT116, RT112 and EJ cells, respectively.

2. Protein synthesis inhibitor (Cycloheximide (CHX)) titration

a.

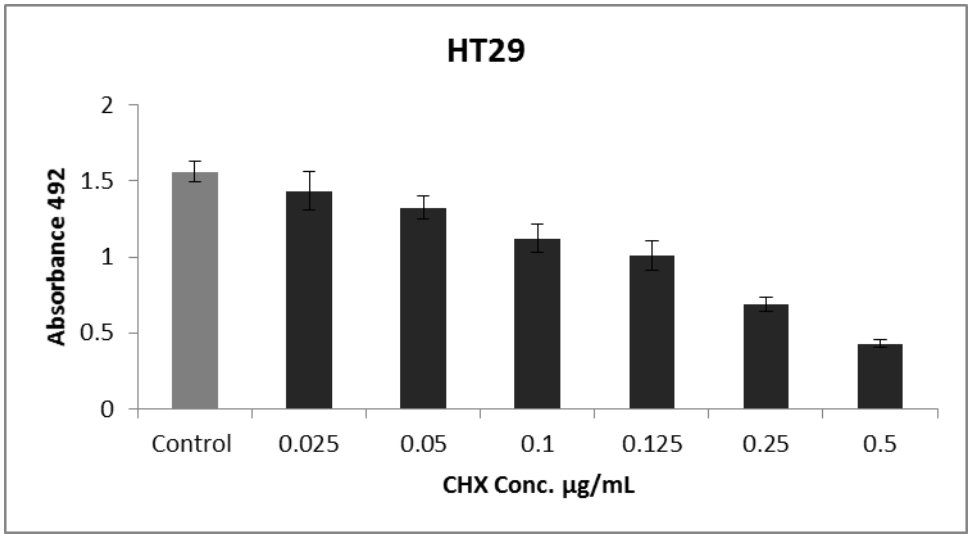

b.

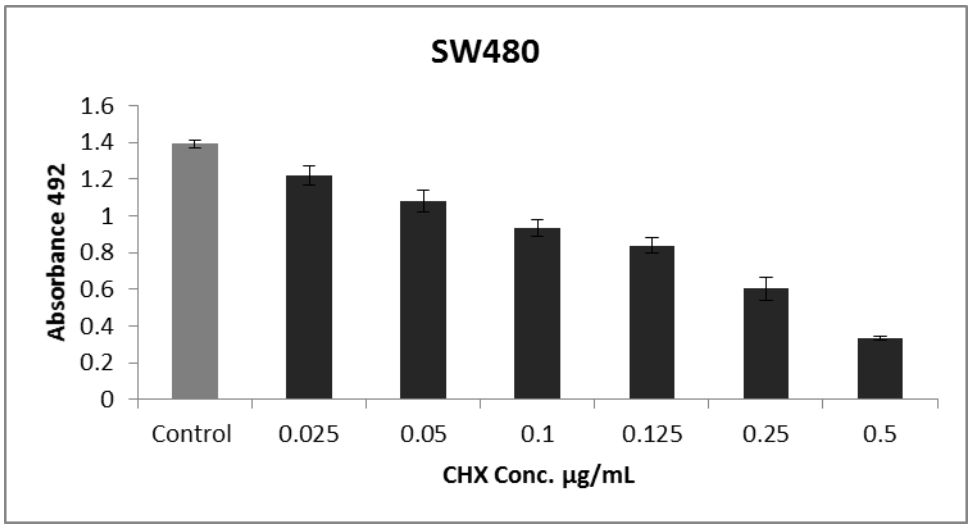

c.

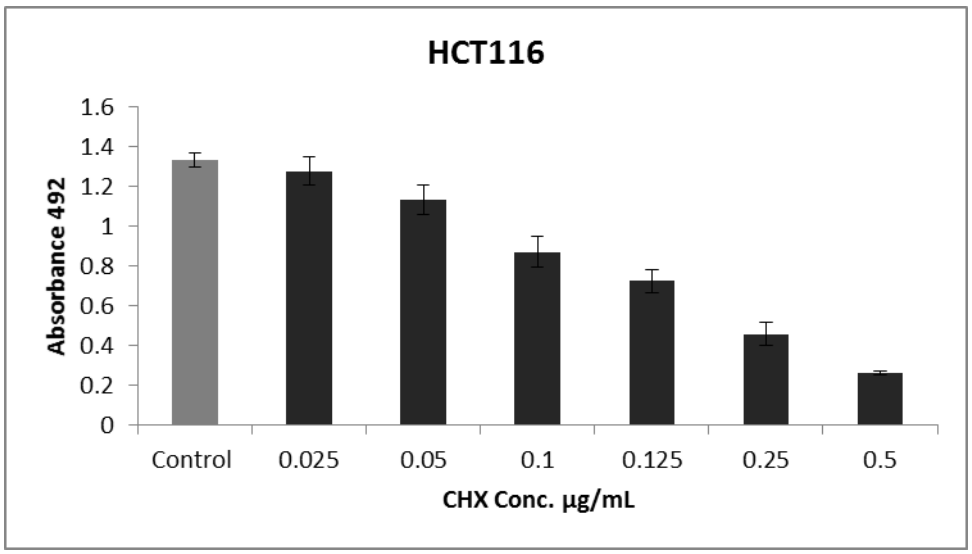
HCT116
Absorbance 492
1.6
1.4
1.2
1
0.8
0.6
0.4
0.2
0
Control
0.025
0.05
0.1
0.125
0.25
0.5
CHX Conc. µg/mL

d.

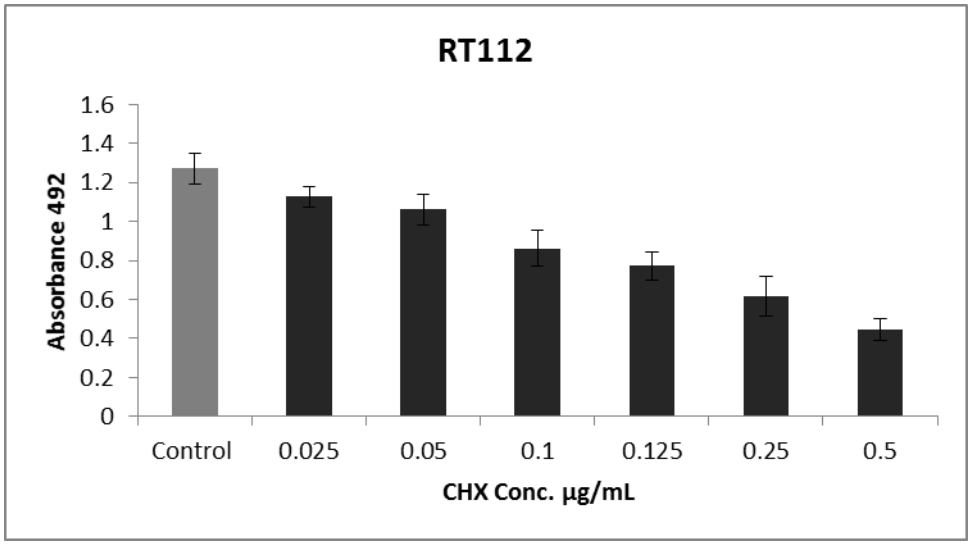
RT112
Absorbance 492
1.6
1.4
1.2
1
0.8
0.6
0.4
0.2
0
Control
0.025
0.05
0.1
0.125
0.25
0.5
CHX Conc. µg/mL

e.

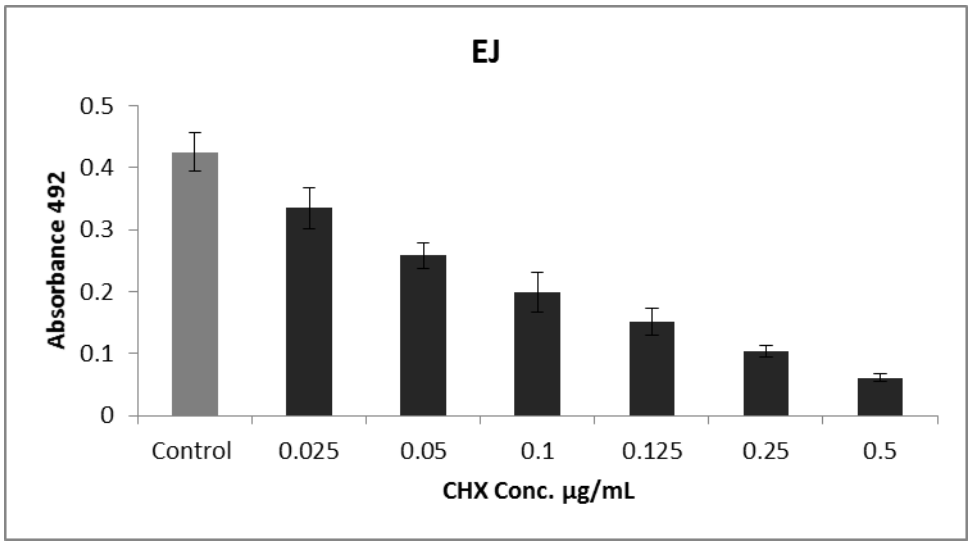

Effects of CHX treatment on carcinoma cell viability

Cells of HT29, EJ, RT112, SW480 and HCT116 were plated in 96-well plates and were then treated with indicated concentrations of CHX for 72hrs. 20µl of MTS solution was added to each well and incubated for 4hrs. Cell viability was determined by a FLUOstar OPTIMA (BMG Labtech) plate reader at absorbance 492nm. Data are represented as mean values of 5-6 replicates ±S.D. a, b, c, d and e show HT29, SW480, HCT116, RT112 and EJ cells, respectively.

Appendix III:

1. BS-1/IFN-γ

a.

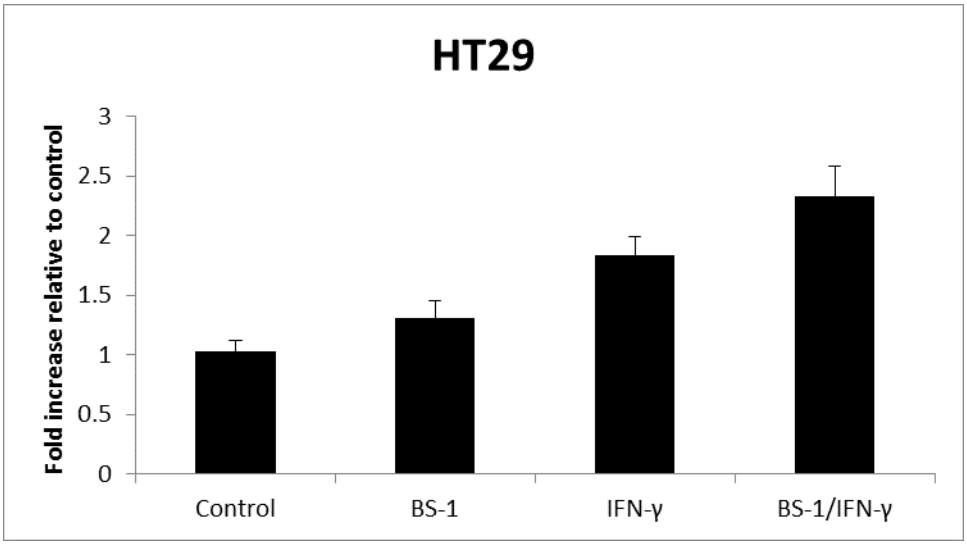

b.

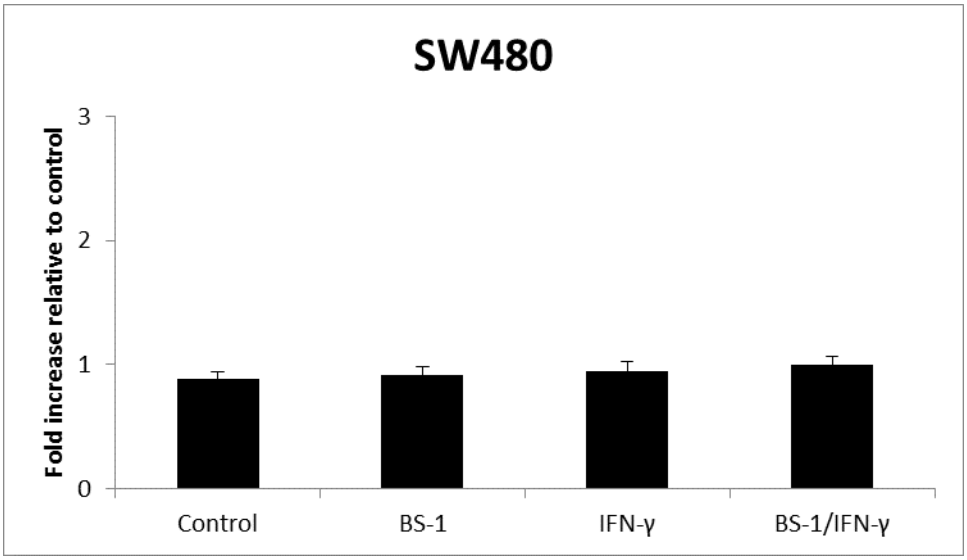

c.

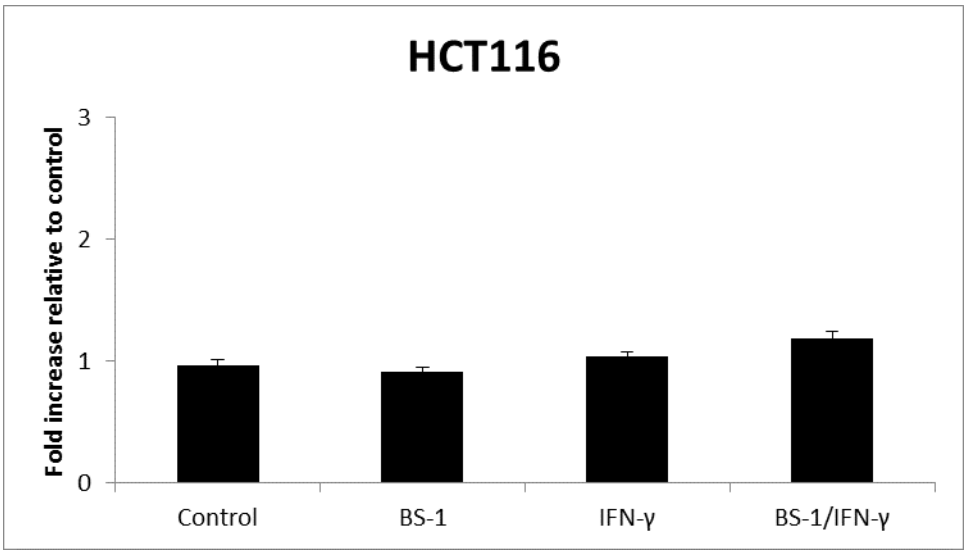
HCT116
Fold increase relative to control
0
1
2
3
Control
BS-1
IFN-γ
BS-1/IFN-γ

d.

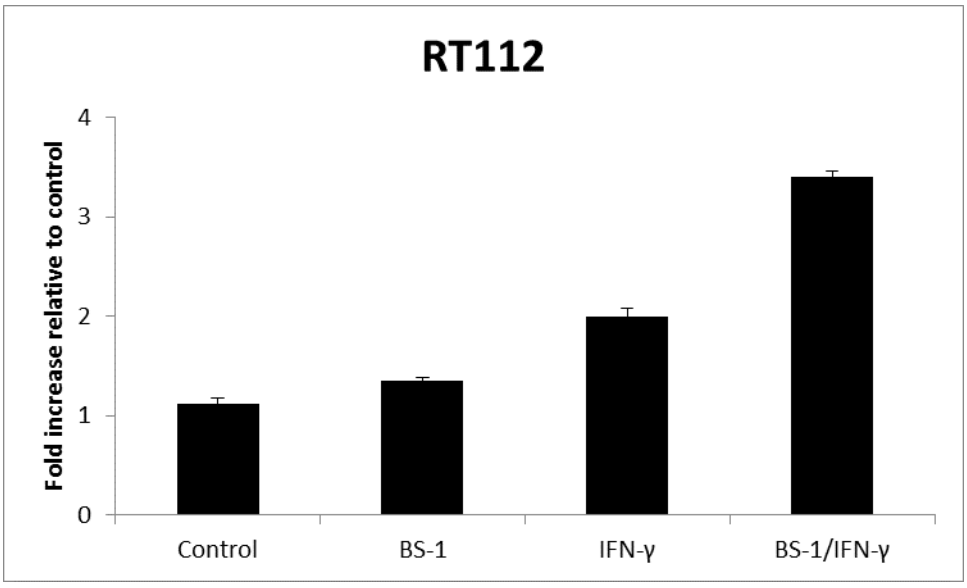
RT112
Fold increase relative to control
0
1
2
3
4
Control
BS-1
IFN-γ
BS-1/IFN-γ

e.

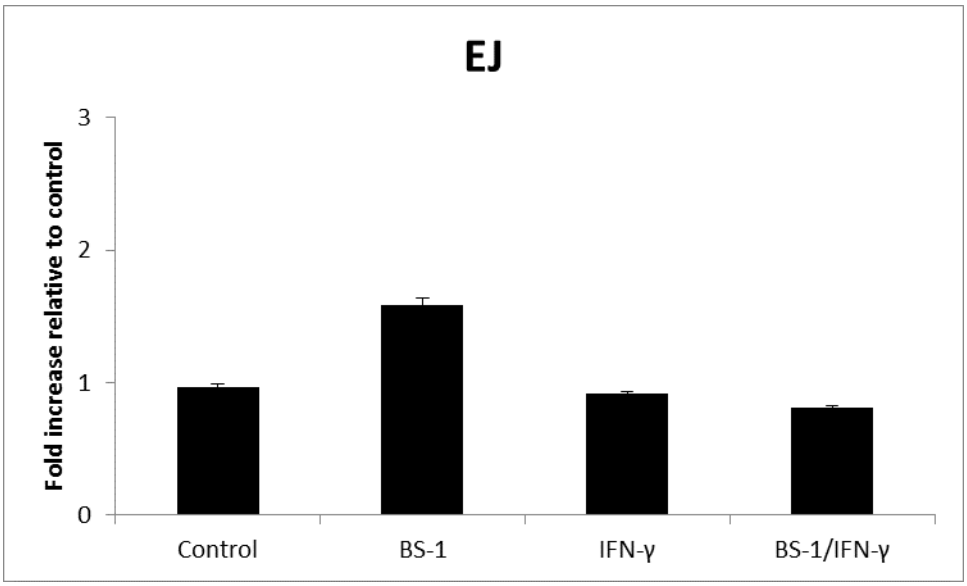

Detection of cell death following carcinoma cell treatment with BS-1 and BS-1/IFN-γ

HT29, SW480, HCT116, RT112 and EJ were seeded in 96-well plates. Cells were treated with BS-1 (30µg/mL), MOPC-21 (10µg/mL), in the absence or presence of IFN-γ (180U/mL) and incubated for 96hrs. CytoTox-Glo reagents were prepared and added to each well and then relative luminescence unit (RLU) was measured by a FLUOstar OPTIMA (BMG Labtech) plate reader. The intensity of the RLU signal corresponds to the degree of dead cells in a population (as described in section 2.13.2). Fold increase relative to control was generated from raw RLU data by comparing treated cells *versus* untreated cells as shown in right panels. a, b, c, d and e show HT29, SW480, HCT116, RT112 and EJ cells, respectively. Data are represented as mean values of 4-5 replicates ±S.D.

2. LIGHT/IFN-γ

a.

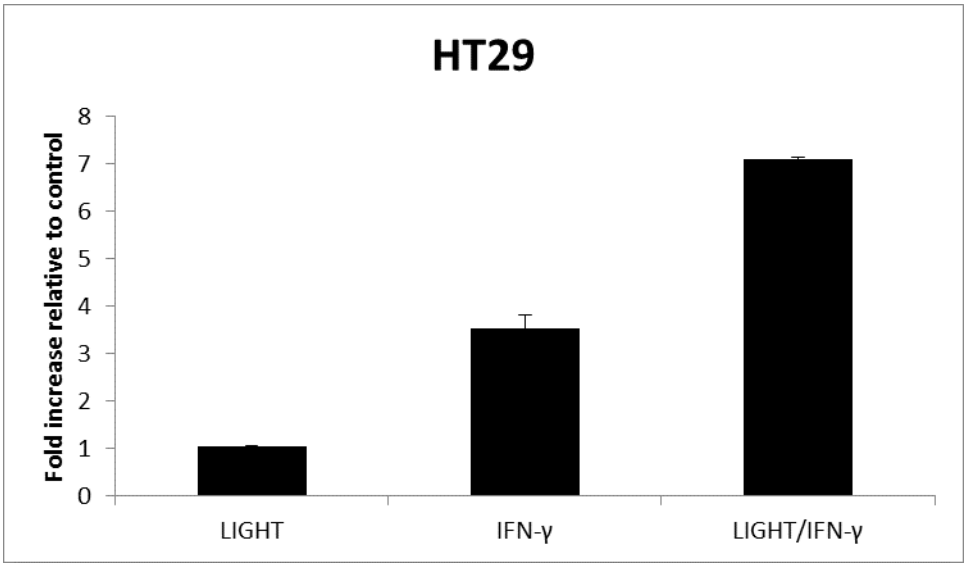

b.

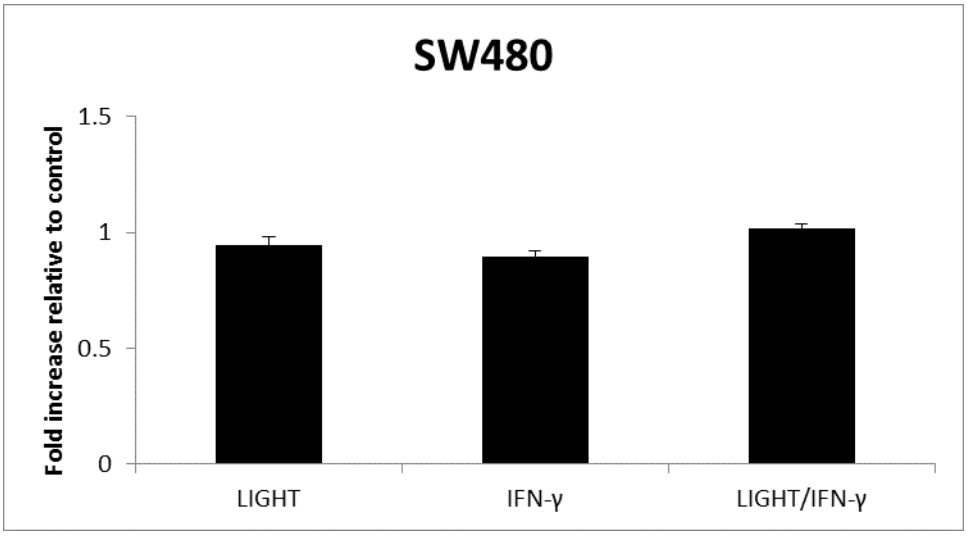

c.

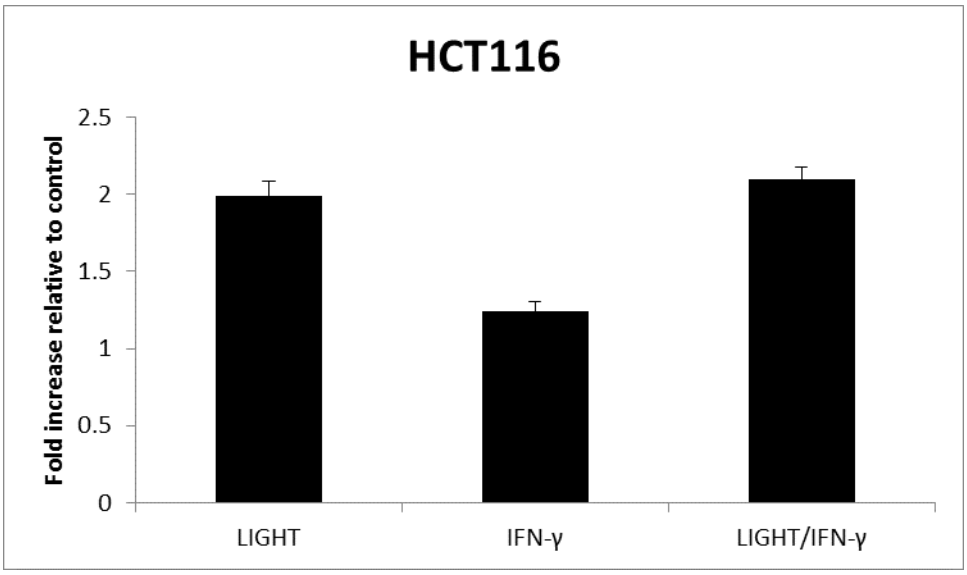
HCT116
Fold increase relative to control
2.5
2
1.5
1
0.5
0
LIGHT
IFN-γ
LIGHT/IFN-γ

d.

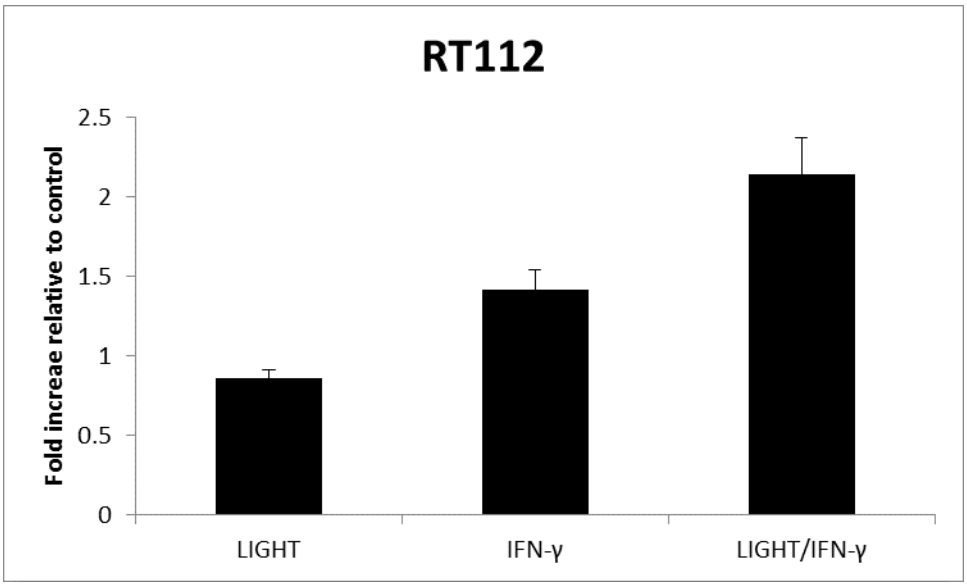
RT112
Fold increae relative to control
2.5
2
1.5
1
0.5
0
LIGHT
IFN-γ
LIGHT/IFN-γ

e.

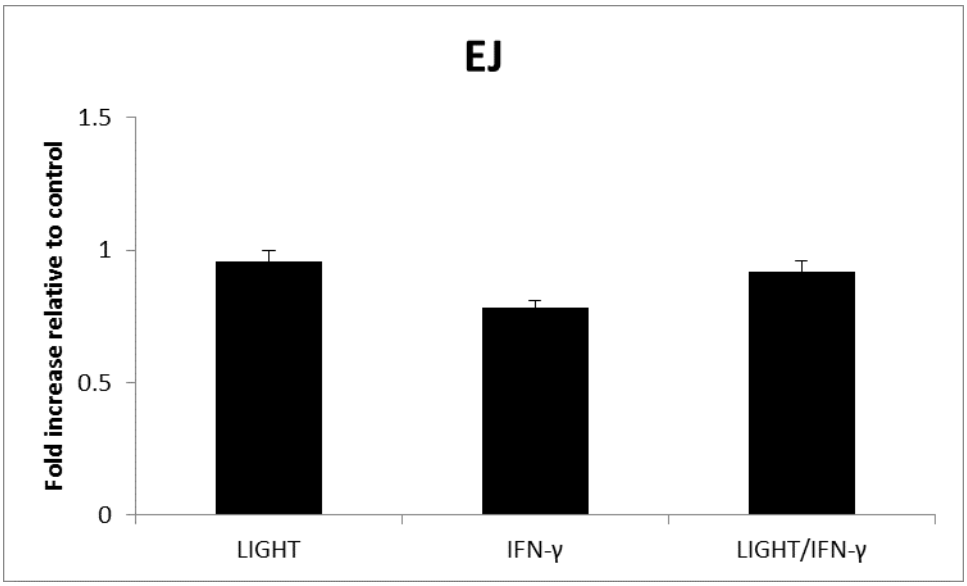

Detection of cell death following carcinoma cell treatment with LIGHT and LIGHT/IFN-γ

HT29, SW480, HCT116, RT112 and EJ were plated in 96-well plates. Cells were treated with LIGHT (1µg/mL), in the absence or presence of IFN-γ (180U/mL) and incubated for 96hrs. CytoTox-Glo was prepared and added to each well and then relative luminescence unit (RLU) was measured by a FLUOstar OPTIMA (BMG Labtech) plate reader. The intensity of the RLU signal corresponds to the degree of dead cells in a population (as described in section 2.13.2). Fold increase relative to control was generated from raw RLU data used in left panels by comparing treated cells *versus* untreated cells as shown in right panels. a, b, c, d and e show HT29, SW480, HCT116, RT112 and EJ cells, respectively. Data are represented as mean values of 4 replicates ±S.D.

Appendix IV:

1. Absence of LIGHT expression on NT-L cells

Control (NT-L) cells

a.

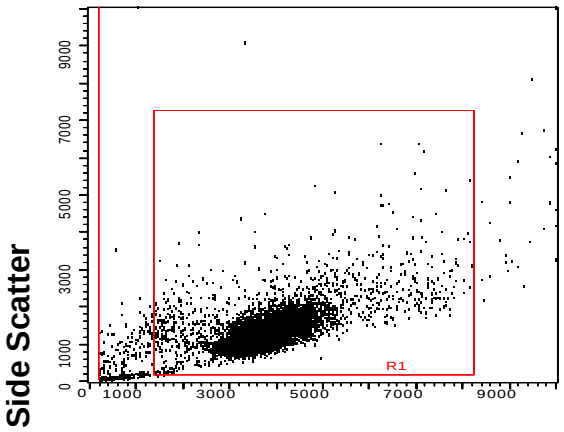

b.

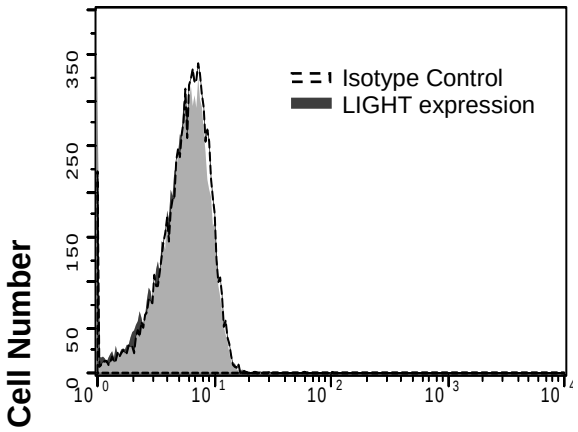

LIGHT expression on NT-L cells

NT-L cells were harvested and labelled with anti-LIGHT or isotype control antibody PE-conjugated for 20-30mins. Cells were then washed and re-suspended in FACS buffer. Samples were acquired on an EasyCyte Guava flow cytometer and data analysed using InCyte2.6 Guava software (Millipore). a, Forward and side scatter plots for acquired cells; b, Control isotype antibody PE was used (dashed white left histogram). LIGHT expression was determined by using PE-conjugated anti-LIGHT antibody (filled grey histograms) and this was compared with control PE.

2. Photos of MMC-treated cells

a. Control (NT-L) cells

Untreated cells

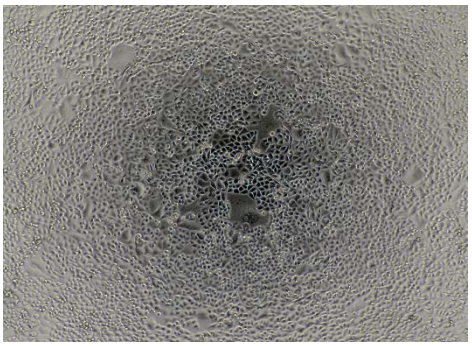

MMC-treated cells (10µg/mL)

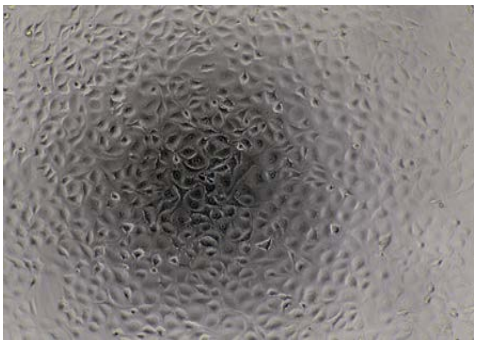

MMC-treated cells (15µg/mL)

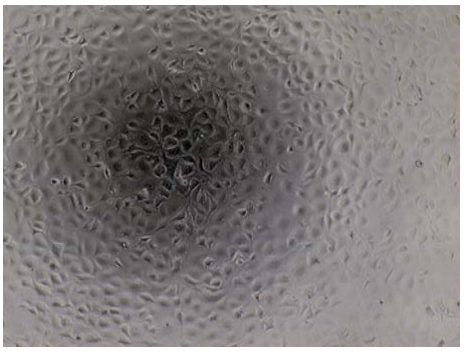

MMC-treated cells (20µg/mL)

b. mLIGHT-L cells

Untreated cells

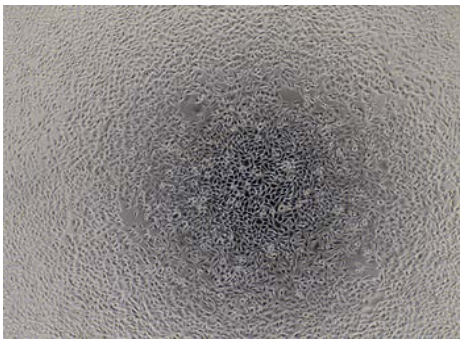

MMC-treated cells (10µg/mL)

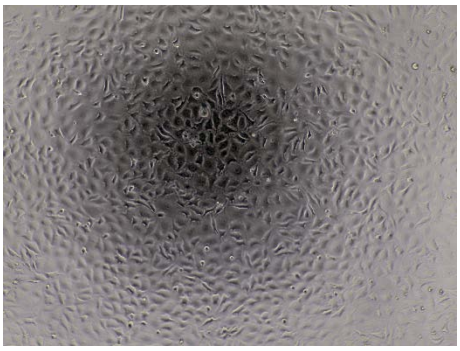

MMC-treated cells (15µg/mL)

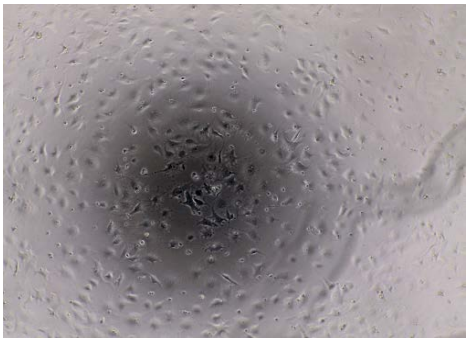

MMC-treated cells (20µg/mL)

Microscopy images of untreated and treated NT-L and mLIGHT-L cells with MMC

Cells were treated with various concentrations of MMC (10, 15 and 20µg/mL) as indicated in different flasks and incubated for 2hrs at 37°C and 5% (v/v) CO_2. Cells were then harvested, counted and seeded in 96-well plates for 72hrs. a. shows control (NT-L) cells, while b. shows mLIGHT-L cells. Photos were taken at magnification a 100x using an EVOSXL inverted microscope (PeqLab).

Appendix V:

Titrations of MAPK inhibitors

1. MEK/ERK inhibitor (U0126)

a.

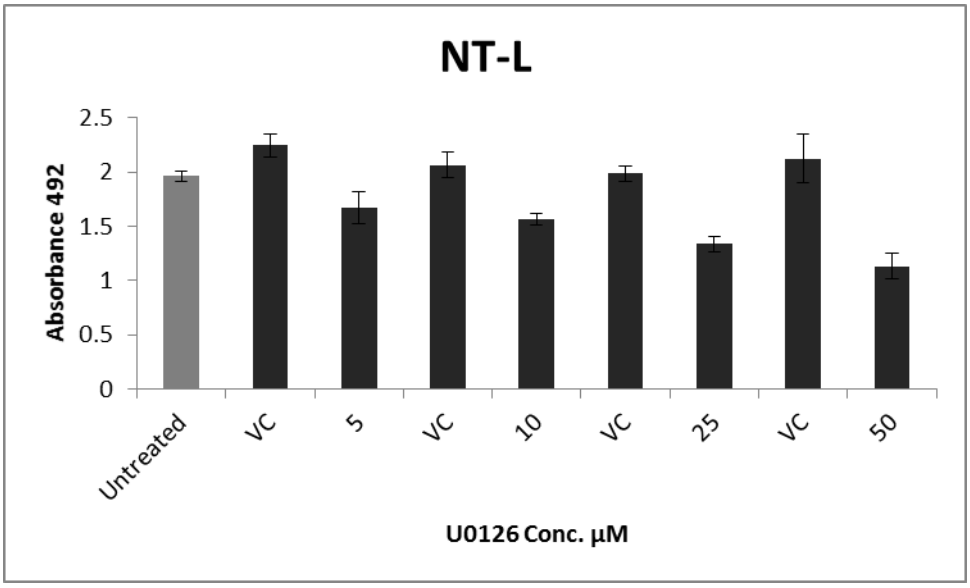

b.

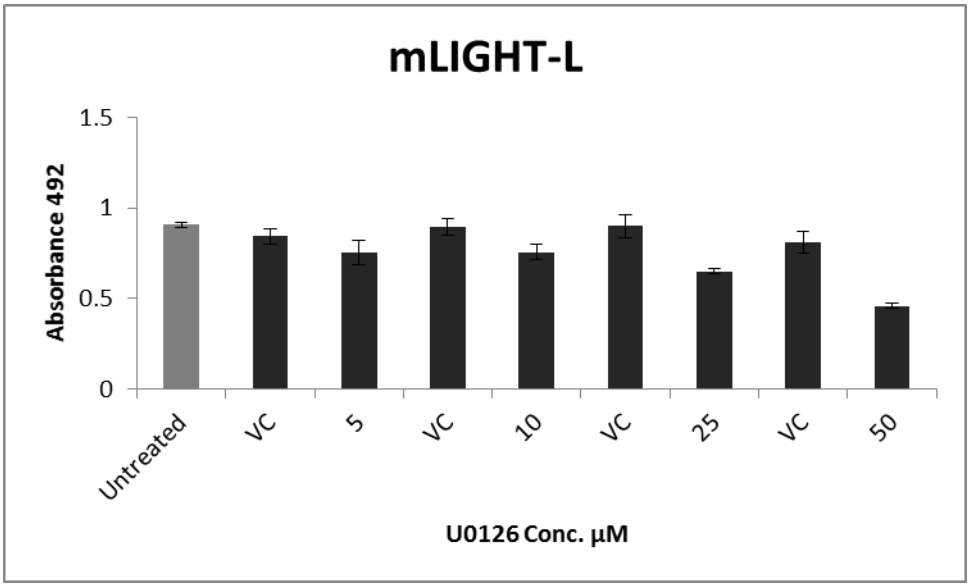

c.

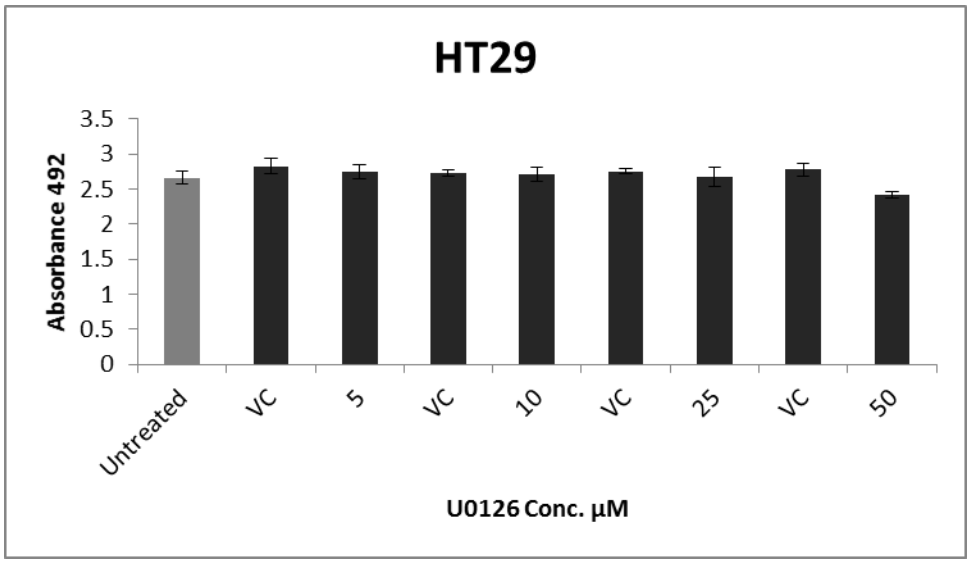
HT29
Absorbance 492
3.5
3
2.5
2
1.5
1
0.5
0
Untreated
VC
5
VC
10
VC
25
VC
50
U0126 Conc. µM

d.

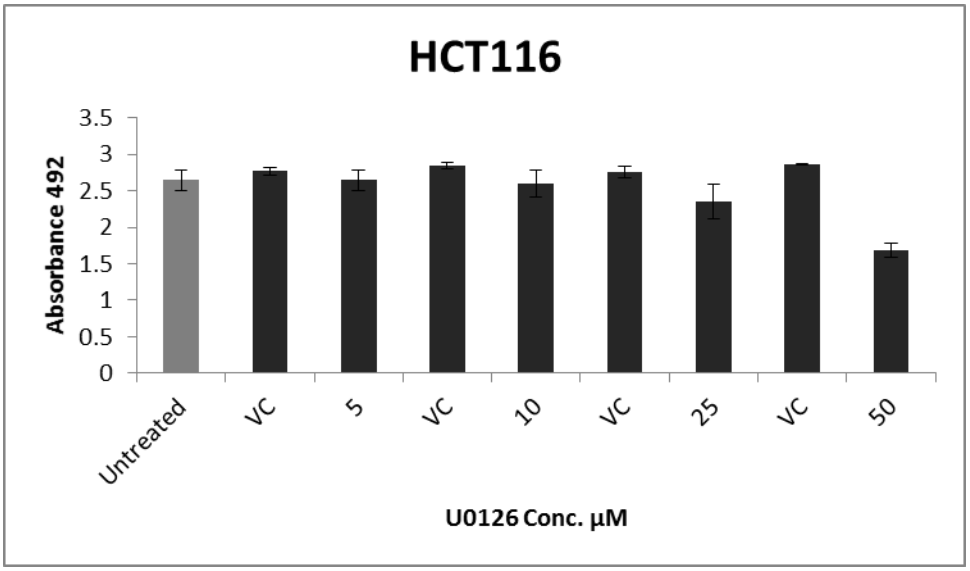
HCT116
Absorbance 492
3.5
3
2.5
2
1.5
1
0.5
0
Untreated
VC
5
VC
10
VC
25
VC
50
U0126 Conc. µM

e.

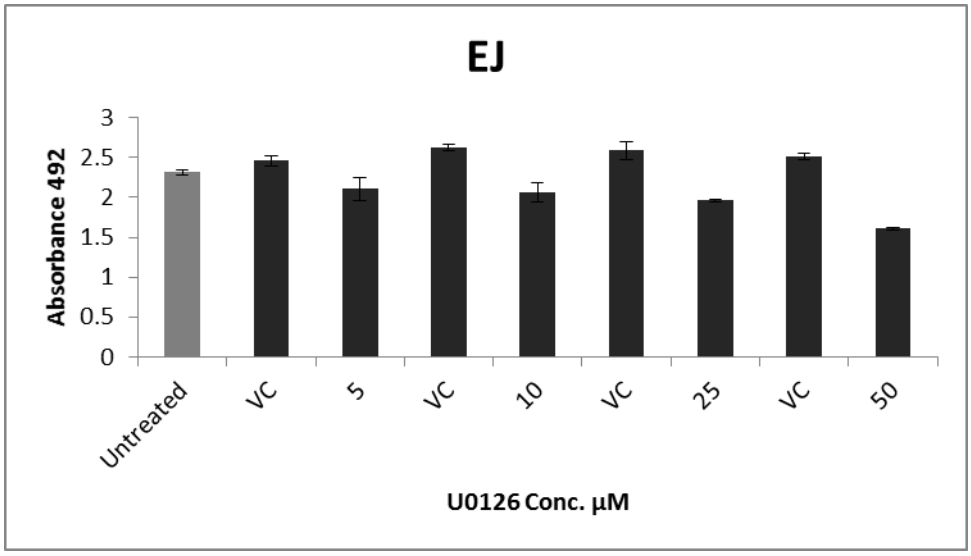

Effects of the MEK/ERK inhibitor (U0126) on carcinoma cell viability

NT-L, mLIGHT-L, HT29, HCT116 and EJ were in 96-well plates. Cells were then treated with MAPKs inhibitors: MEK/ERK inhibitor (U0126), as indicated, and vehicle control (VC) was also included. 20µl of MTS solution was added to each well and incubated for 4hrs. Cell viability was determined by a FLUOstar OPTIMA (BMG Labtech) plate reader at absorbance 492nm. Data are represented as mean values of 4-5 replicates ±S.D. a, b, c, d and e show NT-L, mLIGHT-L, HT29, HCT116 and EJ cells, respectively.

2. JNK inhibitor (SP600125)

a.

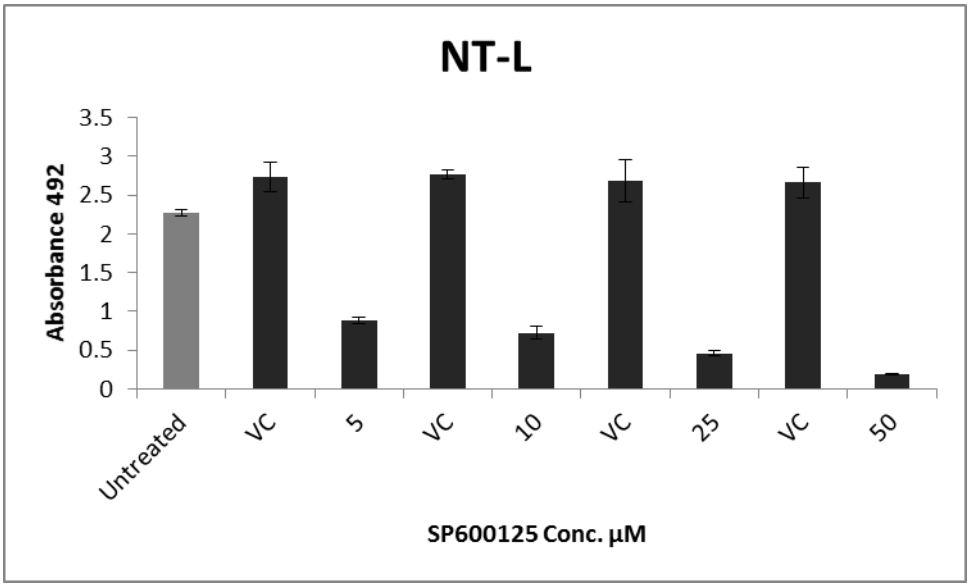

b.

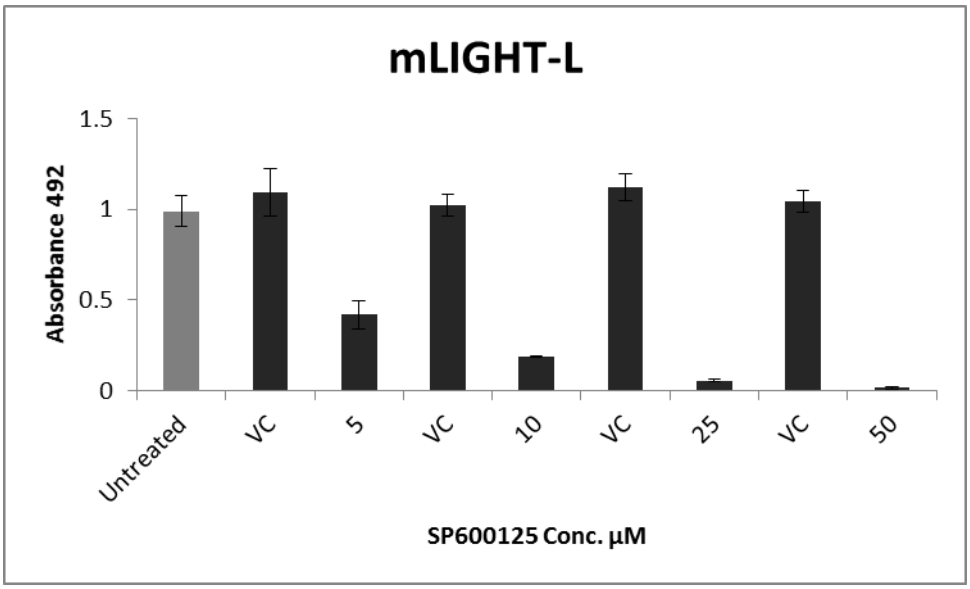

c.

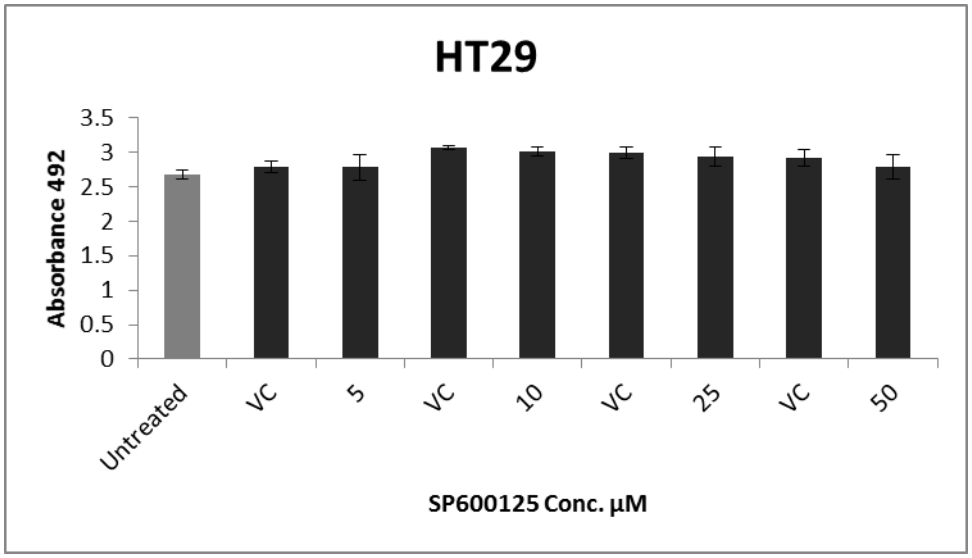
HT29
Absorbance 492
3.5
3
2.5
2
1.5
1
0.5
0
Untreated
VC
5
VC
10
VC
25
VC
50
SP600125 Conc. µM

d.

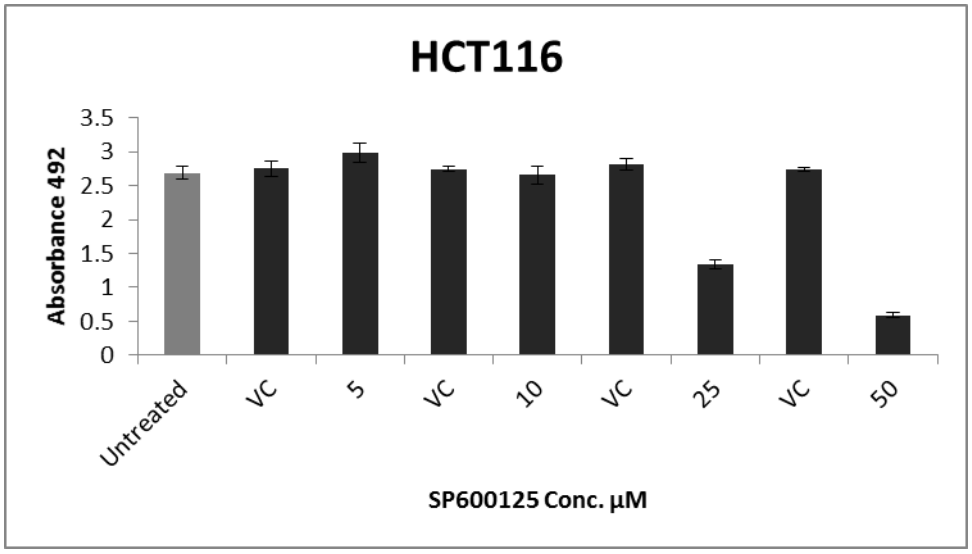
HCT116
Absorbance 492
3.5
3
2.5
2
1.5
1
0.5
0
Untreated
VC
5
VC
10
VC
25
VC
50
SP600125 Conc. µM

e.

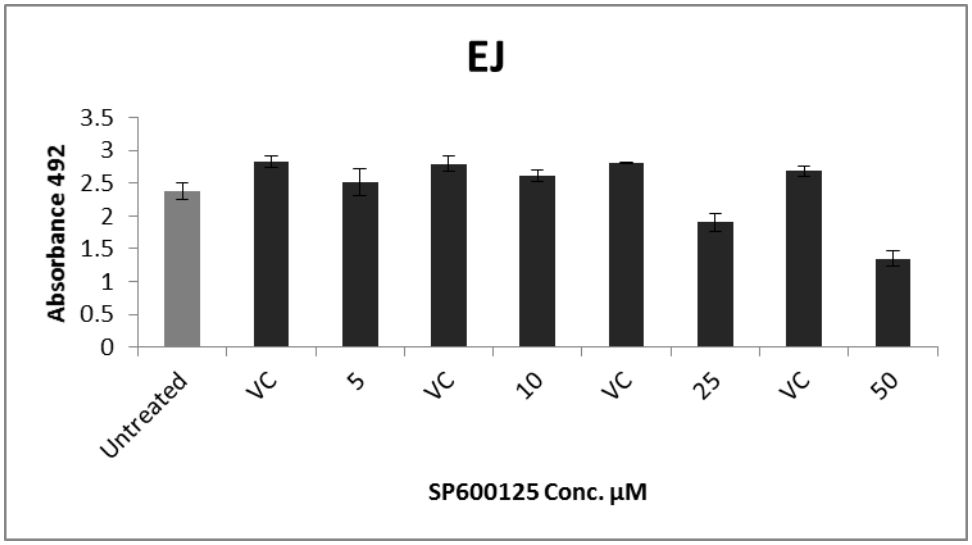

Effects of the JNK inhibitor (SP600125) on carcinoma cell viability

NT-L, mLIGHT-L, HT29, HCT116 and EJ were in 96-well plates. Cells were then treated with MAPKs inhibitors: JNK inhibitor (SP600125), as indicated, and vehicle control (VC) was also included. 20µl of MTS solution was added to each well and incubated for 4hrs. Cell viability was determined by a FLUOstar OPTIMA (BMG Labtech) plate reader at absorbance 492nm. Data are represented as mean values of 4-5 replicates ±S.D. a, b, c, d and e show NT-L, mLIGHT-L, HT29, HCT116 and EJ cells, respectively.

3. p38 inhibitor (SB202190)

a.

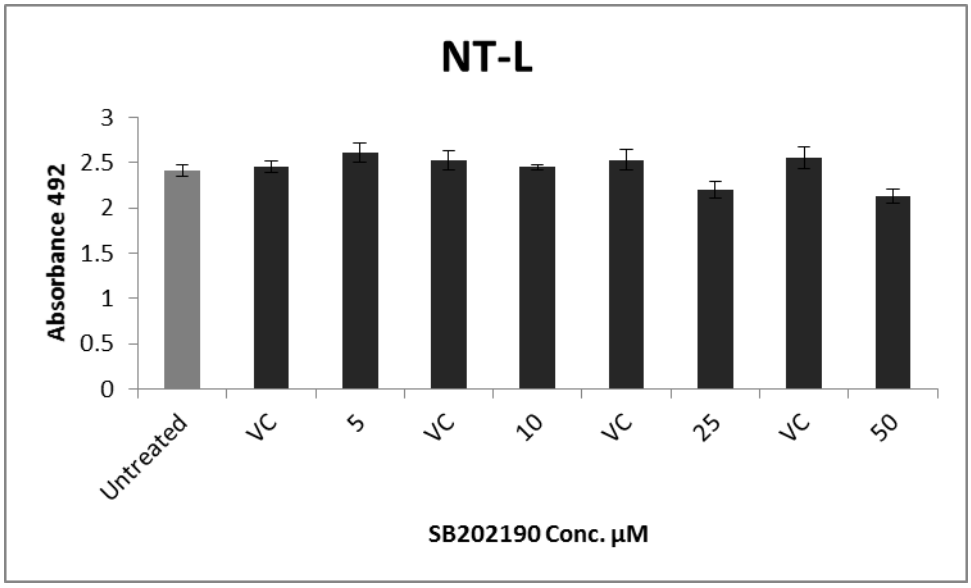

b.

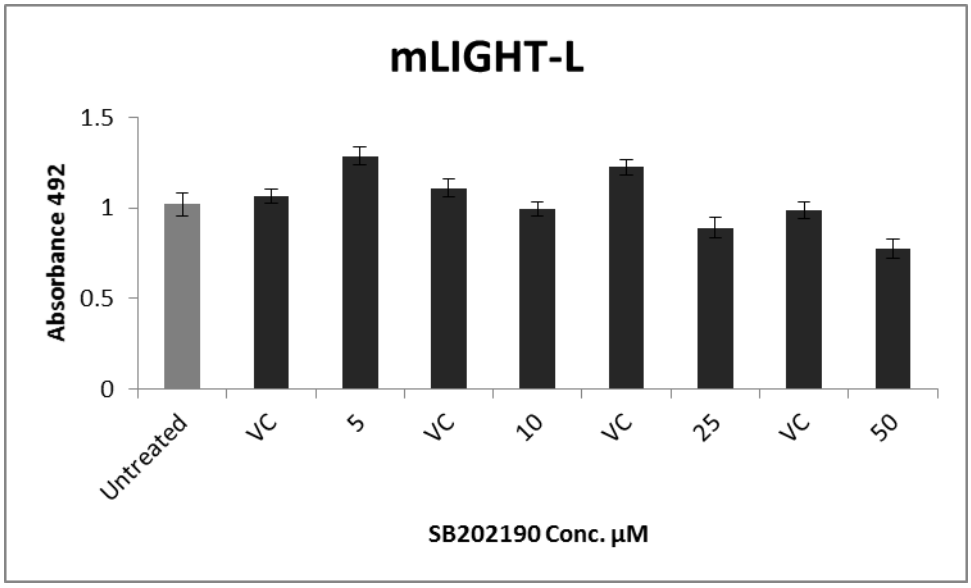

c.

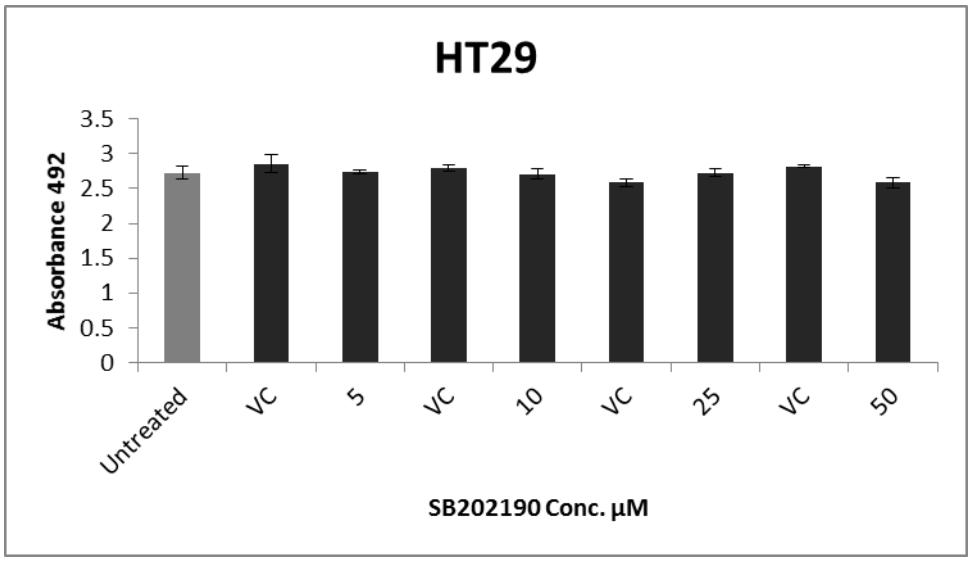
HT29
Absorbance 492
3.5
3
2.5
2
1.5
1
0.5
0
Untreated
VC
5
VC
10
VC
25
VC
50
SB202190 Conc. µM

d.

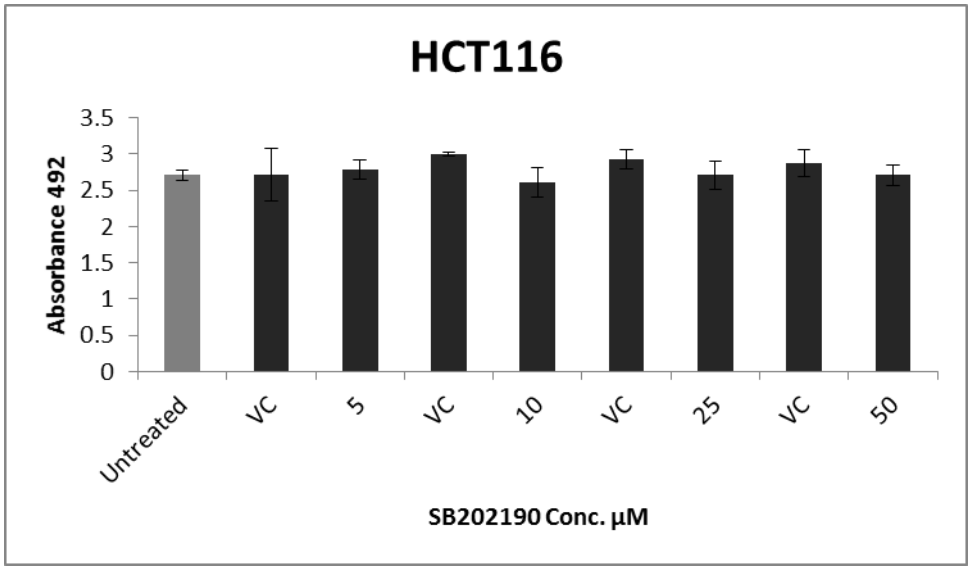
HCT116
Absorbance 492
3.5
3
2.5
2
1.5
1
0.5
0
Untreated
VC
5
VC
10
VC
25
VC
50
SB202190 Conc. µM

e.

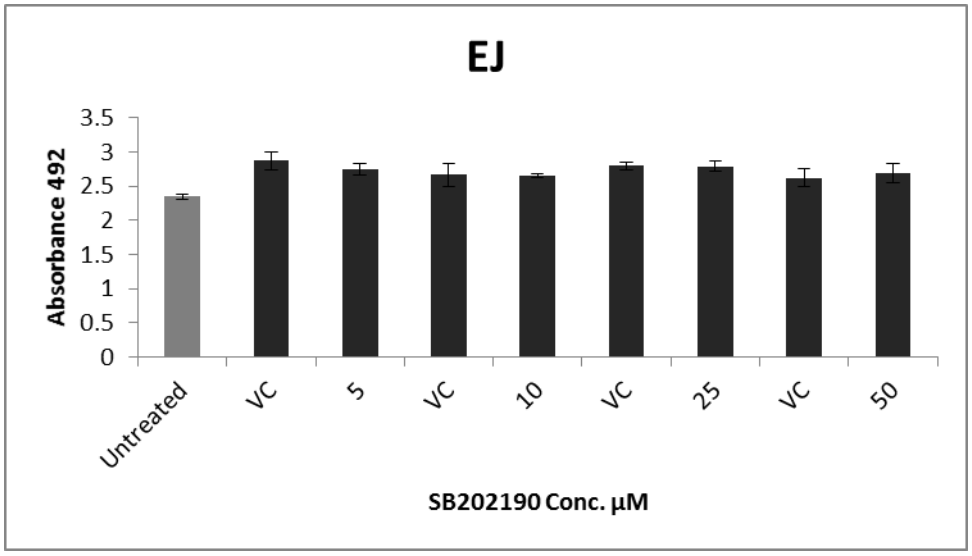

Effects of the p38 inhibitor (SB202190) on carcinoma cell viability

NT-L, mLIGHT-L, HT29, HCT116 and EJ were in 96-well plates. Cells were then treated with MAPKs inhibitors: p38 inhibitor (SB202190), as indicated, and vehicle control (VC) was also included. 20µl of MTS solution was added to each well and incubated for 4hrs. Cell viability was determined by a FLUOstar OPTIMA (BMG Labtech) plate reader at absorbance 492nm. Data are represented as mean values of 4-5 replicates ±S.D. a, b, c, d and e show NT-L, mLIGHT-L, HT29, HCT116 and EJ cells, respectively.

Appendix VI:

The antioxidant (NAC) titration

a.

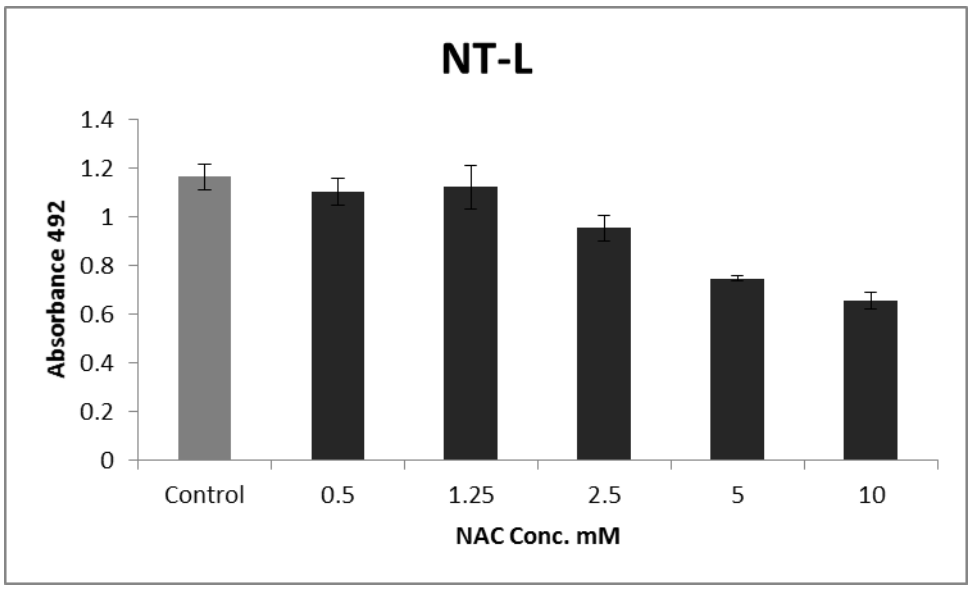

b.

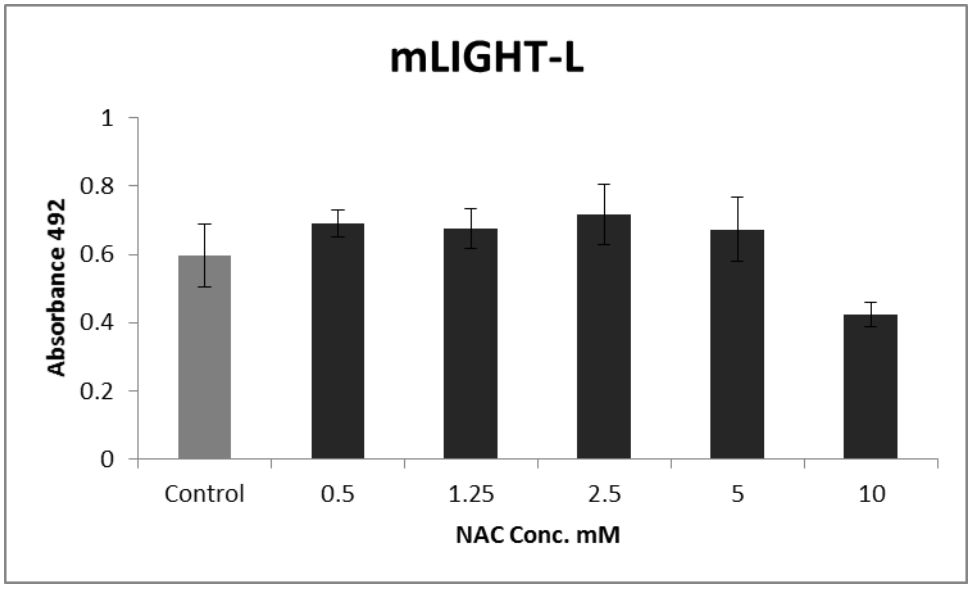

c.

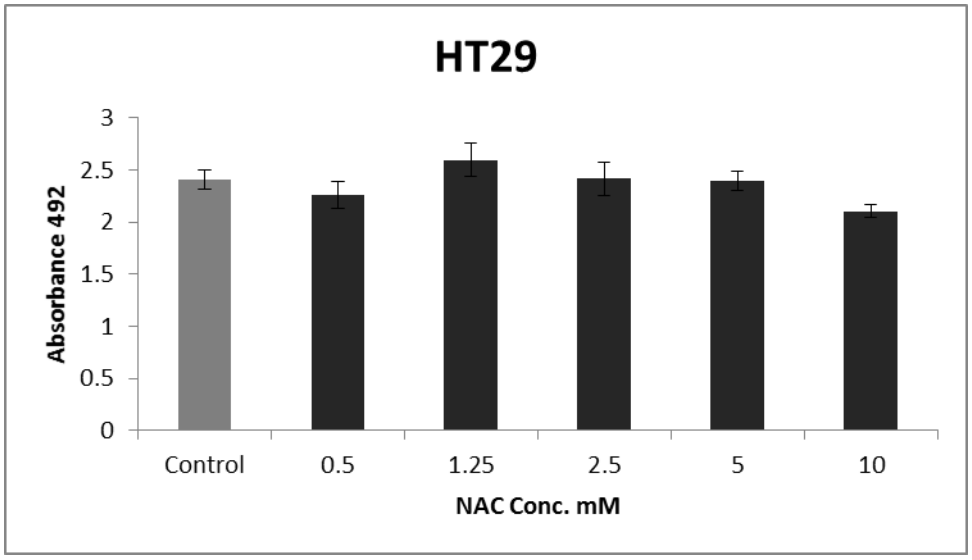
HT29
Absorbance 492
3
2.5
2
1.5
1
0.5
0
Control
0.5
1.25
2.5
5
10
NAC Conc. mM

d.

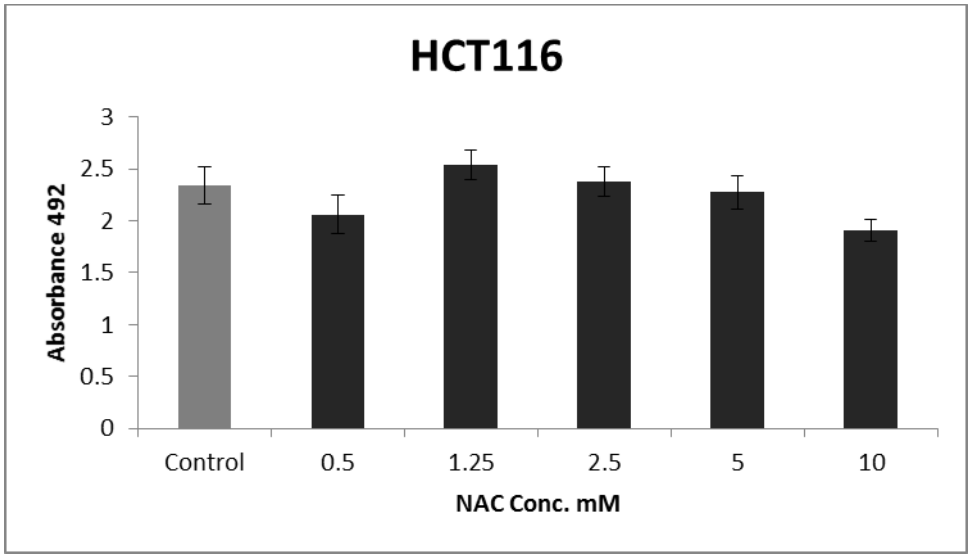
HCT116
Absorbance 492
3
2.5
2
1.5
1
0.5
0
Control
0.5
1.25
2.5
5
10
NAC Conc. mM

e.

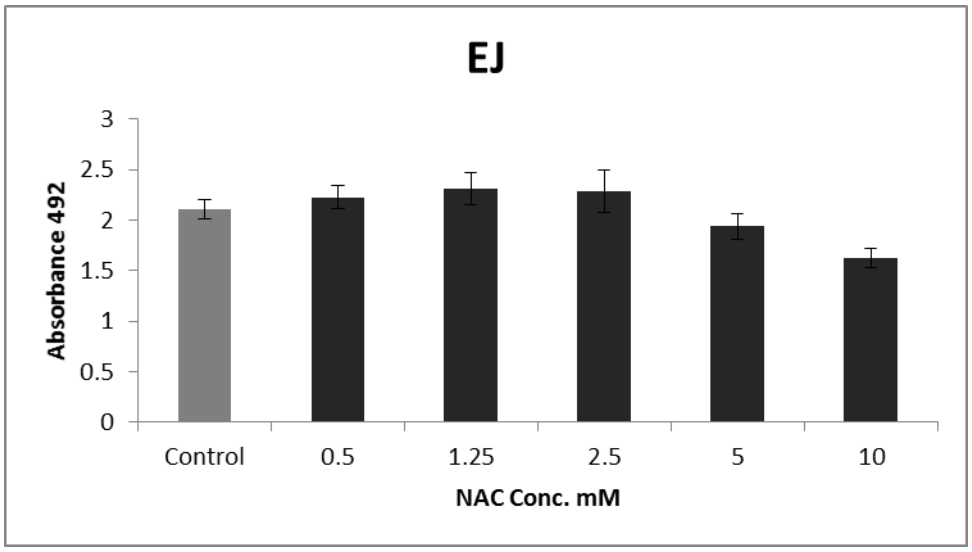

Effects of the antioxidant NAC on carcinoma cell viability

NT-L, mLIGHT-L, HT29, HCT116 and EJ were in 96-well plates. Cells were then treated with NAC as indicated. 20µl of MTS solution was added to each well and incubated for 4hrs. Cell viability was determined by a FLUOstar OPTIMA (BMG Labtech) plate reader at absorbance 492nm. Data are represented as mean values of 5-6 replicates ±S.D. a, b, c, d and e show NT-L, mLIGHT-L, HT29, HCT116 and EJ cells, respectively.

Appendix VII:

The NOX inhibitor (DPI) titration

a.

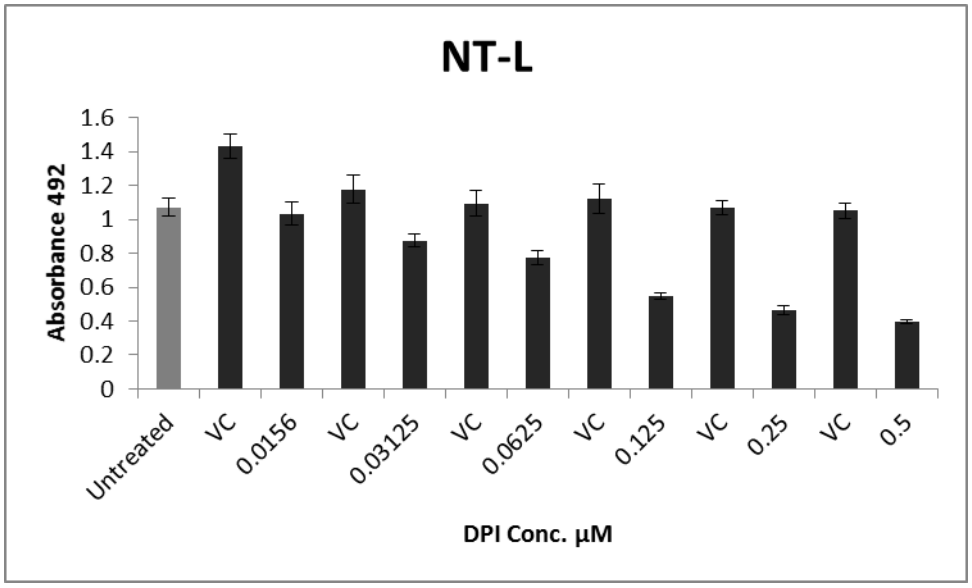

b.

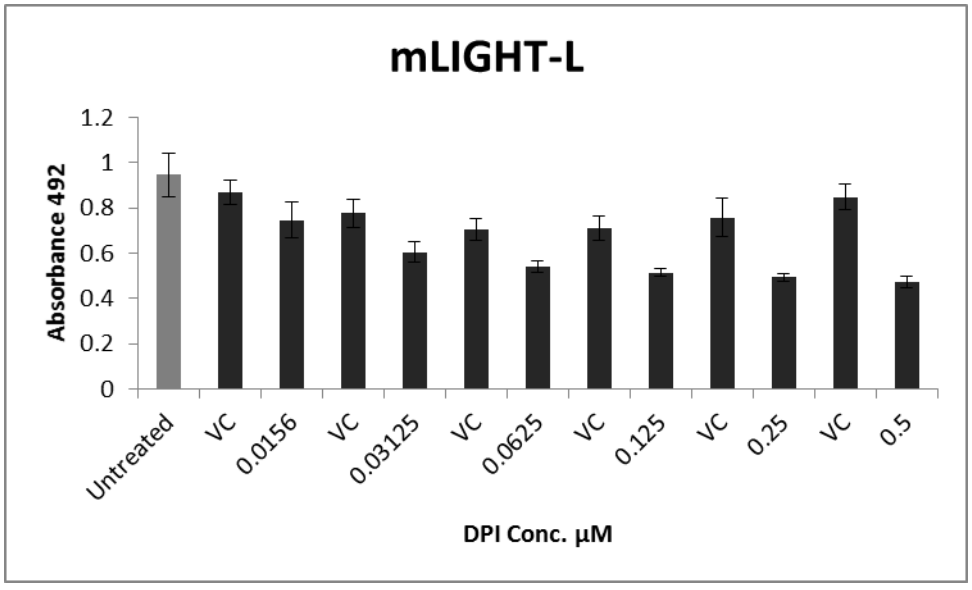

c.

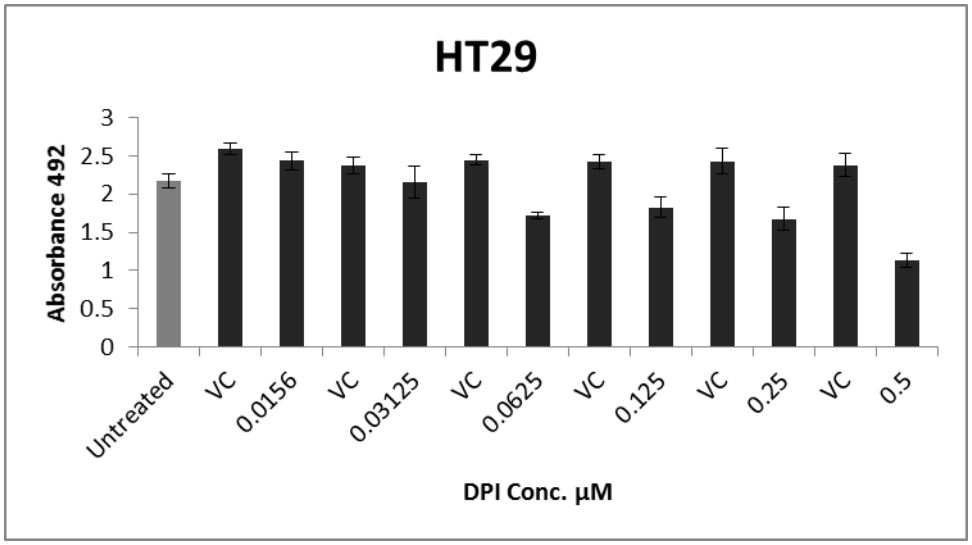
HT29
Absorbance 492
3
2.5
2
1.5
1
0.5
0
Untreated
VC
0.0156
VC
0.03125
VC
0.0625
VC
0.125
VC
0.25
VC
0.5
DPI Conc. µM

d.

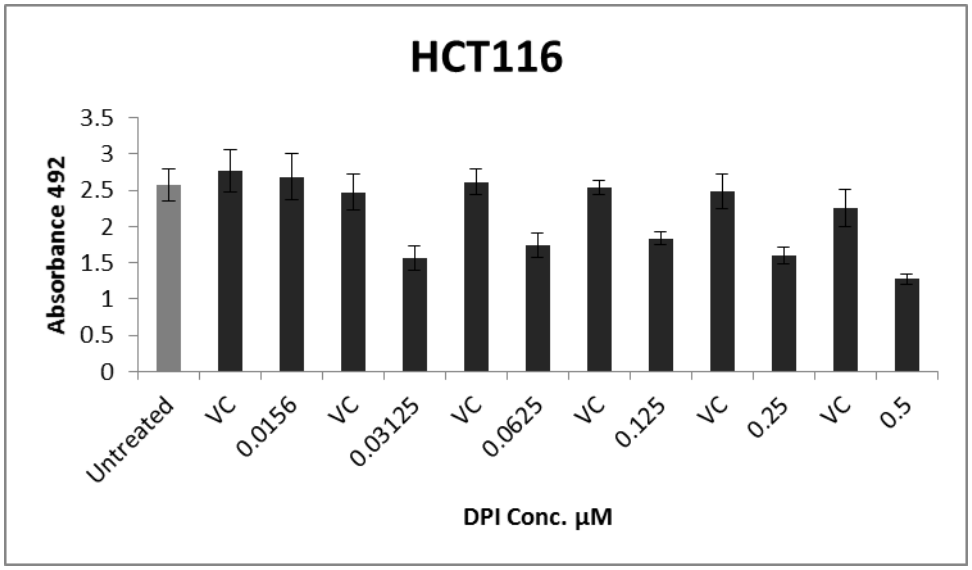
HCT116
Absorbance 492
3.5
3
2.5
2
1.5
1
0.5
0
Untreated
VC
0.0156
VC
0.03125
VC
0.0625
VC
0.125
VC
0.25
VC
0.5
DPI Conc. µM

e.

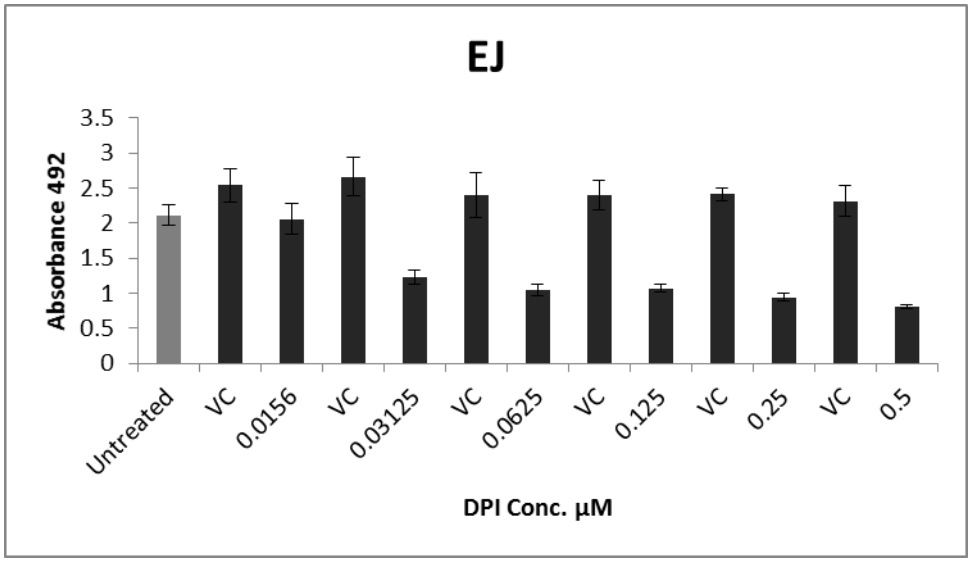

Effects of DPI on carcinoma cell viability

NT-L, mLIGHT-L, HT29, HCT116 and EJ were in 96-well plates. Cells were then treated with NOX inhibitor (DPI), as indicated, and vehicle control (VC) was also included. 20µl of MTS solution was added to each well and incubated for 4hrs. Cell viability was determined by a FLUOstar OPTIMA (BMG Labtech) plate reader at absorbance 492nm. Data are represented as mean values of 5-6 replicates ±S.D. a, b, c, d and e show NT-L, mLIGHT-L, HT29, HCT116 and EJ cells, respectively.

References

Abreu-Martin, M. T., Vidrich, A., Lynch, D. H., Targan, S. R., 1995. Divergent induction of apoptosis and IL-8 secretion in HT-29 cells in response to TNF-alpha and ligation of Fas antigen. The Journal of Immunology 155, 4147-4154.

Afford, S. C., Ahmed-choudhury, J., Randhawa, S., Russell, C., Youster, J., Crosby, H. A., Eliopoulos, A., Hubscher, S. G., Young, L. S., Adams, D. H., 2001. CD40 activation-induced, Fas-dependent apoptosis and NF-κB/AP-1 signaling in human intrahepatic biliary epithelial cells. The FASEB Journal 15, 2345-2354.

Agathanggelou, A., Niedobitek, G., Chen, R., Nicholls, J., Yin, W., Young, L. S., 1995. Expression of immune regulatory molecules in Epstein-Barr virus-associated nasopharyngeal carcinomas with prominent lymphoid stroma. Evidence for a functional interaction between epithelial tumor cells and infiltrating lymphoid cells. The American journal of pathology 147, 1152.

Aggarwal, B. B., 2000. Tumour necrosis factors receptor associated signalling molecules and their role in activation of apoptosis, JNK and NF-kappa B. Annals of the Rheumatic Diseases 59, 6-16.

Aggarwal, B. B., 2004. Nuclear factor-κB: the enemy within. Cancer cell 6, 203-208.

Aizawa, S., Nakano, H., Ishida, T., Horie, R., Nagai, M., Ito, K., Yagita, H., Okumura, K., Inoue, J., Watanabe, T., 1997. Tumor necrosis factor receptor-associated factor (TRAF) 5 and TRAF2 are involved in CD30-mediated NFκB activation. Journal of Biological Chemistry 272, 2042-2045.

Akiba, H., Nakano, H., Nishinaka, S., Shindo, M., Kobata, T., Atsuta, M., Morimoto, C., Ware, C. F., Malinin, N. L., Wallach, D., 1998. CD27, a member of the tumor necrosis factor receptor superfamily, activates NF-κB and stress-activated protein kinase/c-Jun N-terminal kinase via TRAF2, TRAF5, and NF-κB-inducing kinase. Journal of Biological Chemistry 273, 13353-13358.

Albarbar, B., Dunnill, C., Georgopoulos, N. T., 2015. Regulation of cell fate by Lymphotoxin (LT) receptor signalling: Functional differences and similarities of the LT system to other TNF superfamily (TNFSF) members. Cytokine & Growth Factor Reviews.

Albert, M. L., 2004. Death-defying immunity: do apoptotic cells influence antigen processing and presentation? Nature Reviews Immunology 4, 223-231.

Aldinucci, D., Poletto, D., Nanni, P., Degan, M., Rupolo, M., Pinto, A., Gattei, V., 2002. CD40L induces proliferation, self-renewal, rescue from apoptosis, and production of cytokines by CD40-expressing AML blasts. Experimental hematology 30, 1283-1292.

Alimonti, J. B., Shi, L., Baijal, P. K., Greenberg, A. H., 2001. Granzyme B induces BID-mediated cytochrome c release and mitochondrial permeability transition. Journal of Biological Chemistry 276, 6974-6982.

Altenburg, A., Baldus, S. E., Smola, H., Pfister, H., Hess, S., 1999. CD40 ligand-CD40 interaction induces chemokines in cervical carcinoma cells in synergism with IFN-γ. The Journal of Immunology 162, 4140-4147.

Ambrosone, C. B., 2000. Oxidants and antioxidants in breast cancer. Antioxidants & redox signaling 2, 903-917.

Andera, L., 2009. Signaling activated by the death receptors of the TNFR family. Biomedical Papers-Olomouc 153, 173-180.

Androlewicz, M. J., Browning, J. L., Ware, C. F., 1992. Lymphotoxin is expressed as a heteromeric complex with a distinct 33-KDa glycoprotein on the surface of an activated human T-cell hybridoma. Journal of Biological Chemistry 267, 2542-2547.

Arch, R. H., Gedrich, R. W., Thompson, C. B., 1998. Tumor necrosis factor receptor-associated factors (TRAFs)—a family of adapter proteins that regulates life and death. Genes & development 12, 2821-2830.

Ardestani, S., Deskins, D. L., Young, P. P., 2013a. Membrane TNF-alpha-activated programmed necrosis is mediated by Ceramide-induced reactive oxygen species. Journal of molecular signaling 8, 12.

Ardestani, S., Li, B., Deskins, D. L., Wu, H., Massion, P. P., Young, P. P., 2013b. Membrane versus soluble isoforms of TNF-α exert opposing effects on tumor growth and survival of tumor-associated myeloid cells. Cancer research 73, 3938-3950.

Armitage, R. J., 1994. Tumor necrosis factor receptor superfamily members and their ligands. Curr Opin Immunol 6, 407-13.

Aruffo, A., Farrington, M., Hollenbaugh, D., Li, X., Milatovich, A., Nonoyama, S., Bajorath, J., Grosmaire, L. S., Stenkamp, R., Neubauer, M., 1993. The CD40 ligand, gp39, is defective in activated T cells from patients with X-linked hyper-IgM syndrome. Cell 72, 291-300.

Arur, S., Uche, U. E., Rezaul, K., Fong, M., Scranton, V., Cowan, A. E., Mohler, W., Han, D. K., 2003. Annexin I is an endogenous ligand that mediates apoptotic cell engulfment. Developmental Cell 4, 587-598, doi:10.1016/s1534-5807(03)00090-x.

Asao, H., Fu, X.-Y., 2000. Interferon-γ has dual potentials in inhibiting or promoting cell proliferation. Journal of Biological Chemistry 275, 867-874.

Ashkenazi, A., 2002. Targeting death and decoy receptors of the tumour-necrosis factor superfamily. Nature Reviews Cancer 2, 420-430.

Ashkenazi, A., Dixit, V. M., 1998. Death receptors: Signaling and modulation. Science 281, 1305-1308, doi:10.1126/science.281.5381.1305.

Baehrecke, E. H., 2002. How death shapes life during development. Nature Reviews Molecular Cell Biology 3, 779-787.

Baker, A., Payne, C. M., Briehl, M. M., Powis, G., 1997. Thioredoxin, a gene found overexpressed in human cancer, inhibits apoptosis in vitro and in vivo. Cancer Research 57, 5162-5167.

Baldin, V., Lukas, J., Marcote, M., Pagano, M., Draetta, G., 1993. Cyclin D1 is a nuclear protein required for cell cycle progression in G1. Genes & development 7, 812-821.

Baldwin Jr, A. S., 1996. The NF-κB and IκB proteins: new discoveries and insights. Annual review of immunology 14, 649-681.

Banner, D. W., Darcy, A., Janes, W., Gentz, R., Schoenfeld, H. J., Broger, C., Loetscher, H., Lesslauer, W., 1993. Crystal-structure of the soluble human 55 kd tnf receptor-human tnf-beta complex - implications for tnf receptor activation. Cell 73, 431-445, doi:10.1016/0092-8674(93)90132-a.

Basak, S., Kim, H., Kearns, J. D., Tergaonkar, V., O'Dea, E., Werner, S. L., Benedict, C. A., Ware, C. F., Ghosh, G., Verma, I. M., 2007. A fourth IκB protein within the NF-κB signaling module. Cell 128, 369-381.

Bechill, J., Muller, W. J., 2014. Herpesvirus entry mediator (HVEM) attenuates signals mediated by the lymphotoxin β receptor (LTβR) in human cells stimulated by the shared ligand LIGHT. Molecular immunology 62, 96-103.

Belperio, J. A., Keane, M. P., Arenberg, D. A., Addison, C. L., Ehlert, J. E., Burdick, M. D., Strieter, R. M., 2000. CXC chemokines in angiogenesis. Journal of leukocyte biology 68, 1-8.

Ben-Levy, R., Hooper, S., Wilson, R., Paterson, H. F., Marshall, C. J., 1998. Nuclear export of the stress-activated protein kinase p38 mediated by its substrate MAPKAP kinase-2. Current Biology 8, 1049-1057.

Beresford, P. J., Xia, Z., Greenberg, A. H., Lieberman, J., 1999. Granzyme A loading induces rapid cytolysis and a novel form of DNA damage independently of caspase activation. Immunity 10, 585-595.

Beutler, B., Cerami, A., 1989. The biology of cachectin/TNF--a primary mediator of the host response. Annual review of immunology 7, 625-655.

Bhogal, R. H., Weston, C. J., Curbishley, S. M., Adams, D. H., Afford, S. C., 2012. Activation of CD40 with platelet derived CD154 promotes reactive oxygen species dependent death of human hepatocytes during hypoxia and reoxygenation. PloS one 7, e30867.

Bishop, G. A., 2004. The multifaceted roles of TRAFs in the regulation of B-cell function. Nature Reviews Immunology 4, 775-786.

Bishop, G. A., Moore, C. R., Xie, P., Stunz, L. L., Kraus, Z. J., 2007. TRAF proteins in CD40 signaling. TNF Receptor Associated Factors (TRAFs). Springer, pp. 131-151.

Bista, P., Zeng, W., Ryan, S., Bailly, V., Browning, J. L., Lukashev, M. E., 2010. TRAF3 controls activation of the canonical and alternative NFκB by the lymphotoxin beta receptor. Journal of Biological Chemistry 285, 12971-12978.

Biswas, S., Chida, A. S., Rahman, I., 2006. Redox modifications of protein–thiols: emerging roles in cell signaling. Biochemical pharmacology 71, 551-564.

Black, R., Doedens, J., Mahimkar, R., Johnson, R., Guo, L., Wallace, A., Virca, D., Eisenman, J., Slack, J., Castner, B., 2002. Substrate specificity and inducibility of TACE (tumour necrosis factor alpha-converting enzyme) revisited: the Ala-Val preference, and induced intrinsic activity. Biochemical Society symposium, pp. 39-52.

Black, R. A., Rauch, C. T., Kozlosky, C. J., Peschon, J. J., Slack, J. L., Wolfson, M. F., Castner, B. J., Stocking, K. L., Reddy, P., Srinivasan, S., Nelson, N., Boiani, N., Schooley, K. A., Gerhart, M., Davis, R., Fitzner, J. N., Johnson, R. S., Paxton, R. J., March, C. J., Cerretti, D. P., 1997. A metalloproteinase disintegrin that releases tumour-necrosis factor-alpha from cells. Nature 385, 729-733, doi:10.1038/385729a0.

Bodmer, J.-L., Schneider, P., Tschopp, J., 2002. The molecular architecture of the TNF superfamily. Trends in biochemical sciences 27, 19-26.

Bodmer, J.-L., Burns, K., Schneider, P., Hofmann, K., Steiner, V., Thome, M., Bornand, T., Hahne, M., Schröter, M., Becker, K., 1997. TRAMP, a novel apoptosis-mediating receptor with sequence homology to tumor necrosis factor receptor 1 and Fas (Apo-1/CD95). Immunity 6, 79-88.

Boldin, M. P., Goncharov, T. M., Goltseve, Y. V., Wallach, D., 1996. Involvement of MACH, a novel MORT1/FADD-interacting protease, in Fas/APO-1-and TNF receptor–induced cell death. Cell 85, 803-815.

Bonizzi, G., Karin, M., 2004. The two NF-kappa B activation pathways and their role in innate and adaptive immunity. Trends Immunol 25, 280-288, doi:10.1016/j.it.2004.03.008.

Bourgeois, C., Rocha, B., Tanchot, C., 2002. A role for CD40 expression on CD8+ T cells in the generation of CD8+ T cell memory. Science 297, 2060-2063.

Boyle, W. J., Simonet, W. S., Lacey, D. L., 2003. Osteoclast differentiation and activation. Nature 423, 337-342.

Bradley, J. R., Pober, J. S., 2001. Tumor necrosis factor receptor-associated factors (TRAFs). Oncogene 20, 6482-91.

Bratton, D. L., Fadok, V. A., Richter, D. A., Kailey, J. M., Guthrie, L. A., Henson, P. M., 1997. Appearance of phosphatidylserine on apoptotic cells requires calcium-mediated nonspecific flip-flop and is enhanced by loss of the aminophospholipid translocase. Journal of Biological Chemistry 272, 26159-26165, doi:10.1074/jbc.272.42.26159.

Bromberg, J. F., Horvath, C. M., Wen, Z., Schreiber, R. D., Darnell, J. E., 1996. Transcriptionally active Stat1 is required for the antiproliferative effects of both interferon alpha and interferon gamma. Proceedings of the National Academy of Sciences 93, 7673-7678.

Brown, K. D., Hostager, B. S., Bishop, G. A., 2002. Regulation of TRAF2 signaling by self-induced degradation. Journal of Biological Chemistry 277, 19433-19438.

Browning, J. L., Androlewicz, M. J., Ware, C. F., 1991. Lymphotoxin and an associated 33-kDa glycoprotein are expressed on the surface of an activated human T cell hybridoma. The Journal of Immunology 147, 1230-1237.

Browning, J. L., Miatkowski, K., Sizing, I., Griffiths, D., Zafari, M., Benjamin, C. D., Meier, W., Mackay, F., 1996. Signaling through the lymphotoxin beta receptor induces the death of some adenocarcinoma tumor lines. Journal of Experimental Medicine 183, 867-878, doi:10.1084/jem.183.3.867.

Browning, J. L., Ngamek, A., Lawton, P., Demarinis, J., Tizard, R., Chow, E. P. C., Hession, C., Obrinegreco, B., Foley, S. F., Ware, C. F., 1993. Lymphotoxin-beta, a novel member of the tnf family that forms a heteromeric complex with lymphotoxin on the cell-surface. Cell 72, 847-856, doi:10.1016/0092-8674(93)90574-a.

Browning, J. L., Dougas, I., Ngamek, A., Bourdon, P. R., Ehrenfels, B. N., Miatkowski, K., Zafari, M., Yampaglia, A. M., Lawton, P., Meier, W., Benjamin, C. P., Hession, C., 1995. Characterization of surface lymphotoxin forms - use of specific monoclonal-antibodies and soluble receptors. Journal of Immunology 154, 33-46.

Browning, J. L., Sizing, I. D., Lawton, P., Bourdon, P. R., Rennert, P. D., Majeau, G. R., Ambrose, C. M., Hession, C., Miatkowski, K., Griffiths, D. A., Ngamek, A., Meier, W., Benjamin, C. D., Hochman, P. S., 1997. Characterization of lymphotoxin-alpha beta complexes on the surface of mouse lymphocytes. Journal of Immunology 159, 3288-3298.

Bugajska, U., Georgopoulos, N. T., Southgate, J., Johnson, P. W., Graber, P., Gordon, J., Selby, P. J., Trejdosiewicz, L. K., 2002. The effects of malignant transformation on susceptibility of human urothelial cells to CD40-mediated apoptosis. Journal of the National Cancer Institute 94, 1381-1395.

Bush, T. J. V., Bishop, G. A., 2008. TLR7 and CD40 cooperate in IL-6 production via enhanced JNK and AP-1 activation. European journal of immunology 38, 400-409.

Cabal-Hierro, L., Lazo, P. S., 2012. Signal transduction by tumor necrosis factor receptors. Cellular signalling 24, 1297-1305.

Cabal-Hierro, L., Rodríguez, M., Artime, N., Iglesias, J., Ugarte, L., Prado, M. A., Lazo, P. S., 2014. TRAF-mediated modulation of NF-kB AND JNK Activation by TNFR2. Cellular signalling 26, 2658-2666.

Cagnoni, F., Oddera, S., Giron-Michel, J., Riccio, A. M., Olsson, S., Dellacasa, P., Melioli, G., Canonica, G. W., Azzarone, B., 2004. CD40 on adult human airway epithelial cells: expression and proinflammatory effects. J Immunol 172, 3205-14.

Cai, G., Anumanthan, A., Brown, J. A., Greenfield, E. A., Zhu, B., Freeman, G. J., 2008. CD160 inhibits activation of human CD4(+) T cells through interaction with herpesvirus entry mediator. Nat Immunol 9, 176-185, doi:10.1038/ni1554.

Cain, K., Brown, D. G., Langlais, C., Cohen, G. M., 1999. Caspase activation involves the formation of the aposome, a large (~ 700 kDa) caspase-activating complex. Journal of Biological Chemistry 274, 22686-22692.

Cain, K., Bratton, S. B., Langlais, C., Walker, G., Brown, D. G., Sun, X.-M., Cohen, G. M., 2000. Apaf-1 oligomerizes into biologically active~ 700-kDa and inactive~ 1.4-MDa apoptosome complexes. Journal of Biological Chemistry 275, 6067-6070.

Camerini, D., Walz, G., Loenen, W. A. M., Borst, J., Seed, B., 1991. The T-cell activation antigen CD27 is a member of the nerve growth-factor tumor-necrosis-factor receptor gene family. Journal of Immunology 147, 3165-3169.

Campbell, S. L., Khosravi-Far, R., Rossman, K. L., Clark, G. J., Der, C. J., 1998. Increasing complexity of Ras signaling. Oncogene 17, 1395-1413.

Cao, Z., Xiong, J., Takeuchi, M., Kurama, T., Goeddel, D. V., 1996. TRAF6 is a signal transducer for interleukin-1. Nature 383, 443-446.

Cargnello, M., Roux, P. P., 2011. Activation and function of the MAPKs and their substrates, the MAPK-activated protein kinases. Microbiology and Molecular Biology Reviews 75, 50-83.

Cassatella, M., Bazzoni, F., Flynn, R. M., Dusi, S., Trinchieri, G., Rossi, F., 1990. Molecular basis of interferon-gamma and lipopolysaccharide enhancement of phagocyte respiratory

burst capability. Studies on the gene expression of several NADPH oxidase components. Journal of Biological Chemistry 265, 20241-20246.
Cavigelli, M., Dolfi, F., Claret, F.-X., Karin, M., 1995. Induction of c-fos expression through JNK-mediated TCF/Elk-1 phosphorylation. The EMBO Journal 14, 5957.
Chan, F. K.-M., 2000. The pre-ligand binding assembly domain: a potential target of inhibition of tumour necrosis factor receptor function. Annals of the rheumatic diseases 59, i50-i53.
Chan, F. K.-M., 2007. Three is better than one: Pre-ligand receptor assembly in the regulation of TNF receptor signaling. Cytokine 37, 101-107, doi:10.1016/j.cyto.2007.03.005.
Chan, F. K.-M., Chun, H. J., Zheng, L., Siegel, R. M., Bui, K. L., Lenardo, M. J., 2000. A domain in TNF receptors that mediates ligand-independent receptor assembly and signaling. Science 288, 2351-2354.
Chang, H. Y., Nishitoh, H., Yang, X., Ichijo, H., Baltimore, D., 1998. Activation of apoptosis signal-regulating kinase 1 (ASK1) by the adapter protein Daxx. Science 281, 1860-1863.
Chang, L., Karin, M., 2001. Mammalian MAP kinase signalling cascades. Nature 410, 37-40.
Chang, Y.-H., Hsieh, S.-L., Chen, M.-C., Lin, W.-W., 2002. Lymphotoxin β receptor induces interleukin 8 gene expression via NF-κB and AP-1 activation. Experimental cell research 278, 166-174.
Chang, Y. H., Chao, Y., Hsieh, S. L., Lin, W. W., 2004. Mechanism of LIGHT/Interferon-gamma-induced cell death in HT-29 cells. J Cell Biochem 93, 1188-1202, doi:10.1002/jcb.20282.
Chaudhary, P. M., Eby, M., Jasmin, A., Bookwalter, A., Murray, J., Hood, L., 1997. Death receptor 5, a new member of the TNFR family, and DR4 induce FADD-dependent apoptosis and activate the NF-κB pathway. Immunity 7, 821-830.
Chen, M.-C., Hsu, T.-L., Luh, T.-Y., Hsieh, S.-L., 2000. Overexpression of Bcl-2 enhances LIGHT-and interferon-γ-mediated apoptosis in Hep3BT2 cells. Journal of Biological Chemistry 275, 38794-38801.
Chen, M. C., Hwang, M. J., Chou, Y. C., Chen, W. H., Cheng, G., Nakano, H., Luh, T. Y., Mai, S. C., Hsieh, S. L., 2003. The role of apoptosis signal-regulating kinase 1 in lymphotoxin-beta receptor-mediated cell death. J Biol Chem 278, 16073-81.
Chen, Z., Gibson, T. B., Robinson, F., Silvestro, L., Pearson, G., Xu, B.-e., Wright, A., Vanderbilt, C., Cobb, M. H., 2001. MAP kinases. Chemical reviews 101, 2449-2476.
Chen, Z., Seimiya, H., Naito, M., Mashima, T., Kizaki, A., Dan, S., Imaizumi, M., Ichijo, H., Miyazono, K., Tsuruo, T., 1999. ASK1 mediates apoptotic cell death induced by genotoxic stress. Oncogene 18, 173-180.
Cheng, E., Wei, M. C., Weiler, S., Flavell, R. A., Mak, T. W., Lindsten, T., Korsmeyer, S. J., 2001. BCL-2, BCL-X-L sequester BH3 domain-only molecules preventing BAX- and BAK-mediated mitochondrial apoptosis. Mol Cell 8, 705-711, doi:10.1016/s1097-2765(01)00320-3.
Cheng, G., Cleary, A. M., Ye, Z.-S., Hong, D. I., Lederman, S., Baltimore, D., 1995. Involvement of CRAF1, a relative of TRAF, in CD40 signaling. Science 267, 1494-1498.
Cheung, T. C., Humphreys, I. R., Potter, K. G., Norris, P. S., Shumway, H. M., Tran, B. R., Patterson, G., Jean-Jacques, R., Yoon, M., Spear, P. G., 2005. Evolutionarily divergent herpesviruses modulate T cell activation by targeting the herpesvirus entry mediator cosignaling pathway. Proceedings of the National Academy of Sciences of the United States of America 102, 13218-13223.
Chin, Y. E., Kitagawa, M., Kuida, K., Flavell, R. A., Fu, X.-Y., 1997. Activation of the STAT signaling pathway can cause expression of caspase 1 and apoptosis. Molecular and Cellular Biology 17, 5328-5337.
Chinnaiyan, A. M., 1999. The apoptosome: Heart and soul of the cell death machine. Neoplasia (New York) 1, 5-15, doi:10.1038/sj.neo.7900003.

Chinnaiyan, A. M., O'Rourke, K., Tewari, M., Dixit, V. M., 1995. FADD, a novel death domain-containing protein, interacts with the death domain of Fas and initiates apoptosis. Cell 81, 505-512.

Chinnaiyan, A. M., O'Rourke, K., Yu, G.-L., Lyons, R. H., Garg, M., Duan, D. R., Xing, L., Gentz, R., Ni, J., Dixit, V. M., 1996. Signal transduction by DR3, a death domain-containing receptor related to TNFR-1 and CD95. Science 274, 990-992.

Chipuk, J., Bouchier-Hayes, L., Green, D., 2006. Mitochondrial outer membrane permeabilization during apoptosis: the innocent bystander scenario. Cell Death & Differentiation 13, 1396-1402.

Chipuk, J. E., Green, D. R., 2008. How do BCL-2 proteins induce mitochondrial outer membrane permeabilization? Trends in cell biology 18, 157-164.

Chong, H., Vikis, H. G., Guan, K.-L., 2003. Mechanisms of regulating the Raf kinase family. Cellular signalling 15, 463-469.

Choudhury, J. A., Russell, C. L., Randhawa, S., Young, L. S., Adams, D. H., Afford, S. C., 2003. Differential induction of nuclear factor-κB and activator protein-1 activity after CD40 ligation is associated with primary human hepatocyte apoptosis or intrahepatic endothelial cell proliferation. Molecular biology of the cell 14, 1334-1345.

Chung, J. Y., Park, Y. C., Ye, H., Wu, H., 2002. All TRAFs are not created equal: common and distinct molecular mechanisms of TRAF-mediated signal transduction. J Cell Sci 115, 679-88.

Cohen, G. M., 1997. Caspases: the executioners of apoptosis. Biochemical Journal 326, 1-16.

Collette, Y., Gilles, A., Pontarotti, P., Olive, D., 2003. A co-evolution perspective of the TNFSF and TNFRSF families in the immune system. Trends Immunol 24, 387-394, doi:10.1016/s1471-4906(03)00166-2.

Collins, T. S., Lee, L.-F., Ting, J. P.-Y., 2000. Paclitaxel up-regulates interleukin-8 synthesis in human lung carcinoma through an NF-κB-and AP-1-dependent mechanism. Cancer Immunology, Immunotherapy 49, 78-84.

Colombini, M., 2004. VDAC: the channel at the interface between mitochondria and the cytosol. Molecular and cellular biochemistry 256, 107-115.

Compaan, D. M., Gonzalez, L. C., Tom, I., Loyet, K. M., Eaton, D., Hymowitz, S. G., 2005. Attenuating lymphocyte activity - The crystal structure of the BTLA-HVEM complex. Journal of Biological Chemistry 280, 39553-39561, doi:10.1074/jbc.M507629200.

Cooke, P. W., James, N. D., Ganesan, R., Wallace, M., Burton, A., Young, L. S., 1999. CD40 expression in bladder cancer. The Journal of pathology 188, 38-43.

Costello, R., Mallet, F., Barbarat, B., De Colella, J. S., Sainty, D., Sweet, R., Truneh, A., Olive, D., 2003. Stimulation of non-Hodgkin's lymphoma via HVEM: an alternate and safe way to increase Fas-induced apoptosis and improve tumor immunogenicity. Leukemia 17, 2500-2507.

Crallan, R., Georgopoulos, N. T., Southgate, J., 2006. Experimental models of human bladder carcinogenesis. Carcinogenesis 27, 374-381.

Croft, M., So, T., Duan, W., Soroosh, P., 2009. The significance of OX40 and OX40L to T-cell biology and immune disease. Immunological reviews 229, 173-191.

Crompton, M., 1999. The mitochondrial permeability transition pore and its role in cell death. Biochem. j 341, 233-249.

Crowe, P. D., Vanarsdale, T. L., Walter, B. N., Ware, C. F., Hession, C., Ehrenfels, B., Browning, J. L., Din, W. S., Goodwin, R. G., Smith, C. A., 1994. A lymphotoxin-beta-specific receptor. Science 264, 707-710, doi:10.1126/science.8171323.

Cuenda, A., Dorow, D., 1998. Differential activation of stress-activated protein kinase kinases SKK4/MKK7 and SKK1/MKK4 by the mixed-lineage kinase-2 and mitogen-activated protein kinase kinase (MKK) kinase-1. Biochem. J 333, 11-15.

Dadgostar, H., Cheng, G., 2000. Membrane localization of TRAF 3 enables JNK activation. Journal of Biological Chemistry 275, 2539-2544.
Dallman, C., Johnson, P., Packham, G., 2003. Differential regulation of cell survival by CD40. Apoptosis 8, 45-53.
Danese, S., de la Motte, C., Sturm, A., Vogel, J. D., West, G. A., Strong, S. A., Katz, J. A., Fiocchi, C., 2003. Platelets trigger a CD40-dependent inflammatory response in the microvasculature of inflammatory bowel disease patients. Gastroenterology 124, 1249-1264.
Darnay, B. G., Ni, J., Moore, P. A., Aggarwal, B. B., 1999. Activation of NF-κB by RANK Requires Tumor Necrosis Factor Receptor-associated Factor (TRAF) 6 and NF-κB-inducing Kinase IDENTIFICATION OF A NOVEL TRAF6 INTERACTION MOTIF. Journal of Biological Chemistry 274, 7724-7731.
Davies, C. C., Bem, D., Young, L. S., Eliopoulos, A. G., 2005a. NF-kappaB overrides the apoptotic program of TNF receptor 1 but not CD40 in carcinoma cells. Cell Signal 17, 729-38.
Davies, C. C., Mak, T. W., Young, L. S., Eliopoulos, A. G., 2005b. TRAF6 is required for TRAF2-dependent CD40 signal transduction in nonhemopoietic cells. Mol Cell Biol 25, 9806-19.
Davis, R., 1998. Signal transduction by the c-Jun N-terminal kinase. Biochemical Society symposium, Vol. 64, pp. 1-12.
Davis, R. J., 2000. Signal transduction by the JNK group of MAP kinases. Cell 103, 239-252.
De Marchi, U., Campello, S., Szabò, I., Tombola, F., Martinou, J.-C., Zoratti, M., 2004. Bax does not directly participate in the Ca2+-induced permeability transition of isolated mitochondria. Journal of Biological Chemistry 279, 37415-37422.
De Smaele, E., Zazzeroni, F., Papa, S., Nguyen, D. U., Jin, R., Jones, J., Cong, R., Franzoso, G., 2001. Induction of gadd45beta by NF-kappaB downregulates pro-apoptotic JNK signalling. Nature 414, 308-13.
de Vries, E. G., Gietema, J. A., de Jong, S., 2006. Tumor Necrosis Factor–Related Apoptosis-Inducing Ligand Pathway and Its Therapeutic Implications. Clinical cancer research 12, 2390-2393.
De Vries, N., De Flora, S., 1993. N-acetyl-l-cysteine. Journal of Cellular Biochemistry 53, 270-277.
De Zutter, G. S., Davis, R. J., 2001. Pro-apoptotic gene expression mediated by the p38 mitogen-activated protein kinase signal transduction pathway. Proceedings of the National Academy of Sciences 98, 6168-6173.
Dealtry, G. B., Naylor, M. S., Fiers, W., Balkwill, F. R., 1987. DNA fragmentation and cytotoxicity caused by tumor necrosis factor is enhanced by interferon-γ. European journal of immunology 17, 689-693.
Debatin, K.-M., Krammer, P. H., 2004. Death receptors in chemotherapy and cancer. Oncogene 23, 2950-2966.
Degenhardt, K., Mathew, R., Beaudoin, B., Bray, K., Anderson, D., Chen, G., Mukherjee, C., Shi, Y., Gélinas, C., Fan, Y., 2006. Autophagy promotes tumor cell survival and restricts necrosis, inflammation, and tumorigenesis. Cancer cell 10, 51-64.
Degli-Esposti, M. A., Dougall, W. C., Smolak, P. J., Waugh, J. Y., Smith, C. A., Goodwin, R. G., 1997a. The novel receptor TRAIL-R4 induces NF-κB and protects against TRAIL-mediated apoptosis, yet retains an incomplete death domain. Immunity 7, 813-820.
Degli-Esposti, M. A., Davis-Smith, T., Din, W. S., Smolak, P. J., Goodwin, R. G., Smith, C. A., 1997b. Activation of the lymphotoxin beta receptor by cross-linking induces chemokine production and growth arrest in A375 melanoma cells. The Journal of Immunology 158, 1756-1762.
Degli-Esposti, M. A., Smolak, P. J., Walczak, H., Waugh, J., Huang, C.-P., DuBose, R. F., Goodwin, R. G., Smith, C. A., 1997c. Cloning and characterization of TRAIL-R3, a novel

member of the emerging TRAIL receptor family. The Journal of experimental medicine 186, 1165-1170.
Degterev, A., Zhou, W., Maki, J. L., Yuan, J., 2014. Assays for Necroptosis and Activity of RIP Kinases. Regulated Cell Death Part B: Necroptotic, Autophagic and other Non-apoptotic Mechanisms 545, 1.
Degterev, A., Huang, Z., Boyce, M., Li, Y., Jagtap, P., Mizushima, N., Cuny, G. D., Mitchison, T. J., Moskowitz, M. A., Yuan, J., 2005. Chemical inhibitor of nonapoptotic cell death with therapeutic potential for ischemic brain injury. Nature chemical biology 1, 112-119.
Degterev, A., Hitomi, J., Germscheid, M., Ch'en, I. L., Korkina, O., Teng, X., Abbott, D., Cuny, G. D., Yuan, C., Wagner, G., 2008. Identification of RIP1 kinase as a specific cellular target of necrostatins. Nature chemical biology 4, 313-321.
Dempsey, P. W., Doyle, S. E., He, J. Q., Cheng, G., 2003. The signaling adaptors and pathways activated by TNF superfamily. Cytokine & growth factor reviews 14, 193-209.
Deng, Y., Ren, X., Yang, L., Lin, Y., Wu, X., 2003. A JNK-dependent pathway is required for TNFalpha-induced apoptosis. Cell 115, 61-70.
Deshaies, R. J., Joazeiro, C. A., 2009. RING domain E3 ubiquitin ligases. Annual review of biochemistry 78, 399-434.
Devary, Y., Rosette, C., DiDonato, J. A., Karin, M., 1993. NF-kappa B activation by ultraviolet light not dependent on a nuclear signal. Science 261, 1442-1445.
Deveraux, Q. L., Reed, T. C., 1999. IAP family proteins - suppressors of apoptosis. Genes Dev 13, 239-252, doi:10.1101/gad.13.3.239.
Devin, A., Lin, Y., Liu, Z. g., 2003. The role of the death-domain kinase RIP in tumour-necrosis-factor-induced activation of mitogen-activated protein kinases. EMBO reports 4, 623-627.
Dhanasekaran, D., Johnson, G., 2007. MAPKs: function, regulation, role in cancer and therapeutic targeting. Oncogene 26, 3097-3099.
Dhawan, P., Su, Y., Thu, Y. M., Yu, Y., Baugher, P., Ellis, D. L., Sobolik-Delmaire, T., Kelley, M., Cheung, T. C., Ware, C. F., 2008. The lymphotoxin-β receptor is an upstream activator of NF-κB-mediated transcription in melanoma cells. Journal of biological chemistry 283, 15399-15408.
Dickinson, B. C., Chang, C. J., 2011. Chemistry and biology of reactive oxygen species in signaling or stress responses. Nature chemical biology 7, 504-511.
Du, C., Fang, M., Li, Y., Li, L., Wang, X., 2000. Smac, a mitochondrial protein that promotes cytochrome c–dependent caspase activation by eliminating IAP inhibition. cell 102, 33-42.
Duff, J. L., Quinlan, K. L., Paxton, L. L., Naik, S. M., Caughman, S. W., 1997. Pervanadate Mimics IFNγ-Mediated Induction of ICAM-1 Expression via Activation of STAT Proteins. Journal of investigative dermatology 108.
Duhen, T., Pasero, C., Mallet, F., Barbarat, B., Olive, D., Costello, R. T., 2004. LIGHT costimulates CD40 triggering and induces immunoglobulin secretion; a novel key partner in T cell-dependent B cell terminal differentiation. European journal of immunology 34, 3534-3541.
Dunnill, C., Patton, T., Brennan, J., Barrett, J., Dryden, M., Cooke, J., Leaper, D., Georgopoulos, N. T., 2015. Reactive oxygen species (ROS) and wound healing: the functional role of ROS and emerging ROS-modulating technologies for augmentation of the healing process. International wound journal.
Dürkop, H., Latza, U., Himmelreich, P., Stein, H., 1995. Expression of the human OX40 (hOX40) antigen in normal and neoplastic tissues. British journal of haematology 91, 927-931.
Edwards, A. D., Chaussabel, D., Tomlinson, S., Schulz, O., Sher, A., e Sousa, C. R., 2003. Relationships among murine CD11chigh dendritic cell subsets as revealed by baseline gene expression patterns. The Journal of Immunology 171, 47-60.

Elbashir, S. M., Lendeckel, W., Tuschl, T., 2001a. RNA interference is mediated by 21-and 22-nucleotide RNAs. Genes & development 15, 188-200.
Elbashir, S. M., Harborth, J., Lendeckel, W., Yalcin, A., Weber, K., Tuschl, T., 2001b. Duplexes of 21-nucleotide RNAs mediate RNA interference in cultured mammalian cells. nature 411, 494-498.
Elgueta, R., Benson, M. J., De Vries, V. C., Wasiuk, A., Guo, Y., Noelle, R. J., 2009. Molecular mechanism and function of CD40/CD40L engagement in the immune system. Immunological reviews 229, 152-172.
Eliopoulos, A. G., Davies, C., Knox, P. G., Gallagher, N. J., Afford, S. C., Adams, D. H., Young, L. S., 2000. CD40 induces apoptosis in carcinoma cells through activation of cytotoxic ligands of the tumor necrosis factor superfamily. Mol Cell Biol 20, 5503-15.
Eliopoulos, A. G., Dawson, C. W., Mosialos, G., Floettmann, J. E., Rowe, M., Armitage, R. J., Dawson, J., Zapata, J. M., Kerr, D. J., Wakelam, M. J., Reed, J. C., Kieff, E., Young, L. S., 1996. CD40-induced growth inhibition in epithelial cells is mimicked by Epstein-Barr Virus-encoded LMP1: involvement of TRAF3 as a common mediator. Oncogene 13, 2243-54.
Elmetwali, T., Young, L. S., Palmer, D. H., 2010. CD40 ligand-induced carcinoma cell death: a balance between activation of TNFR-associated factor (TRAF) 3-dependent death signals and suppression of TRAF6-dependent survival signals. The journal of immunology 184, 1111-1120.
Elmore, S., 2007. Apoptosis: a review of programmed cell death. Toxicologic pathology 35, 495-516.
Enari, M., Sakahira, H., Yokoyama, H., Okawa, K., Iwamatsu, A., Nagata, S., 1998. A caspase-activated DNase that degrades DNA during apoptosis, and its inhibitor ICAD. Nature 391, 43-50.
Engelmann, H., Novick, D., Wallach, D., 1990. Two tumor necrosis factor-binding proteins purified from human urine. Evidence for immunological cross-reactivity with cell surface tumor necrosis factor receptors. Journal of Biological Chemistry 265, 1531-1536.
Engels, I. H., Totzke, G., Fischer, U., Schulze-Osthoff, K., Janicke, R. U., 2005. Caspase-10 sensitizes breast carcinoma cells to TRAIL-induced but not tumor necrosis factor-induced apoptosis in a caspase-3-dependent manner. Mol Cell Biol 25, 2808-18.
Enslen, H., Brancho, D. M., Davis, R. J., 2000. Molecular determinants that mediate selective activation of p38 MAP kinase isoforms. The EMBO Journal 19, 1301-1311.
Esparza, E., Arch, R., 2004. TRAF4 functions as an intermediate of GITR-induced NF-κB activation. Cellular and Molecular Life Sciences CMLS 61, 3087-3092.
Esparza, E. M., Lindsten, T., Stockhausen, J. M., Arch, R. H., 2006. Tumor necrosis factor receptor (TNFR)-associated factor 5 is a critical intermediate of costimulatory signaling pathways triggered by glucocorticoid-induced TNFR in T cells. Journal of Biological Chemistry 281, 8559-8564.
Fan, Z., Yu, P., Wang, Y., Wang, Y., Fu, M. L., Liu, W., Sun, Y., Fu, Y.-X., 2006. NK-cell activation by LIGHT triggers tumor-specific CD8+ T-cell immunity to reject established tumors. Blood 107, 1342-1351.
Farber, J. M., 1997. Mig and IP-10: CXC chemokines that target lymphocytes. Journal of leukocyte biology 61, 246-257.
Fava, R. A., Notidis, E., Hunt, J., Szanya, V., Ratcliffe, N., Ngam-ek, A., de Fougerolles, A. R., Sprague, A., Browning, J. L., 2003. A role for the lymphotoxin/LIGHT axis in the pathogenesis of murine collagen-induced arthritis. The Journal of Immunology 171, 115-126.
Fernandes, M. T., Dejardin, E., dos Santos, N. R., 2016. Context-dependent roles for lymphotoxin-β receptor signaling in cancer development. Biochimica et Biophysica Acta (BBA)-Reviews on Cancer 1865, 204-219.

Ferri, K. F., Kroemer, G., 2000. Control of apoptotic DNA degradation. Nature cell biology 2, E63-E64.
Fesik, S. W., 2000. Insights into programmed cell death through structural biology. Cell 103, 273-282, doi:10.1016/s0092-8674(00)00119-7.
Fiers, W., Beyaert, R., Declercq, W., Vandenabeele, P., 1999. More than one way to die: apoptosis, necrosis and reactive oxygen damage. Oncogene 18, 7719-7730.
Force, W. R., Cheung, T. C., Ware, C. F., 1997. Dominant negative mutants of TRAF3 reveal an important role for the coiled coil domains in cell death signaling by the lymphotoxin-beta receptor. J Biol Chem 272, 30835-40.
Fransen, L., Ruysschaert, M. R., Vanderheyden, J., Fiers, W., 1986. Recombinant tumor-necrosis-factor - species specificity for a variety of human and murine transformed-cell lines. Cell Immunol 100, 260-267, doi:10.1016/0008-8749(86)90025-0.
Fruehauf, J. P., Meyskens, F. L., 2007. Reactive oxygen species: a breath of life or death? Clinical Cancer Research 13, 789-794.
Fujioka, S., Niu, J., Schmidt, C., Sclabas, G. M., Peng, B., Uwagawa, T., Li, Z., Evans, D. B., Abbruzzese, J. L., Chiao, P. J., 2004. NF-κB and AP-1 connection: mechanism of NF-κB-dependent regulation of AP-1 activity. Molecular and cellular biology 24, 7806-7819.
Fujiwara, S.-i., Yamashita, Y., Choi, Y. L., Wada, T., Kaneda, R., Takada, S., Maruyama, Y., Ozawa, K., Mano, H., 2005. Transforming activity of the lymphotoxin-β receptor revealed by expression screening. Biochemical and biophysical research communications 338, 1256-1262.
Fulda, S., Debatin, K., 2006. Extrinsic versus intrinsic apoptosis pathways in anticancer chemotherapy. Oncogene 25, 4798-4811.
Fulda, S., Wick, W., Weller, M., Debatin, K.-M., 2002. Smac agonists sensitize for Apo2L/TRAIL- or anticancer drug-induced apoptosis and induce regression of malignant glioma in vivo. Nature medicine 8, 808-815.
Fütterer, A., Mink, K., Luz, A., Kosco-Vilbois, M. H., Pfeffer, K., 1998. The lymphotoxin β receptor controls organogenesis and affinity maturation in peripheral lymphoid tissues. Immunity 9, 59-70.
Galibert, L., Tometsko, M. E., Anderson, D. M., Cosman, D., Dougall, W. C., 1998. The involvement of multiple tumor necrosis factor receptor (TNFR)-associated factors in the signaling mechanisms of receptor activator of NF-κB, a member of the TNFR superfamily. Journal of Biological Chemistry 273, 34120-34127.
Gallagher, E., Enzler, T., Matsuzawa, A., Anzelon-Mills, A., Otero, D., Holzer, R., Janssen, E., Gao, M., Karin, M., 2006. Kinase MEKK1 is required for CD40-dependent activation of the kinases Jnk and p38, germinal center formation, B cell proliferation and antibody production. Nature immunology 8, 57-63.
Gallagher, N. J., Eliopoulos, A. G., Agathangelo, A., Oates, J., Crocker, J., Young, L. S., 2002. CD40 activation in epithelial ovarian carcinoma cells modulates growth, apoptosis, and cytokine secretion. Mol Pathol 55, 110-20.
Galluzzi, L., Kepp, O., Kroemer, G., 2012. Mitochondria: master regulators of danger signalling. Nature reviews Molecular cell biology 13, 780-788.
Galluzzi, L., Maiuri, M., Vitale, I., Zischka, H., Castedo, M., Zitvogel, L., Kroemer, G., 2007. Cell death modalities: classification and pathophysiological implications. Cell Death & Differentiation 14, 1237-1243.
Gamper, C., Omene, C. O., van Eyndhoven, W. G., Glassman, G. D., Lederman, S., 2001. Expression and function of TRAF-3 splice-variant isoforms in human lymphoma cell lines. Human immunology 62, 1167-1177.
Geetha, T., Zheng, C., McGregor, W. C., Douglas White, B., Diaz-Meco, M. T., Moscat, J., Babu, J. R., 2012. TRAF6 and p62 inhibit amyloid β-induced neuronal death through p75 neurotrophin receptor. Neurochemistry international 61, 1289-1293.

Gelbmann, C. M., Leeb, S. N., Vogl, D., Maendel, M., Herfarth, H., Scholmerich, J., Falk, W., Rogler, G., 2003. Inducible CD40 expression mediates NFkappaB activation and cytokine secretion in human colonic fibroblasts. Gut 52, 1448-56.

Georgopoulos, N. T., Steele, L. P., Thomson, M., Selby, P. J., Southgate, J., Trejdosiewicz, L. K., 2006. A novel mechanism of CD40-induced apoptosis of carcinoma cells involving TRAF3 and JNK/AP-1 activation. Cell Death & Differentiation 13, 1789-1801.

Georgopoulos, N. T., Merrick, A., Scott, N., Selby, P. J., Melcher, A., Trejdosiewicz, L. K., 2007. CD40-mediated death and cytokine secretion in colorectal cancer: A potential target for inflammatory tumour cell killing. International journal of cancer 121, 1373-1381.

Geyer, M., Wittinghofer, A., 1997. GEFs, GAPs, GDIs and effectors: taking a closer (3D) look at the regulation of Ras-related GTP-binding proteins. Current opinion in structural biology 7, 786-792.

Ghamande, S., Hylander, B. L., Oflazoglu, E., Lele, S., Fanslow, W., Repasky, E. A., 2001. Recombinant CD40 ligand therapy has significant antitumor effects on CD40-positive ovarian tumor xenografts grown in SCID mice and demonstrates an augmented effect with cisplatin. Cancer research 61, 7556-7562.

Ghosh, S., Karin, M., 2002. Missing pieces in the NF-kappa B puzzle. Cell 109, S81-S96, doi:10.1016/s0092-8674(02)00703-1.

Giménez-Cassina, A., Danial, N. N., 2015. Regulation of mitochondrial nutrient and energy metabolism by BCL-2 family proteins. Trends in Endocrinology & Metabolism 26, 165-175.

Giroir, B. P., Brown, T., Beutler, B., 1992. Constitutive synthesis of tumor necrosis factor in the thymus. Proceedings of the National Academy of Sciences 89, 4864-4868.

Goetz, F. W., Planas, J. V., MacKenzie, S., 2004. Tumor necrosis factors. Developmental and Comparative Immunology 28, 487-497, doi:10.1016/j.dci.2003.09.008.

Golstein, P., Kroemer, G., 2005. Redundant cell death mechanisms as relics and backups. Cell Death & Differentiation 12, 1490-1496.

Golstein, P., Kroemer, G., 2007. Cell death by necrosis: towards a molecular definition. Trends in biochemical sciences 32, 37-43.

Gommerman, J. L., Browning, J. L., 2003. Lymphotoxin/LIGHT, lymphoid microenvironments and autoimmune disease. Nature Reviews Immunology 3, 642-655, doi:10.1038/nri1151.

Gommerman, J. L., Summers deLuca, L., 2011. LTβR and CD40: working together in dendritic cells to optimize immune responses. Immunological reviews 244, 85-98.

Gonzalez, F. A., Seth, A., Raden, D. L., Bowman, D. S., Fay, F. S., Davis, R. J., 1993. Serum-induced translocation of mitogen-activated protein kinase to the cell surface ruffling membrane and the nucleus. The Journal of cell biology 122, 1089-1101.

Gonzalez, L. C., Loyet, K. M., Calemine-Fenaux, J., Chauhan, V., Wranik, B., Ouyang, W., Eaton, D. L., 2005. A coreceptor interaction between the CD28 and TNF receptor family members B and T lymphocyte attenuator and herpesvirus entry mediator. Proc Natl Acad Sci U S A 102, 1116-1121, doi:10.1073/pnas.0409071102.

Gotoh, Y., Cooper, J. A., 1998. Reactive oxygen species-and dimerization-induced activation of apoptosis signal-regulating kinase 1 in tumor necrosis factor-α signal transduction. Journal of Biological Chemistry 273, 17477-17482.

Granger, S. W., Ware, C. F., 2001. Turning on LIGHT. The Journal of clinical investigation 108, 1741-1742.

Granger, S. W., Rickert, S., 2003. LIGHT–HVEM signaling and the regulation of T cell-mediated immunity. Cytokine & growth factor reviews 14, 289-296.

Granger, S. W., Butrovich, K. D., Houshmand, P., Edwards, W. R., Ware, C. F., 2001. Genomic characterization of LIGHT reveals linkage to an immune response locus on chromosome 19p13.3 and distinct isoforms generated by alternate splicing or proteolysis. Journal of Immunology 167, 5122-5128.

Gravestein, L. A., Borst, J., 1998. Tumor necrosis factor receptor family members in the immune system. Seminars in immunology, Vol. 10. Elsevier, pp. 423-434.
Green, D. R., Kroemer, G., 2004. The pathophysiology of mitochondrial cell death. Science 305, 626-629.
Grell, M., Wajant, H., Zimmermann, G., Scheurich, P., 1998. The type 1 receptor (CD120a) is the high-affinity receptor for soluble tumor necrosis factor. Proc Natl Acad Sci U S A 95, 570-575, doi:10.1073/pnas.95.2.570.
Grell, M., Douni, E., Wajant, H., Lohden, M., Clauss, M., Maxeiner, B., Georgopoulos, S., Lesslauer, W., Kollias, G., Pfizenmaier, K., Scheurich, P., 1995. The transmembrane form of tumor necrosis factor is the prime activating ligand of the 80 kDa tumor necrosis factor receptor. Cell 83, 793-802.
Gross, A., McDonnell, J. M., Korsmeyer, S. J., 1999. Bcl-2 family members and the mitochondria in apoptosis. Genes Dev 13, 1899-1911, doi:10.1101/gad.13.15.1899.
Ha, H., Han, D., Choi, Y., 2009. TRAF-Mediated TNFR-Family Signaling. Current protocols in immunology, 11.9 D. 1-11.9 D. 19.
Ha, Y. J., Lee, J. R., 2004. Role of TNF receptor-associated factor 3 in the CD40 signaling by production of reactive oxygen species through association with p40phox, a cytosolic subunit of nicotinamide adenine dinucleotide phosphate oxidase. The Journal of Immunology 172, 231-239.
Ha, Y. J., Seul, H. J., Lee, J. R., 2011. Ligation of CD40 receptor in human B lymphocytes triggers the 5-lipoxygenase pathway to produce reactive oxygen species and activate p38 MAPK. Experimental & molecular medicine 43, 101-110.
Häcker, H., Tseng, P.-H., Karin, M., 2011. Expanding TRAF function: TRAF3 as a tri-faced immune regulator. Nature Reviews Immunology 11, 457-468.
Hagemann, T., Balkwill, F., Lawrence, T., 2007. Inflammation and cancer: a double-edged sword. Cancer cell 12, 300-301.
Hallberg, B., Rayter, S. I., Downward, J., 1994. Interaction of Ras and Raf in intact mammalian cells upon extracellular stimulation. Journal of Biological Chemistry 269, 3913-3916.
Halliwell, B., 2007. Oxidative stress and cancer: have we moved forward? Biochem. j 401, 1-11.
Hamanaka, R. B., Chandel, N. S., 2010. Mitochondrial reactive oxygen species regulate cellular signaling and dictate biological outcomes. Trends in biochemical sciences 35, 505-513.
Han, J., Lee, J.-D., Tobias, P., Ulevitch, R., 1993. Endotoxin induces rapid protein tyrosine phosphorylation in 70Z/3 cells expressing CD14. Journal of Biological Chemistry 268, 25009-25014.
Han, J., Lee, J., Bibbs, L., Ulevitch, R., 1994. A MAP kinase targeted by endotoxin and hyperosmolarity in mammalian cells. Science 265, 808-811.
Haranaka, K., Satomi, N., 1981. Cytotoxic activity of tumor necrosis factor (TNF) on human cancer cells in vitro. The Japanese journal of experimental medicine 51, 191-194.
Harrop, J. A., Reddy, M., Dede, K., Brigham-Burke, M., Lyn, S., Tan, K. B., Silverman, C., Eichman, C., DiPrinzio, R., Spampanato, J., 1998a. Antibodies to TR2 (herpesvirus entry mediator), a new member of the TNF receptor superfamily, block T cell proliferation, expression of activation markers, and production of cytokines. The Journal of Immunology 161, 1786-1794.
Harrop, J. A., McDonnell, P. C., Brigham-Burke, M., Lyn, S. D., Minton, J., Tan, K. B., Dede, K., Spampanato, J., Silverman, C., Hensley, P., DiPrinzio, R., Emery, J. G., Deen, K., Eichman, C., Chabot-Fletcher, M., Truneh, A., Young, P. R., 1998b. Herpesvirus entry mediator ligand (HVEM-L), a novel ligand for HVEM/TR2, stimulates proliferation of T cells and inhibits HT29 cell growth. J Biol Chem 273, 27548-27556, doi:10.1074/jbc.273.42.27548.
Hauer, J., Püschner, S., Ramakrishnan, P., Simon, U., Bongers, M., Federle, C., Engelmann, H., 2005. TNF receptor (TNFR)-associated factor (TRAF) 3 serves as an inhibitor of

TRAF2/5-mediated activation of the noncanonical NF-κB pathway by TRAF-binding TNFRs. Proceedings of the National Academy of Sciences of the United States of America 102, 2874-2879.
Hayakawa, J., Mittal, S., Wang, Y., Korkmaz, K. S., Adamson, E., English, C., Omichi, M., McClelland, M., Mercola, D., 2004. Identification of promoters bound by c-Jun/ATF2 during rapid large-scale gene activation following genotoxic stress. Molecular cell 16, 521-535.
Haybaeck, J., Zeller, N., Wolf, M. J., Weber, A., Wagner, U., Kurrer, M. O., Bremer, J., Iezzi, G., Graf, R., Clavien, P.-A., 2009. A lymphotoxin-driven pathway to hepatocellular carcinoma. Cancer cell 16, 295-308.
Hayden, M. S., Ghosh, S., 2008. Shared principles in NF-κB signaling. Cell 132, 344-362.
He, L., Wu, X., Siegel, R., Lipsky, P. E., 2006. TRAF6 regulates cell fate decisions by inducing caspase 8-dependent apoptosis and the activation of NF-κB. Journal of Biological Chemistry 281, 11235-11249.
Hehlgans, T., Männel, D. N., 2001. Recombinant, soluble LIGHT (HVEM ligand) induces increased IL-8 secretion and growth arrest in A375 melanoma cells. Journal of Interferon & Cytokine Research 21, 333-338.
Hehlgans, T., Pfeffer, K., 2005. The intriguing biology of the tumour necrosis factor/tumour necrosis factor receptor superfamily: players, rules and the games. Immunology 115, 1-20, doi:10.1111/j.1365-2567.2005.02143.x.
Hehlgans, T., Stoelcker, B., Stopfer, P., Müller, P., Cernaianu, G., Guba, M., Steinbauer, M., Nedospasov, S. A., Pfeffer, K., Männel, D. N., 2002. Lymphotoxin-β receptor immune interaction promotes tumor growth by inducing angiogenesis. Cancer research 62, 4034-4040.
Hengartner, M. O., 2000. The biochemistry of apoptosis. Nature 407, 770-776, doi:10.1038/35037710.
Hernandez-Caselles, T., Stutman, O., 1993. Immune functions of tumor necrosis factor. I. Tumor necrosis factor induces apoptosis of mouse thymocytes and can also stimulate or inhibit IL-6-induced proliferation depending on the concentration of mitogenic costimulation. The Journal of Immunology 151, 3999-4012.
Hess, S., Engelmann, H., 1996. A novel function of CD40: induction of cell death in transformed cells. The Journal of experimental medicine 183, 159-167.
Higuchi, T., Aiba, Y., Nomura, T., Matsuda, J., Mochida, K., Suzuki, M., Kikutani, H., Honjo, T., Nishioka, K., Tsubata, T., 2002. Cutting edge: ectopic expression of CD40 ligand on B cells induces lupus-like autoimmune disease. The Journal of Immunology 168, 9-12.
Hill, K. S., Errington, F., Steele, L. P., Merrick, A., Morgan, R., Selby, P. J., Georgopoulos, N. T., O'Donnell, D. M., Melcher, A. A., 2008. OK432-activated human dendritic cells kill tumor cells via CD40/CD40 ligand interactions. The Journal of Immunology 181, 3108-3115.
Hill, M. M., Adrain, C., Duriez, P. J., Creagh, E. M., Martin, S. J., 2004. Analysis of the composition, assembly kinetics and activity of native Apaf-1 apoptosomes. Embo Journal 23, 2134-2145, doi:10.1038/sj.emboj.7600210.
Hipskind, R. A., Büscher, D., Nordheim, A., Baccarini, M., 1994. Ras/MAP kinase-dependent and-independent signaling pathways target distinct ternary complex factors. Genes & development 8, 1803-1816.
Hitoshi, Y., Lorens, J., Kitada, S. I., Fisher, J., LaBarge, M., Ring, H. Z., Francke, U., Reed, J. C., Kinoshita, S., Nolan, G. P., 1998. Toso, a cell surface, specific regulator of Fas-induced apoptosis in T cells. Immunity 8, 461-471, doi:10.1016/s1074-7613(00)80551-8.
Hoeijmakers, J. H., 2009. DNA damage, aging, and cancer. New England Journal of Medicine 361, 1475-1485.
Hofmann, W. A., 2009. Cell and molecular biology of nuclear actin. International review of cell and molecular biology 273, 219-263.

Hofmann, W. A., de Lanerolle, P., 2006. Nuclear actin: to polymerize or not to polymerize. The Journal of cell biology 172, 495-496.
Hohmann, H.-P., Remy, R., Brockhaus, M., Van Loon, A., 1989. Two different cell types have different major receptors for human tumor necrosis factor (TNF alpha). Journal of Biological Chemistry 264, 14927-14934.
Holler, N., Tardivel, A., Kovacsovics-Bankowski, M., Hertig, S., Gaide, O., Martinon, F., Tinel, A., Deperthes, D., Calderara, S., Schulthess, T., 2003. Two adjacent trimeric Fas ligands are required for Fas signaling and formation of a death-inducing signaling complex. Molecular and cellular biology 23, 1428-1440.
Holmes, T. D., Wilson, E. B., Black, E. V., Benest, A. V., Vaz, C., Tan, B., Tanavde, V. M., Cook, G. P., 2014. Licensed human natural killer cells aid dendritic cell maturation via TNFSF14/LIGHT. Proceedings of the National Academy of Sciences 111, E5688-E5696.
Hostager, B. S., Haxhinasto, S. A., Rowland, S. L., Bishop, G. A., 2003. Tumor necrosis factor receptor-associated factor 2 (TRAF2)-deficient B lymphocytes reveal novel roles for TRAF2 in CD40 signaling. Journal of Biological Chemistry 278, 45382-45390.
Hsu, H., Shu, H. B., Pan, M. G., Goeddel, D. V., 1996a. TRADD-TRAF2 and TRADD-FADD interactions define two distinct TNF receptor 1 signal transduction pathways. Cell 84, 299-308.
Hsu, H., Solovyev, I., Colombero, A., Elliott, R., Kelley, M., Boyle, W. J., 1997. ATAR, a novel tumor necrosis factor receptor family member, signals through TRAF2 and TRAF5. Journal of Biological Chemistry 272, 13471-13474.
Hsu, H. L., Xiong, J., Goeddel, D. V., 1995. The TNF receptor 1-associated protein tradd signals cell-death and NF-kappa-B activation. Cell 81, 495-504, doi:10.1016/0092-8674(95)90070-5.
Hsu, H. L., Huang, J. N., Shu, H. B., Baichwal, V., Goeddel, D. V., 1996b. TNF-Dependent recruitment of the protein kinase RIP to the TNF receptor-1 signaling complex. Immunity 4, 387-396, doi:10.1016/s1074-7613(00)80252-6.
Hu, H. M., O'Rourke, K., Boguski, M. S., Dixit, V. M., 1994. A novel RING finger protein interacts with the cytoplasmic domain of CD40. Journal of Biological Chemistry 269, 30069-30072.
Hu, S. M., Snipas, S. J., Vincenz, C., Salvesen, G., Dixit, V. M., 1998. Caspase-14 is a novel developmentally regulated protease. Journal of Biological Chemistry 273, 29648-29653, doi:10.1074/jbc.273.45.29648.
Hu, X., Zimmerman, M. A., Bardhan, K., Yang, D., Waller, J. L., Liles, G. B., Lee, J. R., Pollock, R., Lev, D., Ware, C. F., 2013. Lymphotoxin β receptor mediates caspase-dependent tumor cell apoptosis in vitro and tumor suppression in vivo despite induction of NF-κB activation. Carcinogenesis 34, 1105-1114.
Hübner, A., Barrett, T., Flavell, R. A., Davis, R. J., 2008. Multisite phosphorylation regulates Bim stability and apoptotic activity. Molecular cell 30, 415-425.
Ichijo, H., 1999. From receptors to stress-activated MAP kinases. Oncogene 18.
Ichijo, H., Nishida, E., Irie, K., ten Dijke, P., Saitoh, M., Moriguchi, T., Takagi, M., Matsumoto, K., Miyazono, K., Gotoh, Y., 1997. Induction of apoptosis by ASK1, a mammalian MAPKKK that activates SAPK/JNK and p38 signaling pathways. Science 275, 90-94.
Idriss, H. T., Naismith, J. H., 2000. TNF alpha and the TNF receptor superfamily: Structure-function relationship(s). Microscopy Research and Technique 50, 184-195, doi:10.1002/1097-0029(20000801)50:3<184::aid-jemt2>3.0.co;2-h.
Imura, A., Hori, T., Imada, K., Kawamata, S., Tanaka, Y., Imamura, S., Uchiyama, T., 1997. OX40 expressed on fresh leukemic cells from adult T-cell leukemia patients mediates cell adhesion to vascular endothelial cells: implication for the possible involvement of OX40 in leukemic cell infiltration. Blood 89, 2951-2958.

Inoue, J.-i., Ishida, T., Tsukamoto, N., Kobayashi, N., Naito, A., Azuma, S., Yamamoto, T., 2000. Tumor necrosis factor receptor-associated factor (TRAF) family: adapter proteins that mediate cytokine signaling. Experimental cell research 254, 14-24.

Irmler, M., Thome, M., Hahne, M., Schneider, P., Hofmann, K., Steiner, V., Bodmer, J.-L., Schröter, M., Burns, K., Mattmann, C., 1997. Inhibition of death receptor signals by cellular FLIP. Nature 388, 190-195.

Ishida, T., ToJo, T., Aoki, T., Kobayashi, N., Ohishi, T., Watanabe, T., Yamamoto, T., Inoue, J.-I., 1996a. TRAF5, a novel tumor necrosis factor receptor-associated factor family protein, mediates CD40 signaling. Proceedings of the National Academy of Sciences 93, 9437-9442.

Ishida, T., Mizushima, S.-i., Azuma, S., Kobayashi, N., Tojo, T., Suzuki, K., Aizawa, S., Watanabe, T., Mosialos, G., Kieff, E., 1996b. Identification of TRAF6, a novel tumor necrosis factor receptor-associated factor protein that mediates signaling from an amino-terminal domain of the CD40 cytoplasmic region. Journal of Biological Chemistry 271, 28745-28748.

Izumi, K. M., McFarland, E. C., Ting, A. T., Riley, E. A., Seed, B., Kieff, E. D., 1999. The Epstein-Barr virus oncoprotein latent membrane protein 1 engages the tumor necrosis factor receptor-associated proteins TRADD and receptor-interacting protein (RIP) but does not induce apoptosis or require RIP for NF-κB activation. Molecular and cellular biology 19, 5759-5767.

Javelaud, D., BesancËon, F., 2001. NF-kB activation results in rapid inactivation of JNK in TNFa-treated Ewing sarcoma cells: a mechanism for the anti-apoptotic e ect of NF-kB. Oncogene 20, 4365-4372.

Jiang, E., He, X., Chen, X., Sun, G., Wu, H., Wei, Y., Zhao, X., 2008. Expression of CD40 in ovarian cancer and adenovirus-mediated CD40 ligand therapy on ovarian cancer in vitro. Tumori 94, 356.

Jiang, Y., Chen, C., Li, Z., Guo, W., Gegner, J. A., Lin, S., Han, J., 1996. Characterization of the structure and function of a new mitogen-activated protein kinase (p38β). Journal of Biological Chemistry 271, 17920-17926.

Jobin, C., Holt, L., Bradham, C. A., Streetz, K., Brenner, D. A., Sartor, R. B., 1999. TNF receptor-associated factor-2 is involved in both IL-1β and TNF-α signaling cascades leading to NF-κB activation and IL-8 expression in human intestinal epithelial cells. The Journal of Immunology 162, 4447-4454.

Johnson, G. L., Nakamura, K., 2007. The c-jun kinase/stress-activated pathway: regulation, function and role in human disease. Biochimica et Biophysica Acta (BBA)-Molecular Cell Research 1773, 1341-1348.

Joza, N., Susin, S. A., Daugas, E., Stanford, W. L., Cho, S. K., Li, C. Y. J., Sasaki, T., Elia, A. J., Cheng, H. Y. M., Ravagnan, L., Ferri, K. F., Zamzami, N., Wakeham, A., Hakem, R., Yoshida, H., Kong, Y. Y., Mak, T. W., Zuniga-Pflucker, J. C., Kroemer, G., Penninger, J. M., 2001. Essential role of the mitochondrial apoptosis-inducing factor in programmed cell death. Nature 410, 549-554, doi:10.1038/35069004.

Junt, T., Tumanov, A. V., Harris, N., Heikenwalder, M., Zeller, N., Kuprash, D. V., Aguzzi, A., Ludewig, B., Nedospasov, S. A., Zinkernagel, R. M., 2006. Expression of lymphotoxin beta governs immunity at two distinct levels. European journal of immunology 36, 2061-2075.

Juo, P., Kuo, C. J., Reynolds, S. E., Konz, R. F., Raingeaud, J., Davis, R. J., Biemann, H.-P., Blenis, J., 1997. Fas activation of the p38 mitogen-activated protein kinase signalling pathway requires ICE/CED-3 family proteases. Molecular and Cellular Biology 17, 24-35.

Kamata, H., Honda, S.-i., Maeda, S., Chang, L., Hirata, H., Karin, M., 2005. Reactive oxygen species promote TNFα-induced death and sustained JNK activation by inhibiting MAP kinase phosphatases. Cell 120, 649-661.

Kanamoto, T., Mota, M., Takeda, K., Rubin, L. L., Miyazono, K., Ichijo, H., Bazenet, C. E., 2000. Role of apoptosis signal-regulating kinase in regulation of the c-Jun N-terminal kinase pathway and apoptosis in sympathetic neurons. Molecular and Cellular Biology 20, 196-204.

Kanazawa, K., Azuma, Y., Nakano, H., Kudo, A., 2003. TRAF5 Functions in Both RANKL-and TNFα-Induced Osteoclastogenesis. Journal of Bone and Mineral Research 18, 443-450.

Kang, H.-S., Chin, R. K., Wang, Y., Yu, P., Wang, J., Newell, K. A., Fu, Y.-X., 2002. Signaling via LTβR on the lamina propria stromal cells of the gut is required for IgA production. Nature immunology 3, 576-582.

Karin, M., 1998. Mitogen-activated protein kinase cascades as regulators of stress responses. Annals of the New York Academy of Sciences 851, 139-146.

Karin, M., Lin, A., 2002. NF-kappaB at the crossroads of life and death. Nat Immunol 3, 221-7.

Karin, M., Greten, F. R., 2005. NF kappa B: Linking inflammation and immunity to cancer development and progression. Nature Reviews Immunology 5, 749-759, doi:10.1038/nri1703.

Karin, M., Liu, Z.-g., Zandi, E., 1997. AP-1 function and regulation. Current opinion in cell biology 9, 240-246.

Kathiria, A. S., Butcher, L. D., Feagins, L. A., Souza, R. F., Boland, C. R., Theiss, A. L., 2012. Prohibitin 1 modulates mitochondrial stress-related autophagy in human colonic epithelial cells. PloS one 7, e31231.

Kato, K., Cantwell, M. J., Sharma, S., Kipps, T. J., 1998. Gene transfer of CD40-ligand induces autologous immune recognition of chronic lymphocytic leukemia B cells. Journal of Clinical Investigation 101, 1133.

Kawabe, T., Matsushima, M., Hashimoto, N., Imaizumi, K., Hasegawa, Y., 2011. CD40/CD40 ligand interactions in immune responses and pulmonary immunity. Nagoya journal of medical science 73, 69-78.

Kawamata, S., Hori, T., Imura, A., Takaori-Kondo, A., Uchiyama, T., 1998. Activation of OX40 signal transduction pathways leads to tumor necrosis factor receptor-associated factor (TRAF) 2-and TRAF5-mediated NF-κB activation. Journal of Biological Chemistry 273, 5808-5814.

Kelliher, M. A., Grimm, S., Ishida, Y., Kuo, F., Stanger, B. Z., Leder, P., 1998. The death domain kinase RIP mediates the TNF-induced NF-κB signal. Immunity 8, 297-303.

Kerr, J. F., 1965. A histochemical study of hypertrophy and ischaemic injury of rat liver with special reference to changes in lysosomes. The Journal of pathology and bacteriology 90, 419-435.

Kerr, J. F. R., Wyllie, A. H., Currie, A. R., 1972. Apoptosis - basic biological phenomenon with wide-ranging implications in tissue kinetics. British Journal of Cancer 26, 239-&, doi:10.1038/bjc.1972.33.

Khursigara, G., Orlinick, J. R., Chao, M. V., 1999. Association of the p75 neurotrophin receptor with TRAF6. Journal of Biological Chemistry 274, 2597-2600.

Kim, E. K., Choi, E.-J., 2010. Pathological roles of MAPK signaling pathways in human diseases. Biochimica et Biophysica Acta (BBA)-Molecular Basis of Disease 1802, 396-405.

Kim, S., McAuliffe, W. J., Zaritskaya, L. S., Moore, P. A., Zhang, L. R., Nardelli, B., 2004. Selective induction of tumor necrosis receptor factor 6/decoy receptor 3 release by bacterial antigens in human monocytes and myeloid dendritic cells. Infect Immun 72, 89-93, doi:10.1128/iai.72.1.89-93.2004.

Kim, Y.-S., Nedospasov, S. A. & Liu, Z.-G., 2005. TRAF2 plays a key, nonredundant role in LIGHT-lymphotoxin β receptor signaling. Molecular and cellular biology 25, 2130-2137.

Kim, Y. K., Kim, H. J., Kwon, C. H., Kim, J. H., Woo, J. S., Jung, J. S., Kim, J. M., 2005. Role of ERK activation in cisplatin-induced apoptosis in OK renal epithelial cells. Journal of Applied Toxicology 25, 374-382.

Kim, Y. S., Jung, H. W., Choi, J., Kwon, B. S., Ham, S.-Y., Jung, A. K., Ko, B. K., 2007. Expression of AITR and AITR ligand in breast cancer patients. Oncology reports 18, 1189-1194.

Kischkel, F. C., Lawrence, D. A., Chuntharapai, A., Schow, P., Kim, K. J., Ashkenazi, A., 2000. Apo2L/TRAIL-dependent recruitment of endogenous FADD and caspase-8 to death receptors 4 and 5. Immunity 12, 611-620.

Kischkel, F. C., Hellbardt, S., Behrmann, I., Germer, M., Pawlita, M., Krammer, P. H., Peter, M. E., 1995. Cytotoxicity-dependent apo-1 (fas/cd95)-associated proteins form a death-inducing signaling complex (disc) with the receptor. Embo Journal 14, 5579-5588.

Kitson, J., Raven, T., Jiang, Y.-P., Goeddel, D. V., Giles, K. M., Pun, K.-T., Grinham, C. J., Brown, R., Farrow, S. N., 1996. A death-domain-containing receptor that mediates apoptosis. Nature 384, 372-375.

Kobayashi, C. I., Suda, T., 2012. Regulation of reactive oxygen species in stem cells and cancer stem cells. Journal of cellular physiology 227, 421-430.

Koff, J. L., Ramachandiran, S., Bernal-Mizrachi, L., 2015. A time to kill: targeting apoptosis in cancer. International journal of molecular sciences 16, 2942-2955.

Kooten, C. v., Banchereau, J., 1997. Functions of CD40 on B cells, dendritic cells and other cells. Current opinion in immunology 9, 330-337.

Korniluk, A., Kemona, H., Dymicka-Piekarska, V., 2014. Multifunctional CD40L: pro-and anti-neoplastic activity. Tumor Biology, 1-11.

Korsmeyer, S. J., Shutter, J. R., Veis, D. J., Merry, D. E., Oltvai, Z., 1994. Bcl-2/Bax: A rheostat that regulates an anti-oxidant pathway and cell death. Proceedings of the American Association for Cancer Research Annual Meeting 35, 671-672.

Kroemer, G., Reed, J. C., 2000. Mitochondrial control of cell death. Nature medicine 6, 513-519.

Kroemer, G., Martin, S. J., 2005. Caspase-independent cell death. Nat Med 11, 725-30.

Kroemer, G., Galluzzi, L., Brenner, C., 2007. Mitochondrial membrane permeabilization in cell death. Physiological reviews 87, 99-163.

Kroemer, G., El-Deiry, W., Golstein, P., Peter, M., Vaux, D., Vandenabeele, P., Zhivotovsky, B., Blagosklonny, M., Malorni, W., Knight, R., 2005. Classification of cell death: recommendations of the Nomenclature Committee on Cell Death. Cell Death & Differentiation 12, 1463-1467.

Kroemer, G., Galluzzi, L., Vandenabeele, P., Abrams, J., Alnemri, E., Baehrecke, E., Blagosklonny, M., El-Deiry, W., Golstein, P., Green, D., 2009. Classification of cell death: recommendations of the Nomenclature Committee on Cell Death 2009. Cell Death & Differentiation 16, 3-11.

Kuai, J., Nickbarg, E., Wooters, J., Qiu, Y., Wang, J., Lin, L.-L., 2003. Endogenous association of TRAF2, TRAF3, cIAP1, and Smac with lymphotoxin β receptor reveals a novel mechanism of apoptosis. Journal of Biological Chemistry 278, 14363-14369.

Kuchroo, V. K., Dardalhon, V., Xiao, S., Anderson, A. C., 2008. New roles for TIM family members in immune regulation. Nature Reviews Immunology 8, 577-580.

Kuhné, M. R., Robbins, M., Hambor, J. E., Mackey, M. F., Kosaka, Y., Nishimura, T., Gigley, J. P., Noelle, R. J., Calderhead, D. M., 1997. Assembly and regulation of the CD40 receptor complex in human B cells. The Journal of experimental medicine 186, 337-342.

Kumar, S., McDonnell, P. C., Gum, R. J., Hand, A. T., Lee, J. C., Young, P. R., 1997. Novel homologues of CSBP/p38 MAP kinase: activation, substrate specificity and sensitivity to inhibition by pyridinyl imidazoles. Biochemical and biophysical research communications 235, 533-538.

Kummer, J. L., Rao, P. K., Heidenreich, K. A., 1997. Apoptosis induced by withdrawal of trophic factors is mediated by p38 mitogen-activated protein kinase. Journal of Biological Chemistry 272, 20490-20494.

Kuwana, T., Mackey, M. R., Perkins, G., Ellisman, M. H., Latterich, M., Schneiter, R., Green, D. R., Newmeyer, D. D., 2002. Bid, Bax, and lipids cooperate to form supramolecular openings in the outer mitochondrial membrane. Cell 111, 331-342.

Kwon, B. S., Tan, K. B., Ni, J., KwiOkOh, Lee, Z. H., Kim, K. K., Kim, Y. J., Wang, S., Gentz, R., Yu, G. L., Harrop, J., Lyn, S. D., Silverman, C., Porter, T. G., Truneh, A., Young, P. R., 1997. A newly identified member of the tumor necrosis factor receptor superfamily with a wide tissue distribution and involvement in lymphocyte activation. Journal of Biological Chemistry 272, 14272-14276, doi:10.1074/jbc.272.22.14272.

Kyriakis, J. M., Avruch, J., 1990. pp54 microtubule-associated protein 2 kinase. A novel serine/threonine protein kinase regulated by phosphorylation and stimulated by poly-L-lysine. Journal of Biological Chemistry 265, 17355-17363.

Kyriakis, J. M., Avruch, J., 2001. Mammalian mitogen-activated protein kinase signal transduction pathways activated by stress and inflammation. Physiological reviews 81, 807-869.

Kyriakis, J. M., Avruch, J., 2012. Mammalian MAPK signal transduction pathways activated by stress and inflammation: a 10-year update. Physiological reviews 92, 689-737.

La, S., Kim, J., Kwon, B. S., Kwon, B., 2002. Herpes simplex virus type 1 glycoprotein D inhibits T-cell proliferation. Molecules and cells 14, 398-403.

Labbe, K., Saleh, M., 2008. Cell death in the host response to infection. Cell Death & Differentiation 15, 1339-1349.

Lakhani, S. A., Masud, A., Kuida, K., Porter, G. A., Booth, C. J., Mehal, W. Z., Inayat, I., Flavell, R. A., 2006. Caspases 3 and 7: key mediators of mitochondrial events of apoptosis. Science 311, 847-851.

Larsen, C. P., Pearson, T. C., 1997. The CD40 pathway in allograft rejection, acceptance, and tolerance. Current opinion in immunology 9, 641-647.

Lechner, C., Zahalka, M. A., Giot, J.-F., Møller, N., Ullrich, A., 1996. ERK6, a mitogen-activated protein kinase involved in C2C12 myoblast differentiation. Proceedings of the National Academy of Sciences 93, 4355-4359.

Lee, J. C., Laydon, J. T., McDonnell, P. C., Gallagher, T. F., Kumar, S., Green, D., McNulty, D., Blumenthal, M. J., Keys, J. R., Strickler, J. E., 1994. A protein kinase involved in the regulation of inflammatory cytokine biosynthesis.

Lee, K. W., Lee, D. J., Lee, J. Y., Kang, D. H., Kwon, J., Kang, S. W., 2011. Peroxiredoxin II restrains DNA damage-induced death in cancer cells by positively regulating JNK-dependent DNA repair. Journal of Biological Chemistry 286, 8394-8404.

Lee, M.-W., Park, S. C., Yang, Y. G., Yim, S. O., Chae, H. S., Bach, J.-H., Lee, H. J., Kim, K. Y., Lee, W. B., Kim, S. S., 2002. The involvement of reactive oxygen species (ROS) and p38 mitogen-activated protein (MAP) kinase in TRAIL/Apo2L-induced apoptosis. FEBS letters 512, 313-318.

Lee, S. Y., Kandala, G., Liou, M., Liou, H., Choi, Y., 1996. CD30/TNF receptor-associated factor interaction: NF-kappa B activation and binding specificity. Proceedings of the National Academy of Sciences 93, 9699-9703.

Lee, S. Y., Reichlin, A., Santana, A., Sokol, K. A., Nussenzweig, M. C., Choi, Y., 1997. TRAF2 is essential for JNK but not NF-κB activation and regulates lymphocyte proliferation and survival. Immunity 7, 703-713.

Legler, D. F., Micheau, O., Doucey, M. A., Tschopp, J., Bron, C., 2003. Recruitment of TNF receptor 1 to lipid rafts is essential for TNFalpha-mediated NF-kappaB activation. Immunity 18, 655-64.

Lei, K., Davis, R. J., 2003. JNK phosphorylation of Bim-related members of the Bcl2 family induces Bax-dependent apoptosis. Proceedings of the National Academy of Sciences 100, 2432-2437.

Leithäuser, F., Dhein, J., Mechtersheimer, G., Koretz, K., Brüderlein, S., Henne, C., Schmidt, A., Debatin, K., Krammer, P., Möller, P., 1993. Constitutive and induced expression of APO-1, a new member of the nerve growth factor/tumor necrosis factor receptor superfamily, in normal and neoplastic cells. Laboratory investigation; a journal of technical methods and pathology 69, 415-429.

Lennicke, C., Rahn, J., Lichtenfels, R., Wessjohann, L. A., Seliger, B., 2015. Hydrogen peroxide - production, fate and role in redox signaling of tumor cells. Cell Commun Signal 13, 39, doi:10.1186/s12964-015-0118-6.

Lenormand, P., Sardet, C., Pages, G., L'Allemain, G., Brunet, A., Pouysségur, J., 1993. Growth factors induce nuclear translocation of MAP kinases (p42mapk and p44mapk) but not of their activator MAP kinase kinase (p45mapkk) in fibroblasts. The Journal of cell biology 122, 1079-1088.

Leo, E., Welsh, K., Matsuzawa, S., Zapata, J. M., Kitada, S., Mitchell, R. S., Ely, K. R., Reed, J. C., 1999. Differential requirements for tumor necrosis factor receptor-associated factor family proteins in CD40-mediated induction of NF-kappaB and Jun N-terminal kinase activation. J Biol Chem 274, 22414-22.

Letai, A., Bassik, M. C., Walensky, L. D., Sorcinelli, M. D., Weiler, S., Korsmeyer, S. J., 2002. Distinct BH3 domains either sensitize or activate mitochondrial apoptosis, serving as prototype cancer therapeutics. Cancer cell 2, 183-192.

Ley, R., Balmanno, K., Hadfield, K., Weston, C., Cook, S. J., 2003. Activation of the ERK1/2 signaling pathway promotes phosphorylation and proteasome-dependent degradation of the BH3-only protein, Bim. Journal of Biological Chemistry 278, 18811-18816.

Ley, R., Ewings, K. E., Hadfield, K., Howes, E., Balmanno, K., Cook, S. J., 2004. Extracellular signal-regulated kinases 1/2 are serum-stimulated “BimEL kinases” that bind to the BH3-only protein BimEL causing its phosphorylation and turnover. Journal of Biological Chemistry 279, 8837-8847.

Li, H., Zhu, H., Xu, C. J., Yuan, J., 1998. Cleavage of BID by caspase 8 mediates the mitochondrial damage in the Fas pathway of apoptosis. Cell 94, 491-501, doi:S0092-8674(00)81590-1 [pii].

Li, J., Yuan, J., 2008. Caspases in apoptosis and beyond. Oncogene 27, 6194-6206.

Li, L. Y., Luo, L., Wang, X. D., 2001. Endonuclease G is an apoptotic DNase when released from mitochondria. Nature 412, 95-99, doi:10.1038/35083620.

Li, N., Ragheb, K., Lawler, G., Sturgis, J., Rajwa, B., Melendez, J. A., Robinson, J. P., 2003. DPI induces mitochondrial superoxide-mediated apoptosis. Free Radical Biology and Medicine 34, 465-477.

Li, P., Nijhawan, D., Budihardjo, I., Srinivasula, S. M., Ahmad, M., Alnemri, E. S., Wang, X., 1997. Cytochrome c and dATP-dependent formation of Apaf-1/caspase-9 complex initiates an apoptotic protease cascade. Cell 91, 479-489.

Li, Q., Verma, I. M., 2002. NF-κB regulation in the immune system. Nature Reviews Immunology 2, 725-734.

Li, Z.-W., Rickert, R. C., Karin, M., 2004. Genetic dissection of antigen receptor induced-NF-κB activation. Molecular immunology 41, 701-714.

Li, Z., Jiang, Y., Ulevitch, R. J., Han, J., 1996. The primary structure of p38γ: a new member of p38 group of MAP kinases. Biochemical and biophysical research communications 228, 334-340.

Lin, Y., Choksi, S., Shen, H.-M., Yang, Q.-F., Hur, G. M., Kim, Y. S., Tran, J. H., Nedospasov, S. A., Liu, Z.-g., 2004. Tumor necrosis factor-induced nonapoptotic cell death requires receptor-interacting protein-mediated cellular reactive oxygen species accumulation. Journal of Biological Chemistry 279, 10822-10828.

Liston, P., Fong, W. G., Korneluk, R. G., 2003. The inhibitors of apoptosis: there is more to life than Bcl2. Oncogene 22, 8568-8580, doi:10.1038/sj.onc.1207101.

Liu, Y., Min, W., 2002. Thioredoxin promotes ASK1 ubiquitination and degradation to inhibit ASK1-mediated apoptosis in a redox activity-independent manner. Circulation research 90, 1259-1266.
Lockshin, R. A., Williams, C. M., 1964. Programmed cell death—II. Endocrine potentiation of the breakdown of the intersegmental muscles of silkmoths. Journal of Insect Physiology 10, 643-649.
Lockshin, R. A., Williams, C. M., 1965. Programmed cell death—I. Cytology of degeneration in the intersegmental muscles of the Pernyi silkmoth. Journal of insect physiology 11, 123-133.
Locksley, R. M., Killeen, N., Lenardo, M. J., 2001. The TNF and TNF receptor superfamilies: Integrating mammalian biology. Cell 104, 487-501, doi:10.1016/s0092-8674(01)00237-9.
Loetscher, H., Pan, Y. C. E., Lahm, H. W., Gentz, R., Brockhaus, M., Tabuchi, H., Lesslauer, W., 1990. Molecular-cloning and expression of the human 55-kd tumor-necrosis-factor receptor. Cell 61, 351-359, doi:10.1016/0092-8674(90)90815-v.
Look, D., Pelletier, M. R., Holtzman, M. J., 1994. Selective interaction of a subset of interferon-gamma response element-binding proteins with the intercellular adhesion molecule-1 (ICAM-1) gene promoter controls the pattern of expression on epithelial cells. Journal of Biological Chemistry 269, 8952-8958.
Low, H. B., Zhang, Y., 2016. Regulatory Roles of MAPK Phosphatases in Cancer. Immune network 16, 85-98.
Luftig, M. A., Cahir-McFarland, E., Mosialos, G., Kieff, E., 2001. Effects of the NIK aly mutation on NF-κB activation by the Epstein-Barr virus latent infection membrane protein, lymphotoxin β receptor, and CD40. Journal of Biological Chemistry 276, 14602-14606.
Lukashev, M., LePage, D., Wilson, C., Bailly, V., Garber, E., Lukashin, A., Ngam-ek, A., Zeng, W., Allaire, N., Perrin, S., Xu, X., Szeliga, K., Wortham, K., Kelly, R., Bottiglio, C., Ding, J., Griffith, L., Heaney, G., Silverio, E., Yang, W., Jarpe, M., Fawell, S., Reff, M., Carmillo, A., Miatkowski, K., Amatucci, J., Crowell, T., Prentice, H., Meier, W., Violette, S. M., Mackay, F., Yang, D., Hoffman, R., Browning, J. L., 2006. Targeting the lymphotoxin-beta receptor with agonist antibodies as a potential cancer therapy. Cancer Res 66, 9617-24.
Luo, X., Budihardjo, I., Zou, H., Slaughter, C., Wang, X. D., 1998. Bid, a Bcl2 interacting protein, mediates cytochrome c release from mitochondria in response to activation of cell surface death receptors. Cell 94, 481-490, doi:10.1016/s0092-8674(00)81589-5.
Luther, S. A., Bidgol, A., Hargreaves, D. C., Schmidt, A., Xu, Y., Paniyadi, J., Matloubian, M., Cyster, J. G., 2002. Differing activities of homeostatic chemokines CCL19, CCL21, and CXCL12 in lymphocyte and dendritic cell recruitment and lymphoid neogenesis. Journal of Immunology 169, 424-433.
Ma, D. Y., Clark, E. A., 2009. The role of CD40 and CD154/CD40L in dendritic cells. Seminars in immunology, Vol. 21. Elsevier, pp. 265-272.
MacEwan, D. J., 2002. TNF ligands and receptors - a matter of life and death. British Journal of Pharmacology 135, 855-875, doi:10.1038/sj.bjp.0704549.
MacFarlane, M., Ahmad, M., Srinivasula, S. M., FernandesAlnemri, T., Cohen, G. M., Alnemri, E. S., 1997. Identification and molecular cloning of two novel receptors for the cytotoxic ligand TRAIL. Journal of Biological Chemistry 272, 25417-25420, doi:10.1074/jbc.272.41.25417.
Mackay, F., Browning, J. L., 1998. Turning off follicular dendritic cells. Nature 395, 26-27.
Mackay, F., Majeau, G. R., Hochman, P. S., Browning, J. L., 1996. Lymphotoxin beta receptor triggering induces activation of the nuclear factor kappaB transcription factor in some cell types. J Biol Chem 271, 24934-8.

Mackay, F., Majeau, G. R., Lawton, P., Hochman, P. S., Browning, J. L., 1997. Lymphotoxin but not tumor necrosis factor functions to maintain splenic architecture and humoral responsiveness in adult mice. European journal of immunology 27, 2033-2042.

Mallett, S., Fossum, S., Barclay, A. N., 1990. Characterization of the MRC ox40 antigen of activated CD4 positive lymphocytes-T - a molecule related to nerve growth-factor receptor. Embo Journal 9, 1063-1068.

Mansell, A., Jenkins, B. J., 2013. Dangerous liaisons between interleukin-6 cytokine and toll-like receptor families: a potent combination in inflammation and cancer. Cytokine & growth factor reviews 24, 249-256.

Marsters, S., Sheridan, J., Pitti, R., Huang, A., Skubatch, M., Baldwin, D., Yuan, J., Gurney, A., Goddard, A., Godowski, P., 1997a. A novel receptor for Apo2L/TRAIL contains a truncated death domain. Current Biology 7, 1003-1006.

Marsters, S. A., Ayres, T. M., Skubatch, M., Gray, C. L., Rothe, M., Ashkenazi, A., 1997b. Herpesvirus entry mediator, a member of the tumor necrosis factor receptor (TNFR) family, interacts with members of the TNFR-associated factor family and activates the transcription factors NF-κB and AP-1. Journal of Biological Chemistry 272, 14029-14032.

Marsters, S. A., Sheridan, J. P., Donahue, C. J., Pitti, R. M., Gray, C. L., Goddard, A. D., Bauer, K. D., Ashkenazi, A., 1996. Apo-3, a new member of the tumor necrosis factor receptor family, contains a death domain and activates apoptosis and NF-κB. Current Biology 6, 1669-1676.

Martinez, M. M., Reif, R. D., Pappas, D., 2010. Detection of apoptosis: A review of conventional and novel techniques. Analytical methods 2, 996-1004.

Martinvalet, D., Zhu, P., Lieberman, J., 2005. Granzyme A induces caspase-independent mitochondrial damage, a required first step for apoptosis. Immunity 22, 355-370.

MatÉs, J. M., Pérez-Gómez, C., De Castro, I. N., 1999. Antioxidant enzymes and human diseases. Clinical biochemistry 32, 595-603.

Matés, J. M., Segura, J. A., Alonso, F. J., Márquez, J., 2010. Roles of dioxins and heavy metals in cancer and neurological diseases using ROS-mediated mechanisms. Free Radical Biology and Medicine 49, 1328-1341.

Matés, J. M., Segura, J. A., Alonso, F. J., Márquez, J., 2012. Oxidative stress in apoptosis and cancer: an update. Archives of toxicology 86, 1649-1665.

Mauri, D. N., Ebner, R., Montgomery, R. I., Kochel, K. D., Cheung, T. C., Yu, G. L., Ruben, S., Murphy, M., Eisenberg, R. J., Cohen, G. H., Spear, P. G., Ware, C. F., 1998. LIGHT, a new member of the TNF superfamily, and lymphotoxin alpha are ligands for herpesvirus entry mediator. Immunity 8, 21-30, doi:10.1016/s1074-7613(00)80455-0.

Meager, A., 1991. A cytotoxicity assay for tumour necrosis using a human rhabdomyosarcoma cell line. Journal of immunological methods 144, 141-143.

Mebratu, Y., Tesfaigzi, Y., 2009. How ERK1/2 activation controls cell proliferation and cell death: Is subcellular localization the answer? Cell cycle 8, 1168-1175.

Melichar, B., Patenia, R., Gallardo, S., Melicharová, K., Hu, W., Freedman, R. S., 2007. Expression of CD40 and growth-inhibitory activity of CD40 ligand in ovarian cancer cell lines. Gynecologic oncology 104, 707-713.

Micheau, O., Tschopp, J., 2003. Induction of TNF receptor I-mediated apoptosis via two sequential signaling complexes. Cell 114, 181-90.

Migone, T.-S., Zhang, J., Luo, X., Zhuang, L., Chen, C., Hu, B., Hong, J. S., Perry, J. W., Chen, S.-F., Zhou, J. X., 2002. TL1A is a TNF-like ligand for DR3 and TR6/DcR3 and functions as a T cell costimulator. Immunity 16, 479-492.

Miura, M., Friedlander, R. M., Yuan, J., 1995. Tumor necrosis factor-induced apoptosis is mediated by a CrmA-sensitive cell death pathway. Proceedings of the National Academy of Sciences 92, 8318-8322.

Moll, R., Krepler, R., Franke, W. W., 1982a. Complex cytokeratin polypeptide patterns observed in certain human carcinomas. Differentiation 23, 256-269.

Moll, R., Franke, W. W., Schiller, D. L., Geiger, B., Krepler, R., 1982b. The catalog of human cytokeratins: patterns of expression in normal epithelia, tumors and cultured cells. cell 31, 11-24.

Montgomery, R. I., Warner, M. S., Lum, B. J., Spear, P. G., 1996. Herpes simplex virus-1 entry into cells mediated by a novel member of the TNF/NGF receptor family. Cell 87, 427-436, doi:10.1016/s0092-8674(00)81363-x.

Moore, C. R., Bishop, G. A., 2005. Differential regulation of CD40-mediated TNF receptor-associated factor degradation in B lymphocytes. The Journal of Immunology 175, 3780-3789.

Morel, Y., Truneh, A., Sweet, R. W., Olive, D., Costello, R. T., 2001. The TNF superfamily members LIGHT and CD154 (CD40 ligand) costimulate induction of dendritic cell maturation and elicit specific CTL activity. J Immunol 167, 2479-86.

Morel, Y., Schiano de Colella, J. M., Harrop, J., Deen, K. C., Holmes, S. D., Wattam, T. A., Khandekar, S. S., Truneh, A., Sweet, R. W., Gastaut, J. A., Olive, D., Costello, R. T., 2000. Reciprocal expression of the TNF family receptor herpes virus entry mediator and its ligand LIGHT on activated T cells: LIGHT down-regulates its own receptor. J Immunol 165, 4397-404.

Mortarini, R., Scarito, A., Nonaka, D., Zanon, M., Bersani, I., Montaldi, E., Pennacchioli, E., Patuzzo, R., Santinami, M., Anichini, A., 2005. Constitutive expression and costimulatory function of LIGHT/TNFSF14 on human melanoma cells and melanoma-derived microvesicles. Cancer research 65, 3428-3436.

Mosialos, G., Birkenbach, M., Yalamanchili, R., VanArsdale, T., Ware, C., Kieff, E., 1995. The Epstein-Barr virus transforming protein LMP1 engages signaling proteins for the tumor necrosis factor receptor family. Cell 80, 389-99.

Moss, M. L., Jin, S. L. C., Milla, M. E., Burkhart, W., Carter, H. L., Chen, W. J., Clay, W. C., Didsbury, J. R., Hassler, D., Hoffman, C. R., Kost, T. A., Lambert, M. H., Leesnitzer, M. A., McCauley, P., McGeehan, G., Mitchell, J., Moyer, M., Pahel, G., Rocque, W., Overton, L. K., Schoenen, F., Seaton, T., Su, J. L., Warner, J., Willard, D., Becherer, J. D., 1997. Cloning of a disintegrin metalloproteinase that processes precursor tumour-necrosis factor-alpha. Nature 385, 733-736, doi:10.1038/385733a0.

Motyka, B., Korbutt, G., Pinkoski, M. J., Heibein, J. A., Caputo, A., Hobman, M., Barry, M., Shostak, I., Sawchuk, T., Holmes, C. F., 2000. Mannose 6-phosphate/insulin-like growth factor II receptor is a death receptor for granzyme B during cytotoxic T cell–induced apoptosis. Cell 103, 491-500.

Mukundan, L., Milhorn, D. M., Matta, B., Suttles, J., 2004. CD40-mediated activation of vascular smooth muscle cell chemokine production through a Src-initiated, MAPK-dependent pathway. Cellular signalling 16, 375-384.

Muntané, J., 2011. Harnessing tumor necrosis factor receptors to enhance antitumor activities of drugs. Chemical research in toxicology 24, 1610-1616.

Muzio, M., Chinnaiyan, A. M., Kischkel, F. C., O'Rourke, K., Shevchenko, A., Ni, J., Scaffidi, C., Bretz, J. D., Zhang, M., Gentz, R., 1996. FLICE, a novel FADD-homologous ICE/CED-3–like protease, is recruited to the CD95 (Fas/APO-1) death-inducing signaling complex. Cell 85, 817-827.

Nagata, S., 1997. Apoptosis by death factor. cell 88, 355-365.

Nakano, H., Oshima, H., Chung, W., Williams-Abbott, L., Ware, C. F., Yagita, H., Okumura, K., 1996. TRAF5, an activator of NF-κB and putative signal transducer for the lymphotoxin-β receptor. Journal of Biological Chemistry 271, 14661-14664.

Nakano, H., Sakon, S., Koseki, H., Takemori, T., Tada, K., Matsumoto, M., Munechika, E., Sakai, T., Shirasawa, T., Akiba, H., 1999. Targeted disruption of TRAF5 gene causes

defects in CD40-and CD27-mediated lymphocyte activation. Proceedings of the National Academy of Sciences 96, 9803-9808.
Nechushtan, A., Smith, C. L., Lamensdorf, I., Yoon, S.-H., Youle, R. J., 2001. Bax and Bak coalesce into novel mitochondria-associated clusters during apoptosis. The Journal of cell biology 153, 1265-1276.
Nemes, Z., Friis, R. R., Aeschlimann, D., Saurer, S., Paulsson, M., Fesus, L., 1996. Expression and activation of tissue transglutaminase in apoptotic cells of involuting rodent mammary tissue. European Journal of Cell Biology 70, 125-133.
Ngo, V. N., Korner, H., Gunn, M. D., Schmidt, K. N., Riminton, D. S., Cooper, M. D., Browning, J. L., Sedgwick, J. D., Cyster, J. G., 1999. Lymphotoxin α/β and tumor necrosis factor are required for stromal cell expression of homing chemokines in B and T cell areas of the spleen. The Journal of experimental medicine 189, 403-412.
Nicotera, P., Leist, M., Ferrando-May, E., 1998. Intracellular ATP, a switch in the decision between apoptosis and necrosis. Toxicology letters 102, 139-142.
Niwa, Y., Hirose, K., Matsuo, K., Tajima, K., Ikoma, Y., Nakanishi, T., Nawa, A., Kuzuya, K., Tamakoshi, A., Hamajima, N., 2005. < i> Lymphotoxin-α</i> polymorphism and the risk of cervical cancer in Japanese subjects. Cancer letters 218, 63-68.
Nocentini, G., Giunchi, L., Ronchetti, S., Krausz, L. T., Bartoli, A., Moraca, R., Migliorati, G., Riccardi, C., 1997. A new member of the tumor necrosis factor nerve growth factor receptor family inhibits T cell receptor-induced apoptosis. Proc Natl Acad Sci U S A 94, 6216-6221, doi:10.1073/pnas.94.12.6216.
Nonomura, N., Tokizane, T., Nakayama, M., Inoue, H., Nishimura, K., Muramatsu, M., Okuyama, A., 2006. Possible correlation between polymorphism in the tumor necrosis factor-beta gene and the clinicopathological features of bladder cancer in Japanese patients. International journal of urology 13, 971-976.
Norbury, C. J., Hickson, I. D., 2001. Cellular responses to DNA damage. Annual Review of Pharmacology and Toxicology 41, 367-401, doi:10.1146/annurev.pharmtox.41.1.367.
Nowak, G., Bakajsova, D., Clifton, G. L., 2004. Protein kinase C-ϵ modulates mitochondrial function and active Na+ transport after oxidant injury in renal cells. American Journal of Physiology-Renal Physiology 286, F307-F316.
Ono, K., Han, J., 2000. The p38 signal transduction pathway activation and function. Cellular signalling 12, 1-13.
Ossina, N. K., Cannas, A., Powers, V. C., Fitzpatrick, P. A., Knight, J. D., Gilbert, J. R., Shekhtman, E. M., Tomei, L. D., Umansky, S. R., Kiefer, M. C., 1997. Interferon-γ modulates a p53-independent apoptotic pathway and apoptosis-related gene expression. Journal of Biological Chemistry 272, 16351-16357.
Pahl, H. L., 1999. Activators and target genes of Rel/NF-kappaB transcription factors. Oncogene 18, 6853-6866.
Pan, G. H., Ni, J., Yu, G. L., Wei, Y. F., Dixit, V. M., 1998a. TRUNDD, a new member of the TRAIL receptor family that antagonizes TRAIL signalling. FEBS Lett 424, 41-45, doi:10.1016/s0014-5793(98)00135-5.
Pan, G. H., Orourke, K., Chinnaiyan, A. M., Gentz, R., Ebner, R., Ni, J., Dixit, V. M., 1997. The receptor for the cytotoxic ligand TRAIL. Science 276, 111-113, doi:10.1126/science.276.5309.111.
Pan, G. H., Bauer, J. H., Haridas, V., Wang, S. X., Liu, D., Yu, G. L., Vincenz, C., Aggarwal, B. B., Ni, J., Dixit, V. M., 1998b. Identification and functional characterization of DR6, a novel death domain-containing TNF receptor. FEBS Lett 431, 351-356, doi:10.1016/s0014-5793(98)00791-1.
Papa, S., Zazzeroni, F., Bubici, C., Jayawardena, S., Alvarez, K., Matsuda, S., Nguyen, D. U., Pham, C. G., Nelsbach, A. H., Melis, T., De Smaele, E., Tang, W. J., D'Adamio, L.,

Franzoso, G., 2004. Gadd45 beta mediates the NF-kappa B suppression of JNK signalling by targeting MKK7/JNKK2. Nat Cell Biol 6, 146-53.
Papachristou, D., Batistatou, A., Sykiotis, G., Varakis, I., Papavassiliou, A., 2003. Activation of the JNK–AP-1 signal transduction pathway is associated with pathogenesis and progression of human osteosarcomas. Bone 32, 364-371.
Park, J. M., Brady, H., Ruocco, M. G., Sun, H., Williams, D., Lee, S. J., Kato, T., Richards, N., Chan, K., Mercurio, F., 2004. Targeting of TAK1 by the NF-κB protein Relish regulates the JNK-mediated immune response in Drosophila. Genes & development 18, 584-594.
Park, Y. C., Ye, H., Hsia, C., Segal, D., Rich, R. L., Liou, H.-C., Myszka, D. G., Wu, H., 2000. A novel mechanism of TRAF signaling revealed by structural and functional analyses of the TRADD–TRAF2 interaction. Cell 101, 777-787.
Pasero, C., Truneh, A., Olive, D., 2009a. Cosignaling molecules around LIGHT-HVEM-BTLA: from immune activation to therapeutic targeting. Current molecular medicine 9, 911-927.
Pasero, C., Barbarat, B., Just-Landi, S., Bernard, A., Aurran-Schleinitz, T., Rey, J., Eldering, E., Truneh, A., Costello, R. T., Olive, D., 2009b. A role for HVEM, but not lymphotoxin-beta receptor, in LIGHT-induced tumor cell death and chemokine production. Eur J Immunol 39, 2502-14.
Pastorino, J. G., Shulga, N., Hoek, J. B., 2002. Mitochondrial binding of hexokinase II inhibits Bax-induced cytochrome c release and apoptosis. Journal of Biological Chemistry 277, 7610-7618.
Pastorino, J. G., Hoek, J. B., Shulga, N., 2005. Activation of glycogen synthase kinase 3β disrupts the binding of hexokinase II to mitochondria by phosphorylating voltage-dependent anion channel and potentiates chemotherapy-induced cytotoxicity. Cancer research 65, 10545-10554.
Pellat-Deceunynck, C., Amiot, M., Robillard, N., Wijdenes, J., Bataille, R., 1996. CD11a-CD18 and CD102 interactions mediate human myeloma cell growth arrest induced by CD40 stimulation. Cancer research 56, 1909-1916.
Petreaca, M. L., Yao, M., Ware, C., Martins-Green, M. M., 2008. YOUNG INVESTIGATOR AWARD ARTICLE: Vascular endothelial growth factor promotes macrophage apoptosis through stimulation of tumor necrosis factor superfamily member 14 (TNFSF14/LIGHT). Wound Repair and Regeneration 16, 602-614.
Pham, C. G., Bubici, C., Zazzeroni, F., Papa, S., Jones, J., Alvarez, K., Jayawardena, S., De Smaele, E., Cong, R., Beaumont, C., 2004. Ferritin heavy chain upregulation by NF-κB inhibits TNFα-induced apoptosis by suppressing reactive oxygen species. Cell 119, 529-542.
Phillips, T. M., McBride, W. H., Pajonk, F., 2006. The response of CD24−/low/CD44+ breast cancer–initiating cells to radiation. Journal of the National Cancer Institute 98, 1777-1785.
Pitti, R. M., MARSTERS, S. A., LAWRENCE, D. A., ROY, M., KISCHKEL, F. C., DOWD, P., HUANG, A., DONAHUE, C. J., SHERWOOD, S. W., BALDWIN, D. T., GODOWSKI, P. J., WOOD, W. I., GURNEY, A. L., HILLAN, K. J., COHEN, R. L., GODDARD, A. D., BOTSTEIN, D. & ASHKENAZI, A., 1998. Genomic amplification of a decoy receptor for Fas ligand in lung and colon cancer. Nature 396, 699-703.
Poljsak, B., Šuput, D., Milisav, I., 2013. Achieving the balance between ROS and antioxidants: when to use the synthetic antioxidants. Oxidative medicine and cellular longevity 2013.
Pollok, K. E., Kim, Y.-J., Zhou, Z., Hurtado, J., Kim, K., Pickard, R., Kwon, B., 1993. Inducible T cell antigen 4-1BB. Analysis of expression and function. The Journal of Immunology 150, 771-781.
Porter, A. G., 1990. Human tumour necrosis factors-α and-β: differences in their structure, expression and biological properties. FEMS Microbiology Letters 64, 193-199.

Potapova, O., Basu, S., Mercola, D., Holbrook, N. J., 2001. Protective role for c-Jun in the cellular response to DNA damage. Journal of biological chemistry 276, 28546-28553.
Pouysségur, J., Volmat, V., Lenormand, P., 2002. Fidelity and spatio-temporal control in MAP kinase (ERKs) signalling. Biochemical pharmacology 64, 755-763.
Powell, J. C., Twomey, C., Jain, R., McCarthy, J. V., 2009. Association between Presenilin-1 and TRAF6 modulates regulated intramembrane proteolysis of the p75NTR neurotrophin receptor. Journal of neurochemistry 108, 216-230.
Pullen, S. S., Dang, T. T., Crute, J. J., Kehry, M. R., 1999a. CD40 Signaling through Tumor Necrosis Factor Receptor-associated Factors (TRAFs) binding site specificity and activation of downstream pathways by distinct TRAFs. Journal of Biological Chemistry 274, 14246-14254.
Pullen, S. S., Miller, H. G., Everdeen, D. S., Dang, T. T., Crute, J. J., Kehry, M. R., 1998. CD40-tumor necrosis factor receptor-associated factor (TRAF) interactions: regulation of CD40 signaling through multiple TRAF binding sites and TRAF hetero-oligomerization. Biochemistry 37, 11836-11845.
Pullen, S. S., Labadia, M. E., Ingraham, R. H., McWhirter, S. M., Everdeen, D. S., Alber, T., Crute, J. J., Kehry, M. R., 1999b. High-affinity interactions of tumor necrosis factor receptor-associated factors (TRAFs) and CD40 require TRAF trimerization and CD40 multimerization. Biochemistry 38, 10168-10177.
Pulverer, B. J., Kyriakis, J. M., Avruch, J., Nikolakaki, E., Woodgett, J. R., 1991. Phosphorylation of c-jun mediated by MAP kinases. Nature 353, 670-674.
Radeke, H. H., Meier, B., Topley, N., Floge, J., Habermehl, G. G., Resch, K., 1990. Interleukin-1-alpha and tumor necrosis factor-alpha induce oxygen radical production in mesangial cells. Kidney International 37, 767-775, doi:10.1038/ki.1990.44.
Rai, N. K., Tripathi, K., Sharma, D., Shukla, V. K., 2005. Apoptosis: a basic physiologic process in wound healing. The international journal of lower extremity wounds 4, 138-44, doi:10.1177/1534734605280018.
Raingeaud, J., Gupta, S., Rogers, J. S., Dickens, M., Han, J., Ulevitch, R. J., Davis, R. J., 1995. Pro-inflammatory cytokines and environmental stress cause p38 mitogen-activated protein kinase activation by dual phosphorylation on tyrosine and threonine. Journal of Biological Chemistry 270, 7420-7426.
Ransone, L. J., Verma, I. M., 1990. Nuclear proto-oncogenes fos and jun. Annual review of cell biology 6, 539-557.
Rao, V. N., Reddy, E., 1994. elk-1 proteins interact with MAP kinases. Oncogene 9, 1855-1860.
Rauert, H., Wicovsky, A., Müller, N., Siegmund, D., Spindler, V., Waschke, J., Kneitz, C., Wajant, H., 2010. Membrane tumor necrosis factor (TNF) induces p100 processing via TNF receptor-2 (TNFR2). Journal of Biological Chemistry 285, 7394-7404.
Reed, J. C., 2002. Apoptosis-based therapies. Nature reviews Drug discovery 1, 111-121.
Remouchamps, C., Boutaffala, L., Ganeff, C., Dejardin, E., 2011. Biology and signal transduction pathways of the Lymphotoxin-αβ/LTβR system. Cytokine & growth factor reviews 22, 301-310.
Rennert, P. D., Browning, J. L., Mebius, R., Mackay, F., Hochman, P. S., 1996. Surface lymphotoxin alpha/beta complex is required for the development of peripheral lymphoid organs. The Journal of experimental medicine 184, 1999-2006.
Rissoan, M., Van Kooten, C., Chomarat, P., Galibert, L., Durand, I., THIVOLET-BEJUI, F., Miossec, P., Banchereau, J., 1996. The functional CD40 antigen of fibroblasts may contribute to the proliferation of rheumatoid synovium. Clinical & Experimental Immunology 106, 481-490.
Rizzuto, R., Pozzan, T., 2006. Microdomains of intracellular Ca2+: molecular determinants and functional consequences. Physiological reviews 86, 369-408.

Roach, H., Clarke, N., 2000. Physiological cell death of chondrocytes in vivo is not confined to apoptosis NEW OBSERVATIONS ON THE MAMMALIAN GROWTH PLATE. Journal of Bone & Joint Surgery, British Volume 82, 601-613.

Robey, R. B., Hay, N., 2005. Mitochondrial hexokinases: guardians of the mitochondria. Cell Cycle 4, 654-658.

Rodríguez, M., Cabal-Hierro, L., Carcedo, M. T., Iglesias, J. M., Artime, N., Darnay, B. G., Lazo, P. S., 2011. NF-κB signal triggering and termination by tumor necrosis factor receptor 2. Journal of Biological Chemistry 286, 22814-22824.

Rooney, I. A., Butrovich, K. D., Glass, A. A., Borboroglu, S., Benedict, C. A., Whitbeck, J. C., Cohen, G. H., Eisenberg, R. J., Ware, C. F., 2000. The lymphotoxin-β receptor is necessary and sufficient for LIGHT-mediated apoptosis of tumor cells. Journal of Biological Chemistry 275, 14307-14315.

Rothe, M., Wong, S. C., Henzel, W. J., Goeddel, D. V., 1994. A novel family of putative signal transducers associated with the cytoplasmic domain of the 75 kDa tumor necrosis factor receptor. Cell 78, 681-692.

Rothe, M., Sarma, V., Dixit, V. M., Goeddel, D. V., 1995. TRAF2-mediated activation of NF-kappa B by TNF receptor 2 and CD40. Science 269, 1424-7.

Roulston, A., Reinhard, C., Amiri, P., Williams, L. T., 1998. Early activation of c-Jun N-terminal kinase and p38 kinase regulate cell survival in response to tumor necrosis factor α. Journal of Biological Chemistry 273, 10232-10239.

Roux, P. P., Barker, P. A., 2002. Neurotrophin signaling through the p75 neurotrophin receptor. Progress in neurobiology 67, 203-233.

Roux, P. P., Blenis, J., 2004. ERK and p38 MAPK-activated protein kinases: a family of protein kinases with diverse biological functions. Microbiology and molecular biology reviews 68, 320-344.

Ruggiero, V., Latham, K., Baglioni, C., 1987. Cytostatic and cytotoxic activity of tumor necrosis factor on human cancer cells. The Journal of Immunology 138, 2711-2717.

Ruland, J., Mak, T. W., 2003. From antigen to activation: specific signal transduction pathways linking antigen receptors to NF-κB. Seminars in immunology, Vol. 15. Elsevier, pp. 177-183.

Sabapathy, K., Hochedlinger, K., Nam, S. Y., Bauer, A., Karin, M., Wagner, E. F., 2004. Distinct roles for JNK1 and JNK2 in regulating JNK activity and c-Jun-dependent cell proliferation. Molecular cell 15, 713-725.

Saitoh, M., Nishitoh, H., Fujii, M., Takeda, K., Tobiume, K., Sawada, Y., Kawabata, M., Miyazono, K., Ichijo, H., 1998. Mammalian thioredoxin is a direct inhibitor of apoptosis signal-regulating kinase (ASK) 1. The EMBO journal 17, 2596-2606.

Sakon, S., Xue, X., Takekawa, M., Sasazuki, T., Okazaki, T., Kojima, Y., Piao, J. H., Yagita, H., Okumura, K., Nakano, H., 2003. NF-κB inhibits TNF-induced accumulation of ROS that mediate prolonged MAPK activation and necrotic cell death. The EMBO journal 22, 3898-3909.

Sakurai, T., Maeda, S., Chang, L., Karin, M., 2006. Loss of hepatic NF-κB activity enhances chemical hepatocarcinogenesis through sustained c-Jun N-terminal kinase 1 activation. Proceedings of the National Academy of Sciences 103, 10544-10551.

Salvesen, G. S., 2002. Caspases and apoptosis. Essays in biochemistry 38, 9-19.

Sanjo, H., Zajonc, D. M., Braden, R., Norris, P. S., Ware, C. F., 2010. Allosteric regulation of the ubiquitin: NIK and ubiquitin: TRAF3 E3 ligases by the lymphotoxin-β receptor. Journal of Biological Chemistry 285, 17148-17155.

Sarin, A., Williams, M. S., Alexander-Miller, M. A., Berzofsky, J. A., Zacharchuk, C. M., Henkart, P. A., 1997. Target cell lysis by CTL granule exocytosis is independent of ICE/Ced-3 family proteases. Immunity 6, 209-215.

Sassone-Corsi, P., Verma, I. M., 1987. Modulation of c-fos gene transcription by negative and positive cellular factors. Nature 326, 507-510.
Sato, M., Hata, N., Asagiri, M., Nakaya, T., Taniguchi, T., Tanaka, N., 1998. Positive feedback regulation of type I IFN genes by the IFN-inducible transcription factor IRF-7. FEBS letters 441, 106-110.
Sato, T., Irie, S., Reed, J. C., 1995a. A novel member of the TRAF family of putative signal transducing proteins binds to the cytosolic domain of CD40. FEBS letters 358, 113-118.
Sato, T., Irie, S., Kitada, S., Reed, J. C., 1995b. FAP-1: a protein tyrosine phosphatase that associates with Fas. Science 268, 411.
Savill, J., Fadok, V., 2000. Corpse clearance defines the meaning of cell death. Nature 407, 784-788.
Scaffidi, C., Schmitz, I., Krammer, P. H., Peter, M. E., 1999. The role of c-FLIP in modulation of CD95-induced apoptosis. Journal of Biological Chemistry 274, 1541-1548, doi:10.1074/jbc.274.3.1541.
Scaffidi, C., Fulda, S., Srinivasan, A., Friesen, C., Li, F., Tomaselli, K. J., Debatin, K. M., Krammer, P. H., Peter, M. E., 1998. Two CD95 (APO-1/Fas) signaling pathways. Embo J 17, 1675-87.
Schneider, P., Holler, N., Bodmer, J.-L., Hahne, M., Frei, K., Fontana, A., Tschopp, J., 1998. Conversion of membrane-bound Fas (CD95) ligand to its soluble form is associated with downregulation of its proapoptotic activity and loss of liver toxicity. The Journal of experimental medicine 187, 1205-1213.
Schneider, P., Thome, M., Burns, K., Bodmer, J.-L., Hofmann, K., Kataoka, T., Holler, N., Tschopp, J., 1997. TRAIL receptors 1 (DR4) and 2 (DR5) signal FADD-dependent apoptosis and activate NF-κB. Immunity 7, 831-836.
Schroder, K., Hertzog, P. J., Ravasi, T., Hume, D. A., 2004. Interferon-γ: an overview of signals, mechanisms and functions. Journal of leukocyte biology 75, 163-189.
Schuler, M., Green, D. R., 2001. Mechanisms of p53-dependent apoptosis. Biochemical Society Transactions 29, 684-688, doi:10.1042/0300-5127:0290684.
Schwabe, R. F., Schnabl, B., Kweon, Y. O., Brenner, D. A., 2001. CD40 activates NF-kappa B and c-Jun N-terminal kinase and enhances chemokine secretion on activated human hepatic stellate cells. J Immunol 166, 6812-9.
Schweichel, J. U., Merker, H. J., 1973. The morphology of various types of cell death in prenatal tissues. Teratology 7, 253-266.
Schwenzer, R., Siemienski, K., Liptay, S., Schubert, G., Peters, N., Scheurich, P., Schmid, R. M., Wajant, H., 1999. The human tumor necrosis factor (TNF) receptor-associated factor 1 gene (TRAF1) is up-regulated by cytokines of the TNF ligand family and modulates TNF-induced activation of NF-kappaB and c-Jun N-terminal kinase. J Biol Chem 274, 19368-74.
Screaton, G., Xu, X.-N., 2000. T cell life and death signalling via TNF-receptor family members. Current opinion in immunology 12, 316-322.
Screaton, G. R., Xu, X. N., Olsen, A. L., Cowper, A. E., Tan, R. S., McMichael, A. J., Bell, J. I., 1997. LARD: A new lymphoid-specific death domain containing receptor regulated by alternative pre-mRNA splicing. Proc Natl Acad Sci U S A 94, 4615-4619, doi:10.1073/pnas.94.9.4615.
Šedý, J., Bekiaris, V., Ware, C. F., 2014. Tumor Necrosis Factor Superfamily in Innate Immunity and Inflammation. Cold Spring Harbor perspectives in biology, a016279.
Sedy, J. R., Gavrieli, M., Potter, K. G., Hurchla, M. A., Lindsley, R. C., Hildner, K., Scheu, S., Pfeffer, K., Ware, C. F., Murphy, T. L., 2004. B and T lymphocyte attenuator regulates T cell activation through interaction with herpesvirus entry mediator. Nature immunology 6, 90-98.

Sharma, S., Yang, S.-C., Hillinger, S., Zhu, L. X., Huang, M., Batra, R. K., Lin, J. F., Burdick, M. D., Strieter, R. M., Dubinett, S. M., 2003. SLC/CCL21-mediated anti-tumor responses require IFNgamma, MIG/CXCL9 and IP-10/CXCL10. Mol Cancer 2, 22.

Shaulian, E., Karin, M., 2001. AP-1 in cell proliferation and survival. Oncogene 20, 2390-2400.

Shaulian, E., Karin, M., 2002. AP-1 as a regulator of cell life and death. Nat Cell Biol 4, E131-6.

Shaw, N. J., Georgopoulos, N. T., Southgate, J., Trejdosiewicz, L. K., 2005. Effects of loss of p53 and p16 function on life span and survival of human urothelial cells. International journal of cancer 116, 634-639.

Sheridan, J. P., Marsters, S. A., Pitti, R. M., Gurney, A., Skubatch, M., Baldwin, D., Ramakrishnan, L., Gray, C. L., Baker, K., Wood, W. I., 1997. Control of TRAIL-induced apoptosis by a family of signaling and decoy receptors. Science 277, 818-821.

Shimizu, S., Narita, M., Tsujimoto, Y., 1999. Bcl-2 family proteins regulate the release of apoptogenic cytochrome c by the mitochondrial channel VDAC. Nature 399, 483-487.

Shimizu, S., Kanaseki, T., Mizushima, N., Mizuta, T., Arakawa-Kobayashi, S., Thompson, C. B., Tsujimoto, Y., 2004. Role of Bcl-2 family proteins in a non-apoptotic programmed cell death dependent on autophagy genes. Nature cell biology 6, 1221-1228.

Shinohara, H., Yano, S., Bucana, C. D., Fidler, I. J., 2000. Induction of chemokine secretion and enhancement of contact-dependent macrophage cytotoxicity by engineered expression of granulocyte-macrophage colony-stimulating factor in human colon cancer cells. J Immunol 164, 2728-37.

Shore, P., Sharrocks, A. D., 1994. The transcription factors Elk-1 and serum response factor interact by direct protein-protein contacts mediated by a short region of Elk-1. Molecular and Cellular Biology 14, 3283-3291.

Shresta, S., Graubert, T. A., Thomas, D. A., Raptis, S. Z., Ley, T. J., 1999. Granzyme A initiates an alternative pathway for granule-mediated apoptosis. Immunity 10, 595-605.

Simonet, W. S., Lacey, D. L., Dunstan, C. R., Kelley, M., Chang, M. S., Luthy, R., Nguyen, H. Q., Wooden, S., Bennett, L., Boone, T., Shimamoto, G., DeRose, M., Elliott, R., Colombero, A., Tan, H. L., Trail, G., Sullivan, J., Davy, E., Bucay, N., RenshawGegg, L., Hughes, T. M., Hill, D., Pattison, W., Campbell, P., Sander, S., Van, G., Tarpley, J., Derby, P., Lee, R., Boyle, W. J., 1997. Osteoprotegerin: A novel secreted protein involved in the regulation of bone density. Cell 89, 309-319, doi:10.1016/s0092-8674(00)80209-3.

Slee, E. A., Harte, M. T., Kluck, R. M., Wolf, B. B., Casiano, C. A., Newmeyer, D. D., Wang, H.-G., Reed, J. C., Nicholson, D. W., Alnemri, E. S., 1999. Ordering the cytochrome c–initiated caspase cascade: hierarchical activation of caspases-2,-3,-6,-7,-8, and-10 in a caspase-9–dependent manner. The Journal of cell biology 144, 281-292.

Smith, C. A., Farrah, T., Goodwin, R. G., 1994. The TNF receptor superfamily of cellular and viral proteins: activation, costimulation, and death. Cell 76, 959-962.

Smith, C. A., Davis, T., Anderson, D., Solam, L., Beckmann, M. P., Jerzy, R., Dower, S. K., Cosman, D., Goodwin, R. G., 1990. A receptor for tumor-necrosis-factor defines an unusual family of cellular and viral-proteins. Science 248, 1019-1023, doi:10.1126/science.2160731.

Smyth, M. J., Trapani, J. A., 1995. Granzymes: exogenous porteinases that induce target cell apoptosis. Immunology today 16, 202-206.

Song, H. Y., Régnier, C. H., Kirschning, C. J., Goeddel, D. V., Rothe, M., 1997. Tumor necrosis factor (TNF)-mediated kinase cascades: bifurcation of nuclear factor-κB and c-jun N-terminal kinase (JNK/SAPK) pathways at TNF receptor-associated factor 2. Proceedings of the National Academy of Sciences 94, 9792-9796.

Soroosh, P., Doherty, T. A., So, T., Mehta, A. K., Khorram, N., Norris, P. S., Scheu, S., Pfeffer, K., Ware, C., Croft, M., 2011. Herpesvirus entry mediator (TNFRSF14) regulates the persistence of T helper memory cell populations. The Journal of experimental medicine 208, 797-809.

Southgate, J., Masters, J. R., Trejdosiewicz, L. K., 2002. Culture of human urothelium. Culture of epithelial cells 2.

Spanaus, K. S., Schlapbach, R., Fontana, A., 1998. TNF-α and IFN-γ render microglia sensitive to Fas ligand-induced apoptosis by induction of Fas expression and down-regulation of Bcl-2 and Bcl-xL. European journal of immunology 28, 4398-4408.

Spear, P. G., Manoj, S., Yoon, M., Jogger, C. R., Zago, A., Myscofski, D., 2006. Different receptors binding to distinct interfaces on herpes simplex virus gD can trigger events leading to cell fusion and viral entry. Virology 344, 17-24, doi:10.1016/j.virol.2005.09.016.

Spets, H., Georgii-Hemming, P., Siljason, J., Nilsson, K., Jernberg-Wiklund, H., 1998. Fas/APO-1 (CD95)–Mediated Apoptosis Is Activated by Interferon-γ and Interferon-□in Interleukin-6 (IL-6)–Dependent and IL-6–Independent Multiple Myeloma Cell Lines. Blood 92, 2914-2923.

Stamenkovic, I., Clark, E., Seed, B., 1989. A B-lymphocyte activation molecule related to the nerve growth factor receptor and induced by cytokines in carcinomas. The EMBO journal 8, 1403.

Stanger, B. Z., Leder, P., Lee, T.-H., Kim, E., Seed, B., 1995. RIP: a novel protein containing a death domain that interacts with Fas/APO-1 (CD95) in yeast and causes cell death. Cell 81, 513-523.

Steele, L. P., Georgopoulos, N. T., Southgate, J., Selby, P. J., Trejdosiewicz, L. K., 2006. Differential susceptibility to TRAIL of normal versus malignant human urothelial cells. Cell Death & Differentiation 13, 1564-1576.

Steinberg, M. W., Cheung, T. C., Ware, C. F., 2011. The signaling networks of the herpesvirus entry mediator (TNFRSF14) in immune regulation. Immunol Rev 244, 169-187, doi:10.1111/j.1600-065X.2011.01064.x.

Stopfer, P., Mannel, D. N., Hehlgans, T., 2004. Lymphotoxin-beta receptor activation by activated T cells induces cytokine release from mouse bone marrow-derived mast cells. Journal of Immunology 172, 7459-7465.

Stordal, B., Davey, R., 2008. A 39 kDa fragment of endogenous ASK1 suggests specific cleavage not degradation by the proteasome. IUBMB life 60, 180-184.

Suda, T., Hashimoto, H., Tanaka, M., Ochi, T., Nagata, S., 1997. Membrane Fas ligand kills human peripheral blood T lymphocytes, and soluble Fas ligand blocks the killing. The Journal of experimental medicine 186, 2045-2050.

Sugarman, B. J., Aggarwal, B. B., Hass, P. E., Figari, I. S., Palladino, M. A., Shepard, H. M., 1985. Recombinant human-tumor necrosis factor-alpha - effects on proliferation of normal and transformed-cells invitro. Science 230, 943-945, doi:10.1126/science.3933111.

Sun, S.-C., 2010. Non-canonical NF-κB signaling pathway. Cell research 21, 71-85.

Susin, S. A., Daugas, E., Ravagnan, L., Samejima, K., Zamzami, N., Loeffler, M., Costantini, P., Ferri, K. F., Irinopoulou, T., Prevost, M. C., Brothers, G., Mak, T. W., Penninger, J., Earnshaw, W. C., Kroemer, G., 2000. Two distinct pathways leading to nuclear apoptosis. Journal of Experimental Medicine 192, 571-579, doi:10.1084/jem.192.4.571.

Suvas, S., Kim, B., Sarangi, P. P., Tone, M., Waldmann, H., Rouse, B. T., 2005. In vivo kinetics of GITR and GITR ligand expression and their functional significance in regulating viral immunopathology. Journal of virology 79, 11935-11942.

Szatrowski, T. P., Nathan, C. F., 1991. Production of large amounts of hydrogen peroxide by human tumor cells. Cancer research 51, 794-798.

Tamada, K., Shimozaki, K., Chapoval, A. I., Zhu, G., Sica, G., Flies, D., Boone, T., Hsu, H., Fu, Y.-X., Nagata, S., 2000a. Modulation of T-cell-mediated immunity in tumor and graft-versus-host disease models through the LIGHT co-stimulatory pathway. Nature medicine 6, 283-289.

Tamada, K., Shimozaki, K., Chapoval, A. I., Zhai, Y., Su, J., Chen, S.-F., Hsieh, S.-L., Nagata, S., Ni, J., Chen, L., 2000b. LIGHT, a TNF-like molecule, costimulates T cell proliferation and is required for dendritic cell-mediated allogeneic T cell response. The Journal of Immunology 164, 4105-4110.

Tan, J., Town, T., Mori, T., Obregon, D., Wu, Y., DelleDonne, A., Rojiani, A., Crawford, F., Flavell, R. A., Mullan, M., 2002. CD40 is expressed and functional on neuronal cells. The EMBO journal 21, 643-652.

Tan, K., Harrop, J., Reddy, M., Young, P., Terrett, J., Emery, J., Moore, G., Truneh, A., 1997. Characterization of a novel TNF-like ligand and recently described TNF ligand and TNF receptor superfamily genes and their constitutive and inducible expression in hematopoietic and non-hematopoietic cells. Gene 204, 35-46.

Tang, G., Minemoto, Y., Dibling, B., Purcell, N. H., Li, Z., Karin, M., Lin, A., 2001. Inhibition of JNK activation through NF-kappaB target genes. Nature 414, 313-7.

Tartaglia, L. A., Ayres, T. M., Wong, G. H. W., Goeddel, D. V., 1993. A novel domain within the 55 kd tnf receptor signals cell-death. Cell 74, 845-853, doi:10.1016/0092-8674(93)90464-2.

Tartaglia, L. A., Weber, R. F., Figari, I. S., Reynolds, C., Palladino, M. A., Goeddel, D. V., 1991. The two different receptors for tumor necrosis factor mediate distinct cellular responses. Proceedings of the National Academy of Sciences 88, 9292-9296.

Temkin, V., Huang, Q., Liu, H., Osada, H., Pope, R. M., 2006. Inhibition of ADP/ATP exchange in receptor-interacting protein-mediated necrosis. Molecular and cellular biology 26, 2215-2225.

Teoh, G., Tai, Y.-T., Urashima, M., Shirahama, S., Matsuzaki, M., Chauhan, D., Treon, S., Raje, N., Hideshima, T., Shima, Y., 2000. CD40 activation mediates p53-dependent cell cycle regulation in human multiple myeloma cell lines. Blood 95, 1039-1046.

Terry Powers, J. L., Mace, K. E., Parfrey, H., Lee, S.-J., Zhang, G., Riches, D. W., 2010. TNF receptor-1 (TNF-R1) ubiquitous scaffolding and signaling protein interacts with TNF-R1 and TRAF2 via an N-terminal docking interface. Biochemistry 49, 7821-7829.

Thompson, C. B., 1995. Apoptosis in the pathogenesis and treatment of disease. Science 267, 1456-1462.

Tobiume, K., Matsuzawa, A., Takahashi, T., Nishitoh, H., Morita, K. i., Takeda, K., Minowa, O., Miyazono, K., Noda, T., Ichijo, H., 2001. ASK1 is required for sustained activations of JNK/p38 MAP kinases and apoptosis. EMBO reports 2, 222-228.

Todt, F., Cakir, Z., Reichenbach, F., Emschermann, F., Lauterwasser, J., Kaiser, A., Ichim, G., Tait, S. W., Frank, S., Langer, H. F., 2015. Differential retrotranslocation of mitochondrial Bax and Bak. The EMBO journal 34, 67-80.

Tong, A. W., Stone, M. J., 2003. Prospects for CD40-directed experimental therapy of human cancer. Cancer gene therapy 10, 1-13.

Tower, J., 2015. Programmed cell death in aging. Ageing research reviews.

Tracey, D., Klareskog, L., Sasso, E. H., Salfeld, J. G., Tak, P. P., 2008. Tumor necrosis factor antagonist mechanisms of action: A comprehensive review. Pharmacology & Therapeutics 117, 244-279, doi:10.1016/j.pharmthera.2007.10.001.

Trapani, J. A., Smyth, M. J., 2002. Functional significance of the perforin/granzyme cell death pathway. Nature Reviews Immunology 2, 735-747.

Trapani, J. A., Jans, D. A., Jans, P. J., Smyth, M. J., Browne, K. A., Sutton, V. R., 1998. Efficient nuclear targeting of granzyme B and the nuclear consequences of apoptosis induced by granzyme B and perforin are caspase-dependent, but cell death is caspase-independent. Journal of Biological Chemistry 273, 27934-27938.

Tsujimoto, M., Yip, Y., Vilcek, J., 1986. Interferon-gamma enhances expression of cellular receptors for tumor necrosis factor. The Journal of Immunology 136, 2441-2444.

Tsujimoto, Y., Shimizu, S., 2000. VDAC regulation by the Bcl-2 family of proteins. Cell death and differentiation 7, 1174-1181.
Tsukamoto, N., Kobayashi, N., Azuma, S., Yamamoto, T., Inoue, J.-i., 1999. Two differently regulated nuclear factor κB activation pathways triggered by the cytoplasmic tail of CD40. Proceedings of the National Academy of Sciences 96, 1234-1239.
Turrens, J. F., 2003. Mitochondrial formation of reactive oxygen species. The Journal of physiology 552, 335-344.
Vakkila, J., Lotze, M. T., 2004. Inflammation and necrosis promote tumour growth. Nature Reviews Immunology 4, 641-648.
Vallabhapurapu, S., Karin, M., 2009. Regulation and Function of NF-kappa B Transcription Factors in the Immune System. Annual Review of Immunology, Vol. 27, pp. 693-733.
Valladares, A., Álvarez, A. M., Ventura, J. J., Roncero, C., Benito, M., Porras, A., 2000. p38 Mitogen-Activated Protein Kinase Mediates Tumor Necrosis Factor-α-Induced Apoptosis in Rat Fetal Brown Adipocytes 1. Endocrinology 141, 4383-4395.
Van De Craen, M., Declercq, W., Fiers, W., Vandenabeele, P., 1999. The proteolytic procaspase activation network: an in vitro analysis. Cell death and differentiation 6, 1117-1124.
Van den Oord, J., Maes, A., Stas, M., Nuyts, J., Battocchio, S., Kasran, A., Garmyn, M., De Wever, I., De Wolf-Peeters, C., 1996. CD40 is a prognostic marker in primary cutaneous malignant melanoma. The American journal of pathology 149, 1953.
Van Eyndhoven, W., Gamper, C., Cho, E., Mackus, W., Lederman, S., 1999. TRAF-3 mRNA splice-deletion variants encode isoforms that induce NF-κB activation. Molecular immunology 36, 647-658.
van Geelen, C. M., Pennarun, B., Le, P. T., de Vries, E. G., de Jong, S., 2011. Modulation of TRAIL resistance in colon carcinoma cells: different contributions of DR4 and DR5. BMC cancer 11, 39.
van Kooten, C., Banchereau, J., 2000. CD40-CD40 ligand. Journal of leukocyte biology 67, 2-17.
van Loo, G., Saelens, X., Van Gurp, M., MacFarlane, M., Martin, S., Vandenabeele, P., 2002. The role of mitochondrial factors in apoptosis: a Russian roulette with more than one bullet. Cell death and differentiation 9, 1031-1042.
van Parijs, L., Abbas, A. K., 1996. Role of Fas-mediated cell death in the regulation of immune responses. Current opinion in immunology 8, 355-361.
VanArsdale, T. L., VanArsdale, S. L., Force, W. R., Walter, B. N., Mosialos, G., Kieff, E., Reed, J. C., Ware, C. F., 1997. Lymphotoxin-β receptor signaling complex: role of tumor necrosis factor receptor-associated factor 3 recruitment in cell death and activation of nuclear factor κB. Proceedings of the National Academy of Sciences 94, 2460-2465.
Vandenabeele, P., Galluzzi, L., Berghe, T. V., Kroemer, G., 2010. Molecular mechanisms of necroptosis: an ordered cellular explosion. Nature reviews Molecular cell biology 11, 700-714.
Vardouli, L., Lindqvist, C., Vlahou, K., Loskog, A., Eliopoulos, A., 2009. Adenovirus delivery of human CD40 ligand gene confers direct therapeutic effects on carcinomas. Cancer gene therapy 16, 848-860.
Varfolomeev, E. E., Ashkenazi, A., 2004. Tumor necrosis factor: an apoptosis JuNKie? Cell 116, 491-7.
Verma, I. M., Sassone-Corsi, P., 1987. Proto-oncogene fos: complex but versatile regulation. Cell 51, 513-514.
Vilcek, J., Lee, T. H., 1991. Tumor necrosis factor. New insights into the molecular mechanisms of its multiple actions. J Biol Chem 266, 7313-7316.
Vinay, D. S., Kwon, B. S., 1999. Differential expression and costimulatory effect of 4-1BB (CD137) and CD28 molecules on cytokine-induced murine CD8(+) Tc1 and Tc2 cells. Cell Immunol 192, 63-71, doi:10.1006/cimm.1998.1433.

Vince, J. E., Pantaki, D., Feltham, R., Mace, P. D., Cordier, S. M., Schmukle, A. C., Davidson, A. J., Callus, B. A., Wong, W. W.-L., Gentle, I. E., 2009. TRAF2 must bind to cellular inhibitors of apoptosis for tumor necrosis factor (TNF) to efficiently activate NF-κB and to prevent TNF-induced apoptosis. Journal of Biological Chemistry 284, 35906-35915.

Wajant, H., 2015. Principles of antibody-mediated TNF receptor activation. Cell Death & Differentiation.

Wajant, H., Scheurich, P., 2001. Tumor necrosis factor receptor-associated factor (TRAF) 2 and its role in TNF signaling. Int J Biochem Cell Biol 33, 19-32.

Wajant, H., Henkler, F., Scheurich, P., 2001a. The TNF-receptor-associated factor family: scaffold molecules for cytokine receptors, kinases and their regulators. Cellular signalling 13, 389-400.

Wajant, H., Pfizenmaier, K., Scheurich, P., 2003. Tumor necrosis factor signaling. Cell Death Differ 10, 45-65.

Wajant, H., Moosmayer, D., Wuest, T., Bartke, T., Gerlach, E., Schonherr, U., Peters, N., Scheurich, P., Pfizenmaier, K., 2001b. Differential activation of TRAIL-R1 and-2 by soluble and membrane TRAIL allows selective surface antigen-directed activation of TRAIL-R2 by a soluble TRAIL derivative. Oncogene 20, 4101-4106.

Walczak, H., Krammer, P. H., 2000. The CD95 (APO-1/Fas) and the TRAIL (APO-2L) apoptosis systems. Exp Cell Res 256, 58-66, doi:10.1006/excr.2000.4840.

Wang, H., Yu, Z., Liu, S., Liu, X., Sui, A., Yao, R., Luo, Z., Li, C., 2013. Lentivirus‐mediated LIGHT overexpression inhibits human colorectal carcinoma cell growth in vitro and in vivo. Oncology letters 6, 927-932.

Wang, J., Chun, H. J., Wong, W., Spencer, D. M., Lenardo, M. J., 2001a. Caspase-10 is an initiator caspase in death receptor signaling. Proceedings of the National Academy of Sciences 98, 13884-13888.

Wang, J., Lo, J. C., Foster, A., Yu, P., Chen, H. M., Wang, Y., Tamada, K., Chen, L., Fu, Y.-X., 2001b. The regulation of T cell homeostasis and autoimmunity by T cell–derived LIGHT. The Journal of clinical investigation 108, 1771-1780.

Wang, J., Chun, T., Lo, J. C., Wu, Q., Wang, Y., Foster, A., Roca, K., Chen, M., Tamada, K., Chen, L., Wang, C. R., Fu, Y. X., 2001c. The critical role of LIGHT, a TNF family member, in T cell development. J Immunol 167, 5099-105.

Wang, T.-H., Popp, D. M., Wang, H.-S., Saitoh, M., Mural, J. G., Henley, D. C., Ichijo, H., Wimalasena, J., 1999. Microtubule dysfunction induced by paclitaxel initiates apoptosis through both c-Jun N-terminal kinase (JNK)-dependent and-independent pathways in ovarian cancer cells. Journal of Biological Chemistry 274, 8208-8216.

Wang, X., Martindale, J. L., Holbrook, N. J., 2000. Requirement for ERK activation in cisplatin-induced apoptosis. Journal of Biological Chemistry 275, 39435-39443.

Wang, Y., Prywes, R., 2000. Activation of the c-fos enhancer by the Erk MAP kinase pathway through two sequence elements: the c-fos AP-1 and p62TCF sites. Oncogene 19, 1379-1385.

Ware, C., VanArsdale, T., Crowe, P., Browning, J., 1995. The ligands and receptors of the lymphotoxin system. Pathways for Cytolysis. Springer, pp. 175-218.

Ware, C. F., 2005. Network communications: lymphotoxins, LIGHT, and TNF. Annu. Rev. Immunol. 23, 787-819.

Ware, C. F., Šedý, J. R., 2011. TNF Superfamily Networks: bidirectional and interference pathways of the herpesvirus entry mediator (TNFSF14). Current opinion in immunology 23, 627-631.

Ware, C. F., VanArsdale, S., VanArsdale, T. L., 1996. Apoptosis mediated by the TNF-related cytokine and receptor families. J Cell Biochem 60, 47-55, doi:10.1002/(sici)1097-4644(19960101)60:1<47::aid-jcb8>3.0.co;2-3.

Ware, C. F., Crowe, P. D., Grayson, M. H., Androlewicz, M. J., Browning, J. L., 1992. Expression of surface lymphotoxin and tumor-necrosis-factor on activated T-cell, B-cell, and natural-killer-cells. Journal of Immunology 149, 3881-3888.

Wei, M. C., Zong, W.-X., Cheng, E. H.-Y., Lindsten, T., Panoutsakopoulou, V., Ross, A. J., Roth, K. A., MacGregor, G. R., Thompson, C. B., Korsmeyer, S. J., 2001. Proapoptotic BAX and BAK: a requisite gateway to mitochondrial dysfunction and death. Science 292, 727-730.

Welsh, S. J., Williams, R. R., Birmingham, A., Newman, D. J., Kirkpatrick, D. L., Powis, G., 2003. The thioredoxin redox inhibitors 1-methylpropyl 2-imidazolyl disulfide and pleurotin inhibit hypoxia-induced factor 1α and vascular endothelial growth factor formation 1. Molecular cancer therapeutics 2, 235-243.

Westwick, J. K., Weitzel, C., Minden, A., Karin, M., Brenner, D. A., 1994. Tumor necrosis factor alpha stimulates AP-1 activity through prolonged activation of the c-Jun kinase. J Biol Chem 269, 26396-401.

Wheeler, E., Gong, H., Grimes, R., Benoit, D., Vazquez, L., 1998. p75NTR and Trk receptors are expressed in reciprocal patterns in a wide variety of non-neural tissues during rat embryonic development, indicating independent receptor functions. Journal of Comparative Neurology 391, 407-428.

Wiens, G. D., Glenney, G. W., 2011. Origin and evolution of TNF and TNF receptor superfamilies. Developmental & Comparative Immunology 35, 1324-1335.

Williams-Abbott, L., Walter, B. N., Cheung, T. C., Goh, C. R., Porter, A. G., Ware, C. F., 1997. The lymphotoxin-α (LTα) subunit is essential for the assembly, but not for the receptor specificity, of the membrane-anchored LTα1β2 heterotrimeric ligand. Journal of Biological Chemistry 272, 19451-19456.

Wilson, C. A., Browning, J. L., 2002. Death of HT29 adenocarcinoma cells induced by TNF family receptor activation is caspase-independent and displays features of both apoptosis and necrosis. Cell Death Differ 9, 1321-33.

Wingett, D. G., Vestal, R. E., Forcier, K., Hadjokas, N., Nielson, C. P., 1998. CD40 is functionally expressed on human breast carcinomas: variable inducibility by cytokines and enhancement of Fas-mediated apoptosis. Breast cancer research and treatment 50, 27-36.

Winter, H., van den Engel, N. K., Poehlein, C. H., Hatz, R. A., Fox, B. A., Hu, H.-M., 2007. Tumor-specific T cells signal tumor destruction via the lymphotoxin β receptor. Journal of translational medicine 5, 14.

Wolter, K. G., Hsu, Y.-T., Smith, C. L., Nechushtan, A., Xi, X.-G., Youle, R. J., 1997. Movement of Bax from the cytosol to mitochondria during apoptosis. The Journal of cell biology 139, 1281-1292.

Wong, B. R., Josien, R., Lee, S. Y., Vologodskaia, M., Steinman, R. M., Choi, Y., 1998. The TRAF family of signal transducers mediates NF-kappaB activation by the TRANCE receptor. J Biol Chem 273, 28355-9.

Wood, K. W., Sarnecki, C., Roberts, T. M., Blenis, J., 1992. ras mediates nerve growth factor receptor modulation of three signal-transducing protein kinases: MAP kinase, Raf-1, and RSK. Cell 68, 1041-1050.

Wu, Y., Han, B., Sheng, H., Lin, M., Moore, P. A., Zhang, J., Wu, J., 2003. Clinical significance of detecting elevated serum DcR3/TR6/M68 in malignant tumor patients. International journal of cancer 105, 724-732.

Wyzgol, A., Müller, N., Fick, A., Munkel, S., Grigoleit, G. U., Pfizenmaier, K., Wajant, H., 2009. Trimer stabilization, oligomerization, and antibody-mediated cell surface immobilization improve the activity of soluble trimers of CD27L, CD40L, 41BBL, and glucocorticoid-induced TNF receptor ligand. The Journal of Immunology 183, 1851-1861.

Xia, Z., Dickens, M., Raingeaud, J., Davis, R. J., Greenberg, M. E., 1995. Opposing effects of ERK and JNK-p38 MAP kinases on apoptosis. Science 270, 1326-1331.
Xie, P., 2013. TRAF molecules in cell signaling and in human diseases. Journal of molecular signaling 8, 7.
Xu, L.-G., Li, L.-Y., Shu, H.-B., 2004. TRAF7 potentiates MEKK3-induced AP1 and CHOP activation and induces apoptosis. Journal of Biological Chemistry 279, 17278-17282.
Xu, X., Fu, X.-Y., Plate, J., Chong, A. S., 1998. IFN-γ induces cell growth inhibition by Fas-mediated apoptosis: requirement of STAT1 protein for up-regulation of Fas and FasL expression. Cancer research 58, 2832-2837.
Yamamoto, H., Kishimoto, T., Minamoto, S., 1998. NF-κB activation in CD27 signaling: involvement of TNF receptor-associated factors in its signaling and identification of functional region of CD27. The Journal of Immunology 161, 4753-4759.
Yang, D., ud Din, N., Browning, D. D., Abrams, S. I., Liu, K., 2007. Targeting lymphotoxin β receptor with tumor-specific T lymphocytes for tumor regression. Clinical Cancer Research 13, 5202-5210.
Yang, X. D., Sun, S. C., 2015. Targeting signaling factors for degradation, an emerging mechanism for TRAF functions. Immunological reviews 266, 56-71.
Yang, Y.-M., Bost, F., Charbono, W., Dean, N., McKay, R., Rhim, J. S., Depatie, C., Mercola, D., 2003. C-Jun NH2-terminal kinase mediates proliferation and tumor growth of human prostate carcinoma. Clinical Cancer Research 9, 391-401.
Yang, Y., Wilson, J. M., 1996. CD40 ligand-dependent T cell activation: requirement of B7-CD28 signaling through CD40. Science 273, 1862-1864.
Yasumoto, K., Okamoto, S.-I., Mukaida, N., Murakami, S., Mai, M., Matsushima, K., 1992. Tumor necrosis factor alpha and interferon gamma synergistically induce interleukin 8 production in a human gastric cancer cell line through acting concurrently on AP-1 and NF-kB-like binding sites of the interleukin 8 gene. Journal of Biological Chemistry 267, 22506-22511.
Yee, C., Yang, W., Hekimi, S., 2014. The intrinsic apoptosis pathway mediates the pro-longevity response to mitochondrial ROS in C. elegans. Cell 157, 897-909.
Young, J., Yu, X., Wolslegel, K., Nguyen, A., Kung, C., Chiang, E., Kolumam, G., Wei, N., Wong, W. L., DeForge, L., 2010. Lymphotoxin-αβ heterotrimers are cleaved by metalloproteinases and contribute to synovitis in rheumatoid arthritis. Cytokine 51, 78-86.
Young, L., Dawson, C., Brown, K., Rickinson, A., 1989. Identification of a human epithelial cell surface protein sharing an epitope with the C3d/epstein-barr virus receptor molecule of B lymphocytes. International Journal of Cancer 43, 786-794.
Yu, K.-Y., Kwon, B., Ni, J., Zhai, Y., Ebner, R., Kwon, B. S., 1999. A newly identified member of tumor necrosis factor receptor superfamily (TR6) suppresses LIGHT-mediated apoptosis. Journal of Biological Chemistry 274, 13733-13736.
Yu, P., Lee, Y., Liu, W., Chin, R. K., Wang, J., Wang, Y., Schietinger, A., Philip, M., Schreiber, H., Fu, Y.-X., 2004. Priming of naive T cells inside tumors leads to eradication of established tumors. Nature immunology 5, 141-149.
Yu, W., Xu, Y.-C., Tao, Y., He, P., Li, Y., Wu, T., Zhu, Y.-P., Li, J., Wu, J.-X., Dai, J., 2013. DcR3 regulates the growth and metastatic potential of SW480 colon cancer cells. Oncology reports 30, 2741-2748.
Zaid, H., Abu-Hamad, S., Israelson, A., Nathan, I., Shoshan-Barmatz, V., 2005. The voltage-dependent anion channel-1 modulates apoptotic cell death. Cell Death & Differentiation 12, 751-760.
Zapata, J. M., Pawlowski, K., Haas, E., Ware, C. F., Godzik, A., Reed, J. C., 2001. A diverse family of proteins containing tumor necrosis factor receptor-associated factor domains. Journal of Biological Chemistry 276, 24242-24252.

Zechner, D., Craig, R., Hanford, D. S., McDonough, P. M., Sabbadini, R. A., Glembotski, C. C., 1998. MKK6 activates myocardial cell NF-κB and inhibits apoptosis in a p38 mitogen-activated protein kinase-dependent manner. Journal of Biological Chemistry 273, 8232-8239.

Zeiss, C., 2003. The apoptosis-necrosis continuum: insights from genetically altered mice. Veterinary Pathology Online 40, 481-495.

Zenz, R., Wagner, E. F., 2006. Jun signalling in the epidermis: From developmental defects to psoriasis and skin tumors. The international journal of biochemistry & cell biology 38, 1043-1049.

Zha, J., Harada, H., Yang, E., Jockel, J., Korsmeyer, S. J., 1996a. Serine phosphorylation of death agonist BAD in response to survival factor results in binding to 14-3-3 not BCL-X L. Cell 87, 619-628.

Zha, J. P., Harada, H., Yang, E., Jockel, J., Korsmeyer, S. J., 1996b. Serine phosphorylation of death agonist BAD in response to survival factor results in binding to 14-3-3 not BGL-X(L). Cell 87, 619-628, doi:10.1016/s0092-8674(00)81382-3.

Zhai, Y., Guo, R., Hsu, T.-L., Yu, G.-L., Ni, J., Kwon, B. S., Jiang, G., Lu, J., Tan, J., Ugustus, M., 1998. LIGHT, a novel ligand for lymphotoxin beta receptor and TR2/HVEM induces apoptosis and suppresses in vivo tumor formation via gene transfer. Journal of Clinical Investigation 102, 1142.

Zhan, C., Patskovsky, Y., Yan, Q., Li, Z., Ramagopal, U., Cheng, H., Brenowitz, M., Hui, X., Nathenson, S. G., Almo, S. C., 2011. Decoy strategies: the structure of TL1A: DcR3 complex. Structure 19, 162-171.

Zhang, A. Y., Yi, F., Zhang, G., Gulbins, E., Li, P.-L., 2006. Lipid raft clustering and redox signaling platform formation in coronary arterial endothelial cells. Hypertension 47, 74-80.

Zhang, D., Lin, J., Han, J., 2010. Receptor-interacting protein (RIP) kinase family. Cellular & molecular immunology 7, 243-249.

Zhang, G., 2004. Tumor necrosis factor family ligand–receptor binding. Current opinion in structural biology 14, 154-160.

Zhang, M. C., LIU, H. P., DEMCHIK, L. L., ZHAI, Y. F., YANG, D. J., 2004. LIGHT sensitizes IFNγ–mediated apoptosis of HT-29 human carcinoma cells through both death receptor and mitochondria pathways. Cell research 14, 117-124.

Zhang, X., Li, L., Choe, J., Krajewski, S., Reed, J. C., Thompson, C., Choi, Y. S., 1996. Up-Regulation of Bcl-xL Expression Protects CD40-Activated

Human B Cells from Fas-Mediated Apoptosis. Cellular immunology 173, 149-154.

Zhang, Y., Chen, F., 2004. Reactive oxygen species (ROS), troublemakers between nuclear factor-κB (NF-κB) and c-Jun NH2-terminal kinase (JNK). Cancer research 64, 1902-1905.

Zheng, H., Luo, R., Zhang, L., Mai, G., 2002. [Interferon-gamma up-regulates Fas expression and increases Fas-mediated apoptosis in tumor cell lines]. Di 1 jun yi da xue xue bao= Academic journal of the first medical college of PLA 22, 1090-1092.

Zhou, W., Yuan, J., 2014. Necroptosis in health and diseases. Seminars in cell & developmental biology, Vol. 35. Elsevier, pp. 14-23.

Zimmermann, K. C., Green, D. R., 2001. How cells die: apoptosis pathways. Journal of Allergy and Clinical Immunology 108, S99-S103.

Zong, W. X., Lindsten, T., Ross, A. J., MacGregor, G. R., Thompson, C. B., 2001. BH3-only proteins that bind pro-survival Bcl-2 family members fail to induce apoptosis in the absence of Bax and Bak. Genes Dev 15, 1481-1486, doi:10.1101/gad.897601.

Zotti, T., Vito, P., 2012. The seventh ring: exploring TRAF7 functions. Journal of cellular physiology 227, 1280-1284.

Zou, G. M., Hu, W. Y., 2005. LIGHT regulates CD86 expression on dendritic cells through NF-κB, but not JNK/AP-1 signal transduction pathway. Journal of cellular physiology 205, 437-443.

Zou, H., Henzel, W. J., Liu, X., Lutschg, A., Wang, X., 1997. Apaf-1, a human protein homologous to C. elegans CED-4, participates in cytochrome c–dependent activation of caspase-3. Cell 90, 405-413.